Creating a protein-protein interaction network for alpha-synuclein

Dissertation zur Erlangung des akademischen Grades des
Doktors der Naturwissenschaften (Dr. rer. nat.)

eingereicht im Fachbereich Biologie, Chemie, Pharmazie
der Freien Universität Berlin

vorgelegt von

Matthias Könn

aus Bergisch Gladbach

Juli 2012

Die Arbeit wurde im Zeitraum von August 2007 bis Juli 2012 unter der Leitung von Herrn Prof. Dr. Erich E. Wanker am Max Delbrück Centrum für Molekulare Medizin Berlin-Buch angefertigt.

1. Gutachter: Prof. Dr. Erich E. Wanker

2. Gutachter: Prof. Dr. Fritz G. Rathjen

Disputation am 03. Dezember 2012

Danksagung

An erster Stelle möchte ich mich bei Herrn Prof. Dr. Erich Wanker für die Überlassung des Themas sowie die Bereitstellung von finanziellen Mitteln und seines Fachwissens bedanken.

Ganz besonders möchte ich mich bei Dr. Angeli Möller für die Supervision während der Endphase der experimentellen Arbeiten, die vielen wertvollen Diskussionen sowie für das Korrekturlesen meiner Dissertation bedanken.

Des Weiteren möchte ich mich bei Anup Arumughan, Ronny Kalis, Susanne Köppen, Pablo Porras Millan, Kirstin Rau, Jenny Russ, Maliha Shah und Martina Zenkner für die Hilfestellung bei vielen Experimenten herzlich bedanken.

Danken möchte ich auch Dr. Sean-Patrick Riechers, Nadine Strempel und Philipp Trepte für das Korrekturlesen meiner Dissertation.

Weiterhin danke ich allen Kollegen der AG Wanker für ihre Hilfe bei alltäglichen Problemen im Labor sowie für die angenehme Arbeitsatmosphäre.

Für die Hilfestellung bei der Durchführung und Auswertung des Illumina deep sequencings möchte ich mich bei Mirjam Feldkamp, Dr. Andreas Gogol-Doering und Claudia Langnick (AG Chen) bedanken.

Ebenfalls bedanke ich mich bei Martin Schaefer (AG Andrade) für die Hilfe beim confidence scoring der Protein-Protein-Interaktionen.

Mein besonderer Dank gilt meinen Eltern und Freunden. Diese waren, besonders in der Endphase meiner Promotion, immer für mich da und haben mich stets motiviert und unterstützt.

Summary

Parkinson's disease (PD) is the second most common neurodegenerative disorder after Alzheimer disease. Early in the disease, patients show motor problems including shaking, rigidity, and a slowness of movement. As the disease progresses, cognitive problems like dementia and behavioral problems arise. The two major pathological features of PD are the death of dopaminergic neurons and diffuse accumulation of the alpha-synuclein protein in intracellular aggregates termed Lewy bodies.

Three point mutations in the SNCA gene encoding alpha-synuclein have been identified in familial cases of PD. Furthermore, duplication and triplication of the SNCA locus have been found in familial dominant PD cases. A role of alpha-synuclein in the pathogenesis of sporadic PD is implicated by single nucleotide polymorphisms in the SNCA gene that are associated with increased PD risk. Even though a lot of research effort has been devoted to the identification of the precise role of alpha-synuclein in PD pathology, the exact mechanism has not been identified yet.

A well-established method for determining the function of a protein of interest is the study of the proteins interacting with it. Although the interaction of alpha-synuclein with numerous proteins has been described in literature, no work aiming to create a comprehensive protein-protein interaction (PPI) network has been published yet.

To find out more about the role of alpha-synuclein in the pathogenesis of PD, the yeast two-hybrid (Y2H) assay was used to generate alpha-synuclein PPI networks. Furthermore, two additional PPI detection methods were established and used to identify proteins interacting with alpha-synuclein. The cytosolic yeast two-hybrid (cytoY2H) system was modified for high-throughput use to detect PPIs in the yeast cytoplasm. The subSEQ method combines a cytoY2H cDNA library screen with next-generation sequencing (NGS) to identify interacting proteins. PPIs detected by the Y2H, cytoY2H and subSEQ methods were validated in mammalian cells using the LUMIER co-immunoprecipitation assay. Subsequently, the interaction data obtained by the different detection methods was used to generate a high-confidence alpha-synuclein PPI network.

All applied methods detected published as well as novel interaction partners of alpha-synuclein. Many of these proteins could be potential therapeutic targets for PD. Several drugs and small molecules targeting interacting proteins were identified and

could be tested for an effect in PD models. Furthermore, the screens detected alpha-synuclein interactions with proteins that are part of signaling pathways inducing neuronal death. The analysis of the generated high-confidence interaction network strongly supports the hypothesis that alpha-synuclein plays an important role in vesicle trafficking.

Finally, it was demonstrated that several human proteins interacting with alpha-synuclein modulate its toxicity when overproduced in a yeast model.

Zusammenfassung

Die Parkinson-Krankheit ist nach der Alzheimer-Krankheit die zweithäufigst auftretende neurodegenerative Erkrankung. Zu Beginn der Krankheit treten bei Parkinson-Patienten motorische Störungen wie Muskelzittern, Muskelstarre sowie verlangsamte Bewegungen auf. Im weiteren Verlauf der Krankheit können kognitive Probleme, Demenz und verschiedene Verhaltensprobleme entstehen. Die pathologischen Hauptbefunde der Parkinson-Krankheit sind die Degeneration dopaminerger Neuronen sowie die diffuse Ansammlung des alpha-Synuclein Proteins in intrazellulären Aggregaten, den sog. Lewy-Körperchen.

In Familien mit bekannter erblicher Form der Parkinson-Krankheit wurden drei Punktmutationen im SNCA-Gen, welches alpha-Synuclein kodiert, identifiziert. Weiterhin konnten die Duplikation und Triplikation des SNCA-Gens in Familien mit dominant vererbter Parkinson-Krankheit festgestellt werden. Ebenfalls wurden in mehreren Studien genetische Varianten (*single nucleotide polymorphisms*) des SNCA-Gens mit der sporadischen Form der Parkinson-Krankheit assoziiert. Trotz intensiver Forschung ist die Rolle von alpha-Synuclein bei der Entstehung der Parkinson-Krankheit jedoch noch ungeklärt.

Eine gängige Methode um Informationen über die Funktion eines unbekannten Proteins zu erhalten, ist die Identifizierung der Proteine, die mit ihm interagieren. In der wissenschaftlichen Literatur wurden bereits zahlreiche Interaktionspartner von alpha-Synuclein beschrieben. Bis jetzt wurde jedoch noch kein umfassendes Protein-Protein-Interaktionsnetzwerk für alpha-Synuclein beschrieben.

Um mehr über seine Rolle bei Entstehung der Parkinson-Krankheit zu erfahren, wurde in der vorliegenden Arbeit das *yeast two-hybrid* (Y2H) System verwendet, um neue Interaktionspartner von alpha-Synuclein zu identifizieren. Zusätzlich wurden zwei weitere Methoden zur Bestimmung von Protein-Protein-Interaktionen (PPIs) etabliert und zur Identifizierung von alpha-Synuclein Interaktionspartnern verwendet. Zum einen handelt es sich dabei um das *cytosolic yeast two-hybrid* (cytoY2H) System. Dieses wurde für den Hochdurchsatz modifiziert und zur Bestimmung von PPIs im Cytoplasma von Hefe verwendet. Zum anderem wurde das subSEQ-System etabliert. Bei dieser Methode wurde ein cytoY2H cDNA-Bank-Screen mit *next-generation sequencing* (NGS) kombiniert, um interagierende Proteine zu identifizieren. Die durch die o.g. Methoden detektierten Interaktionen wurden in Säugetierzellen mit dem LUMIER Assay validiert. Anschließend wurden alle

Interaktionsdaten in ein *high-confidence* Protein-Protein-Interaktionsnetzwerk integriert.

Durch alle verwendeten Methoden konnten bereits publizierte als auch neue Interaktionspartner von alpha-Synuclein identifiziert werden. Viele dieser Proteine könnten potentielle therapeutische Ziele für die Parkinson-Krankheit darstellen. Weiterhin konnten diverse chemische Moleküle identifiziert werden, die an Modellsystemen für die Parkinson-Krankheit getestet werden können. Durch die Interaktions-Screens konnten Interaktionspartner von alpha-Synuclein identifiziert werden, die als Teil von Signal-Kaskaden den Tod neuronaler Zellen induzieren. Durch die Analyse des *high-confidence* Protein-Protein-Interaktionsnetzwerkes von alpha-Synuclein konnte die Hypothese unterstützt werden, dass alpha-Synuclein eine wichtige Rolle beim intrazellulären Vesikeltransport spielt.

Außerdem konnte in einem Hefe Modellsystem der Parkinson-Krankheit gezeigt werden, dass viele Interaktionspartner von alpha-Synuclein dessen Toxizität modulieren können.

Abbreviations

°C	degrees Celsius
µg	microgram
µl	microliter
µM	micro molar
3-AT	3-amino-1,2,4-triazole
6-OHDA	6-hydroxydopamine
A30P	alpha-synuclein mutation (alanine to proline)
A53T	alpha-synuclein mutation (alanine to threonine)
AD	Alzheimer's disease / transcription activation domain
ADP	adenosine diphosphate
ALS	amylotrophic lateral sclerosis
Amp	Ampicillin
ATP	adenosine triphosphate
β-gal	ß-galactosidase
BD	DNA-binding domain
bp	base pair
C. elegans	*Caenorhabditis elegans*
cDNA	complementary DNA
CMA	chaperone-mediated autophagy
CNS	central nervous system
Co-IP	Co-immunoprecipitation
Cub	C-terminal half of ubiquitin
cytoY2H	cytosolic yeast two-hybrid
D. melanogaster	*Drosophila melanogaster*
ddH_2O	double-distilled water
DMSO	Dimethylsulfoxide
DNA	Desoxiribonucleic acid
DTT	Dithiothreitole
E46K	alpha-synuclein mutation (glutamic acid to lysine)
E. coli	*Escherichia coli*
EDTA	ethylenediaminetetraacetic acid
ER	endoplasmatic reticulum
FL	Firefly luciferase
GFP	green fluorescent protein
GWAS	genome wide association studies
h	hours
HD	Huntington's disease
HEK	Human Embryonic Kidney 293 cells
HEPES	4-(2-hydroxyethyl)-1-piperazineethanesulfonic acid
Htt	Huntingtin
Kan	Kanamyin
KEGG	Kyoto Encyclopedia of Genes and Genomes
kDa	kilodalton
LB	Lewy body
LB-medium	Luria Bertani medium
LUMIER	luminescence-based mammalian interactome mapping
MATα	yeast mating type α
MATa	yeast mating type a
mg	milligram

min	minutes
ml	mililiter
MPTP	1-methyl-4-phenyl-1,2,3,6-tetrahydropyridine
mRNA	messenger ribonucleic acid
MS	mass spectrometry
MTP	microtiter plate
MYTH	membrane yeast two-hybrid
NAC	non-Aβ component of AD amyloid
NGF	nerve growth factor
Nub	N-terminal half of ubiquitin
nm	nanometer
OD600	optical density at 600nm wavelength
ORF	open reading frame
PA	Protein A
PBS	phospho-buffered saline
PCR	polymerase chain reaction
PD	Parkinson's disease
PPI	protein-protein interaction
PTM	post-translational modification
ROS	reactive oxygen species
RL	Renilla luciferase
RNAi	RNA interference
S. cerevisiae	*Saccharomyces cerevisiae*
SCA	spinocerebellar ataxias
SD	synthetic defined broth
SDS	sodium dodecyl sulfate
SDS-PAGE	sodium dodecyl sulfate polyacrylamide gel electrophoresis
sec	seconds
siRNA	small interfering ribonucleic acid
SNCA	gene encoding alpha-synuclein
SNpc	substantia nigra pars compacta
subSEQ	split-ubiquitin screen combined with sequencing
TAP	tandem affinity purification
Tet	Tetracycline
TH	tyroxine hydroxylase
TF	transcription factors
TNF	tumor necrosis factor
Tris	tris(hydroxymethyl)aminomethane
U	enzyme unit
Ub	ubiquitin
UBP	ubiquitin binding proteases
UPS	ubiquitin-proteasome system
WB	Western blotting
x g	earth's gravity
Y2H	yeast two-hybrid
YPD	Yeast Peptone Dextran medium

Table of contents

List of Figures

List of Tables

1 Introduction

1.1 Parkinson’s disease

Parkinson's disease (PD) is a progressive neurodegenerative disorder that was first described by James Parkinson in 1817 [1]. PD is the second most common neurodegenerative disease, following Alzheimer's disease. The disease symptoms appear at a mean age of onset of 57 years [2]. The disease affects 1% of the population over the age of 60 years [3]. However, about 5% of the individuals diagnosed with PD are younger than 40 years of age (early-onset PD) [4].

Clinically, PD patients show motor symptoms collectively termed as parkinsonism. The symptoms include shaking, bradykinesia (slowness of movement), reduced spontaneous movement, rigidity, balance problems and hypomimia (reduced facial expression). In addition, PD patients can show non-motoric symptoms including autonomic, cognitive and psychiatric problems like depression and anxiety [5]. Cognitive impairment, such as slowness in memory and thought, increases with age and disease progression [6].

The main cellular pathological characteristic of PD are intracellular proteinaceous inclusions termed Lewy bodies (LB) that were first described in 1912 [7]. The analysis of LBs revealed that their major constituents are amyloid fibrils composed of the protein alpha-synuclein [8], a protein expressed in presynaptic terminals in the central nervous system (CNS). LBs are particularly abundant in the substania nigra [9], specifically in the substantia nigra pars compacta (SNpc) [10]. Another pathological feature of PD are Lewy neurites, which correspond to abnormal neurites containing inclusions similar to those found in LBs [11].

Along with the formation of LBs, the progressive loss of dopaminergic neurons was observed in the SNpc of PD patients [10]. Although all PD patients show parkinsonism, the symptoms described by this term can also be observed in the absence of alpha-synuclein accumulation (secondary parkinsonism) [12]. The SNpc is an area of the midbrain and plays a role in the control of voluntary movement, learning and reward seeking. Although dopaminergic neurons represent less than 1% of the total neurons in the human brain, these cells play an important role in the regulation of basic brain functions in the brain regions they innervate [13]. The major disease symptoms become evident after the loss of about 50% of the dopaminergic neurons of the nigrostriatal pathway, projecting from the SNpc to the striatum [3] (Figure 1-1 A). Parts of the SNpc appear darker than neighboring areas due to high

levels of melanin and iron. Neuronal degeneration leads to a depigmentation of the area in post-mortem brains of PD patients (Figure 1-1 B) [14]. However, PD pathology is not limited to the nigrostriatal pathway, as LBs have also been found in the cortex, amygdala, locus coeruleus and the peripheral autonomic system [15, 16].

PD, dementia with LBs and multiple system atrophy are collectively referred to as synucleinopathies [17]. Synucleinopathies are a heterogeneous group of neurodegenerative disorders that are characterized by LBs containing large amounts of aggregated alpha-synuclein [17]. In summary, PD is a complex neurodegenerative disorder and until today no cure has been found.

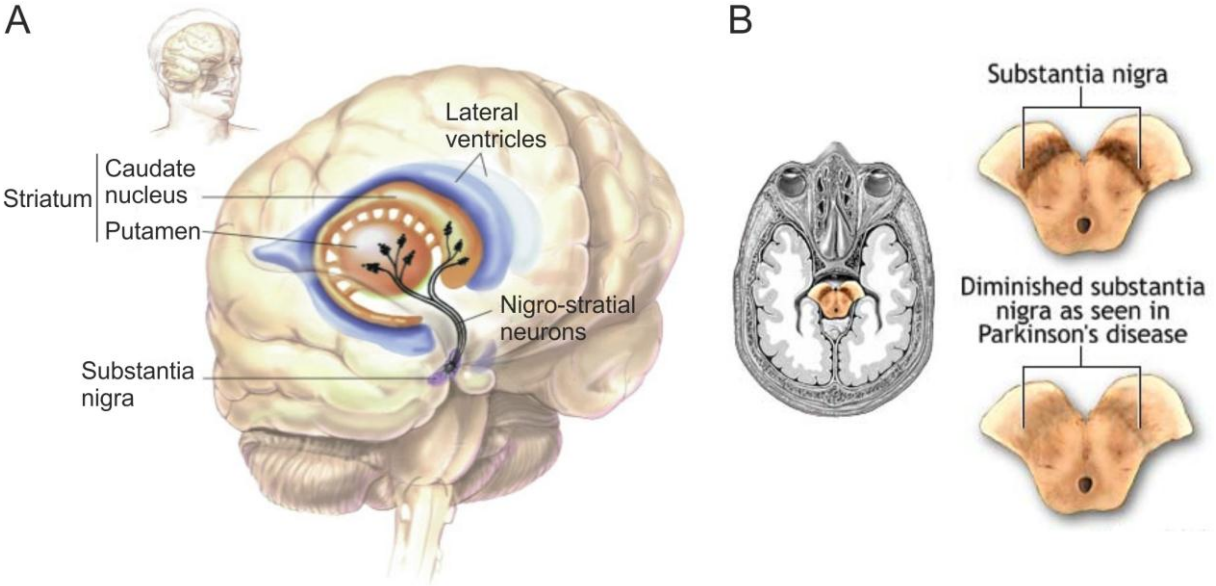

Figure 1-1: Neuronal degeneration in Parkinson's disease. A: Affected brain regions: Neurons projecting from the substantia nigra to the caudate nucleus and putamen (collectively called the striatum) transmit signals controlling body movements. These neurons release the neurotransmitter dopamine at their targets in the striatum. Dopaminergic neurons in the nigro-striatal pathway degenerate in PD patients for unknown reasons. (adapted from Terese Winslow and Lydia Kibiuk, 2001). B: The loss of dopaminergic neurons in substantia nigra pars compacta leads to depigmentation of the area in post-mortem brains of PD patients (modified from A.D.A.M., Inc website, 2011).

1.2 Causes of PD

1.2.1 Environmental causes of PD

Most PD cases are considered to be idiopathic or sporadic, meaning that the origin of the disease is unknown. Several environmental factors that could cause this form of the disease have been identified.

An association between pesticide exposure and PD has been demonstrated by several studies [18-20]. Regardless of these findings, these chemicals are still commonly used. The herbicide paraquat is utilized to eliminate weeds. Rotenone, which naturally occurs in several plant roots, is used as insecticide, piscicide and

pesticide. It has been demonstrated that exposure to paraquat and rotenone leads to development of neurodegenerative phenotypes resembling PD in mice, rats and primates [21-23]. Furthermore, exposure to 1-methyl-4-phenyl-1,2,3,6-tetrahydropyridine (MPTP) directly causes parkinsonism [24, 25]. MPTP is a contaminant of artificial heroin [1-methyl-4-phenyl-propionoxypiperidine (MPPP)] and has a similar structure as paraquat. Both paraquat and MPTP are thought to have an identical mechanism of action. The chemicals bind to the mitochondrial complex I and interfere with oxidative phosphorylation, leading to mitochondrial dysfunction [26]. Disturbed mitochondrial function leads to an increase in reactive oxygen species (ROS), which oxidize and damage different components of a cell and thereby propagate toxicity.

1.2.2 Genetic causes of PD

Although the majority of PD cases are considered to be idiopathic or sporadic, an estimated 5-10% of all parkinsonian cases are familial [27]. Most of these familial cases are caused by mutations in the genes SNCA, PARK2, PINK1, DJ-1 and LRRK2 [28]. Table 1-1 gives a brief overview of the major identified genes.

Table 1-1: Selected genes involved in PD [28].

Locus	MOI	Gene (protein)	Protein function	Clinical presentation	Neuropathology	Age at onset
PARK1 (PARK4)	AD	SNCA (a-synuclein)	Unknown synaptic function	Duplications: Idiopathic PD; some postural tremor; slow progression	LBs	Mid 30–mid 60
				Triplications: PD; PD with dementia; diffuse LBs disease; aggressive course	LBs and LNs; ± glial inclusions; hippocampal CA2 and CA3 loss	Mid 20–30
				Mutations A53T, A30P, E46K: Idiopathic PD; parkinsonism and diffuse LBs	LBs and LNs; ± tau inclusions; amyloid plaques	30–60
PARK2	AR	Parkin	E3 ubiquitin ligase	Parkinsonism; slow progression	Variable presence of LBs	Juvenile to 40
PARK5	AD	UCHL1	Ubiquitin hydrolase and ligase	PD	Unknown	30–50
PARK6	AR	PINK1	Mitochondrial Ser–Thr kinase	Parkinsonism	Unknown	30–50
PARK7	AR	DJ-1	Oxidative stress response?	Parkinsonism	Unknown	20–40
PARK8	AD	LRRK2 (dardarin)	Unknown protein kinase	PD	Diffuse LBs; LNs;± tau inclusions; ± amyloid plaques	40–60

Abbreviations: AD, autosomal dominant; AR, autosomal recessive; LBs, Lewy bodies; LNs, Lewy neurites; MOI, mode of inheritance; OE, overexpressed; PD, Parkinson's disease.

The best studied gene is SNCA, the gene encoding alpha-synuclein. This protein is the main focus of this thesis and will be described in detail in the following section.

The E3 ubiquitin protein ligase Parkin encoded by the gene PARK2 targets misfolded proteins for degradation by the ubiquitin proteasome pathway [29]. Mutations in the PARK2 gene are linked to autosomal recessive early-onset PD [29-31].

The serine/threonine-protein kinase PINK1 accumulates within the intermembrane space of mitochondria [32]. Some rare forms of familial PD are correlated to mutated PINK1 [32]. Overexpression of wild type PINK1 in cell lines prevents the release of mitochondrial cytochrome c and subsequent apoptosis, but this function is abolished in familial PD-linked PINK1 mutants [33].

Loss-of-function mutations in the DJ-1 gene have been associated with rare forms of autosomal recessive early-onset parkinsonism [34]. The homo-dimeric protein may function as a scavenger of reactive oxygen species (ROS) [35, 36]. It was also suggested that oxidized DJ-1 acts as a chaperone and might prevent early steps in the formation of alpha-synuclein aggregates [37].

Mutations in the leucine-rich repeat kinase 2 (LRRK2) cause autosomal dominant PD [38, 39]. Furthermore, LRRK2 point mutations have been associated with 1-2% of the idiopathic PD cases [40, 41]. A role for LRRK2 as a modulator in a mitochondrial dependent cell death pathway has been suggested [38].

1.3 The role of alpha-synuclein in PD

1.3.1 Role of alpha-synuclein in familial PD

Several mutations identified in the SNCA locus have linked alpha-synuclein to familial PD. The first mutation was found in Italian and Greek families with a dominantly inherited form of PD [42]. The authors identified the G209A missense mutation leading to an A53T (alanine to threonine) amino acid exchange. The age of disease onset in affected patients was around 40 years. Subsequently, additional point mutations associated with autosomal dominant PD were identified. The G88C missense mutation leads to an A30P (alanine to proline) amino acid exchange in German PD patients [43]. The third missense mutation was discovered in a Spanish family [44]. In these patients, the G188A mutation caused the E46K (glutamic acid to lysine) amino acid exchange, leading to autosomal dominant PD [44]. In addition, duplication and triplication of the SNCA locus has been reported in families with an autosomal dominant inheritance pattern [45, 46], further confirming the important role of alpha-synuclein in the pathogenesis of PD. Strikingly, even more severe symptoms were observed in PD cases with SNCA triplication [47].

1.3.2 The role of alpha-synuclein in sporadic PD

Several genome wide association studies (GWAS) performed recently have associated polymorphisms in the SNCA locus with PD [48-50]. Taken together, these studies suggest that alpha-synuclein also plays an important role in sporadic PD.

Consistent with this hypothesis, alpha-synuclein mRNA levels are increased in sporadic PD brains [51] and LBs containing aggregated alpha-synuclein are also present in sporadic disease cases [52].

1.4 Properties of alpha-synuclein

1.4.1 The synuclein protein family

Alpha-synuclein belongs to the family of synucleins, which also includes beta-synuclein and gamma-synuclein [53]. The members of this family have a similar domain organization and are 55-62% identical in sequence [54]. Synucleins are highly conserved between vertebrate species [55]. All members of the synuclein family are abundantly present in the human brain, but their exact physiological function remains to be determined.

1.4.2 Structure of alpha-synuclein

Alpha-synuclein was first isolated in 1988 from *Torpedo californica* (an electric ray) using an antiserum against cholinergic vesicles [56]. The protein was localized to the nuclear envelope and presynaptic nerve terminals of neurons and was thus named synuclein [56]. Later, a peptide termed NAC (non-Aβ component of AD amyloid) was found in amyloid plaques of Alzheimer's disease (AD) patients. The precursor protein of this peptide (NACP) was identified as a homologue of rat alpha-synuclein [57].

The human SNCA gene is located on chromosome 4q21.3-q22 and spans a region of 111 kb. The gene consists of seven exons, but only five of them correspond to a region encoding the 140 amino acid alpha-synuclein protein. In solution, the protein lacks a defined tertiary structure and therefore belongs to the group of natively unfolded or intrinsically disordered proteins [58]. In the presence of lipids and membranes, alpha-synuclein adopts an α-helical conformation that can bind to the anionic phospholipid surfaces of vesicles [59].

Alpha-synuclein is a highly abundant protein primarily found in neural tissues. The sequence of alpha-synuclein can be divided into three domains (Figure 1-2): The highly conserved amphipathic N-terminal domain (residues 1-60) contains a series of imperfect 11 amino acid repeats. These repeats include the consensus sequence KTKEGV, which has a structural alpha helix propensity and is highly similar to apolipoprotein lipid-binding motifs. This region adopts an α-helical secondary structure when bound to phospholipids. The three missense mutations associated with familial PD (A30P, E46K and A53T) are located in this domain, suggesting that this region has an important cellular function. The central hydrophobic NAC domain

(non-Aβ component, residues 61-95) of alpha-synuclein is associated with an increased propensity of the protein to convert into a β-sheet conformation and to form fibrils [60]. The other members of the synuclein family lack the NAC region and do not tend to aggregate [54], further underlining the importance of this region for alpha-synuclein aggregation. The highly acidic and proline-rich C-terminal tail (residues 96-140) contains mostly negatively charged residues and has no distinct structural propensity.

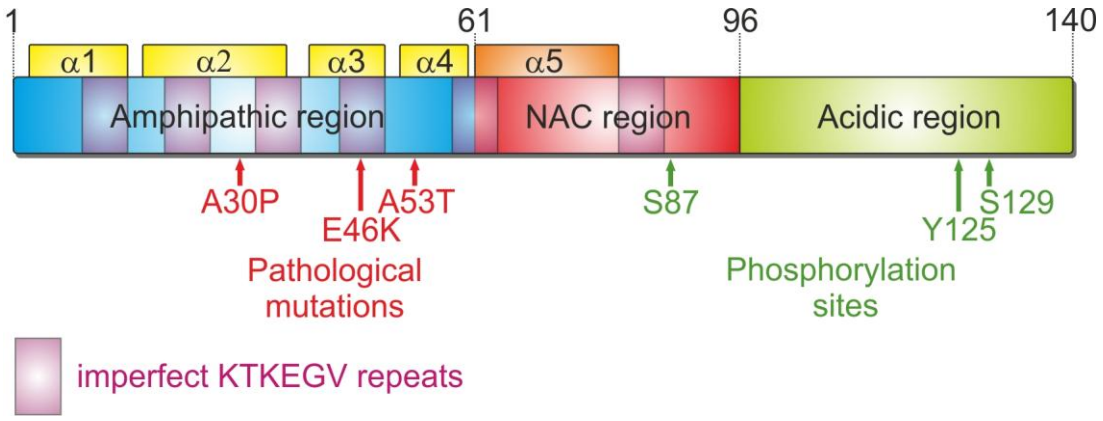

Figure 1-2: Modular domain structure of alpha-synuclein. The α-helices in the N-terminal amphipathic region (α1-α4; in yellow) are required for phospholipid binding. The non-Aβ component (NAC) region promotes β-sheet formation. The highly acidic C-terminal region is prone to be unstructured and subject to post-translational modifications. Amino-acid positions are indicated above the regions. The imperfect KTKEGV repeats that form amphipathic α-helices are shown in purple. Pathological mutations and the major (S129) and minor phosphorylation sites are indicated by red or green arrows, respectively. The figure is based on published information [61].

Several studies have reported four different alpha-synuclein isoforms (SNCA140, SNCA126, SNCA112, and SNCA98) that are generated by alternative splicing of exon 3 and 5 [62]. One of these isoforms (SNCA112) is only found in brains from patients with LB disease [63]. In addition, this isoform is upregulated in PD cell culture models treated with MPTP or rotenone [63].

1.4.3 Aggregation of alpha-synuclein

It is well established that monomers of alpha-synuclein can convert into a β-sheet conformation and form soluble prefibrillar aggregates known as protofibrils, which can further aggregate into even larger insoluble fibrils [64-66]. A widely accepted hypothesis proposes that alpha-synuclein protofibrils are the cytotoxic species, while the insoluble aggregates might represent a cytoprotective aggregate species [67, 68]. Protofibrils induce neurotoxicity in cell models and in mice overexpressing alpha-synuclein [64, 69] and are increased in their abundance in PD patient brains [70], supporting the hypothesis of protofibril-induced cytotoxicity. The known pathological mutations of alpha-synuclein affect the protein's propensity to form fibrils *in vitro*:

A30P and A53T alpha-synuclein variants form protofibrils more efficiently than the wild-type protein [66], while the E46K mutation reduces the formation of protofibrillar structures [71]. Both E46K and A53T alpha-synuclein form more mature fibrils than the wild-type protein [66, 71].

1.4.4 Posttranslational modification of alpha-synuclein

Post-translational modification (PTM) in the C-terminal domain of alpha-synuclein influences the aggregation properties of the protein [62]. These modifications include phosphorylation, oxidation and nitration of specific amino acids [72-74]. Phosphorylation is the best studied alpha-synuclein PTM, and addition of a phosphate group to serine 129 increases fibrilization, while modification of tyrosine 125 prevents this process [75]. In addition, the reported C-terminal truncation of alpha-synuclein increases the protein's propensity for fibrilization [76].

1.4.5 Degradation of alpha-synuclein

In neuronal cells, monomeric alpha-synuclein is mainly degraded by the lysosomal pathway, in particular by chaperone-mediated autophagy (CMA) and macroautophagy [77-82]. Furthermore, alpha-synuclein can also be degraded by the proteasome in a ubiquitin-independent manner [78, 83].

1.5 Potential pathogenic effects of alpha-synuclein

Various cellular roles of alpha-synuclein in PD pathogenesis have been suggested. Overexpression studies of alpha-synuclein in cell culture and in *in vivo* models have identified several roles of the protein in the synapse: Increased alpha-synuclein levels lead to decreased neurotransmitter release, loss of presynaptic proteins, redistribution of SNARE proteins, enlargement of synaptic vesicles as well the inhibition of vesicle recycling [84-86]. Alpha-synuclein might also impair cytoskeletal dynamics, as it interacts with and influences the polymerization of tubulin [87, 88]. Furthermore, several studies have demonstrated that aberrant alpha-synuclein can induce proteasomal dysfunction [89-92] and impair the function of the lysosomal degradation system [79, 93, 94]. Alpha-synuclein localizes to mitochondria and causes down-regulation of complex I activity, similar to mitochondrial toxins [95-97]. In addition, mice overexpressing alpha-synuclein show aberrant mitochondrial morphology [98]. Mitochondrial dysfunction might generate reactive oxygen species (ROS) and induce neuronal death [99]. Other studies in yeast, worms and mammalian cells described ER/Golgi stress and impaired cellular transport caused

by alpha-synuclein [100-102]. Finally, it was shown that alpha-synuclein can reduce histone acetylation in the nucleus and thereby promote neurotoxicity [103]. Despite of these numerous lines of evidence for a role of alpha-synuclein in PD, its exact role in the disease remains to be identified.

1.6 Disease models of PD

1.6.1 Toxin induced models of PD

Several models for PD have been designed to produce nigrostriatal dopaminergic lesions. These rodent models function by intracerebral infusion of the neurotoxins 6-hydroxydopamine (6-OHDA), MPTP, paraquat or rotenone (reviewed by Bove *et al.* [104]). The toxins inhibit mitochondrial function and/or create reactive oxygen species, however none of them completely reproduces the human clinical symptoms and pathology of PD [105].

1.6.2 Alpha-synuclein overexpression models of PD

Numerous disease models of PD primarily based on the transgenic overexpression of wild-type or mutant alpha-synuclein have been developed. These include cell models of primary neurons and neuroblastoma derived cell lines (reviewed by Falkenburger *et al.* [106]). Recently, pluripotent stem cells derived from a PD patient with triplication of the SNCA locus have been generated, which better mimic the disease phenotype [107]. Overexpression of wild-type and mutant alpha-synuclein in yeast limits cell growth, and several new insights in the mechanism of PD have been obtained using this disease model [108]. Alpha-synuclein overexpression also induces loss of dopaminergic neurons in invertebrates like *D. melanogaster*, and these flies are used as a common model to study the disease mechanisms of PD [109]. Furthermore, the worm *C. elegans* is used to examine the toxic effects of alpha-synuclein on dopaminergic neurons in an *in vivo* setting [110]. In addition, several mouse strains overexpressing wild type [69] or mutant alpha-synuclein [111] have been generated. However, no degeneration or loss of nigrostriatal dopaminergic neurons in the substantia nigra was observed in these transgenic mice [111]. The loss of nigrostriatal dopaminergic neurons can be induced by viral vector mediated expression of alpha-synuclein in a rat model [112].

1.7 Study of protein-protein interactions

To function in a cellular environment, proteins rarely act alone but rather form complexes and work as ‘‘molecular machines’’ with intricate physicochemical

dynamic connections. Most cellular processes, for example the regulation of gene expression or the transport across biological membranes, depend on defined protein-protein interactions (PPIs). A common approach to gain insight into the function of an uncharacterized protein is to identify the proteins interacting with it. For example, if a protein is found to interact with known components of the proteasome, it is quite likely that it also plays a role in ubiquitin-mediated protein degradation.

1.8 Alpha-synuclein interactions modulate cellular processes disturbed in PD

Alpha-synuclein has been shown to regulate the production of dopamine in cell culture by physically interacting with tyroxine hydroxylase (TH), a rate-limiting enzyme in the dopamine synthesis pathway [113, 114]. Alpha-synuclein binds TH, prevents its phosphorylation and inhibits TH activation by increasing protein phosphatase 2A activity [113, 115]. In agreement with these findings, suppression of alpha-synuclein in cell culture models leads to increased TH phosphorylation and activity [114]. Consistent with a role of alpha-synuclein in dopamine biosynthesis, reduced TH activity has also been demonstrated in mouse models overexpressing alpha-synuclein [69, 112]. These examples show that alpha-synuclein can modulate cellular processes by physically interacting with proteins involved in these processes. Thus, the identification of novel interaction partners of alpha-synuclein could reveal processes regulated by alpha-synuclein, which might be disturbed in PD when alpha-synuclein is misfolded or its protein levels are increased.

1.9 Interacting proteins modulate alpha-synuclein aggregation and toxicity

It has been demonstrated that several proteins interacting with alpha-synuclein can modulate the toxicity caused by alpha-synuclein while other proteins influence its propensity to form protofibrils or aggregates. One of these proteins is synphilin-1, which was initially identified in a Y2H screen and promotes alpha-synuclein aggregation and inclusion formation [116]. Strikingly, expression of synphilin-1 in an A53T alpha-synuclein expressing mouse strain reduces neurodegeneration, while enhancing the formation of insoluble alpha-synuclein inclusions, further supporting the hypothesis that insoluble species might represent a cytoprotective mechanism [117]. The E3 ubiquitin ligase Siah-1 interacts with and facilitates mono- and di-ubiquitination of alpha-synuclein *in vivo* [118]. However, ubiquitination by Siah-1 does not target alpha-synuclein for the degradation by the proteasome but promotes its aggregation and increases apoptotic cell death [118]. The detection of novel

interaction partners of alpha-synuclein could could allow the identification of proteins that directly or indirectly modulate the aggregation properties of alpha-synuclein.

1.10 Common methods to detect PPIs

1.10.1 The Y2H system

The yeast two-hybrid (Y2H) system is a powerful tool for the identification of binary PPIs. It was originally developed by Stanley Fields [119] and takes advantage of the modular architecture of transcription factors, which consist of a DNA-binding domain (BD) and a transcription activation domain (AD). In the Y2H system, the proteins of interest are expressed as BD and AD fusion proteins designated as bait and prey proteins, respectively. The interaction between a bait and a prey protein in the nucleus of yeast cells expressing both hybrid proteins brings the BD and AD into proximity, leading to reconstitution of the transcription factor. The functional transcription factor activates the expression of one or more reporter genes integrated into the yeast genome, allowing the selection of yeast cells expressing interacting protein pairs.

In the last decade, high-throughput Y2H screening assays have been applied to detect interactions across the entire proteome of several organisms. Two different Y2H methods have been used, the matrix-based and library-based approach. In the library approach, a bait protein is screened separately against a pool of preys (the prey library). This library contains random cDNA fragments or open reading frames (ORFs). Yeast clones expressing interacting proteins are selected based on reporter gene activation and the resulting ability to grow on selective media. Subsequently, the interacting prey proteins have to be determined by DNA sequencing. This laborious process is circumvented in the Y2H matrix approach where bait proteins are tested against an array of individually subcloned prey clones, each expressing a particular prey protein. The prey clones can be identified by their position in the microtiter plates containing the matrix. The yeast strains carrying the plasmids encoding the bait proteins are mated individually with this array of prey strains. Subsequently, diploid cells expressing interacting protein pairs are identified based on the activation of reporter genes and the resulting growth in a specific plate position. To further enhance the throughput of the matrix approach, a pool of bait strains can be tested against the prey matrix. However, the pooling strategy requires a subsequent deconvolution step to identify the specific bait (or baits) interacting with the prey protein [120]. Y2H studies have been used to generate interaction maps for

yeast [121], worms [122], flies [123], and humans [124-127]. The Y2H system is the most robust technology for the *in vivo* identification of protein interactions and was used in this thesis to identify proteins interacting with alpha-synuclein. However, the system is biased against certain protein classes, like membrane proteins or proteins involved in transcriptional regulation. For example, membrane proteins have been found under-represented in interaction networks generated by Y2H methods [128, 129]. These limitations arise as the Y2H system requires the translocation of both the bait and prey protein into the yeast nucleus [130].

1.10.2 The split ubiquitin system

The cytosolic yeast two-hybrid (cytoY2H) and membrane yeast two-hybrid (MYTH) system are based on the split-ubiquitin system. These methods detect PPIs in the yeast cytosol, leading to cleavage and the release of a TF, which then can translocate into the nucleus. The split-ubiquitin system takes advantage of the specific cleavage of ubiquitin by ubiquitin binding proteases (UBPs) [131]. The small 76 amino acid protein ubiquitin (ub) is highly conserved in eukaryotes [132]. Ubiquitin is conjugated to lysine residues of target proteins by the E1-E2-E3 enzyme cascade [133]. After target proteins have been covalently modified with at least four ubiquitin molecules, they are marked for proteasomal degradation by the 26S proteasome [134]. Prior to the degradation of the target protein, the ubiquitin moieties are recognized by UBPs and cleaved [135]. Ubiquitin can be expressed as an N-terminal (Nub) and a C-terminal half (Cub), which spontaneously reassociate into the so called "split-ubiquitin", which is recognized and cleaved by UBPs [136]. The introduction of the point mutation isoleucine 13 to glycine prevents the spontaneous association of the mutated N-terminal ubiquitin half (NubG) and Cub [136]. Reassociation of the ubiquitin halves only occurs if they are located in close proximity to each other, which can be facilitated by the fusion to two interacting proteins. In addition, a transcription factor consisting of the bacterial LexA DNA-binding domain (*E. coli*) and the activation domain of the viral transcriptional activator VP16 (*Herpes simplex*) is fused to Cub [136]. Cleavage by UBPs releases the transcription factor fused to split-ubiquitin and allows its translocation into the nucleus to activate one or more reporter genes. Activation of reporter genes allows the selection of yeast cells expressing interacting protein pairs.

Two variants of the split-ubiquitin system have been developed. The MYTH system is used to study interactions between full-length integral membrane proteins (fused to

Cub-TF) and their putative interaction partners (fused to NubG) [137]. It is suitable for all proteins facing at least one terminus to the cytosol in yeast. Membrane proteins are difficult to analyze in classical Y2H assays, as their hydrophobic nature prevents their translocation into the yeast nucleus [130]. The prey proteins used for interacting screening in MYTH can be membrane or soluble proteins. A number of reports have shown the capacity of the MYTH system to detect interactions of integral and membrane-associated proteins in yeast [138], plants [139] and human [140].

The cytoY2H system is used to detect protein interactions of soluble proteins. It was predominantly designed for proteins of the transcription machinery [141], a class of proteins which is difficult to analyze with classic Y2H assays. In the cytoY2H system, the bait protein is inserted between the yeast ER integral membrane protein Ost4p and the C-terminal half of ubiquitin (Cub). Anchoring of the bait to the ER membrane makes the method especially suitable for screening transcriptionally active proteins by keeping them in the cytosol and thereby preventing autoactivation [141]. The prey proteins used for interaction screening in MYTH can be membrane or soluble proteins. The cytoY2H method was successfully used to determine novel interactions for yeast proteins [141]. In this thesis, both systems were modified for high-throughput screening and utilized to identify proteins interacting with alpha-synuclein.

1.10.3 Tandem affinity purification / mass spectrometry (TAP-MS)

The two-hybrid systems described in the previous section are used to detect binary PPIs *in vivo*. In contrast, classical biochemical techniques for the detection of PPIs, immunoprecipitation and pull-down assays, identify complexes of proteins that co-immunopurify with a bait protein *in vitro*. Tandem affinity purification (TAP) [142] combined with mass spectrometry (MS) has become a powerful tool for large-scale interactome research [129]. After expression of the TAP-tagged baits in a target cell, protein complexes are purified using the TAP-tag in two consecutive steps (Figure 1-3). Subsequently, the protein complexes are separated by SDS-PAGE and proteins are identified by mass spectrometry. A major advantage of this technique is that only the bait protein has to be fused to an affinity tag, while the whole proteome is ‘fished’ for potential prey proteins. Furthermore, the combination of different datasets allows the identification of individual protein interactions within a complex. However, it is difficult to detect transient interactions and complexes using TAP-MS. In a large study, the method was applied to identify more than 200 distinct protein complexes in yeast, which were further characterized and validated by TAP [143]. TAP-MS has

been successfully applied to other organisms and derived cell lines, including human cells [144], insect cells [145], plants [146] and *E. coli* [147]. In addition, it has been demonstrated that TAP is particularly powerful when used in combination with Y2H [122].

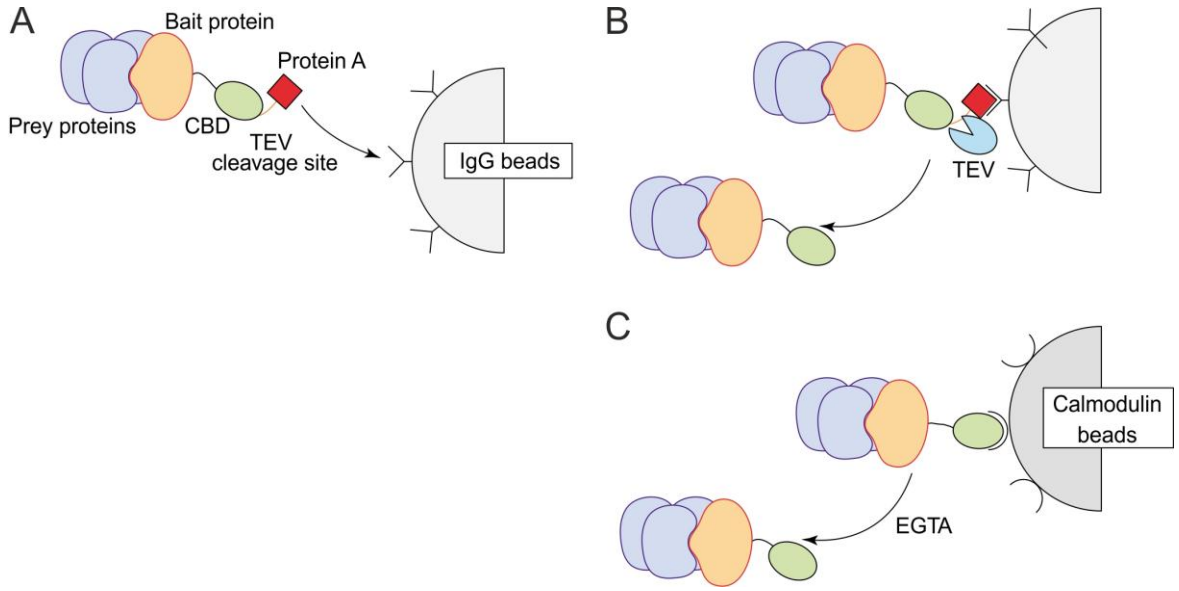

Figure 1-3: Identification of protein interactions by tandem affinity purification (TAP). A: TAP of bait/prey protein complexes via the TAP tag using two sequential steps of purification. B: First cleavage step by TEV protease. C: Elution with EGTA in the second purification step ensures high specificity and a minimum effect on the eluted protein complexes. CBD (calmodulin-binding domain). Figure modified from Piehler *et al*. [148].

1.10.4 LUMIER assay

The LUMIER-assay (luminescence-based mammalian interactome mapping) is used to identify binary PPIs in mammalian cells. It is based on the co-purification of two tagged proteins from transiently transfected HEK293 cells [149]. One protein is expressed as a fusion with the Renilla luciferase enzyme, while the other protein is expressed as fusion with a purification tag. After successful purification, binding of bait and prey proteins is monitored by measuring the bioluminescence activity of the luciferase. A high-throughput version of the LUMIER assay has been used to generate large PPI networks, which can for example be used to explore human signaling pathways [149, 150]. Furthermore, the assay is used as a common tool to validate interactions generated by other assays like Y2H [151]. Several modifications of the technique have been described [151, 152]. In the LUMIER method used for this thesis, the bait protein is expressed as a fusion to protein A (PA) and Renilla luciferase (RL), while the prey protein is tagged with Firefly luciferase (FL) [153]. This modification allows the convenient control of bait and prey fusion protein expression. In this thesis, interactions detected by two-hybrid systems were validated in mammalian cells unsing the LUMIER assay.

2 Aims of this thesis

Parkinson's disease is a progressive neurodegenerative disorder. Alpha-synuclein is a well-studied synaptic protein that plays a major role in both sporadic and familial forms or the disease. However, its precise physiological function and its role in Parkinson's disease remain to be identified.

Therefore, the main aim of this thesis project was to generate a protein-protein interaction network for alpha-synuclein, including novel interaction partners. These could potentially help to better understand the cellular mechanisms that are impaired by mutant alpha-synuclein, finally leading to familial PD. In addition, the interaction screen might identify novel potential therapeutic targets for PD.

To identify proteins interacting with alpha-synuclein, two well-established methods for PPI detection, the Y2H and the LUMIER assay, were combined with two novel methods, high-throughput cytoY2H and subSEQ. All these methods detect binary PPIs, which were integrated into a high-confidence interaction network.

Finally, the ability of interacting proteins to modulate alpha-synuclein toxicity in a yeast model of PD was to be tested.

3 Materials and Methods

3.1 Gateway™ LR cloning reaction

Gateway™ LR cloning reactions (protocol modified from Gateway™ LR Clonase II Enzyme mix protocol, Invitrogen) were performed to rapidly transfer open reading frames (ORFs) from entry clones into expression vectors. Each reaction was composed of 1 µl destination vector (75 ng/µl), 1 µl entry vector (25 ng/µl), 0.5 µl Gateway™ LR Clonase II Enzyme mix (Invitrogen) and 2.5 µl with TE buffer (pH 8.0, see section 3.20). To allow site specific recombination, the reaction was incubated at 25°C for 2 h. Reactions were directly used for chemical *E. coli* transformation or stored at -20°C.

3.2 Chemical *E. coli* transformation

This protocol (modified from manual: MultiShot^{TM} StripWell Mach1^{TM}-T1^{R} Chemically Competent *E. coli,* Invitrogen) was used for 96-well format chemical transformation of *E. coli* cells with LR-reaction products or other plasmid DNA. Competent bacterial cells were thawed on ice for 15 min. 8 µl cells were distributed into each well of 96-well PCR plates (Thermo Scientific), each well containing 5 µl LR reaction solution or 1 µl (~100 ng) plasmid DNA. PCR plates were sealed, vortexed at low speed and incubated on ice for 15 min. The plates were incubated at 42°C for 45 sec and kept on ice for additional 5 min. 100 µl SOC-medium (see section 3.20, prewarmed to 37°C) was added to each well and the plate was incubated at 37°C for 1 h. 25 µl from each well were streaked out as a line on selective LB-plates (see section 3.14). Plates were incubated for 16 h at 37°C. Subsequently, single colonies were transferred into 96-well deep well plates, each well containing 1.2 ml liquid LB-medium (see section 3.14) including the appropriate antibiotic. The deep well plates were incubated with shaking (250 rpm) for 16 h at 37°C.

3.3 *E. coli* plasmid DNA isolation

Transformed *E. coli* cells were grown in selective LB-medium (see section 3.14) with shaking (250 rpm) for 16 h at 37°C. Subsequently, plasmid DNA was isolated using the QIAprep 96 Turbo Miniprep Kit (Qiagen) and eluted with 100 µl EB buffer (Qiagen) into 96-well microtiter plates (MTPs, Nunc). To obtain larger quantities of plasmid DNA, for example for the cytoY2H and MYTH destination vectors, the Plasmid Midi Kit (Qiagen) was used according to the manufacturer's instructions.

3.4 Chemical *S.cerevisiae* transformation

This protocol (modified from Gietz *et al.* [154]) was used for 96-well format chemical transformation of *S. cerevisiae* cells with expression plasmids generated by Gateway™ LR cloning (see section 3.1) or other plasmid DNA. 3 ml liquid YPD medium (see section 3.16) were inoculated as overnight culture of the yeast strains L40ccua, L40ccα, W303-1A (CRY1) or DSY-6 (see section 3.15) and incubated with shaking (250 rpm) at 30°C for 16 h. From this culture, 30 ml liquid YPD medium were inoculated at 0.1 OD600 and grown with shaking (250 rpm) to an OD600 of 0.5 at 30°C (~4 h). Cells were centrifuged for 5 min at 1.300 g, washed with 10 ml TE buffer (see section 3.20) and incubated with 1.100 µl Transformation Mix 1 (see section 3.20). Herring Sperm Carrier DNA (Clontech) was boiled for 10 min, cooled on ice for 2 min and 1.5 µl were distributed to each well of a 96-well PCR plate (Thermo Scientific). 5 µl mini-prep plasmid DNA, 12 µl yeast in Transformation Mix 1 and 60 µl Transformation Mix 2 (see section 3.20) were distributed to each well. The PCR plates were sealed and incubated at 30°C for 30 min. 8 µl DMSO were added to each well and the yeast cells were heat shocked at 42°C for 7 min. Subsequently, yeast cells were stamped onto SD media (see section 3.16). After incubation at 30°C for 72 h several clones were transferred into liquid SD media (see section 3.16).

3.5 Y2H screen procedure

3.5.1 Y2H bait auto-activation test

Generated Y2H bait plasmids (pBTM116-D9) [124] encoding wild-type or mutant alpha-synuclein fused to the LexA DNA binding domain were transformed into the yeast strain L40ccua (MATa) and tested for auto-activation. Therefore, yeast clones carrying bait plasmids were grown in liquid SD-t/hul (-Trp, see section 3.16) medium and each mixed in 384-well MTPs (Greiner Bio-One) with yeast (L40ccα, MATα) carrying one of 32 random Y2H prey plasmids (pACT4-DM) [124] or the empty prey plasmid. Mixing steps were performed using a pipetting robot (Freedom EVO, Tecan). The yeast mixtures were stamped onto YPD agar plates (see section 3.14) using a spotting robot (K4, KBiosystems) and incubated at 30°C for 36 h. After mating, yeast colonies were transferred into 384-well MTPs containing liquid SD2 (-Leu-Trp, see section 3.14) medium. Diploid yeasts were spotted onto SD4 (-Leu-Trp-Ura-His, see section 3.14) agar plates. After 5 days of incubation at 30°C, digital images of the agar plates were assessed for growth. Yeast clones carrying a

bait plasmid that grow in combination with more than 50% of the preys were considered as auto-activating and were not used for interaction screening.

3.5.2 Y2H pool screen and backmating

Single yeast clones (L40ccua, MATa) transformed with Y2H bait plasmids that passed the auto-activation test were grown to saturation in liquid SD-t/hul (-Trp) medium at 30°C. Afterwards, grown yeast clones were combined into pools of 16 baits with yeast clones carrying unrelated bait plasmids. 16098 clones of the yeast strain L40ccα (MATα), each previously transformed with a unique Y2H prey plasmid (Y2H prey matrix), were replicated in 384-well MTPs (Greiner Bio-One) containing liquid SD–l/haut (-Leu, see section 3.14) medium using a pipetting robot (Biomek® FXP, Beckman Coulter). Pooled MATa strains (16 baits) were added to each well and mixed using the pipetting robot. The yeast mixtures were spotted onto YPD agar plates using a spotting robot (K4, KBiosystems) and incubated for 36 h at 30°C. After mating, yeast colonies were transferred into 384-well MTPs containing liquid SD2 (-Leu-Trp) medium. Diploid yeasts were spotted onto SD4 agar plates and SD4 plates covered with sterile nylon membranes (Hybond™-N, GE Healthcare). After 5 days of incubation at 30°C, digital images of the agar plates and membranes were assessed for growth and β-galactosidase activity (see section 3.5.3) using the software Visual Grid (GPC Biotech). Growing colonies of single preys interacting with a pool of baits were identified by their position in the matrix.

To determine which specific bait protein from a pool interacted with a given prey protein, 16 baits from each pool were arrayed in 384-well MTPs using a pipetting robot (Freedom EVO, Tecan) and mated on YPD agar plates with the positive preys identified in the pool screen. After incubation for 36 h at 30°C, yeast cultures were spotted onto SD4 agar plates and SD4 plates covered with nylon membranes using the spotting robot. After 5 days of incubation at 30°C, digital images of the agar plates and membranes were assessed for growth and β-galactosidase activity (see section 3.5.3) using the software Visual Grid (GPC Biotech). Y2H protocols modified from Goehler *et al.* [124].

3.5.3 β-galactosidase assay

This protocol was used to detect transcription of the lacZ gene and subsequent β-galactosidase activity [155]. For each nylon membrane with growing yeast spots to be assayed, 20 ml Z-Puffer, 312 µl X-Gal solution (see section 3.20) and 200 µl DTT (1M) were mixed (X-gal-mix). 2 Whatman filter papers (Whatman) were soaked with

X-gal-mix and placed in an empty Q-tray petri dish (22 x 22 cm). Excessive liquid was removed from the filter papers. The nylon membranes spotted with yeast were removed from the SD4 agar plates and incubated in liquid nitrogen for 1 min. Membranes were thawed for 1 min at room temperature and frozen again in liquid nitrogen for 1 min. After thawing, the membranes were placed (without bubbles) onto the Whatman filter papers. The Q-tray petri dishes were closed with a lid and incubated for 4 h at 37°C. Afterwards, the membranes were removed from the Whatman filter papers and placed in a new Q-tray petri dish for drying under a fume hood overnight.

3.6 Modification of cytoY2H and MYTH vectors

The MYTH bait vectors pGBT3-N, pGBT3-Ste, pGBT3-Suc and cytoY2H/MYTH prey-vectors pGPR3-N, pGPR3-Ste and pGPR3-Suc were kind gifts from Prof. I. Stagljar [137]. The cytoY2H bait vector pDHB1 [141] was purchased from Dualsystems Biotech. The Y2H bait vector pBTM116-D9 [124] served as template for the Gateway™ cloning cassette to be inserted into the multiple cloning sites (MCS) of all bait and prey vectors. The Gateway™ cassette for modification of pGBT3-N and pGPR3-N was amplified with the primers MK14 and MK34. The cassette for all other vectors was amplified using the primers MK14 and MK15. The PCR reactions were performed using Pwo DNA polymerase (Roche) were performed as following:

component	amount [µl]
dNTP mix (10 mM)	1
MK14	1
MK15 / MK34	1
pBTM116-D9 (50 ng/µl)	1
Pwo DNA polymerase	0.5
10x PCR buffer with 20 mM $MgSO_4$	5
ddH_2O	40.5

cycle step	temperature [°C]	time [s]	cycles
Initial denaturation	94	120	1
Denaturation	94	15	25
Annealing	55	30	
Extension	72	60	
Final extension	72	240	1
	4	∞	

The resulting PCR products were gel purified using the Qiaex2 kit (Qiagen). PCR products were subcloned into the vector pCR2.1-TOPO using the TOPO TA cloning kit (Invitrogen). After chemical transformation into *E. coli* (strain DB3.1, Invitrogen), several clones growing were analyzed by restriction digestion and sequencing. 5 µg of the bait- and prey vectors as well as the corresponding sub-cloning vectors containing the Gateway™ cassettes were digested with the restriction enzyme SfiI (NEB) and gel purified (Qiaex2 kit, Qiagen). 1 µg vector and 1 µg insert were ligated

with T4 ligase (NEB). Ligation reactions were transformed into chemically competent *E. coli* (strain DB3.1, Invitrogen) and plated on LB-Kan (baits) or LB-Amp (preys) agar plates. Several clones of each construct were analyzed by restriction digestion and sequencing. LR cloning of random ORFs was used to generate expression plasmids from all modified vectors, and correct recombination was confirmed by restriction digestion. Figure 3-1 A depicts the insertion of the Gateway™ cloning cassette into the cytoY2H bait vector pDHB1.

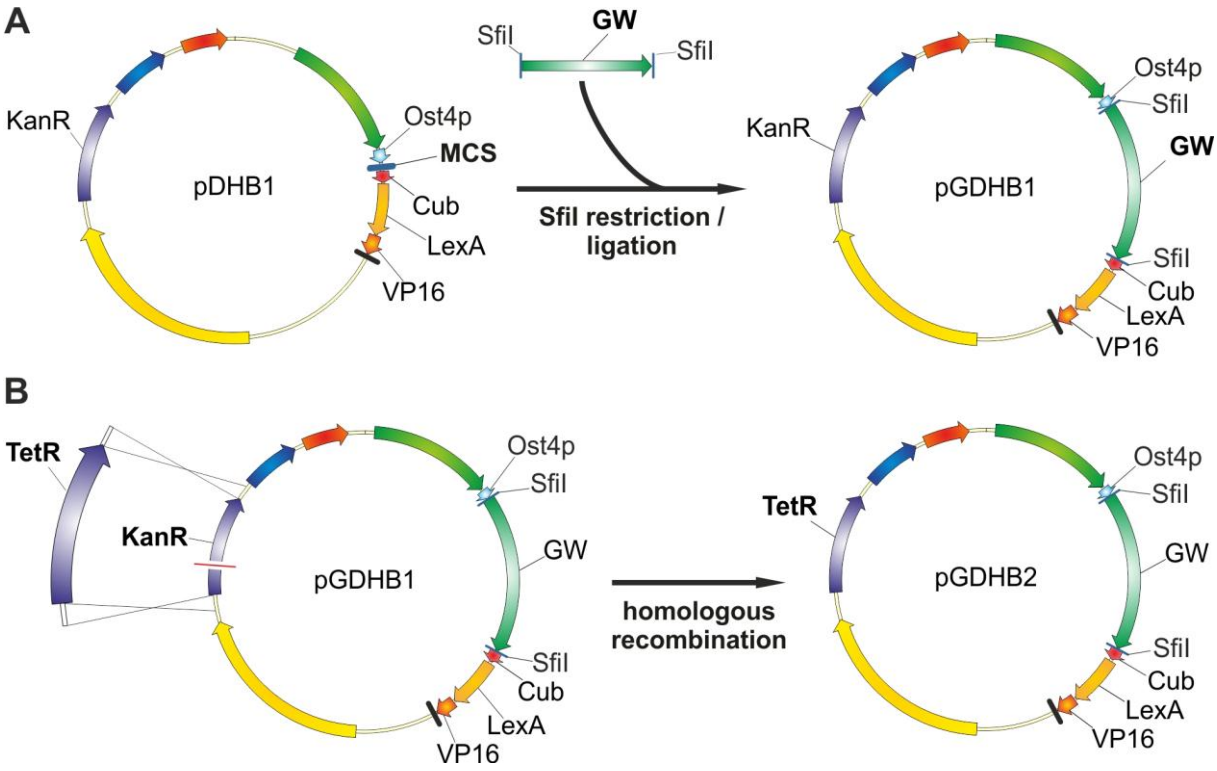

Figure 3-1: Adaptation of the cytoY2H bait vector to the Gateway™ system. A: Insertion of the Gateway™ Cassette (GW). The recombination-cassette was PCR amplified and ligated with the SfiI restriction sites of the multiple cloning site (MCS) of the cytoY2H bait vector (pDHB1). ORFs cloned into the vector are fused in frame with the membrane anchor protein Ost4p and the C-terminal half of ubiquitin (Cub) fused to the transcription factor (LexA+VP16). B: Replacement of the Kanamycin-resistance marker. The tetracycline resistance marker (TetR) was PCR amplified with primers containing homology to the sequence up- and downstream of the Kanamycin marker (KanR). Purified PCR products and linearized bait vectors (indicated by red line in KanR) were co-transformed into yeast to allow homologous recombination by gap repair.

To replace the *E. coli* selection marker, the Tetracycline-marker was PCR amplified from the vector pBTM116-D9 with primers containing homology to the sequence up- or downstream the Kanamycin-marker (MK43 and MK44). The PCR reaction was performed using Pwo DNA polymerase (Roche) was performed as following:

component	amount [µl]
dNTP mix (10 mM)	1
MK43	1
MK44	1
pBTM116-D9 (50 ng/µl)	1
Pwo DNA polymerase	0.5
10x PCR buffer with 20 mM $MgSO_4$	5
ddH_2O	40.5

cycle step	temperature [°C]	time [s]	cycles
Initial denaturation	94	120	1
Denaturation	94	15	25
Annealing	58	30	
Extension	72	60	
Final extension	72	240	1
	4	∞	

The resulting PCR products were gel purified using the Qiaex2 kit (Qiagen). 5 µl of each bait plasmid were digested with the restriction enzyme NruI (NEB) and linearization was confirmed on a 0.8% agarose gel. The vectors were dephosphorylated with shrimp alkaline phosphatase (Roche). 1 µg vector and 1 µg PCR product were co-transformed into 30 µl yeast (W303-1A, see section 3.4) to allow recombinational repair [156]. Yeast was plated on SD-l/haut (-Leu) medium and grown at 30°C for 72 h. Single colonies were each transferred into 1 ml liquid SD-l/haut medium and grown at 30°C for 36 h. Subsequently, DNA plasmids were isolated using the Zymoprep II Yeast Plasmid Miniprep Kit (Zymo Research) and eluted with 10 µl EB. 5 µl of each plasmid were transformed into 12 µl chemically competent *E. coli* (strain DB3.1, Invitrogen). Bacteria were plated on LB-Tet agar and incubated at 37°C for 16 h. Several single clones were each transferred into 5 ml liquid LB-Tet medium and incubated with shaking (250 rpm) at 37°C for 24 h. After plasmid isolation, final plasmids were confirmed by restriction digestion and sequencing. Figure 3-1 B depicts the exchange of the *E. coli* selection marker cassette in the cytoY2H bait plasmid.

3.7 cytoY2H screen procedure

3.7.1 High throughput NubG/NubI genetic test

The positive (pOst1-NubI, pAlg5-NubI, pFur4-NubI) and negative control plasmids (pOst1-NubG, pAlg5-NubG, pFur4-NubG, p414-NubG) [137] were individually transformed into the yeast strain L40ccua (MATa). Single clones were transferred into liquid SD-t/hul (-Trp) medium and grown to saturation at 30°C. Clones carrying control plasmids were mixed with up to 72 yeast clones (strain L40ccα, MATα) carrying cytoY2H or MYTH bait plasmids in 384-well MTPs using a pipetting robot (Freedom EVO, Tecan). Each bait protein was tested against each a control prey protein in four repetitions and in eight repetitions against NubG alone (expressed

from p414-NubG). For details, see section 4.4.3. The yeast mixtures were stamped onto YPD agar plates with a spotting robot (K4, KBiosystems) and incubated for 36 h at 30°C. After mating, yeast colonies were transferred into 384-well MTPs containing liquid SD2 (-Leu-Trp) medium. Subsequently, diploid yeasts were spotted onto SD4 (-Leu-Trp-Ura-His) agar plates. After 5 days of incubation at 30°C, digital images of the agar plates were assessed for growth. Bait proteins growing only in the presence of positive controls were used for screening. Bait proteins growing when tested with positive control preys along with smaller colonies when tested with negative controls were screened on selective SD4 medium containing 1 mM 3-amino-1,2,4-triazole (3-AT). Bait proteins that showed robust growth with all control prey proteins or did not grow at all were not used for screening. Protocols modified from Iyer *et al.* [137].

3.7.2 cytoY2H screen

Single yeast clones (L40ccα, MATα) transformed with cytoY2H or MYTH bait plasmids that passed the NubG/NubI genetic test were grown to saturation in liquid SD-l/haut (-Leu) medium at 30°C. Afterwards, grown yeast clones were combined into pools of 16 baits with yeast clones carrying unrelated bait plasmids. 490 ORFs encoding synaptic proteins were Gateway™ cloned (see section 3.1) into the vector pGPR4-Ns. Subsequently, plasmids were individually transformed (see section 3.4) into the yeast strain L40ccua (MATa) and arrayed in 384-well MTPs containing liquid SD–t/hul (-Trp) medium (cytoY2H/MYTH prey matrix). This matrix of clones was replicated using a pipetting robot (Biomek® FXP, Beckman Coulter). Pooled MATα strains (16 baits) were added to each well and mixed. The yeast mixtures were spotted onto YPD agar plates using a spotting robot (K4, KBiosystems) and incubated for 36 h at 30°C. After mating, yeast colonies were transferred into 384-well MTPs containing liquid SD2 (-Leu-Trp) medium. Diploid yeasts were spotted onto SD4 agar plates and SD4 plates covered with sterile nylon membranes. After 5 days of incubation at 30°C, digital images of the agar plates and membranes were assessed for growth and β-galactosidase activity (as described in section 3.5.3) using the software Visual Grid (GPC Biotech). Growing colonies of single preys interacting with a pool of baits were identified by their position in the matrix.

To determine which specific bait protein from a pool interacted with a given prey protein, 16 baits from each pool were arrayed in 384-well MTPs using the pipetting robot and mated on YPD agar plates with the positive preys identified in the pool screen. After incubation for 36 h at 30°C, yeast cultures were spotted onto SD4 agar

plates and SD4 plates covered with nylon membranes. After 5 days of incubation at 30°C, digital images of the agar plates and membranes were assessed for growth and β-galactosidase activity (as described in section 3.5.3) using the software Visual Grid (GPC Biotech). Protocols modified from Iyer *et al.* [137].

3.8 Fractionation of yeast cell extracts

3.8.1 Total yeast cell extracts

Yeast clones (strain DSY-6, see section 3.15) carrying cytoY2H or MYTH bait plasmids (see section 3.4) were used to inoculate 2 ml SD-l/haut (-Leu) precultures that were grown with shaking (250 rpm) at 30°C for 72 h. Subsequently, 10 ml cultures were inoculated at 0.05 OD600 and grown with shaking (250 rpm) at 30°C to an OD600 of 1. The cells were centrifuged at 700 *g* for 5 min at room temperature. After discarding the supernatant, cells were resuspended in 200 µl Protein Lysis Buffer (see section 3.20) and transferred to 1.5 ml reaction tubes. 200 µl glass beads (400-600 µm, unwashed) were added. The samples were vortexed for 30 s and cooled on ice for 60 s; steps were repeated seven times. After centrifugation at 700 *g* for 20 min at 4°C, the supernatant was transferred to a new 1.5 ml reaction tube. The protein concentration was determined (660 nm Protein Assay, Pierce) and samples were processed as described in section 3.8.2. Protocol modified from Iyer *et al*. [137].

3.8.2 Cytosolic and membrane fractionation

Yeast clones (strain DSY-6, see section 3.15) transformed with cytoY2H or MYTH bait plasmids (see section 3.4) were used to inoculate 2 ml SD-l/haut (-Leu) precultures that were grown with shaking (250 rpm) at 30°C for 72 h. Subsequently, 50 ml cultures were inoculated at 0.05 OD600 and grown with shaking (250 rpm) at 30°C to an OD600 of 1. The cells were centrifuged at 700 *g* for 5 min at room temperature and the supernatant was discarded. Subsequently, cells were resuspended in 1 ml Protein Lysis Buffer (see section 3.20) and transferred to 2 ml reaction tubes. 300 µl glass beads (400-600 µm, unwashed) were added and samples were vortexed for 30 s and cooled on ice for 60 s; steps were repeated seven times. The extracts were centrifuged at 700 *g* for 20 min at 4°C and the supernatant was transferred to a 1.5 ml reaction tube suitable for ultracentrifugation. Subsequently, the samples were centrifuged at 150.000 *g* at 4°C for 2 h. The supernatant (representing the cytosolic fraction) was transferred to a new 1.5 ml reaction tube suitable for ultracentrifugation. After resuspending the pellet in 200 µl Protein Lysis Buffer supplied with 1% Triton X-100, the samples were centrifuged at

150.000 *g* at 4°C for 2 h. The supernatant (representing the membrane fraction) was transferred to a new 1.5 ml reaction tube. Protein concentrations of the cytosolic and membrane fractions were determined (660 nm Protein Assay, Pierce) and 30 µg of each fraction including the total extracts (section 3.8.1) were boiled in 4x SDS sample buffer (see section 3.20). Proteins were separated on SDS-PAGE gradient gels (Invitrogen) and subjected to immunoblotting (see section 3.9). Bait fusion proteins were probed using a LexA antibody (Millipore, 1:1000). Separation of the fractions was confirmed using yeast-specific antibodies against the cytosolic protein Pgk1p (Invitrogen, 1:10.000) and the ER protein Dpm1p (Invitrogen, 1:250). For details on the antibodies see section 3.19. Protocol modified from Iyer *et al*. [137].

3.9 SDS-PAGE and immunoblotting

Protein samples were supplied with 4x SDS sample buffer (see section 3.20) and boiled for 5 min at 99°C. The proteins were separated on SDS-PAGE gradient gels (NuPAGE Novex 4-12% Bis-Tris Gels, 1.0-mm thick, 12-well, Invitrogen) using the supplied buffer. For immunoblotting, proteins were transferred to nylon membranes (Hybond™-N, GE Healthcare) using semi-dry blotting (Trans-Blot SD Semi-Dry Electrophoretic Transfer Cell, BioRad) according to the manufacturer's instructions. The membranes were blocked in 5% milk in PBS-T (see section 3.20) at room temperature for 1 h, washed 3x with PBS-T and incubated with primary antibodies (diluted in 5% milk in PBS-T) at 4°C for 16 h. After washing 3x with PBS-T, the membranes were incubated with a secondary antibody conjugated to alkaline phosphatase (diluted in 5% milk in PBS-T) for 1 h. Membranes were washed 3x with PBS-T, 3x with PBS (see section 3.20) and 3x with AttoPhos buffer (Promega). After incubation of the membranes with AttoPhos reagent (Promega) for 1 min, the fluorescence signal was visualized using an image reader (LAS 3000, Fujifilm).

3.10 SubSEQ sample preparation

3.10.1 Selective plasmid enrichment

100 µl (28 µg) cDNA library (P12221 Human adult brain cDNA library, NubG-x, Dualsystems Biotech) were transformed (see section 3.4) into 200 µl yeast cells (strain: L40ccua). Yeast transformants were spread on 5 Q-tray petri dishes (22 x 22 cm) containing SD-t/hul (-Trp) medium. After 48 h incubation at 30°C, yeast colonies were washed off the plate with sterile NBG medium (see section 3.16), mixed well and frozen as aliquots of 1 ml each. For mating, 50 µl yeast cells (strain L40ccα, grown to saturation) carrying a single bait and 50 µl yeast transformed with

the cDNA library (thawed aliquots) were mixed and spread on YPD agar plates. Separate petri dishes (10 cm diameter) were used for each mating. After 48 h incubation at 30°C, yeast colonies were washed off the plate with sterile NBG medium and 40 OD600 yeast cells were transferred to a Q-tray petri dish containing SD4 (-Leu-Trp-Ura-His) agar. After 72 h incubation at 30°C, yeast cells were washed off the plate with sterile ddH_2O. Plasmid DNA was isolated from 20 OD600 cells with a yeast DNA plasmid preparation kit (Zymoprep™ Yeast Plasmid Miniprep II, Zymo Research) and eluted with 20 µl EB (Zymo Research). Subsequently, the DNA concentration was determined using a NanoDrop spectrophotometer (ND-8000, Thermo Scientific).

3.10.2 PCR-enrichment of cDNA inserts

100 ng of each plasmid DNA preparation served as template for the PCR reaction using Phusion® High-Fidelity PCR Master Mix (NEB) with GC Buffer. The PCR reactions were performed as following:

component	amount [µl]
MK62	1
MK63	1
2x Phusion master mix (GC)	25
ddH_2O	21
Template DNA (50 ng/µl)	2

cycle step	temperature [°C]	time [s]	cycles
Initial denaturation	98	60	1
Denaturation	98	10	35
Annealing	58	30	
Extension	72	300	
Final extension	72	600	1
	4	∞	

After PCR amplification, 5 µl of PCR products were visualized on a 1% agarose gel.

3.10.3 Acoustic DNA shearing

After addition of 55 µl TE buffer (pH 8.0, see section 3.20), the PCR mixtures were transferred to Snap-Cap microTUBEs with AFA fiber and pre-split Teflon/silicone/Teflon septa (100µl, Covaris). DNA was fragmented using an S2 DNA Shearing Instrument (AFA technology, Covaris). Fragmentation was performed using the following parameters: Duty cycle: 10%, Intensity: 5, 200 bursts / cycle, Temperature: 4°C, Time: 180 s, Power mode: Frequency sweeping. Subsequently, 10 µl of the fragments were visualized on a 2% agarose gel. The remaining DNA fragments were purified using the QIAEX II Gel Extraction Kit (Qiagen) and eluted with 30 µl EB (Qiagen).

3.10.4 End repair / adenine addition / adapter ligation

Using the Quick Blunting Kit (NEB, 4 µl enzyme mix), single strand overhanging DNA ends were removed from the fragments. DNA was purified using the QIAEX II Gel Extraction Kit (Qiagen) and eluted with 32 µl EB (Qiagen). A single overhanging adenine (A) nucleotide was added to the 3' end of the DNA fragments using Klenow fragment (NEB, 5 U). Subsequently, DNA was purified using the QIAEX II Gel Extraction Kit and eluted with 32 µl EB. One of eight multiplexing adapters (SeqAdapter_1 - SeqAdapter_8, 50 µM, 1 µl each, see section 3.17) was ligated to the fragments using ultrapure T4 DNA Ligase (Enzymatics, 3000 U). Samples were purified using AMPure XP beads (Beckmann Coulter) and eluted with 30 µl EB. Subsequently, DNA-concentration was determined with a NanoDrop spectrophotometer (ND-8000, Thermo Scientific).

3.10.5 PCR enrichment of cDNA inserts

The multiplexing adapters were extended by PCR using Platinum *Pfx* DNA Polymerase (Invitrogen) according to the following setup:

component	amount [µl]
10x PCR buffer	5
dNTPs (10 mM)	2
$MgSO_4$ (50 mM)	2
SeqP1	1
SeqP2	1
Platinum *Pfx* Polymerase	0.8
ddH_2O	37.2
Template DNA (4 ng/µl)	1

cycle step	temperature [°C]	time [s]	cycles
Initial denaturation	94	300	1
Denaturation	94	15	15
Annealing	65	30	
Extension	68	60	
Final extension	68	300	1
	4	∞	

For comparison, PCR was also performed with Phusion High-Fidelity DNA Polymerase (NEB) with the following parameters:

component	amount [µl]
SeqP1	1
SeqP2	1
2x Phusion master mix (GC)	25
ddH_2O	22
Template DNA (4 ng/µl)	1

cycle step	temperature [°C]	time [s]	cycles
Initial denaturation	98	30	1
Denaturation	98	10	15
Annealing	65	30	
Extension	72	30	
Final extension	72	300	1
	4	∞	

The samples were purified with AMPure XP beads and eluted with 25 µl EB (Qiagen). 5µl of all generated libraries were visualized on a 1% agarose gel. Subsequently, sample quality was controlled by chip-based capillary electrophoresis on a BioAnalzyer (Agilent). Cluster generation and the final sequencing run were performed on a Genome Analyzer II (Illumina) according to manufacturer's protocols.

3.11 LUMIER screen procedure

Protein A (PA)-Renilla luciferase (RL)-tagged bait proteins were co-produced with Firefly luciferase (FL)-tagged prey proteins in transiently transfected HEK293 cells. The assay was performed in two parallel steps: First, alpha-synuclein was expressed from the bait vector (pcDNA3.1-PA-Renilla-DM) [153] while a putative interaction partner was expressed from the prey vector (pcDNA3.1-Firefly-V5-DM) [153]. In the second step, the putative interaction partner was expressed from the bait vector and alpha-synuclein was expressed from the prey vector. All vectors were generated by Gateway™ LR cloning (see section 3.1) and transfected into HEK293 cells in 96-well MTPs using Polyethylenimine (PEI) as transfection reagent [157]. 48 h after transfection, cells were lysed with HEPES buffer and the lysates were transferred into IgG coated 384-well MTPs. Subsequently, protein complexes were co-immunoprecipitated from cell extracts. Luciferase activity (bioluminescence) was quantified using the Dual-Glo Luciferase Assay System (Promega) in a luminescence plate reader (TECAN Infinite M1000). Interactions between bait (PA-RL fusions) and prey proteins (FL fusions) were monitored by quantification of FL activity. Successful immunoprecipitation of PA-RL-tagged bait proteins from cell extracts was confirmed by quantification of RL activity. All co-immunoprecipitation experiments were performed in triplicate. A scoring system based on two calculated ratios (R_{op} and R_{ob}, see formula below) was used to evaluate the binding specificity. R_{op} is the ratio of the FL luminescence detected after immunoprecipitation of a bait protein (PA-RL-bait) with a potentially-interacting prey protein (FL-prey) and the FL luminescence detected after immunoprecipitation of PA-RL alone (empty PA-RL) with a prey protein (FL-prey). R_{ob} is the ratio of the FL luminescence detected after immunoprecipitation of a bait protein (PA-RL-bait) with a potentially-interacting prey protein (FL-prey) and the FL luminescence detected after immunoprecipitation of a bait protein (PA-RL-bait) with FL alone (empty FL).

$$R_{op} = \frac{\text{FL luminescence (IP PA-RL-bait and FL-prey)}}{\text{FL luminescence (IP empty PA-RL and FL-prey)}}$$

$$R_{ob} = \frac{\text{FL luminescence (IP PA-RL-bait and FL-prey)}}{\text{FL luminescence (IP PA-RL-bait and empty FL)}}$$

Low R_{op} values indicate unspecific prey protein interactions, while low R_{ob} values indicate unspecific bait protein interactions. Based on empirical studies with a set of well-characterized positive and negative interaction pairs, it was defined that R_{op} and R_{ob} binding ratios of >1.5 are indicative of reliable protein-protein interactions. An interaction of alpha-synuclein with a putative interaction partner was considered validated if the interaction was detected using alpha-synuclein as bait, prey or both as bait and prey. Protocol modified from Barrios-Rodiles *et al*. [149].

3.12 Modifiers of alpha-synuclein induced toxicity

ORFs encoding human toxicity modifier orthologs were Gateway™ cloned (see section 3.1) into the yeast expression vector pAG425-FLAG (modified from pAG425GAL-ccdB-HA (Addgene) by T. Rasko, unpublished). After confirmation by restriction digest, the generated plasmids and the empty pAG425-FLAG vector were rearrayed into 96-well plates (Nunc) in 3 replicates (one for each yeast strain, see below). In these 96-well plaes, plasmid DNA was transformed (see section 3.4) into yeast strains (W303-1A) expressing two copies of either GFP, GFP-tagged wild-type or GFP-tagged A53T alpha-synuclein [108]. Yeast colonies were stamped onto SD-ltu/ha (-Leu-Trp-His, see section 3.16) plates and incubated for 48 h at 30°C. Afterwards, several yeast clones per construct were used to inoculate 5 ml liquid SD-ltu/ha (-Leu-Trp-His, see section 3.16, each construct in a single tube) cultures (carbon source: glucose) that were grown with shaking (250 rpm) for 48 h at 30°C. From these cultures, 2 ml liquid SD–ltu/ha cultures (carbon source: raffinose, each construct in a single tube) were inoculated at an OD600 of 0.1 and grown with shaking (250 rpm) at 30°C to an OD600 of 1. 1:5 serial dilutions of the different yeast strains (carrying different pAG425-FLAG plasmids) were prepared in 96-well MTPs (Nunc) and stamped onto SD-ltu/ha agar plates containing glucose or galactose as carbon source. The plates were incubated at 30°C for 120 h and digital images of yeast colonies were taken. The experiment was performed in triplicates.

3.13 *E. coli* strains

Mach1™ T1® (Invitrogen): ΔrecA1398 endA1 tonA Φ80ΔlacM15 ΔlacX74 hsdR(r_K^- m_K^+), recommended strain for use with the Gateway™ Cloning System.

DB3.1: F- gyrA462 endA1 glnV44 Δ(sr1-recA) mcrB mrr hsdS20(r_B^-, m_B^-) ara14 galK2 lacY1 proA2 rpsL20(Sm^r) xyl5 Δleu mtl1, gyrA462 enables propagation of Gateway-compatible plasmids containing the ccdB gene.

3.14 Media *E. coli*

LB-medium: 10 g/l Bacto peptone, 5 g/l yeast-extract, 10 g/l NaCl, set pH to 7.2

Antibiotics: Ampicillin: 100 mg/ml in ddH_2O (stock), final concentration: 100 µg/ml
Tetracycline: 12.5 mg/ml in 50% EtOH (stock), final concentration: 20 µg/ml
Kanamycin: 30 mg/ml in ddH_2O (stock), final concentration: 15 µg/ml
Spectinomycin: 25 mg/ml in ddH_2O (stock), final concentration: 50 µg/ml

SOB-medium: 20 g Bacto tryptone, 5 g Bacto yeast extract, 0.5 g NaCl, ad 1000 ml ddH_2O, after autoclaving add: 10 ml 1 M $MgCl_2$,10 ml 1 M $MgSO_4$

SOC-medium: 99 ml SOB-medium, 1 ml 20% glucose

3.15 *S. cerevisiae* strains used

L40ccua [124]: *MATa his3Δ200 trp1-901 leu2-3,11 gal8 can cyh2 LYS2::(lexAop)4-HIS3TATA-HIS3 ura3::(lexAop)8-GAL1TATA-LacZ ADE2::(lexAop)8-GAL1TATA-URA3*

L40ccα [124]: *MATα his3Δ200 trp1-901 leu2-3,112 ade2 can1 cyh2 LYS2::(lexAop)4-HIS3TATA-HIS3 URA3::(lexAop)8-GAL1TATA-LacZ*

DSY-6 (Dualsystems biotech): *MATa leu2 trp1Δ63 ura3-52 prb1-22 pep4-3 prc1-407*

W303-1A (CRY1): *MATa ura3-1 trp1-1 his3-11, 15 leu2-3,112 ade2-1 can1-100* GAL+

3.16 Media *S. cerevisiae*

YPD (liquid): 10 g/l Bacto yeast extract, 20 g/l Bacto peptone, 20 g/l glucose

SD (liquid): 6.7 g/l Yeast Nitrogen Base, 20 g/l glucose, add 10 ml supplemental amino acids / nucleosides (100x stock solutions) to 1 l SD medium:

Adenine (Ade):	2 g/l (stock), final concentration: 20 mg/l
Histidine (His):	2 g/l (stock), final concentration: 20 mg/l
Leucine (Leu):	10 g/l (stock), final concentration: 100 mg/l
Tryptophan (Trp):	2 g/l (stock), final concentration: 20 mg/l
Uracil (Ura):	2 g/l (stock), final concentration: 20 mg/l

SD media are named after the missing and required amino acids / nucleosides: Anabolytes omitted are marked by a minus sign, while those that are added to the medium are separated by a slash. For example, SD-l/haut lacks Leucine, but contains Histidine, Adenine, Uracil and Tryptophan.

To prepare solid SD or YPD media, add 17 g/l agar.

NBG (yeast storage medium): 6.7 g/l Yeast Nitrogen Base, 20 g/l glucose, 5% glycerol, 0.5 M Betaine, add 10 ml supplemental amino acids / nucleosides (100x stock solutions) to 1 l NBG medium.

3.17 Oligonucleotides

MK14: GGCCATTACGGCCACAAGTTTGTACAAAAAAGCTGAAC

MK15: GGCCGAGGCGGCCACCACTTTGTACAAGAAAGCTGAACGAGA

MK34: GGCCGAGGCGGCCTCAACCACTTTGTACAAGAAAGCTGAACG

MK43: GTTCCCTCAAGAATTTTACTCTGTCAGAAACGGCCTTACAATAAGGGCGACACGGAAATG

MK44: ATCTCAGCGATCTGTCTATTTCGTTCATCCATAGTTGCCTTCAGGTCGAGGTGGCCCGGC

MK62: GGATCCAAGCAGTGGTATCAACGCAGAGTGGCCATTACGGCCACAAGTTT

MK63: AGCTTGATATCGAATTCTCGAGAGGCCGAGGCGGCCACCACTTTGTACAA

SeqP1: CAAGCAGAAGACGGCATACGAGCTCTTCCGATC*T

SeqP2: AATGATACGGCGACCGAGATCTACACTCTTTCCCTACACGACGCTCTTCCGATC*T

These oligonucleotides were synthesized (MK oligonucleotides by metabion GmbH, Seq oligonucleotides by STRATEC Molecular GmbH) in a quantity of 10 nmol and diluted with nuclease-free H_2O to a concentration of 10 pmol/µl.

SeqAdapter_1a: ACACTCTTTCCCTACACGACGCTCTTCCGATCTACTGA*T

SeqAdapter_1b: p-TCAGTAGATCGGAAGAGCTCGTATGCCGTCTTCTGCTTG

SeqAdapter_2a: ACACTCTTTCCCTACACGACGCTCTTCCGATCTAGCTA*T

SeqAdapter_2b: p-TAGCTAGATCGGAAGAGCTCGTATGCCGTCTTCTGCTTG

SeqAdapter_3a: ACACTCTTTCCCTACACGACGCTCTTCCGATCTCAGTC*T

SeqAdapter_3b: p-GACTGAGATCGGAAGAGCTCGTATGCCGTCTTCTGCTTG

SeqAdapter_4a: ACACTCTTTCCCTACACGACGCTCTTCCGATCTCGTAC*T’

SeqAdapter_4b: p-GTACGAGATCGGAAGAGCTCGTATGCCGTCTTCTGCTTG

SeqAdapter_5a: ACACTCTTTCCCTACACGACGCTCTTCCGATCTGAGAG*T

SeqAdapter_5b: p-CTCTCAGATCGGAAGAGCTCGTATGCCGTCTTCTGCTTG

SeqAdapter_6a: ACACTCTTTCCCTACACGACGCTCTTCCGATCTGCATG*T

SeqAdapter_6b: p-CATGCAGATCGGAAGAGCTCGTATGCCGTCTTCTGCTTG

SeqAdapter_7a: ACACTCTTTCCCTACACGACGCTCTTCCGATCTTGACT*T

SeqAdapter_7b: p-AGTCAAGATCGGAAGAGCTCGTATGCCGTCTTCTGCTTG

SeqAdapter_8a: ACACTCTTTCCCTACACGACGCTCTTCCGATCTTACGT*T

SeqAdapter_8b: ACGTAAGATCGGAAGAGCTCGTATGCCGTCTTCTGCTTG

These oligonucleotides were synthesized (by STRATEC Molecular GmbH) in a quantity of 40 nmol and diluted with TE buffer to a concentration of 200 µM. 50 µl of each adapter pair (a and b) were mixed and heated to 90°C for 2 min. Afterwards, the temperature was decreased at 2°C/min for 30 min. The adapter mixes were cooled on ice and diluted to a working concentration of 50 µM with ddH_2O.
All primers are shown from 5' to 3' end; *- phosphorothioate bond.

3.18 Plasmids

pBTM116-D9	Y2H bait plasmid [124]
pACT4-DM	Y2H prey plasmid [124]
pGBT5-Ns	MYTH bait plasmid [137]
pGBT5-Ste	MYTH bait plasmid [137]
pGBT5-Suc	MYTH bait plasmid [137]
pGDHB2	cytoY2H bait plasmid [137]
pGPR4-Ns	cytoY2H/MYTH prey plasmid [137]
pGPR4-Ste	cytoY2H/MYTH prey plasmid [137]
pGPR4-Suc	cytoY2H/MYTH prey plasmid [137]
pOst1-NubI	cytoY2H/MYTH control plasmid [137]
pOst1-NubG	cytoY2H/MYTH control plasmid [137]
pAlg5-NubI	cytoY2H/MYTH control plasmid [137]
pAlg5-NubG	cytoY2H/MYTH control plasmid [137]
pFur4-NubI	cytoY2H/MYTH control plasmid [137]
pFur4-NubG	cytoY2H/MYTH control plasmid [137]
p414-NubG	cytoY2H/MYTH control plasmid [137]
pAG425-FLAG	yeast expression plasmid, modified from pAG425GAL-ccdB-HA (Addgene) by T. Rasko, unpublished
pCR2.1-TOPO	sub-cloning plasmid (Invitrogen)
pcDNA3.1-PA-Renilla-DM	LUMIER bait plasmid [153]
pcDNA3.1-Firefly-V5-DM	LUMIER prey plasmid [153]

3.19 Antibodies

All antibodies were diluted in 5% milk in PBS-T (5% skim milk powder (w/v)).

Primary antibodies:

Anti-LexA (polyclonal, Millipore, produced in rabbit, # 06-719), 1:1.000

Anti-Pgk1p (clone 22C5D8, Invitrogen, produced in mouse, # 459250), 1:10.000

Anti-Dpm1p (clone 5C5A7, Invitrogen, produced in mouse, # A-6429), 1:250

Secondary antibodies:

Anti-mouse IgG (Sigma-Aldrich, Alkaline Phosphatase, produced in goat, # A3562), 1:10.000

Anti-rabbit IgG (Sigma-Aldrich, Alkaline Phosphatase, produced in goat, (# A3687), 1:10.000

3.20 Buffers

DNA sample buffer (4x): 0.25% bromophenol blue, 0.25% xylene cyanole FF, 30% glycerol.

HEPES lysis buffer (LUMIER): 50 mM Hepes, 150 mM NaCl, 10% Glycerol, 0.1% NP-40, 20 mM NaF, 1.5 mM $MgCl_2$, 1 mM EDTA, 1 mM DTT, 1% Benzonase, 1 mM PMSF, 1 cOmplete EDTA-free Protease Inhibitor Cocktail Tablet.

PBS (10x): 80 g/l NaCl, 2 g/l KCl, 14.4 g/l Na_2HPO_4, 2.4 g/l KH_2PO_4.

PBS-T: 1x PBS, 0.05% Tween 20.

Protein Lysis Buffer: 50 mM Tris-HCl (pH 7.5), dissolve 1 cOmplete EDTA-free Protease Inhibitor Cocktail Tablet (Roche) in 7 ml buffer.

SDS sample buffer (4x): 200 mM Tris-HCl (pH 6.8), 400 mM DTT, 8% SDS, 0.4% bromophenol blue, 40% glycerol.

TE buffer (10x): 100 mM Tris HCl (pH 7.4), 10 mM EDTA (pH 8.0), autoclave.

Transformation Mix1: 1 ml 1 M LiOAc, 0.5 ml 10x TE, 5 ml 2 M Sorbitol, 3.5 ml ddH_2O.

Transformation Mix 2: 6 ml 1 M LiOAc, 6 ml 10x TE, 40 ml 60% PEG 3350, 8 ml ddH_2O.

WB (western blot) buffer (10x): 30 g/l Tris, 144 g/l glycine.

WB buffer: 1 x WB-buffer, 10% EtOH.

X-Gal: 20 g/l X-Gal (5-bromo-4-chloro-3-indolyl-beta-D-galacto-pyranoside) in Dimethylformamide (DMF).

Z-buffer: 10.7 g/l Na_2HPO_4, 5.5 g/l NaH_2PO_4, 750 mg/l KCl, 244 mg/l $MgSO_4$, set pH to 7.0, autoclave.

3.21 Enzymes, proteins and markers

Benchmark pre-stained protein ladder	Invitrogen
Benzonase purity grade II	Merck
Gateway® LR Clonase® II Enzyme mix	Invitrogen
Herring Sperm Carrier DNA	Clontech
Klenow fragment 3' to 5' exo$^-$	NEB
Low Molecular Weight DNA Ladder (LMW marker)	NEB
Phusion High-Fidelity DNA Polymerase	NEB
Platinum *Pfx* DNA Polymerase	Invitrogen
Pwo DNA polymerase	Roche
Quick Blunting Kit	NEB
Ready-Load™ 1 Kb Plus DNA ladder	Invitrogen
Restriction enzymes	NEB
Shrimp alkaline phosphatase	Roche
T4 DNA Ligase	Fermentas
T4 DNA Ligase (Rapid)	Enzymatics

3.22 Kits

660 nm Protein Assay	Pierce
Dual-Glo® Luciferase Assay System	Promega
QIAEX II Gel Extraction Kit	Qiagen
QIAGEN Plasmid Midi Kit	Qiagen
QIAprep 96 Turbo Miniprep Kit	Qiagen
QIAprep Spin Miniprep Kit	Qiagen
Zymoprep Yeast Plasmid Miniprep II	Zymo Research

3.23 Chemicals and consumables

3-amino-1,2,4-triazole (3-AT)	Santa Cruz
386-well microtiter plates	Nunc
96-well microtiter plates	Nunc
96-well PCR plates	Thermo Scientific
Agarose	Invitrogen
Ampicillin-sodium salt	Sigma-Aldrich
Agencourt AMPure XP beads	Beckmann Coulter
AttoPhos buffer	Promega
AttoPhos reagent	Promega

Bacto peptone	Becton Dickinson
Bacto tryptone	Becton Dickinson
Bacto yeast extract	Becton Dickinson
Bromophenol blue	Merck Eurolab
Chloramphenicol	Sigma-Aldrich
Complete™ protease inhibitor cocktail	Roche
Deoxyribonucleotides (dNTPs)	Fermentas
Dimethylsulfoxide (DMSO)	Sigma-Aldrich
Dithiothreitol (DTT)	Serva
Ethidium bromide solution	Sigma-Aldrich
Glass beads, acid washed	Sigma-Aldrich
Glycerol	Merck
Kanamycin A monosulfate	Sigma-Aldrich
microTUBE AFA Fiber Pre-Slit Snap-Cap 6x16mm	Covaris
NuPAGE Novex 4-12% Bis-Tris Gels, 1.0-mm thick, 12-well	Invitrogen
Nylon membranes: Hybond™-N	GE Healthcare
Polyethylene Glycol 3350 (PEG 3350)	Biomatik
Polyethylenimine (PEI)	Sigma-Aldrich
Polyoxyethylensorbitan-Monolaureat (Tween 20)	Sigma-Aldrich
Quartz glass cuvettes 100-QS	neoLab
Tetracycline	Sigma-Aldrich
Whatman chromatography paper 3MM	Whatman
Yeast Nitrogen Base	Sigma-Aldrich

All other chemicals, salts, buffer substances, solvents, acids and bases were purchased from Carl Roth GmbH.

3.24 Laboratory equipment

BioAnalyzer (2100 Bioanalyzer)	Agilent
Biofuge Pico	Heraeus
Biomek® FXP pipetting robot	Beckman Coulter
Biophotometer	Eppendorf
Centrifuge 5810R	Eppendorf
DNA electrophoresis chamber	BioRad
Electrophoresis Power Supply EPS 601	Amersham
Freedom EVO pipetting robot	Tecan

Gene Genius UV imager	Syngene
Genome Analyzer II	llumina
Infinite M200 microplate reader	TECAN
Infinite M1000 microplate reader	TECAN
Innova 4430 incubator shaker	New Brunswick Scientific
K4 stamping robot	KBiosystems
LAS-3000 photo imager	Fujifilm
NanoDROP 8000	Thermo Scientific
Optima TLX Ultracentrifuge	Beckman Coulter
PTC200 Peltier Thermal Cycler	MJ Research
S2 DNA Shearing Instrument	Covaris
Sunrise Horizontal Gel Electrophoresis	GibCo
Thermomixer comfort	Eppendorf
Trans-Blot SD Semi-Dry Electrophoretic Transfer Cell	BioRad
TW8 Water Bath	Julabo
XCell SureLock™ Mini	Invitrogen

3.25 Bioinformatics

3.25.1 Database search for high-confidence PPI data

To collect PPI data for alpha-synuclein from published literature, information was retrieved from the following databases: Human Integrated Protein-Protein Interaction rEference (HIPPIE, release date: 2 August 2, 2011) [163], Human Protein Reference Database (HPRD, release date: April 13, 2010) [158], Unified Human Interactome (UniHI, version 4) [159], Molecular INTeraction database (MINT, release date: March 5, 2009) [160], Database of Interacting Proteins (DIP, release date: January 10, 2010) [161]. Additional interaction data was retrieved by manual literature search using the NCBI pubmed web service (ncbi.nlm.nih.gov/pubmed/).

3.25.2 Gene-term enrichment analysis

For gene-term enrichment, the Functional Annotation Tool provided by the Database for Annotation, Visualization and Integrated Discovery (DAVID, release 6.7) [162, 163] was used with the following settings: Disease: OMIM_DISEASE; Functional_Categories: COG_ONTOLOGY, SP_PIR_KEYWORDS, UP_SEQ_FEATURE; Gene_Ontology: GOTERM_BP_FAT, GOTERM_CC_FAT, GOTERM_MF_FAT; Pathways: BBID, BIOCARTA, KEGG_PATHWAY; Protein_Domains: INTERPRO, PIR_SUPERFAMILY, SMART. Fisher exact

probability was calculated with Bonferroni correction for multiple comparisons. Only results with a p-value <0.05 were considered as statistically significant. Functional Annotation Tool output was imported into Microsoft EXCEL and processed manually.

3.25.3 Bioinformatic confidence scoring

To assign confidence scores to experimentally measured PPIs, several commonly used sources of evidence were integrated into an overall score (manuscript by M. Schaefer in preparation). To identify Gene Ontology (GO) semantic similarity, the FunSimMat score [164] was retrieved for each protein pair using the provided web service. Only the GO categories “biological process” and “cellular component” were considered. Next, the number of potentially interacting domains on the protein pairs as indicated by the database DOMINE (version 2.0) [165] was counted. Additionally, published co-expression data of two protein pairs was assessed by calculating their topological overlap values in the GeneAtlas gene expression data set [166] by weighted gene co-expression network analysis (WGCNA) using the WGCNA package of the statistical environment R [167, 168]. To integrate the number of orthologous interactions, the number of species in which orthologous pairs of proteins were observed to interact was retrieved from the databases HomoMINT (release date: March 5, 2009) [160], I2D (release date: January 7, 2010) [169] and the dataset from Lehner *et al*. [170]. Two additional features to be included in the overall score were extracted from a large integrated network of known PPIs [171]: the length of the shortest path between the two proteins and the number of edge-disjoint paths connecting them.

A Support Vector Machine (SVM) integrating the above features was used to predict whether a measured interaction was a true or a false positive one. The library LIBSVM [172] was used to train an SVM to distinguish a known high-confidence PPI set [171] from an equally sized random interaction set. A RBF kernel was used to perform a grid search in combination with five-fold cross validation to determine the optimal hyperparameters. C = 0.5 and gamma = 2 were found to perform best showing an area under the ROC curve (AUC) of 0.86. Missing values were replaced by the feature-specific median values of the training data in the training and experimental set. All features were scaled to the interval [-1,1]. The SVM decision function was used to categorize each interaction into the classes low confidence (LC), medium confidence (MC) and high confidence (HC). The confidence score was used to categorize each interaction into the classes low confidence (LC), medium

confidence (MC) or high confidence (HC). The value boundaries of confidence categories were arbitrarily chosen to be -0.1 as an upper boundary for LC, [-0.1, 0.1] for MC, and 0.1 as a lower boundary for HC.

3.25.4 subSEQ data processing

Base calling of image data obtained by sequencing was performed using the Real Time Analysis (RTA) software, which is part of the Illumina Sequence Control Software (SCS, Version 1.5). Subsequently, the obtained reads were identified by the multiplexing tags and were assigned to the corresponding baits. In parallel, the sequence of the tags was removed from the sequence of the reads. Multiple sequence alignments from the obtained reads were generated using the program MosaikAssembler (MOSAIK 1.1.0014, bioinformatics.bc.edu/marthlab/Mosaik). 13.885 sequences of genes carried by the entry clones available for this thesis were downloaded from the NCBI Reference Sequence (RefSeq) collection [173] and used as reference set. Only unique read values generated by MosaikAssembler were considered for the following analysis. After sequence alignment, the refSEQ accession numbers were converted to Gene IDs using the tool IDconverter [174]. To normalize for sample quality, the unique reads obtained for each Gene ID were each multiplied by a quality factor, which was calculated separately for each library. The quality factor was obtained by dividing the number of total reads of the library the quality factor was calculated for by 1.135.495. This number represents the total reads obtained from the library with the lowest number of reads (HTT513-Q17). Subsequently, the arithmetical mean of the obtained number of reads for each gene was calculated from the duplicates prepared for each library. Finally, non-specific interactions were removed from the dataset: Unique reads obtained for each Gene ID from a library were corrected by subtracting the arithmetic mean of the unique reads of the same Gene ID obtained from the libraries selected against CYP, YFP and SpecR.

4 Results

4.1 An alpha-synuclein interaction network based on published data

The first aim of this thesis project was to collect all known interactors of alpha-synuclein from published literature. A gene-term enrichment analysis was performed in order to find common biological functions among the published interactors of alpha-synuclein.

4.1.1 Collection of high-confidence interaction data

In order to investigate the currently unknown biological function of alpha-synuclein and its role in Parkinson's disease, high-confidence protein-protein interaction (PPI) data for alpha-synuclein was collected from published literature. Initially, all alpha-synuclein-interactors were extracted from the PPI database "HIPPIE" (Human Integrated Protein-Protein Interaction rEference) [171]. This database contains a collection of published interaction data and provides a confidence score for each interaction. This confidence score is based on the experimental data supporting each reported interaction. The score ranges from 0 (no evidence for an interaction) to 1 (strong evidence for an interaction as it has been reproduced with multiple techniques). To obtain additional PPI data, information was extracted from the UniHI database [159] as well as other PPI databases (HPRD [158], MINT [160], DIP [161]). Finally, a manual search and assessment of publications describing alpha-synuclein PPIs was performed. All of the PPIs collected were manually curated. At least two experiments had to support an interaction in order to be defined as high-confidence (HC). For example, sufficient supporting data was provided by a colocalisation and a pulldown experiment. Interactions were also taken into account if the same experiment, for example a co-immunoprecipitation (Co-IP), was performed in two different model organisms. Furthermore, a single interaction experiment combined with a functional association that requires a physical interaction, e.g., a kinase that caused phosphorylation of alpha-synuclein, was considered as HC. Table 4-1 lists the published HC alpha-synuclein interactors, see Supplementary Table 1 for detailed information including the references and the experimental methods used to identify an interaction. The interactors listed in the lower part of the table, which are not annotated in the HIPPIE database, are indicated as "n.a.". Most of these PPIs were identified through manual curation of the available alpha-synuclein literature. In total, 42 proteins were defined as HC interactors of alpha-synuclein. These proteins

will henceforth be referred to as “published interactors” or “published high-confidence interactors”.

Many publications presented insufficient data for HC scoring, e.g. co-localization only [175]. Discrepancies were also found, for example, one publication demonstrated the absence of the binding between alpha-synuclein and Bcl-2 family proteins [176], whereas two independent publications provided convincing evidence supporting an interaction between these proteins [177, 178]. The absence of the interaction was supported by a binding assay with gluthathione S-transferase (GST) fusion proteins and a co-IP assay in COS7 cells (derived from monkey kidney). In contrast, the presence of the interaction was demonstrated under more physiological conditions; specifically, co-IPs from rat brain N27 (derived from rat mesencephalic dopaminergic neuronal cells) and HEK cell (derived from human embryonic kidney) extracts. After careful analysis of these studies [177, 178], the Bcl-2 family protein BAD was added to the list of high-confidence interactors.

Table 4-1: Published high-confidence alpha-synuclein interactors.

Gene ID	Gene symbol	Protein name	HIPPIE score
9627	SNCAIP	Synphilin-1	0.7
6622	SNCA	Alpha-synuclein	0.69
572	BAD	Bcl2 antagonist of cell death	0.5
4137	MAPT	Microtubule-associated protein tau	0.48
5337	PLD1	Phospholipase D1	0.48
6531	SLC6A3	Sodium-dependent dopamine transporter	0.48
4131	MAP1B	Microtubule-associated protein 1B	0.45
351	APP	Abeta	0.43
801	CALM1	Calmodulin	0.43
4514	MT-CO3	Cytochrome c oxidase subunit 3	0.36
1861	TOR1A	Torsin-1A precursor	0.36
5594	MAPK1	Mitogen-activated protein kinase 1	0.31
5071	PARK2	E3 ubiquitin-protein ligase parkin	0.31
7314	UBB	ubiquitin B	0.31
7533	YWHAH	14-3-3 protein eta	0.31
6850	SYK	Tyrosine-protein kinase SYK	0.3
54205	CYCS	Cytochrome c	0.28
6620	SNCB	Beta-synuclein	0.26
5414	SEPT4	Septin-4	0.21
7054	TH	Tyrosine 3-monooxygenase	0.21
11076	TPPP	Tubulin polymerization-promoting protein	0.21
84570	COL25A1	Collagen alpha-1(XXV) chain	0.18
5653	KLK6	Kallikrein-6	0.18
7846	TUBA1A	Tubulin alpha-1A chain	0.18

Table continued on next page.

Gene ID	Gene symbol	Protein name	HIPPIE score
7529	YWHAB	14-3-3 protein beta/alpha	0.18
7531	YWHAE	14-3-3 protein epsilon	0.18
375790	AGRN	Agrin	n.a.
207	AKT1	RAC-alpha serine/threonine-protein kinase	n.a.
8535	CBX4	E3 SUMO-protein ligase CBX4	n.a.
1271	CNTFR	Ciliary neurotrophic factor receptor subunit alpha	n.a.
1410	CRYAB	Alpha-crystallin B chain	n.a.
3303	HSPA1A	Heat shock 70 kDa protein 1A/1B	n.a.
3920	LAMP2	Lysosome-associated membrane glycoprotein 2	n.a.
120892	LRRK2	Leucine-rich repeat serine/threonine-protein kinase 2	n.a.
11315	PARK7	Protein DJ-1	n.a.
5538	PLD2	Phospholipase D2	n.a.
5524	PPP2R4	Serine/threonine-protein phosphatase 2A activator	n.a.
5578	PRKCA	Protein kinase C alpha type	n.a.
5702	PSMC3	26S protease regulatory subunit 6A	n.a.
6477	SIAH1	E3 ubiquitin-protein ligase SIAH1	n.a.
7052	TGM2	Protein-glutamine gamma-glutamyltransferase 2	n.a.
7189	TRAF6	TNF receptor-associated factor 6	n.a.

See Supplementary Table 1 for detailed information including the references and the experimental methods used identify an interaction.

4.1.2 Gene-term enrichment analysis of published alpha-synuclein interactors

To investigate shared functions and find the most salient biological themes among the high-confidence set of interactors, a gene-term enrichment analysis was performed. The Database for Annotation, Visualization and Integrated Discovery (DAVID) [162, 163] provides a functional annotation tool that identifies gene ontology terms, diseases and pathways strongly associated with a particular gene list. The program was used to quantify the enrichment of gene-terms associated with published alpha-synuclein interactors in comparison with the human genome. The functional annotation tool was used with standard settings (see section 3.25.2). To determine the statistical relevance of the biological themes, Fisher exact probability was calculated with Bonferroni correction for multiple comparisons [179]. Only results with a p-value <0.05 were considered as statistically significant. The results of the analysis are shown as a bar diagram in Figure 4-1. See Supplementary Table 2 for the exact numbers and the corrected p-values behind the gene-term enrichment analysis.

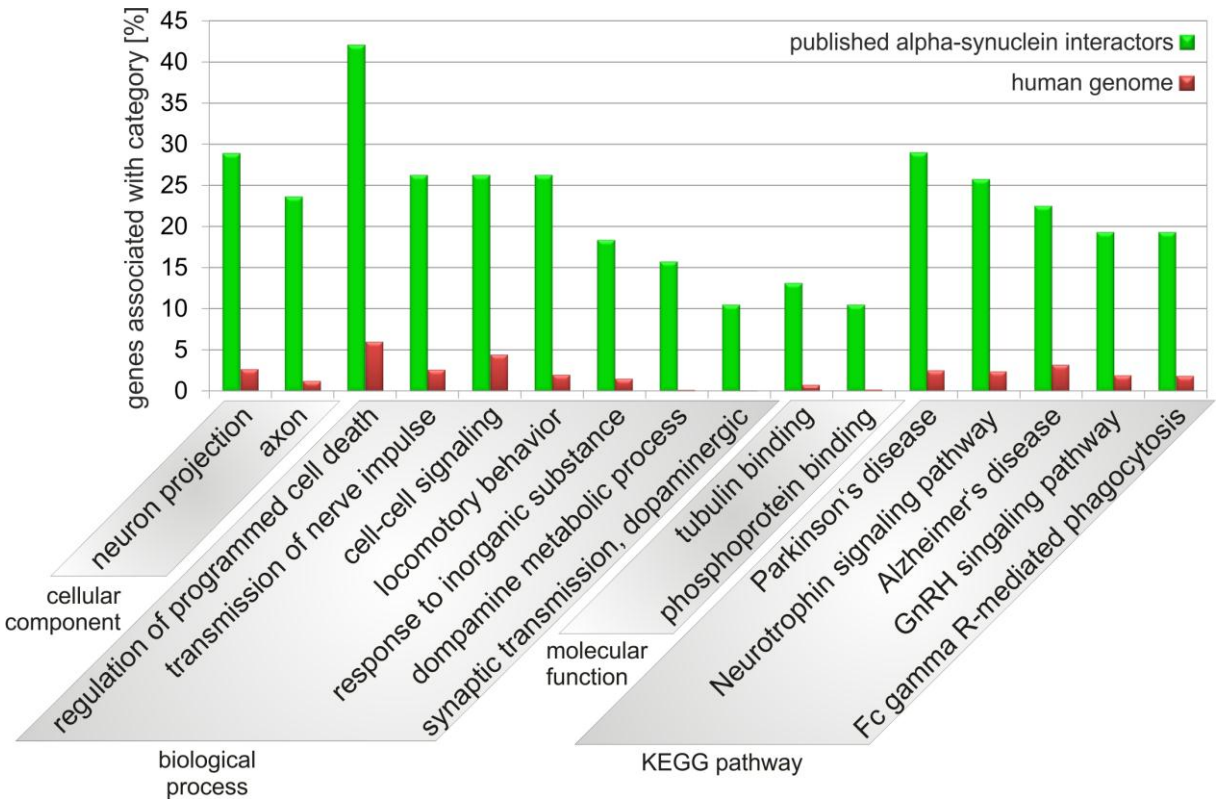

Figure 4-1: Gene-term enrichment analysis of published high-confidence alpha-synuclein interactors. High-confidence alpha-synuclein interactors were analyzed for gene-term enrichment compared to the human genome using the DAVID Functional Annotation Tool. Only statistically significant results (P<0.05, Bonferroni correction) were taken into account.

28.9% of the high-confidence interactors were associated with the term neuron projection, suggesting that alpha-synuclein and the interaction partners play a functional role in the nerve cell. 23.7% of the interactors were localized more specifically to the axon, a sub-term of neuron projection.

4.1.3 Biological processes and molecular functions associated with published alpha-synuclein interactors

A major commonality in the biological function of the published interactors was their involvement in the regulation of programmed cell death; with 42.1% of the interactors being associated with this process. Programmed cell death is known to be activated in PD and other neurodegenerative diseases [180]. The terms “transmission of nerve impulse”, “cell-cell signaling” and “locomotory behavior” were associated with 26.3% of the interactors. Another 18.4% of the proteins were associated with “response to inorganic substance”, a term that describes processes leading for example to movement, secretion, enzyme production or gene expression as a result of an inorganic substance stimulus. 15.8% of the interactors were associated with “dopamine metabolic processes” while 10.5% were involved in dopaminergic synaptic transmission. The progressive loss of dopaminergic neurons in the substantia nigra

pars compacta (SNpc) and their terminals in the dorsal striatum is the primary pathological characteristic of PD [181]. The GO molecular function “tubulin-binding” was associated with 13.2% of the interactors while 10.5% had phosphoprotein binding properties. An interaction between alpha-synuclein and alpha-tubulin has have been demonstrated in several publications [182, 183].

4.1.4 KEGG[1] pathways associated with published alpha-synuclein interactors

As expected, a large fraction of the interactors were associated with the KEGG pathway Parkinson's disease (29.0%); 2.5% of all human genes are related to this pathway. Interestingly, a large fraction (22.6%) of the interactors was also associated with Alzheimer's disease, another prominent neurodegenerative disorder, supporting the view that both diseases are linked [184]; 3.2% of all human genes are related to this disease.

Gene terms for several other KEGG pathways affected by neurodegeneration were also enriched amongst alpha-synuclein interactors. For example, 25.8% of the interactors were involved in the neurotrophin signaling pathway, which is involved in differentiation and survival of neuronal cells [185]. Reduced neurotrophic support is a significant factor in the pathogenesis of neurodegenerative diseases [186]. 19.4% of the interactors are involved in the gonadotropin-releasing hormone (GnRH) signaling pathway. GnRH is secreted from the hypothalamus; the stimulation of its receptor regulates the production and release of the gonadotropins, LH and FSH (KEGG pathway: map04912). It has been demonstrated that GnRH secretion was decreased in a hypothalamic neuronal cell line overexpressing alpha-synuclein [99]. Furthermore, 19.4% of the interactors are associated with Fc gamma R-mediated phagocytosis. Stimulation of this pathway leads to the acquisition of lysosomal proteases and release of reactive oxygen species, which are crucial for the digestion of engulfed materials, e.g. pathogens, in phagosomes [187]. Activated phagocytic microglia, the resident macrophages of the brain and spinal cord, were reported to cluster around dead or dystrophic dopamine neurons in the PD substantia nigra [188]. In addition, the neurotoxin 6-hydroxydopamine (6-OHDA), which is thought to induce oxidative stress, causes the degeneration of dopaminergic neurons and is used to mimic the early stages of PD [189, 190].

4.1.5 Pictorial representation of published alpha-synuclein interactors

[1] KEGG: Kyoto Encyclopedia of Genes and Genomes (www.genome.jp/kegg)

Disease- and biological process-association data obtained from the enrichment analysis as well as the confidence scores from the HIPPIE database are shown in a pictorial representation in Figure 4-2. The HIPPIE score is represented by the color of the nodes: the values range from weak experimental support (blue) to strong experimental support (red), as indicated in the scale bar. After analysis with the official GO search engine AmiGO [191], some interactors were manually added to the created category “cell cycle” (GO Biological Process). As many of the published interactors of alpha-synuclein were involved in several processes, not all disease association/biological process categories are shown. Furthermore, some interactors were only displayed in the most important categories they are associated with. For example, parkinson protein 7 (PARK7) was not shown in the groups “cell-cell signaling” and “response to inorganic substance”, although it is associated with these biological processes.

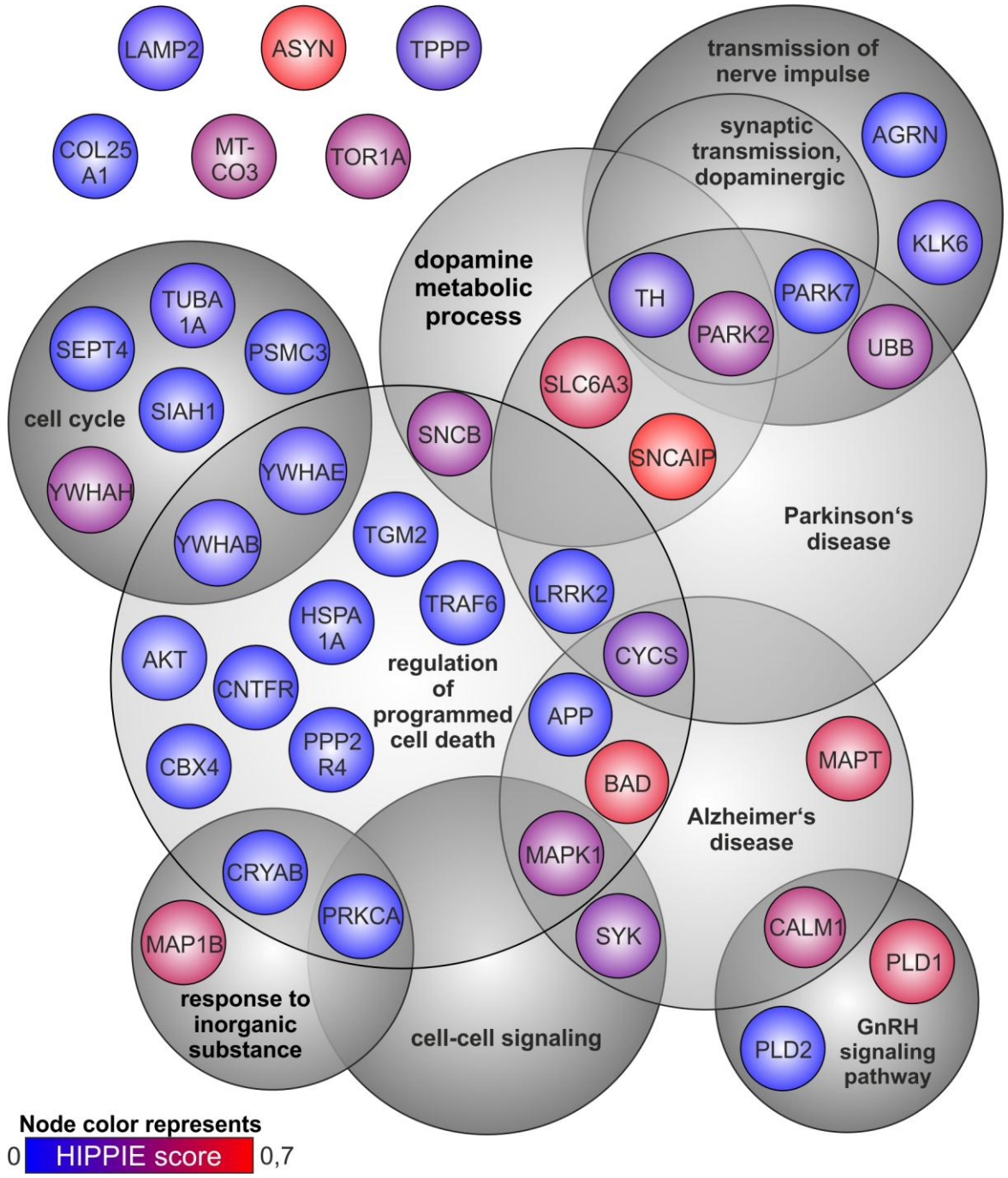

Figure 4-2: Classification of published high-confidence alpha-synuclein interactors. Data extracted from PPI databases, HIPPIE and UniHI information and manual literature curation were combined to define a set of high-confidence alpha-synuclein interactors. The genes encoding the interactors were grouped according to disease association and / or biological process; alpha-synuclein was not displayed in a group. The HIPPIE score is represented by the color of the nodes: the values range from weak experimental support (blue) to strong experimental support (red), as indicated in the scale bar.

4.1.6 Summary of chapter 1

Based on information from PPI interaction databases and manual literature curation, a list of 42 published high-confidence interactors of alpha-synuclein was created. The gene-term enrichment analysis of these interactors highlights various processes that are known to be associated with Parkinson's disease, for example the metabolism of dopamine [192]. Other enriched terms included processes like apoptotic cell death, phagocytosis and the neurotrophin signaling pathway, which also play an important role in other neurodegenerative disorders like Alzheimer's disease [180, 185, 187].

4.2 Creating an alpha-synuclein interaction network based on Y2H screening data

The aim of this chapter was to screen wild-type alpha-synuclein and its pathological mutant isoforms against a library of approximately 16,000 prey proteins and thus generate a comprehensive protein-protein interaction network for alpha-synuclein. In order to find common biological functions among the interactors of alpha-synuclein detected in the Y2H screen, gene-term enrichment analysis was performed. Furthermore, interacting proteins that are associated with genetic diseases and are targets of drugs or compounds were identified via database comparison.

4.2.1 Y2H principle

The Y2H system (Figure 4-3), also referred to here as classic Y2H method, takes advantage of the modular architecture of transcription factors, which consist of a DNA-binding domain (BD) and a transcription activation domain (AD). The Y2H system utilized in this work uses the bacterial LexA BD (*E. coli*) and the yeast GAL4-AD (*S. cerevisiae*). To detect binary interactions between cytosolic or nuclear proteins, a bait protein is fused to the BD domain while a prey protein is fused to the AD domain. Subsequently, the bait and the prey fusion proteins are expressed in a Y2H yeast strain lacking an endogenous copy of the *HIS3* gene. If the bait and the prey proteins interact an artificial transcription factor is reconstituted through the association of the BD and AD. In the system utilized in this study, this functional transcription factor then promotes transcription of the reporter genes *HIS3* (*S. cerevisiae*) and lacZ (*E. coli*). *HIS3* expression enables growth selection on minimal medium lacking the amino acid histidine and ß-galactosidase (β-gal) expression which is detected via blue colonies following X-Gal conversion into 5,5'-dibromo-4,4'-dichloro-indigo [155].

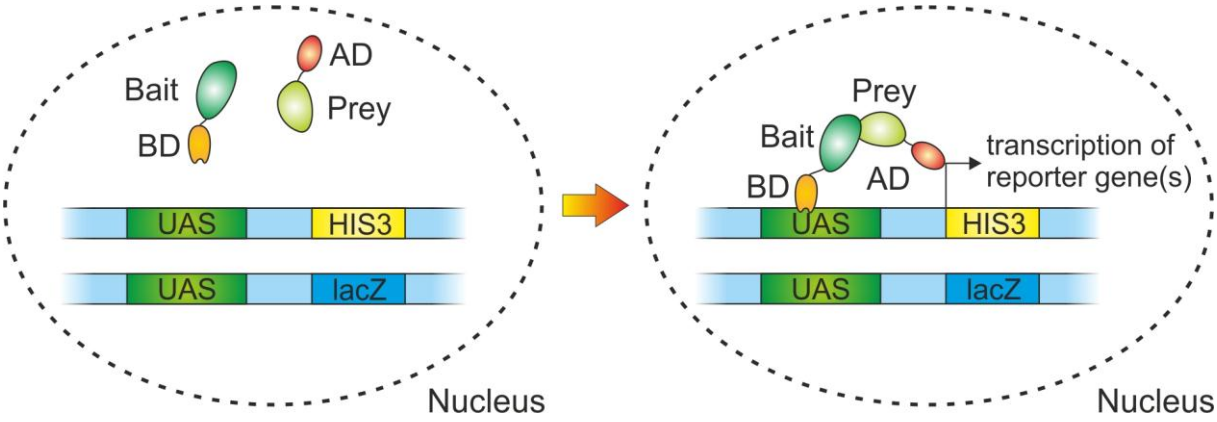

Figure 4-3: Y2H principle. This technique is used to detect binary interactions between cytosolic or nuclear proteins. The bait protein is fused to a DNA-binding domain (BD) while the prey protein is fused to a transcription activation domain (AD). Bait and the prey proteins that physically interact in the yeast nucleus reconstitute a functional transcription factor. It can promote the transcription of the reporter genes *HIS3*, lacZ or both by binding to their upstream activation sequence (UAS), allowing growth selection on minimal medium and colorimetric detection of ß-galactosidase activity to identify protein-protein interactions.

4.2.2 Generation and auto-activation test of alpha-synuclein baits

Three mutations in the SNCA gene have been identified in different families with a dominantly inherited form of PD [42-44]. To facilitate the identification of physiological as well as aberrant disease-associated PPIs, wild-type alpha-synuclein (ASYN) baits as well as baits bearing the pathological mutations were generated (Figure 4-4 A).

Entry clones[2] carrying genes encoding full-length, wild-type alpha-synuclein (CCSB_6120) as well as genes encoding the pathological mutants (A30P, E46K and A53T) were used to generate yeast expression plasmids by Gateway™ LR-cloning (Invitrogen) into the plasmid pBTM116-D9. The open reading frames (ORFs) in the entry clones used to generate these 4 bait constructs lacked a C-terminal stop codon. Furthermore, the vector pBTM116-D9 did not contain a stop codon after the 3' end of the alpha-synuclein sequences inserted by LR-cloning, but only further downstream in the vector backbone. Therefore, a C-terminal tail of 105 nucleotides encoding 30 neutral, 4 basic and 1 acidic amino acid was fused to each of the bait proteins generated from the CCSB clones (Figure 4-4 B). An additional full-length construct containing a stop codon was generated from the entry clone RZPDo834A087D. This construct contained a silent mutation as indicated by a green box in Figure 4-4 A. The identity of all generated baits was confirmed by restriction digestion and sequencing. The restriction enzyme BsrGI was used to analyze the baits and all other Gateway™ compatible plasmids (prey plasmids, entry clones) generated for this

[2] Entry clone: a plasmid containing an open reading frame (ORF) flanked by attL recombination sites, used with Gateway™ Recombination Cloning Technology (Gateway™ nomenclature, Invitrogen).

thesis. Every Gateway™ compatible plasmid contains at least two recognition sites for this restriction endonuclease that are located in the two att-sites flanking the inserted ORF. The BsrGI enzyme therefore releases the ORF-insert from the Gateway™ expression or entry plasmids, which allows the convenient control of the cloning process. Subsequently, the confirmed plamids were transformed into the yeast strain L40ccua (MATa) and tested for auto-activation. In this test, each bait was tested against 32 randomly selected prey proteins and the empty prey vector. An auto-activating bait is a BD-fusion protein that activates the transcription of a reporter gene independent of an interaction with a prey protein [119]. Therefore, these baits are not suitable for screening in the Y2H interaction assay. All clones except CCSB_6120_A53T, which was found to be a strong auto-activator, were used for the subsequent Y2H screening procedure as described in the following sections.

Figure 4-4: Sequence alignment of alpha-synuclein clones used for Y2H bait generation. A: The DNA sequences of the alpha-synuclein clones selected for the Y2H bait generation were aligned using ClustalW; output was manually adjusted and displayed with Jalview. The green box marks a silent mutation; stop codons are marked with an orange box. The entry clones used to generate the CCSB baits lack a C-terminal stop codon. Therefore, these baits contain a tail of 105 additional nucleotides (marked with a yellow box). The Y2H bait generated from the clone CCSB_6120_A53T was auto-activating and was not used for the Y2H screen. B: Amino acid sequence of the C-terminal tail fused to the CCSB baits, shown as yellow box in A. Color of amino acids: yellow: neutral, blue: basic, red: acidic.

4.2.3 Identification of preys interacting with a pool of baits in Y2H

For this thesis a semi-automated, robot-assisted array screening approach was used to find new alpha-synuclein interactors [125]. The yeast strains carrying the generated alpha-synuclein bait plasmids, which successfully passed the auto-activation test, were grown in liquid medium and combined with other baits into pools of up to 16 baits. These pools were screened as part of a larger PPI interaction study. The combination of the pool screen (Figure 4-5) approach combined with a deconvolution step, the so-called backmating (see section 4.2.4), allowed the screening of several baits in parallel, saving time and material. For screening, an existing prey library containing 16098 ORFs cloned into the Y2H prey vector pACT4-DM by Gateway™ technology (Invitrogen) was used. The previously generated prey plasmids, each containing an ORF fused to the AD, were transformed into the haploid yeast strain L40ccα (MATα). To allow yeast mating, the resulting prey clones were mixed with the pooled baits in 384 well microtiter plates (MTPs) and stamped onto rich medium (YPD) with stamping robots (K4, KBiosystems). These robots were also used for all subsequent stamping procedures. The resulting diploid clones were transferred onto SD4 (-Leu-Trp-Ura-His) agar plates selecting for the interaction of bait and prey proteins. SD4 medium lacks the amino acid histidine, which can only be synthesized by yeast upon an interaction of the bait and the prey protein. In parallel, the diploid clones were also spotted onto SD4 agar plates covered with sterile nylon membranes. The membranes were taken for the colorimetric detect of ß-galactosidase (β-gal) expression and its activity. *In silico*, digital images of yeast colonies growing on SD4 agar plates and membranes with blue β-gal signals were overlaid with a grid to mark positive signals (VisualGrid, GPC Biotech). Growing colonies of single preys interacting with a pool of baits were identified by their position in the matrix. An example of detected pool interactions is shown in Figure 4-5 B. The application of stamping robots allowed the production of four technical replicates of the pool screen in parallel. Each interaction of a prey with a pool of baits containing one of the alpha-synuclein constructs was further analyzed in the following backmating step, even if the interaction was only detected in one of the replicates.

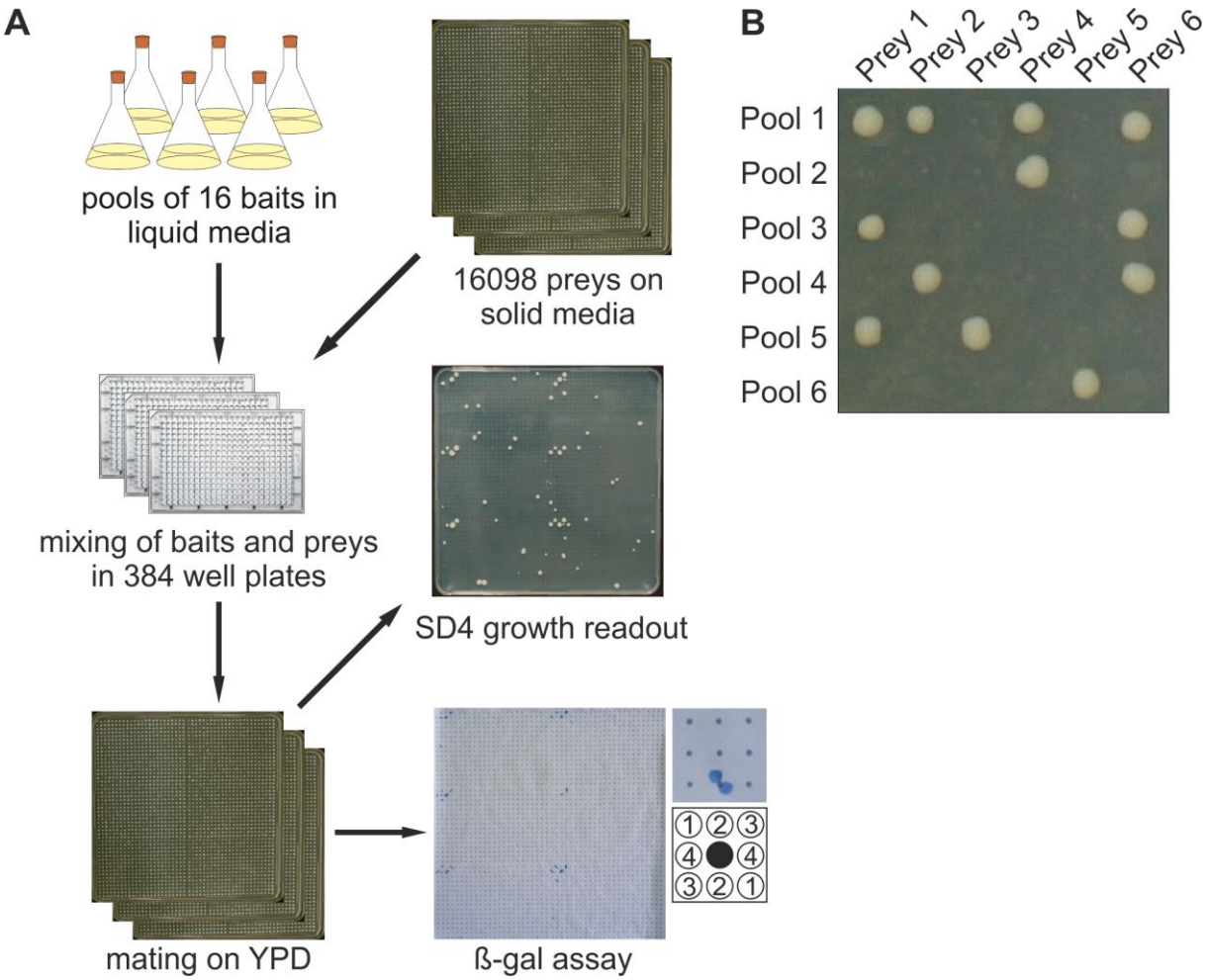

Figure 4-5: A Y2H array screening approach with pooled baits. A: Flow diagram of the pooled interaction screen. Up to 16 baits in a haploid yeast strain (mating type a) were united in a pool. Yeast clones (mating type α), each containing one of 16.098 preys, were mixed with the baits in 384 well plates. After mating on rich medium (YPD), the resulting diploid yeast clones expressing bait and prey proteins were stamped onto selective SD4 (-Leu-Trp-Ura-His) agar plates and onto SD4 plates covered with sterile nylon membranes used for the beta-galactosidase (β-gal) assay. B: Example of results obtained with a pooled interaction screen. Growth patterns on SD4 plates and in the β-gal assay were analyzed to identify preys interacting with bait pools.

4.2.4 Identification of binary PPIs of alpha-synuclein in a Y2H backmating

After the screening of baits in pools, a subsequent backmating step was performed (Figure 4-6) to determine which specific bait protein from a pool interacts with a given prey protein. After completing the pool screen, non-specific PPIs were identified using an in-house generated database. This database contains all prey proteins that constantly activated reporter genes in previously performed Y2H screens, independent of which bait protein the prey proteins were tested against. One reason for these false positive results can be so called “sticky” preys that bind to a broad range of bait proteins, which are functionally unrelated [193]. Furthermore, the interaction of a prey protein with the LexA binding domain fused to the bait protein, but not with the bait protein itself, can generate false positive results [193].

Non-specific interactions with prey proteins obtained in Y2H pool screens were removed from the dataset. All pools containing alpha-synuclein baits were subsequently analyzed in the backmating. In 384-well microtiter plates (MTPs), each bait protein from a pool of 16 baits was tested for interaction with 24 preys. After mating and analysis of reporter gene activation, pairwise interactions between bait and prey proteins were identified. As an example, Figure 4-6 B shows the pairwise interactions detected between the baits in pool 1 and specific preys. The application of stamping robots in the backmating step allowed the production of four technical replicates for this step. This procedure also allowed determining the reproducibility of the results. Some of the interactions were only detected once by growth on SD4 or in the β-gal assay. In contrast, the interactions between other bait and prey protein combinations that activated both reporter genes could be detected in two or more replicates. See Supplementary Table 3 for detailed results. During the analysis of the Y2H results, the sizes of the growing yeast colonies and the size of the blue coloration from the β-galactosidase assay were categorized as small, medium or large. 1 point was awarded for a small colony / spot, 2 points for a medium colony / spot and 3 points were awarded for a large colony / spot. For the final results (“result SD4” or “result lacZ” in Supplementary Table 3) the points from all four repetitions were added. This means that an interaction can get a maxium SD4 and lacZ score of 12 each (large colonies / spots in all 4 repetitions). There is evidence that many biologically important interactions, such as those of various enzymes with their substrates, are often relatively weak and therefore are not easily detectable by Y2H assays [194]. However, the quality of the interactions that can only be detected in one repetition is comparable to highly reproducible interactions [195]. To allow the detection of these weak interactions, all interactors of alpha-synuclein baits that were detected in the backmating step of the Y2H screen, including those that were only detected once by growth on SD4 or in the β-gal assay, were taken into account.

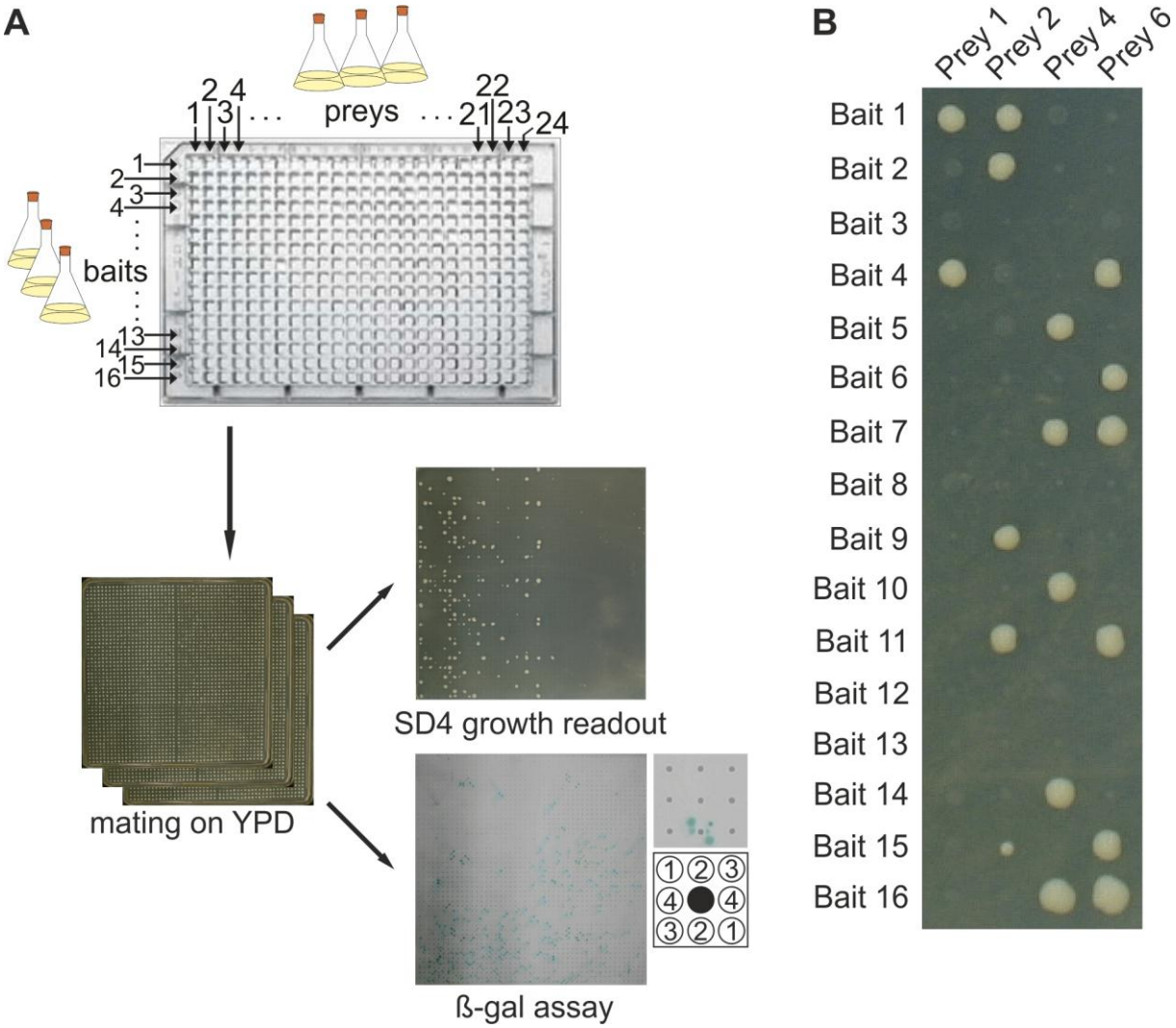

Figure 4-6: Backmating step of Y2H array screening approach. A: Flow diagram of the backmating step. 16 baits from a bait pool in the L40ccua strain (MATa) were tested individually against 24 preys in the L40ccα strain, which has the opposing mating type (MATα). The 384 well plates were stamped on YPD plates for yeast mating. Subsequently, the resulting diploid yeast clones expressing bait and prey proteins were transferred onto SD4 (-Leu-Trp-Ura-His) agar plates and onto SD4 plates covered with sterile nylon membranes, which were used for the colorimetric detection of beta-galactosidase (β-gal) activity. B: Example of results obtained in the backmating. Growth patterns on SD4 plates and in the β-gal assay were analyzed to identify pairwise interactions of baits and preys.

4.2.5 Y2H screening results

The Y2H screen identified 138 interaction partners of the wild-type alpha-synuclein bait generated from the entry clone CCSB_6120 (lacking a stop codon). 98 proteins interacted with the wild-type alpha-synuclein bait generated from the entry clone RZPDo834A087D (including a stop codon). Only 66 proteins interacted with both alpha-synuclein bait proteins. This indicates that the missing stop-codon in the clone CCSB_6120, which leads to the addition of a C-terminal tail of 30 amino acids to the bait protein, changes the interaction spectrum of the bait proteins. In addition, interaction data from previously performed in-house Y2H screens (unpublished data) using prey constructs generated from the wild-type entry clones CCSB_6120 and

RZPDo834A087D (see Figure 4-4 A) was integrated into the dataset. This means that the dataset contains PPI data obtained by screening different clones of wild-type alpha-synuclein both as bait and as prey protein. In total, 200 proteins (211 clones) interacted with wild-type alpha-synuclein. The number of proteins is lower than the actual number of screened clones, as for some proteins different isoforms, fragments or mutants were screened. 103 proteins only interacted with wild-type alpha-synuclein but not with its mutant isoforms. In addition, I detected the interaction of 146 proteins (152 clones) with the bait protein generated from the clone CCSB_6120_A30P, which carries the pathological A30P mutation. 48 of the prey proteins only interacted with CCSB_6120_A30P but not with other baits. Furthermore, the bait construct generated from the clone CCSB_6120_E46K, carrying another pathological mutation, interacted with 46 distinct prey proteins (47 clones). Only 9 of the prey proteins exclusively interacted with CCSB_6120_E46K bait. The complete list of protein-protein interactions detected by Y2H can be found in Supplementary Table 3.

The prey matrix used for the Y2H screen array contained clones potentially expressing 36 published interactors of alpha-synuclein. In the Y2H screen 18 of these proteins did interact with wild-type alpha-synuclein. The fact that published interactions could be reconstructed with the Y2H system validates the method as a powerful tool for the detection of novel interactors of alpha-synuclein.

4.2.6 Confidence scoring of alpha-synuclein interactors detected by Y2H

Apart from false positive results caused by the “sticky” and auto-activating preys (those were removed before the backmating), there are other types of biological false positives that are often detected with the Y2H technique. For example, some protein-protein interactions are detected in yeast cells, but do not occur *in vivo* in human cells because the proteins are not expressed in the same tissue or at the same time [193]. For this thesis, a bioinformatic scoring system was applied to the interactions identified in the Y2H screen to rank the interactions according to their likeliness to occur *in vivo* (Schaefer *et al.*, unpublished). However, that does not necessarily mean that a low ranking interaction cannot be reconstructed with other techniques and/or is biologically irrelevant. The scoring system takes into account the following factors as sub-scores: co-expression, co-localization, known orthologous interactions as well as the presence of domains known to interact in both of the interacting proteins. In addition, shared biological processes, shared cellular components and interaction

network topology features (the length of the shortest path between the two proteins and the number of edge-disjoint paths connecting them) are also taken into account. The interaction network topology features are solely based on published interaction data. All named sub-scores were integrated into a single score using a machine learning approach trained on high-confidence gold standard set of 4203 published interactions. Using this scoring system, the probability for each interaction to be relevant *in vivo* was quantified as a confidence score. The confidence score theoretically ranges from -∞ to +∞, but in practice does not reach values higher than 2. Interactions from the gold standard set receive a value above 0 and random interactions receive a value below 0. A higher score indicates that an interaction is more likely to be relevant than an interaction with a lower score. The confidence score was used to categorize each interaction into the classes low confidence (LC), medium confidence (MC) or high confidence (HC). The value boundaries of confidence categories were arbitrarily chosen to be -0.1 as an upper boundary for LC, [-0.1, 0.1] for MC, and 0.1 as a lower boundary for HC. For the baits generated from wild-type alpha-synuclein clones (CCSB_6120 and RZPDo834A087D), interactions with 200 proteins were subject to the scoring. 81 of the PPIs were ranked as HC (40%), 13 as MC (7%) and 106 of them were ranked as LC (53%). Furthermore, interactions of 146 proteins with A30P alpha-synuclein were ranked as following: 68 as HC (46%), 4 as MC (3%) and 74 as LC (51%). The E46K mutant bait interacted with 46 proteins: 16 of the interactions were ranked as HC (35%) and 29 as LC (63%). None of the interactions was ranked as MC. No confidence score was calculated for homo-dimeric alpha-synuclein interactions.

4.2.7 Gene-term enrichment analysis of alpha-synuclein interactors detected by Y2H

To investigate the shared biological processes for alpha-synuclein interactors detected in the Y2H screen in more detail, gene-term enrichment analysis was performed using the DAVID functional annotation tool [162, 163]. Thus, 81 high-confidence interactors of wild-type alpha-synuclein were annotated. Also annotated were 6 published interactions detected in the Y2H screen that ranked as MC (1) or LC (5). Although there is evidence that alpha-synuclein is not exclusively expressed in the brain [196], the aim was to analyze brain-specific interactions to get hints on alpha-synuclein's role in Parkinson's disease. Therefore, expression data was obtained from HPRD [158] and 14 proteins not expressed in the human brain were removed. Interactions with proteins for which no expression information was available were kept in the list of interactors to prevent a biased analysis towards the better characterized proteins. After these selection steps, the genes encoding the remaining 73 interactors of the wild-type baits were subject for the gene-term enrichment analysis. The terms enriched among these interactors were compared to the terms enriched among all genes in the Y2H prey-matrix. Only results with a p-value <0.05 were considered as statistically significant. The results of the analysis are shown as a bar diagram in Figure 4-7 A. See Supplementary Table 4 for the exact numbers and the corrected p-values behind the gene-term enrichment analysis.

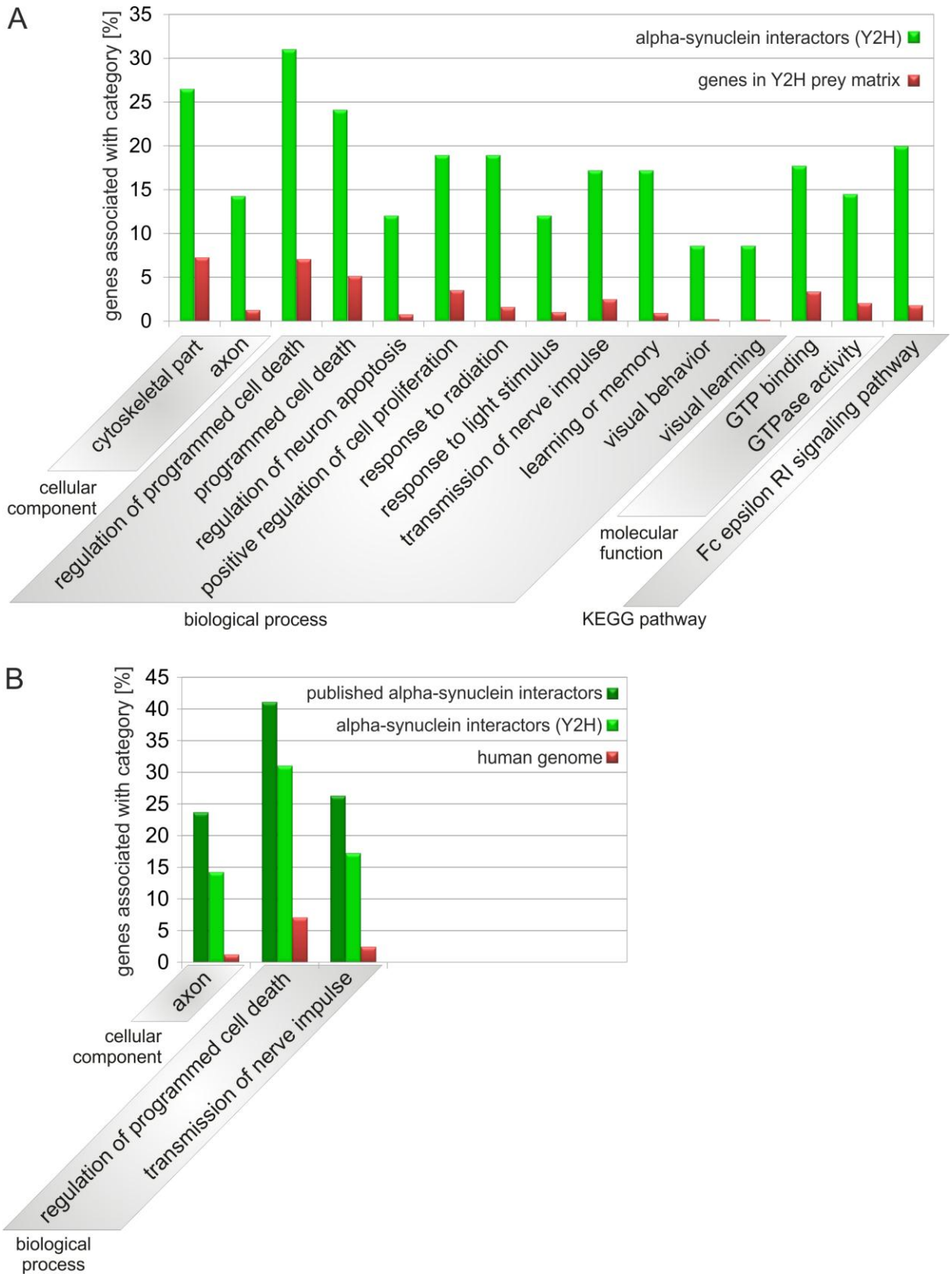

Figure 4-7: Gene-term enrichment analysis of alpha-synuclein interactors detected by Y2H. Predicted high-confidence interactors of wild-type alpha-synuclein detected by Y2H were analyzed for gene-term enrichment compared to all genes in the Y2H prey matrix using the DAVID Functional Annotation Tool. Published interactors that were not ranked as HC were also included in the analysis. Only statistically significant results ($P<0.05$, Bonferroni correction) were taken into account. B: Comparison of terms enriched among published interactors, interactors detected by Y2H and the human genome.

26.5% of the interactors detected by Y2H assays were associated with the term “cytoskeletal part”, a term describing cellular components. The cytoskeleton maintains the cell shape, enables specific cell motion and plays important roles in intra-cellular transport and cellular division [197]. The assembly of abnormal cytoskeletal elements is thought to be a major characteristic of neurodegenerative diseases [198]. 14.3% of the interactors were localized to the axon, suggesting that they might play a functional role in the axon extension. Furthermore, 31.0% of the Y2H interactors were associated with the biological processes “regulation of programmed cell death” while 24.1% of all Y2H interactors were associated with “programmed cell death”. In addition, 12.1% of the interactors were associated with “regulation of neuron apoptosis”, a more specific term related to cell death. There are various lines of evidence suggesting that the activation of programmed cell death pathways may lead to neurodegeneration in PD, specifically the degeneration of dopaminergic neurons in the substantia nigra pars compacta (SNpc) [199]. 19.0% of the Y2H interactors were found to be involved in “positive regulation of cell proliferation”. It has been suggested that cerebral dopamine depletion in PD impairs neural precursor cell proliferation and thereby might affect adult neurogenesis [200]. Furthermore, the terms “response to radiation” (9.0% of Y2H interactors associated with it) and its sub-term “response to light stimulus” (12.1% of Y2H interactors associated with it), both describing a response to external stimuli, were detected in the enrichment analysis. Radiation and chemicals like the neurotoxin MPTP can induce the formation of reactive oxygen species (ROS), which are able to damage to the neurons in the substantia nigra of PD patients [201]. 17.2% of the interactors were associated with the term “transmission of nerve impulse”. Alpha-synuclein localizes to pre-synaptic terminals and is thought to regulate synaptic vesicle formation and neurotransmitter release [202, 203], both crucial processes for the transmission of nerve impulses. An enrichment of the terms “learning or memory” (17.2%) as well as its sub-terms “visual behavior” (8.6%) and “visual learning” (8.6%) was also found. It is published that alpha-synuclein can affect synaptic plasticity during learning [55]. Two gene-terms describing the molecular function of the Y2H interactors were found to be enriched, GTP binding (17.7%) and GTPase activity (14.5%). Finally, an enrichment of the KEGG pathway FC epsiolon RI signaling pathway was found; 20.0% of all HC alpha-synuclein interactors were associated with this term. Stimulation of this pathway leads to the activation of mast cells which play

a key role in inflammatory processes [204]. Activated mast cells release biogenic amines (especially histamines), proteoglycans (especially heparin), leukotrienes, prostaglandins and cytokines into the extracellular environment. Studies using the 6-OHDA-induced rat model of Parkinson's disease suggest that mast cells might participate in neuroprotection [205]. All terms found enriched among the interactors of wild-type alpha-synuclein identified by Y2H are associated with PD or neurodegenerative disorders, indicating that the Y2H screen generated biologically relevant data.

4.2.8 Gene terms enriched among published interactors Y2H interactors of alpha-synuclein

The terms enriched among the published interactors (see section 4.1.2) and the interactors detected by Y2H were compared to each other (Figure 4-7 B). Three terms were found in both analyses: the term “axon”, describing cellular components, as well as the terms “regulation of programmed cell death” and “transmission of nerve impulse”, both describing biological processes known to be associated with Parkinson’s disease [199]. The occurrence of these terms in both analyses indicates that the Y2H screen generated biologically relevant data that could give further hints on the disease mechanisms underlying PD.

4.2.9 Y2H interactions detected with wild-type alpha-synuclein

Molecular function and biological process association data obtained from the enrichment analysis of wild-type alpha-synuclein interactors detected by Y2H are schematically shown in Figure 4-8. The gene symbols are used to show the prey proteins interacting with alpha-synuclein. Only predicted HC and published interactors of alpha-synuclein that were detected by Y2H are shown. As stated previously, some of published interactors were ranked as MC or LC by the confidence scoring system. Furthermore, in Figure 4-8 only major terms are depicted; the sub-terms “response to light stimulus“, as well as “visual behavior” and “visual learning” were not shown. Some interactors were associated with numerous terms and were displayed with as many terms as possible. For example, Huntingtin (HTT) is not shown in the group “learning or memory”, due to the limitations of this data visualization, although it is associated with this biological process.

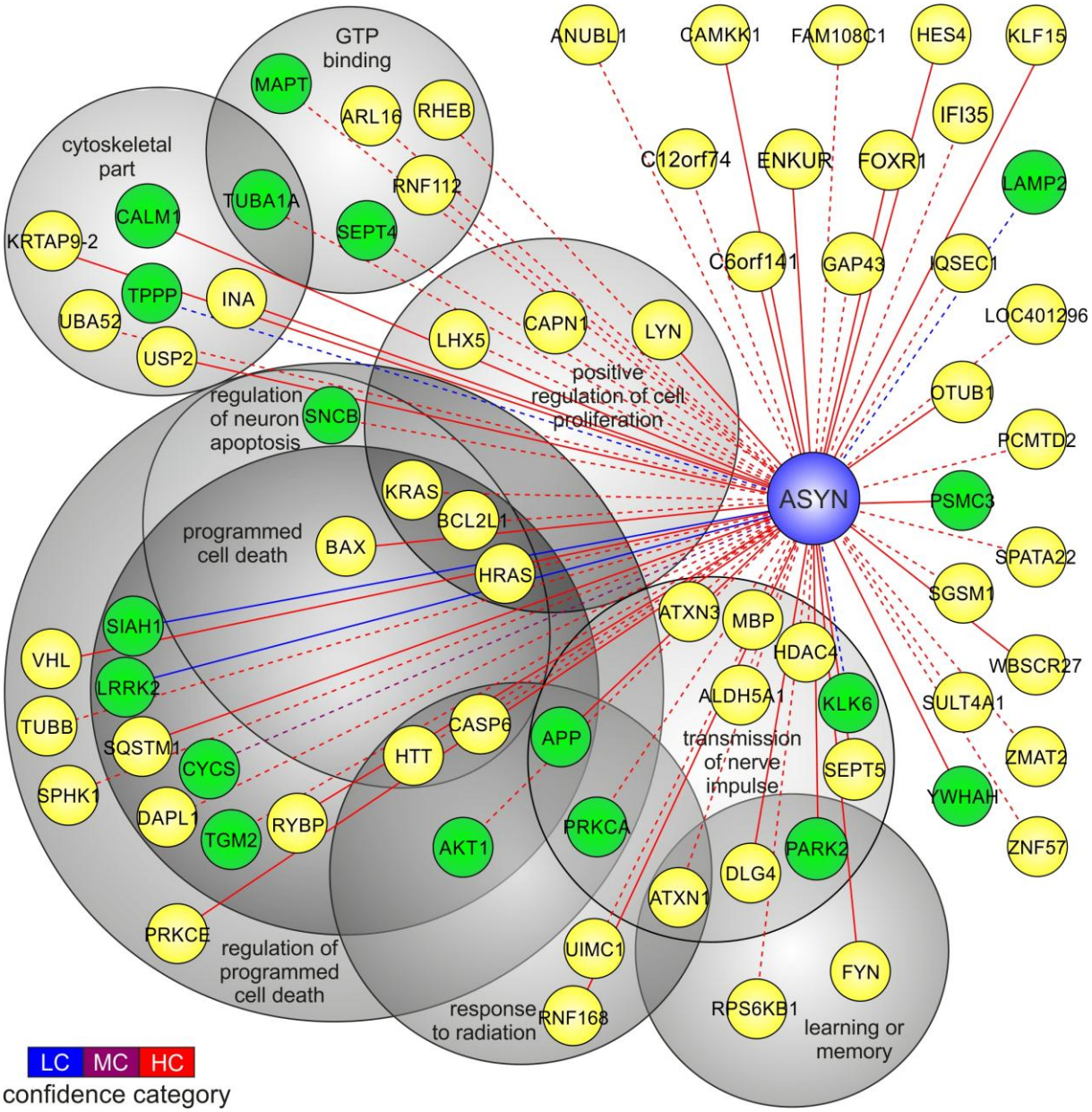

Figure 4-8: Classification of wild-type alpha-synuclein interactors detected by automated Y2H screening. Predicted high-confidence and published interactors of wild-type alpha-synuclein detected by Y2H were grouped according to biological process or molecular function association. The edge color represents predicted low confidence (LC), medium confidence (MC) and high confidence (HC) interactions, as indicated in the scale bar. Known interactors of alpha-synuclein are shown in green while all other proteins are shown with yellow nodes. Bait-prey interactions activating one reporter gene are connected to alpha-synuclein with a dotted edge. Bait-prey interactions activating both reporters are connected with a solid edge. Alpha-synuclein was not assigned to a group.

Strikingly, alpha-synuclein interacted with numerous proteins that are known to be involved in other neurodegenerative disorders. These included BAX, BCL2L1 and CYCS, which are associated with amyotrophic lateral sclerosis (ALS) [206-208] and BAX, CYCS, HTT and TGM2 which are associated with Huntington's disease (HD) [209-212]. Furthermore, alpha-synuclein interacted with ATXN1 and ATXN3, which are associated with spinocerebellar ataxias (SCA) [213, 214] and FYN, which is associated with prion diseases [215]. The proteins APP, CALM1, CALPAIN1 and

MAPT which are associated with Alzheimer's disease (AD) [216-219] also interacted with alpha-synuclein. These findings support a known role of alpha-synuclein in other neurodegenerative diseases [54]. There are several additional lines of evidence for common cellular and molecular mechanisms between PD and other neurodegenerative disorders [220].

Alpha-synuclein also interacted with various proteins which are associated with cancer, such as AKT1, BAX, BCL2L1, CYCS, HRAS, KRAS, PRKCA and VHL [221-228]. Current research is revealing a growing number of proteins that are involved in both cancer and neurodegenerative disorders [229], and reactivation of cell cycle components might contribute to neuronal loss in PD [230].

It is published that the phosphorylation state of alpha-synuclein is important for its ability to form fibrils [72]. Alpha-synuclein is phosphorylated at serine 129 in intracellular Lewy bodies [231]. The phosphorylation of tyrosine 125 [232] and other tyrosine residues [233] has also been demonstrated. Strikingly, the Y2H screen detected the interaction of 9 kinases with alpha-synuclein: the serine/threonine kinases AKT1, CAMKK1, LRRK2, PRKCA, PRKCE, and RPS6KB1 as well as the tyrosine kinases FYN and LYN. Surprisingly, the lipid kinase SPHK1 also interacted with alpha-synuclein in the Y2H assay. Of the kinases found to interact with alpha-synuclein in Y2H, the protein kinases FYN, LRRK2 and LYN [232, 234] are known to phosphorylate alpha-synuclein, which further supports a direct interaction between alpha-synuclein and these kinases. The identified interacting kinases could be tested for their ability to phosphorylate alpha-synuclein *in vitro*. Furthermore, the effect of a possible phosphorylation on the aggregation properties of alpha-synuclein could be assessed.

Alpha-synuclein is degraded by both autophagy and the proteasome [78], an important constituent of cellular protein degradation [92]. However, aggregated and monomeric alpha-synuclein both bind to subunits of the proteasome complex [235] and impair its function. The Y2H assay detected published interactions of alpha-synuclein including the proteasome subunit PSMC3 and the ubiquitin ligases parkin (PARK2) and SIAH1 [118, 235, 236]. Both PARK2 and SIAH1 are known to facilitate the ubiquitination of alpha-synuclein [118, 236]. In addition, the Y2H screen detected the interaction of alpha-synuclein with the E3 ubiquitin-protein ligase RNF168 as well as with the von Hippel-Lindau tumor suppressor protein (VHL), a member of the E3 ubiquitin ligase complex [237]. These proteins could be further tested for their ability

to ubiquitinate alpha-synuclein *in vitro*. It addition, the effect of a possible post-translational modification on the degradation of alpha-synuclein or its tendency to form aggregates could be analyzed.

4.2.10 Y2H interactions detected with wild-type and mutant alpha-synuclein proteins

Only 33% of the publications that were selected to generate the list of published alpha-synuclein interactors (section 4.1.1) presented evidence for interactions with the mutant protein. A detailed insight into the PPI spectrum of mutant alpha-synuclein might help to better understand the disease mechanisms underlying familial PD. In addition to the numerous interactions of the wild-type protein, the Y2H screen detected several interaction partners of A30P and E46K alpha-synuclein. However, a gene-term enrichment analysis of the interactors of the A30P or the E46K mutant using the DAVID functional annotation tool [162, 163] did not return statistically significant results ($P<0.05$, Bonferroni correction).

To identify shared interactions or interactions specific for a certain mutant protein, the interacting proteins were grouped according to the alpha-synuclein isoform they interacted with. Only predicted HC interactions were taken into account. Published interactions of wild-type alpha-synuclein detected in the screen that only ranked as MC or LC were also included. To get information relevant to PD, only proteins surely co-expressed with alpha-synuclein in the human brain were selected. Therefore, expression data was obtained from HPRD [158] and proteins not expressed in the human brain were removed. Proteins for which no expression data was available were kept in the dataset. In Figure 4-9, 73 interactors of wild-type alpha-synuclein, 55 interactors of the A30P mutant and 15 interactors of the E46K mutant were grouped according to the alpha-synuclein isoform they interacted with. In group 1, 33 proteins are summarized, which only interacted with the wild-type baits. A second group contains 27 proteins that interacted with wild-type and A30P alpha-synuclein. The 16 proteins in the third group only interacted with the A30P mutant, while group 4 summarizes 12 proteins that interacted with wild-type alpha-synuclein as well as its A30P and E46K mutant isoforms. Only one prey protein interacted with the wild-type and E46K isoform of alpha-synuclein. In addition, one interaction was detected exclusively with the E46K isoform but not with other baits.

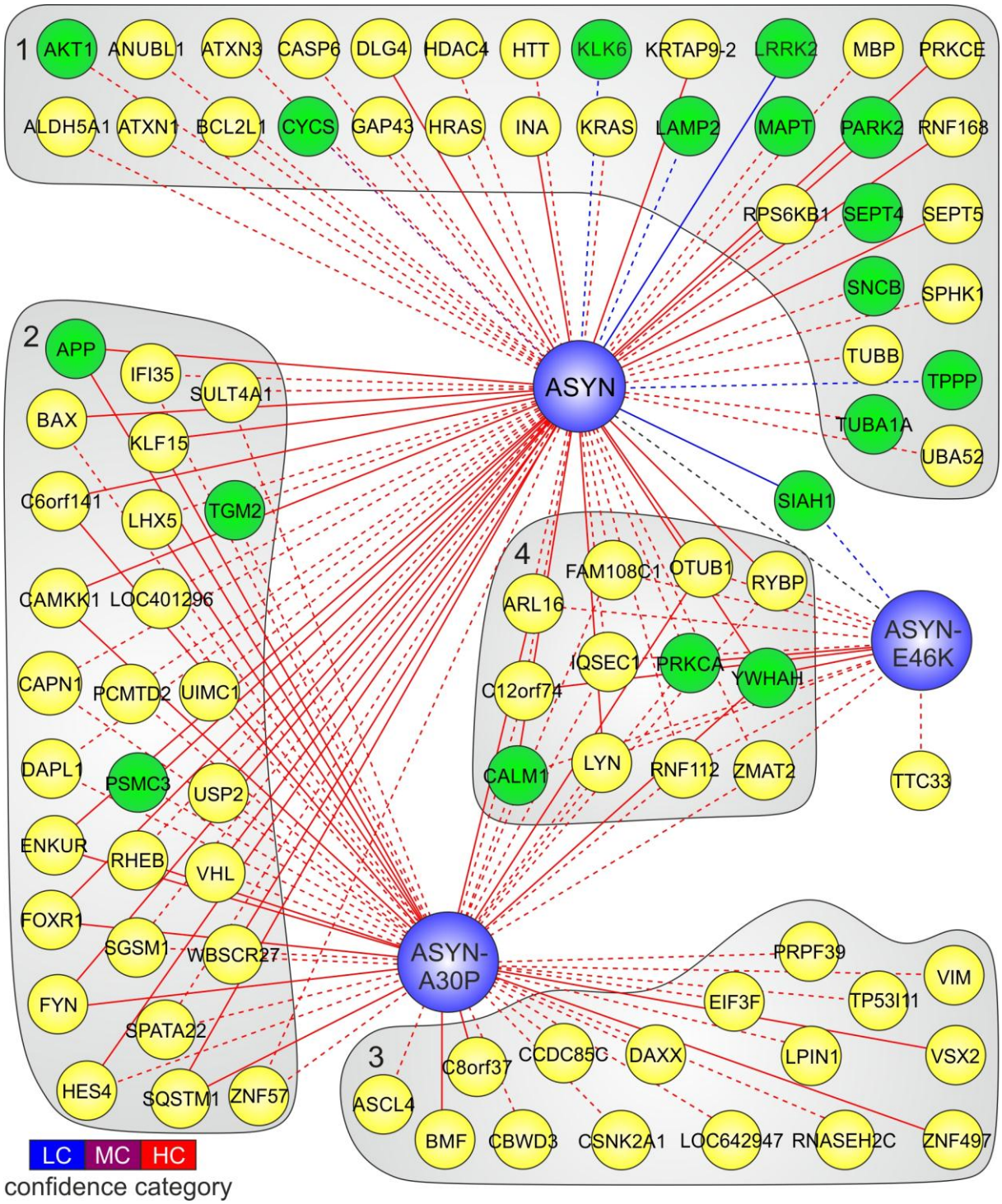

Figure 4-9: Y2H interactions detected with wild-type and mutant alpha-synuclein proteins. Interactors of wild-type and mutant alpha-synuclein proteins were grouped according to their wild-type / mutant specificity, as indicated by the numbered grey outlines. Only predicted high-confidence and published interactors detected by Y2H were taken into account. The edge color represents predicted low confidence (LC), medium confidence (MC) and high confidence (HC) interactions, as indicated in the scale bar. Bait-prey interactions activating one reporter gene are connected to alpha-synuclein with a dotted edge. Bait-prey interactions activating both reporters are connected with a solid edge.

As some interactions were detected exclusively with mutant alpha-synuclein, it is likely that the mutations of alpha-synuclein change its conformation (25, 119), not only leading to different membrane binding properties (121, 123, 124), but also to a different protein interaction spectrum. The serine / threonine specific protein casein kinase 2 (CSNK2A1), which exclusively interacted with the A30P mutant of alpha-synuclein, is known to be associated with the regulation of apoptosis [238]. There is evidence that activation of this pathway may lead to the degeneration of dopaminergic neurons in the substantia nigra pars compacta [199]. By binding and inhibiting casein kinase 2, A30P alpha-synuclein might influence the regulation of apoptosis in the familial forms of PD. In future experiments, A30P mutant alpha-synuclein could be tested for its ability to inhibit casein kinase 2. A30P alpha-synuclein also interacted with the Bcl2 modifying factor (BMF), which is associated with the regulation of apoptosis [239]. BMF functions as an apoptotic activator that binds to BCL2 proteins and is bound to components of the cytoskeleton in healthy cells [239]. A30P alpha-synuclein is known to destabilize the cytoskeleton [240], which could release BMF and thereby promote neuronal apoptosis in familial PD.

4.2.11 Disease association and drug or compound availability for alpha-synuclein interactors

It has been demonstrated that alpha-synuclein interacts with several proteins involved in genetic diseases, for example other neurodegenerative disorders [54] and cancer [229]. The identification of interaction partners of alpha-synuclein with a known disease association might give additional hints on the role of alpha-synuclein in PD pathology. Therefore, the third analysis of the alpha-synuclein interactors detected in the Y2H array screen focused on disease association and the amenability of interactors for available drugs or other small molecules specifically targeting the proteins. For this analysis, all predicted low, medium and high confidence interactors found with wild-type and mutant alpha-synuclein isoforms screened as baits in Y2H (ASYN-A30P and ASYN-E46K) were considered. In order to get high confidence results relevant to PD, only proteins which are co-expressed with alpha-synuclein in the human brain were selected. Expression data was extracted from HPRD [158] and proteins expressed in other tissues were removed. However, proteins for which no expression data was available were left in the dataset. Information on disease association was extracted from the OMIM database [241], while drug target data was available from the DrugBank database [242]. More information on both topics was

retrieved from the GeneCards database [243]. Only interactions with gene products having a disease association and / or where small molecules targeting the gene product are available are shown in Figure 4-10. 61 interactors of wild-type alpha-synuclein, 33 interactors of the A30P and 10 interactors of the E46K mutant isoform of alpha-synuclein were grouped according to their wild-type / mutant specificity. Group 1 contains 35 proteins only interacting with wild-type alpha-synuclein. In group 2, 17 interactors of the wild-type and the A30P isoform are summarized. 8 interactors of the A30P mutant are summarized in group 3, while group 4 contains 8 interactors of wild-type, A30P and E46K alpha-synuclein. No confidence score was calculated for the interaction between wild-type alpha-synuclein and its E46K isoform as indicated by a black edge.

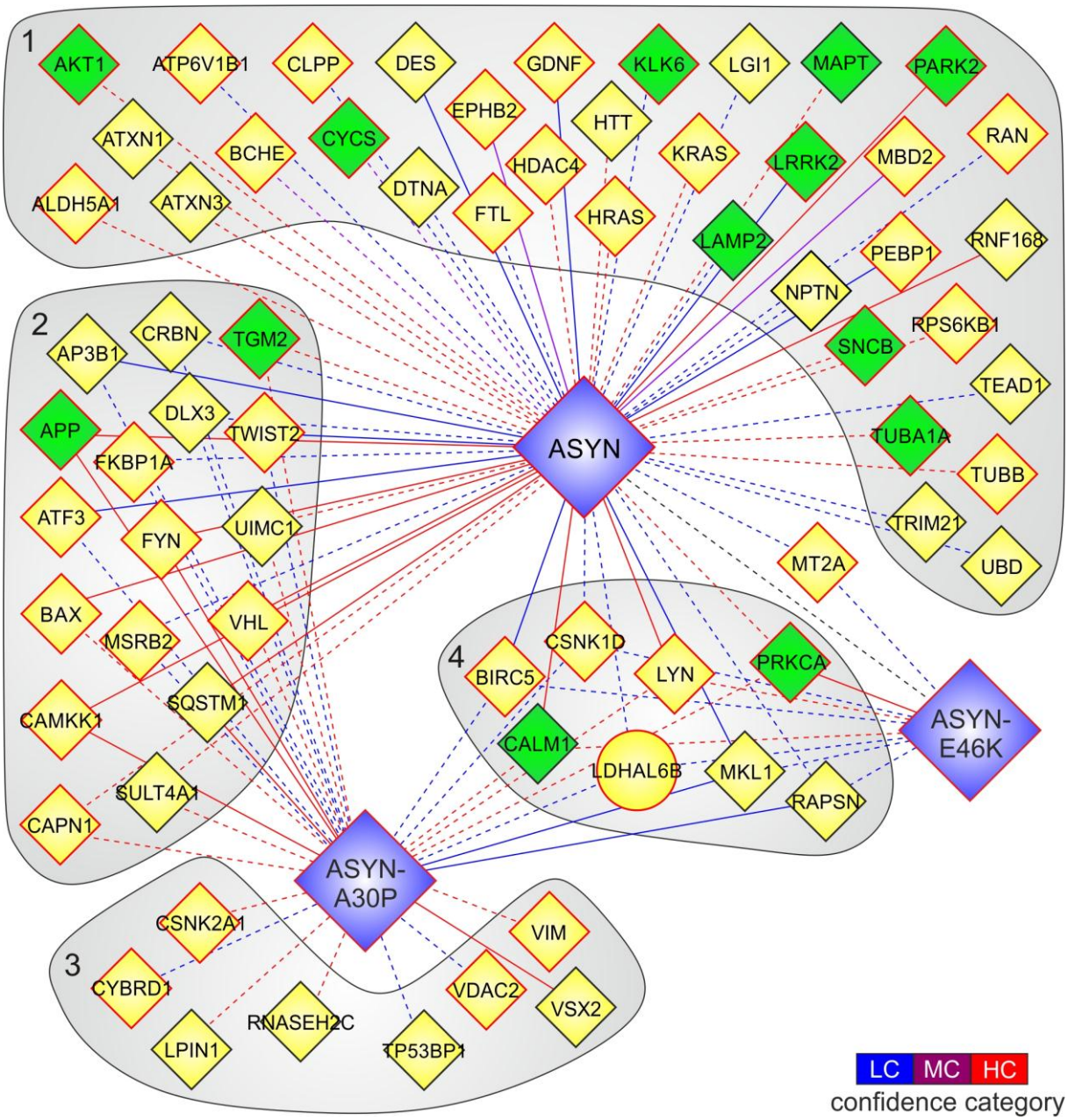

Figure 4-10: Disease association and drug or compound availability for alpha-synuclein interactors detected by Y2H assays. Proteins interacting with alpha-synuclein that had a disease association and / or where small molecules targeting the interacting protein are available were grouped according to their wild-type / mutant specificity, as indicated by the numbered grey outlines. Information was retrieved from OMIM, GeneCards and DrugBank databases. Proteins associated with genetic diseases are shown as a diamond. Known drug or compound targets are shown with a red node border color. Proteins published to interact with alpha-synuclein are shown in green while all others are shown with yellow nodes. The edge color represents predicted low confidence (LC), medium confidence (MC) and high confidence (HC) interactions, as indicated in the scale bar. Bait-prey interactions activating one reporter gene are connected to alpha-synuclein with a dotted edge. Bait-prey interactions activating both reporters are connected with a solid edge.

The Y2H array screen detected an interaction between wild-type alpha-synuclein and histone deacetylase 4 (HDAC4). Mutations and deletions in the HDAC4 gene have been associated with the brachydactyly mental retardation syndrome [244]. In addition, HDAC4 can inhibit cell cycle progression and partially protect cultured

neurons from induced cell death [245]. Interestingly, alpha-synuclein was shown to inhibit histone acetylation in the nucleus and promote neurotoxicity [103]. Strikingly, the authors were able to rescue alpha-synuclein toxicity by administration of histone deacetylase inhibitors in both cell culture and transgenic flies. The database search for drugs or compounds targeting HDAC4 returned several histone deacetylase inhibitors. Many of these small molecules are currently being tested in model systems of PD [246, 247] and other neurodegenerative disorders [248]. The Y2H screen also detected an interaction between the A30P mutant of alpha-synuclein and vimentin (VIM). Vimentin is an intermediate filament protein and a component of aggresomes, proteinaceous inclusion bodies that form when the cellular degradation machinery is impaired or overwhelmed [249]. These inclusion bodies are common features of neurodegenerative diseases like AD, PD, HD and ALS [220]. In a cell-based model of PD, aggresomes formed by alpha-synuclein and synphilin-1 had a cytoprotective effect and the number of aggresome-positive cells was increased in cells expressing the A30P mutant in comparison to cells expressing wild-type alpha-synuclein [250]. The database search identified a compound specifically targeting vimentin: The dipeptide Carnosine, composed of the amino acids histidine and alanine, stimulates vimentin expression in cultured human fibroblasts [251] and has been suggested as a therapeutic agent in AD [252]. Furthermore, Carnosine was found to efficiently protect mice from Parkinsonism induced by MPTP [253] and can be used as dietary supplement for L-DOPA therapy in PD patients [254].

The previous examples demonstrate that the current analysis can identify disease-associated proteins with a published role in PD. Targeting these proteins with chemical compounds or administration of the proteins themselves produces positive effects in models of PD. Administration of the compounds or proteins is even used as therapeutic approach to treat PD patients. The analysis can thus be used to identify new potential therapeutic targets for PD. Agonists or antagonists of these targets could be tested for a possible effect in PD models.

Wild-type, A30P and E46K alpha-synuclein interacted with the baculoviral IAP repeat containing protein 5 (BIRC5). This protein, which is also known as survivin, controls apoptosis and the mitotic spindle checkpoint [255]. It is associated with various types of cancer and has been suggested as a cancer therapeutic target [256]. The mitotic inhibitor Paclitaxel (trade name Taxol, Bristol-Myers Squibb) targets survivin. Strikingly, mitosis-like signals are activated in mature dopaminergic neurons in PD

patients [257]. A possible effect of Paclitaxel on PD disease progression could be tested in animal models mimicking the disease [258].

Several kinases interacted with alpha-synuclein in the Y2H assay, among them the non-receptor tyrosine kinase FYN (oncogene related to SRC, FGR, YES). FYN interacted both with wild-type and A30P alpha-synuclein. There are several lines of evidence for a role of FYN in Alzheimer's disease [259]. The subcellular localization of mutant FYN might influence neurofibrillary pathology and synapse loss in AD [260]. FYN is inhibited by the Src family tyrosine kinase inhibitor Dasatinib (trade name Sprycel, Bristol-Myers Squibb). This small molecule inhibitor can be administered orally and its possible effect on PD could be tested in animal models mimicking the disease [258].

4.2.12 Summary of chapter 2

The Y2H array screen detected 18 published interactors (50% of the interactors that could potentially have been detected) as well as 182 previously unknown interactors of wild-type alpha-synuclein. The gene-term enrichment analysis of the alpha-synuclein interactors detected by Y2H led to the identification of biological processes like "regulation of programmed cell death" and "transmission of nerve impulse", which are known to be associated with Parkinson's disease. These terms were also found enriched among the published interactors of alpha-synuclein, indicating that the Y2H screen generated biologically relevant data. Strikingly, alpha-synuclein interacted with several proteins that are associated with other neurodegenerative disorders like Alzheimer's and Huntington's disease, supporting the hypothesis that there might be similar pathological mechanisms underlying these disorders [220]. Furthermore, the analysis of wild-type and mutant interactions highlighted proteins that are involved in processes like the regulation of apoptosis, which might be altered upon mutation of alpha-synuclein. The disease association analysis identified proteins involved in other known genetic diseases. Chemical compounds targeting these proteins are used as a therapeutic approach for PD and have been tested both in disease models as well as PD patients. In addition, the analysis identified new therapeutic targets of PD as well as compounds targeting these proteins, which could be tested in PD cell or animal models.

4.3 Development of cytoY2H and MYTH high-throughput PPI screening systems

As alpha-synuclein is a membrane associated protein [261], it was assessed if the cytosolic yeast two-hybrid (cytoY2H) system, which localizes the protein better to its usual near membrane environment, delivers different interaction spectra for alpha-synuclein than classic Y2H. Therefore, it was the aim of this chapter to establish a high-throughput version the cytoY2H method. In parallel, the membrane Y2H (MYTH) system was also modified for high-throughput use. The combination of cytoY2H and MYTH would allow screening of PPIs using alpha-synuclein both as bait and prey proteins. To confirm the correct function of both PPI screening systems, the modified vectors were used to reconstruct published interactions between defined protein pairs. Subsequently, alpha-synuclein cytoY2H bait plasmids were generated and the correct expression and function of the bait proteins were analyzed.

4.3.1 Principle of cytoY2H and MYTH interaction assays

The cytoY2H [141] and the MYTH [137] system are based on the split-ubiquitin technique [131, 136] and detect protein-protein interactions which take place in the cytoplasm (Figure 4-11). In the split-ubiquitin technique, the bait protein is produced as a fusion to the C-terminal half of ubiquitin (Cub, residues 35-76) and an artificial transcription factor (TF). The TF consists of the bacterial LexA DNA-binding domain (*E. coli*) and the activation domain of the viral transcriptional activator VP16 (*Herpes simplex*). The prey protein is fused to the N-terminal half of ubiquitin (NubG, residues 1-34). The introduction of the point mutation isoleucine 13 to glycine prevents the spontaneous NubG-Cub association. Only upon interaction of bait and prey proteins, fused Cub and NubG together can form a complete ubiquitin molecule, which is recognized and cleaved after its carboxy-terminus by endogenous ubiquitin binding proteases (UBPs) in the yeast cytosol, leading to the release the artificial transcription factor LexA-VP16. The released TF is then able to enter the nucleus to activate the reporter genes *HIS3* (*S. cerevisiae*) and lacZ (*E. coli*) by binding to their upstream activation sequence (UAS) lexAop. This means the interacting bait and prey proteins do not migrate into the nucleus as they do in the classic Y2H system. An interaction of the bait and prey protein allows growth selection on SD4 agar lacking the amino acid histidine. Further on, β-galactosidase expression can be determined by colorimetric detection of X-gal conversion into 5,5'-dibromo-4,4'-dichloro-indigo [262]. The cytoY2H system is used to study interactions of soluble

proteins and it was predominantly designed for proteins of the transcription machinery [141]. The bait protein is anchored to the membrane by fusing it to the small yeast ER (endoplasmic reticulum) integral membrane protein Ost4p. Anchoring of the bait to the ER membrane makes the method especially suitable for screening transcriptionally active proteins by keeping them in the cytosol and thereby preventing autoactivation, which is often observed in classic Y2H assays. The MYTH system is used to study interactions between full-length integral membrane proteins and their putative interaction partners [137]. It is suitable for all proteins facing at least one terminus to the cytosol in yeast. Membrane proteins are difficult to analyze in classic Y2H assays, as their hydrophobic nature prevents their translocation into the yeast nucleus, a requirement for classic Y2H.

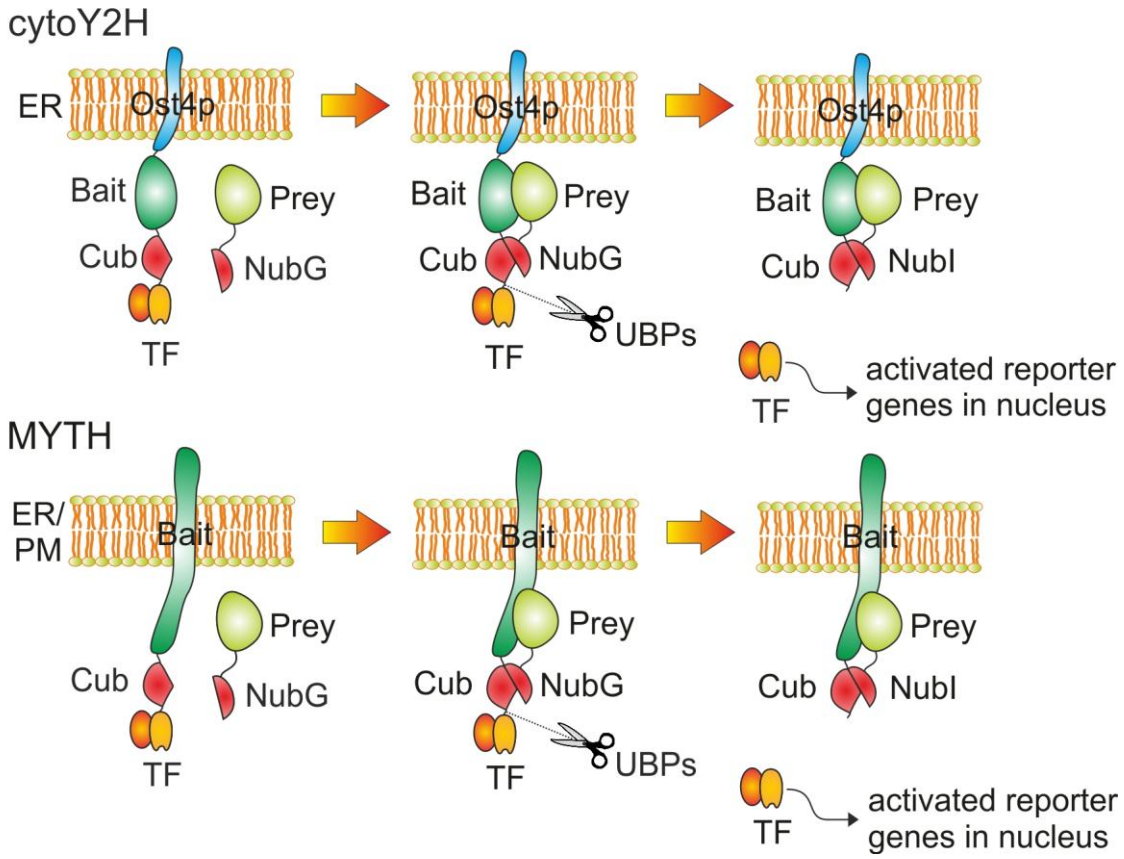

Figure 4-11: The cytosolic yeast two-hybrid (cytoY2H) and the membrane yeast two-hybrid (MYTH) principle. The cytoY2H system is used to detect protein-protein interactions of soluble proteins, especially transactivating proteins, a class of proteins difficult to analyze with classic Y2H methods. The bait protein is inserted between the yeast ER membrane protein Ost4p and the C-terminal half of ubiquitin (Cub, residues 35-76), followed by the artificial transcription factor LexA-VP16 (TF). The prey protein is fused to the mutated N-terminal half of ubiquitin (NubG, residues 1-34). Due to a mutation (Ile13=>Glu), NubG has no intrinsic affinity for Cub, and therefore the two halves do not interact when co-expressed within the yeast cell. Membrane anchorage of the prey proteins is not mandatory. If the bait and prey protein interact, Cub and NubG complement to form split-ubiquitin, which is recognized and cleaved by ubiquitin binding proteases (UBPs), allowing translocation of the TF to the nucleus and subsequent transcriptional activation of endogenous reporter genes. Activation of the *HIS3* gene allows yeast to grow on minimal medium lacking the amino acid histidine. Expression of the lacZ gene can be monitored by colorimetric detection of β-galactosidase activity in the X-gal assay. MYTH: This system is used to detect protein-protein interactions of full-length membrane proteins or proteins firmly attached to the membrane. Baits do not require artificial recruitment to the membrane. The detection of interactions works as described for cytoY2H.

4.3.2 Modification of cytoY2H and MYTH vectors

To allow the time-efficient generation of a large number of constructs, the Gateway™ casette (GW, Invitrogen, site-specific recombination sequence) was inserted into the multiple cloning sites (MCS) of the cytoY2H [141] and MYTH [137] bait vectors by restriction and ligation. The Gateway™ casette was also cloned into the MCS of the prey vectors. The prey vectors are compatible with both the cytoY2H and MYTH system. For this thesis, a collection of 26.122 different entry clones containing human ORFs was available. This collection contained clones from the humanORFeome

collection 5.1[3], the RZPD clone collection[4] as well as various entry-clones generated in our workgroup. Next to full-length sequences and fragments of different human genes, the collection also contained DNA sequences with known pathological mutations of disease-associated genes. 55% of the entry clones available from the library contained a Kanamycin resistance gene, which is also used as selection marker in the cytoY2H and MYTH bait vectors. To ensure their compatibility with all available entry clones, the *E. coli* resistance marker in the cytoY2H and MYTH bait vectors was changed from a Kanamycin to a Tetracycline marker using homologous recombination in yeast [156]. The successful modification of all vectors was confirmed by restriction digestion and sequencing. For further details on the cloning processes, see section 3.6. In total, one cytoY2H bait-vector, three MYTH bait-vectors and three prey-vectors compatible with both systems were generated (Figure 4-12).

[3] http://horfdb.dfci.harvard.edu/hv5/
[4] www.imagenes-bio.de

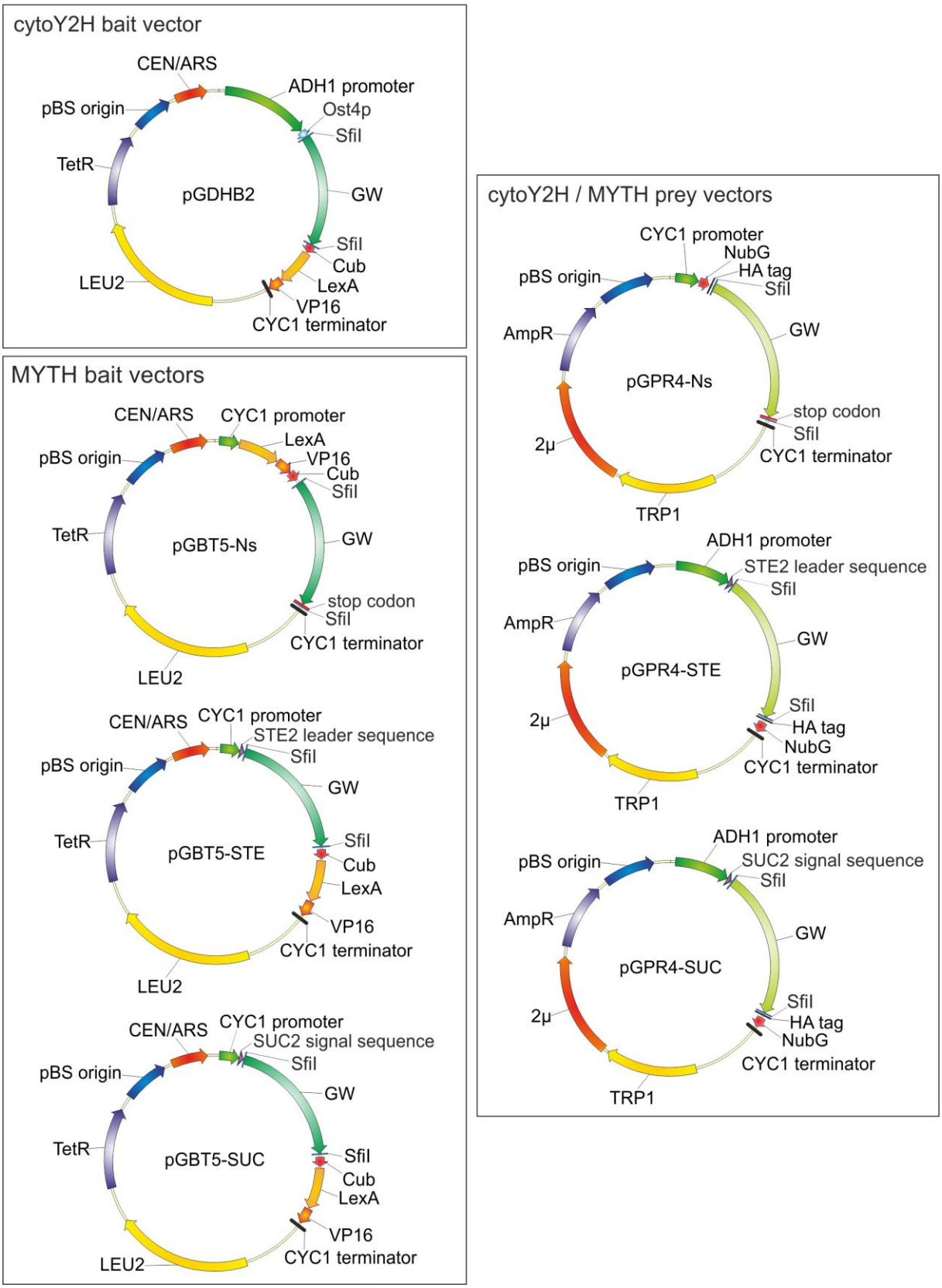

Figure 4-12: Overview of generated cytoY2H / MYTH vectors. One cytoY2H bait-vector, three MYTH bait-vectors and three prey-vectors (compatible with both systems) were modified for high-throughput Gateway™ cloning. All bait plasmids contained the C-terminal half of ubiquitin (Cub) fused to an artificial transcription factor (LexA-VP16). All prey plasmids contained the mutated N-terminal half of ubiquitin (NubG). The Gateway™ Cassettes (GW) inserted into the vectors pGBT5-Ns and pGPR4-Ns included an extra stop codon. See Table 4-2 for additional features.

Table 4-2: Features of generated cytoY2H / MYTH vectors.

Vector	type	entry clone tagged at	promoter	Leader / signal sequence	yeast selection marker	*E. coli* selection marker	plasmid replication yeast	plasmid replication *E. coli*
pGDHB2	cytoY2H bait	N- and C-terminus	ADH1	-	LEU	Tet	CEN/ ARS	pBS origin
pGBT5-Ns	MYTH bait	N-terminus	CYC1	-	LEU	Tet	CEN/ ARS	pBS origin
pGBT5-Ste	MYTH bait	C-terminus	CYC1	STE leader	LEU	Tet	CEN/ ARS	pBS origin
pGBT5-Suc	MYTH bait	C-terminus	CYC1	SUC signal sequence	LEU	Tet	CEN/ ARS	pBS origin
pGPR4-Ns	MYTH / cytoY2H prey	N-terminus	ADH1	-	TRP	Amp	2 µ	pBS origin
pGPR4-Ste	MYTH / cytoY2H prey	C-terminus	ADH1	STE leader	TRP	Amp	2 µ	pBS origin
pGPR4-Suc	MYTH / cytoY2H prey	C-terminus	ADH1	SUC signal sequence	TRP	Amp	2 µ	pBS origin

Table 4-2 lists the features of the generated vectors. The cytoY2H bait vector pGDHB2 is used to identify interactions of soluble proteins (cytosolic or nuclear), especially transcription factors. The vectors pGBT5-Ns (bait vector) and pGPR4-Ns (prey vector) are used for type II integral membrane proteins with their N-terminus in the cytoplasm. The GW cassette inserted into these vectors contained an additional STOP-codon inserted immediately downstream of the cassette. Without this translation termination signal, N-terminally tagged baits and preys generated from entry-clones without a STOP-codon would contain an additional C-terminal tail of amino acids. The vectors pGBT5-Ste (bait vector) and pGPR4-Ste (prey vector) are used for type I integral membrane proteins with their C-terminus inside the cytoplasm, especially proteins without a canonical N-terminal signal sequence. These vectors fuse the N-terminal 15 amino acids of the STE leader sequence of the *S. cerevisiae* Ste2p protein to the N-terminus of the bait or prey protein. The

sequence does not influence membrane targeting of the bait and prey proteins but increases their expression levels in yeast. Targeting of the bait or prey proteins to the membrane can be increased by using the vectors pGBT5-Suc (to generate baits) and pGPR4-Suc (to generate preys). These vectors carry a signal sequence derived from the *S. cerevisiae* invertase (*SUC2*) gene. The invertase signal sequence is often used for secretion of heterologous proteins in yeast [263]. A weak CYC1 promoter drives the constitutive expression of the MYTH baits, whereas the cytoY2H baits and cytoY2H / MYTH preys are under the control of a strong ADH1 promoter. All baits are expressed from low copy plasmids (CEN/ARS), whereas the preys are expressed from high copy plasmids (2μ).[5]

4.3.3 Detection of defined protein interactions using the modified cytoY2H and MYTH vectors

Initially, two well characterized interaction pairs were chosen to perform a proof of principle experiment for the redesigned cytoY2H bait vectors following insertion of the Gateway™ cassette and the *E. coli* selection marker exchange. The two interactions chosen were between the NF-κB subunit p65 and its inhibitor IκB-α [264] and between the S100 calcium binding protein A1 (S100A1) and the S100 calcium binding protein B (S100B) [265, 266]. The NF-κB subunit p65 is a transcription factor that is difficult to handle in the classic Y2H assay [141]. Its interaction with IκB-α was previously shown using the cytoY2H assay [141]. The transcription factor p53 [267] was used as a negative control (no interaction expected). CytoY2H bait constructs were generated by Gateway™ cloning from entry clones carrying the sequences of p65 and S100A1 followed by transformation into the haploid yeast strain L40ccα (MATα). Preys were generated by Gateway™ cloning the sequences of IκB-α, S100A1, S100B, p53 and p65 into the vector pGPR4-Ns, followed by transformation into the haploid yeast strain L40ccua (MATa). After mating, diploid cells were stamped from YPD plates onto SD2 (-Leu-Trp) agar plates selecting for the presence of both bait and prey vectors. Afterwards, colonies were transferred to SD4 (-Leu-Trp-Ura-His) agar plates selecting for the interaction of bait and prey proteins, where co-expression of the IκB-α bait and the p65 prey robustly yielded growth as well as strong blue signals in the β-galactosidase assay (Figure 4-13 A). No growth was observed neither with NubG expressed from the empty prey vector, nor with the

[5] Information on cytoY2H / MYTH vectors was modified from the DUALhunter starter kit manual (P01601-29) and the DUALmembrane vector selection guide available from the Dualsystems website (www.dualsystems.com).

control prey proteins p53, S100A1, and S100B. Likewise, co-expression of the S100A1 bait and the S100B prey also resulted in robust growth under selection conditions and a strong blue signal in the β-galactosidase assay (Figure 4-13 B). Also here, the controls behaved as expected.

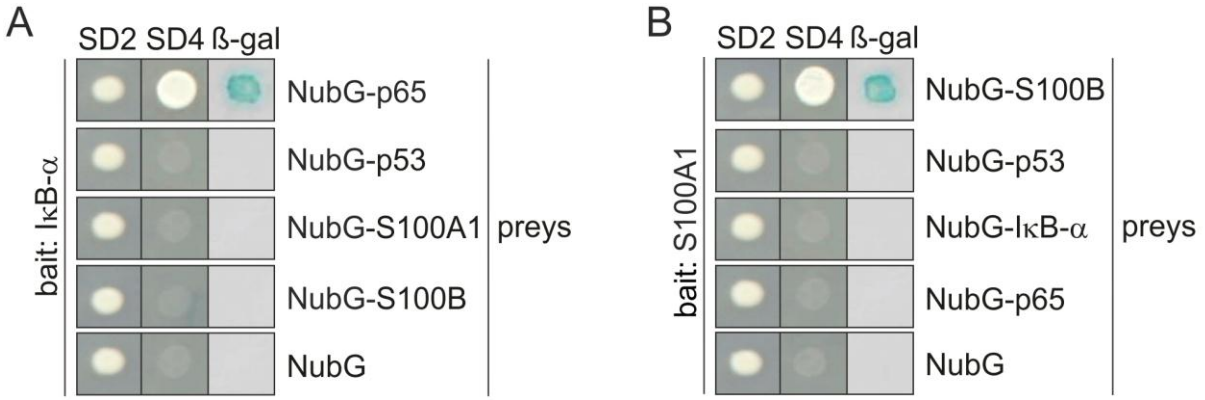

Figure 4-13: Proof of principle experiment for the cytoY2H system with two published interactions. A+B: Diploid yeast cells (L40ccα + L40ccua) co-expressing the indicated cytoY2H bait and prey proteins were plated on SD2 (-Leu-Trp) agar plates selecting for the presence of both bait and prey plasmids. Subsequently, yeast clones were transferred to SD4 (-Leu-Trp-Ura-His) agar plates to select for an interaction of bait and prey proteins. In parallel, yeast colonies were spotted onto SD4 plates covered with nylon membranes for colorimetric detection of active β-galactosidase (β-gal), which is expressed upon interaction of bait and prey proteins. NubG: N-terminal half of ubiquitin.

The function of the MYTH bait vectors pGBT5-Ns, pGBT5-Ste and pGBT5-Suc was confirmed by reconstructing the interaction between the protein tyrosine phosphatase like member b (PTPLB) and BAP31. Both of these human integral membrane proteins resident in the ER have previously been shown to interact in the MYTH system [268]. The authors predicted both the N- and the C-terminus of PTPLB to be facing the cytoplasm. Therefore, the full-length sequence of PTPLB was Gateway™ cloned into all three available MYTH bait vectors, while the full-length BAP31 sequence was Gateway™ cloned into the prey vector pGPR4-Ste. Subsequently, the bait plasmids were transformed into the haploid yeast strain L40ccα (MATα) and tested, as described for the cytoY2H vectors above, with a specific (BAP31) and unspecific prey proteins (p53, p65) as well as the empty prey-vector in the yeast strain L40ccua (MATa). An interaction of PTPLB in all three bait vectors with BAP31, but not with unspecific preys or NubG expressed from the empty prey vector was detected. Taken together, these results indicate that the generated vectors are fully functional and can be used for further detection of PPIs.

4.3.4 Generation and functional test of bait alpha-synuclein baits

After the vectors had been tested successfully, cytoY2H bait plasmids were generated by Gateway™ cloning harboring the full-length sequence encoding wild-type and mutant (A30P, E46K or A53T) alpha-synuclein proteins into the vector pGDHB2. All constructs were confirmed by restriction digestion and sequencing. Subsequently, the function of the bait proteins was tested using the "NubG/NubI" genetic test [137]. In this test, each bait protein was produced in combination with one of 7 specific prey control proteins (Table 4-3, modified from Iyer *et al.* [137]). The test was used to confirm the correct expression of a bait protein and tests its ability to autoactivate the reporter genes.

Table 4-3: NubG/NubI control vectors.

Name of prey plasmid	Localization of control prey protein	Control type	Interpretation of result
pOst1-NubI	ER	positive control	If no growth on SD4 and negative β-gal assay: indication that the bait protein is not expressed.
pAlg5-NubI	ER	positive control	If no growth on SD4 and negative β-gal assay: indication that the bait protein is not expressed.
pFur4-NubI	PM	positive control	If no growth on SD4 and negative β-gal assay: indication that the bait protein is not expressed.
pOst1-NubG	ER	negative control	If growth on SD4 and positive β-gal assay: indication of bait overexpression, nonspecific cleavage or interaction with Ost1p.
pAlg5-NubG	ER	negative control	If growth on SD4 and positive β-gal assay: indication of bait overexpression, nonspecific cleavage or interaction with Alg5p.
pFur4-NubG	PM	negative control	If growth on SD4 and positive β-gal assay: indication of bait overexpression, nonspecific cleavage or interaction with Fur4p.
NubG	cytosol	negative control	auto-activating bait protein

ER: endoplasmatic reticulum, PM: plasma membrane.

In the NubG/NubI control test system, the tested bait proteins are co-produced with both positive and negative control preys in yeast. GFP-tagged alpha-synuclein, when synthesized in yeast, is delivered to the plasma membrane via the secretory pathway [269]. Thus, yeast transmembrane proteins also passing through this pathway were chosen as control preys. The oligosaccharyl transferase Ost1p plays an important role in the N-glycosylation of proteins and is localized in the yeast endoplasmic reticulum (ER) [270]. The dolichyl-phosphate beta-glucosyltransferase Alg5p, another protein involved in N-linked protein glycosylation, is also localized to the ER [271]. The uracil permease Fur4p mediates the uptake of the nucleoside uracil and is

localized in the yeast plasma membrane (PM) [272]. Positive control proteins are fused to the wild-type N-terminal half of ubiquitin (NubI) and interact with the tested bait proteins, which are fused to the C-terminal half of ubiquitin (Cub), via a spontaneous reconstitution of NubI and Cub. The reconstitution is independent of the proteins fused to the ubiquitin halves (Figure 4-14 A). Synthesis and localization of a bait protein in the ER or PM can therefore be monitored, like the interaction of defined protein pairs (see section 4.3.3), by growth under selective conditions on SD4 (-Leu-Trp-Ura-His) agar plates and colorimetric detection of active β-galactosidase (β-gal). Negative control preys fused to the mutated N-terminal half of ubiquitin (NubG, without affinity for Cub) should not interact with a control prey (Figure 4-14 B). Growth upon coproduction of a bait protein with negative control prey proteins indicates bait auto-activation, which can be caused by bait overexpression, nonspecific cleavage of the bait protein or an interaction of the bait protein with either Ost1p, Alg5p or Fur4p. Weak auto-activation can be suppressed by adding 3-amino-1,2,4-triazole (3-AT) to the medium used for screening (see section 4.4.3). Tested baits had to grow on selective medium in the presence of at least one positive control, but not in the presence of any negative control, to be immediately suitable for cytoY2H screening.

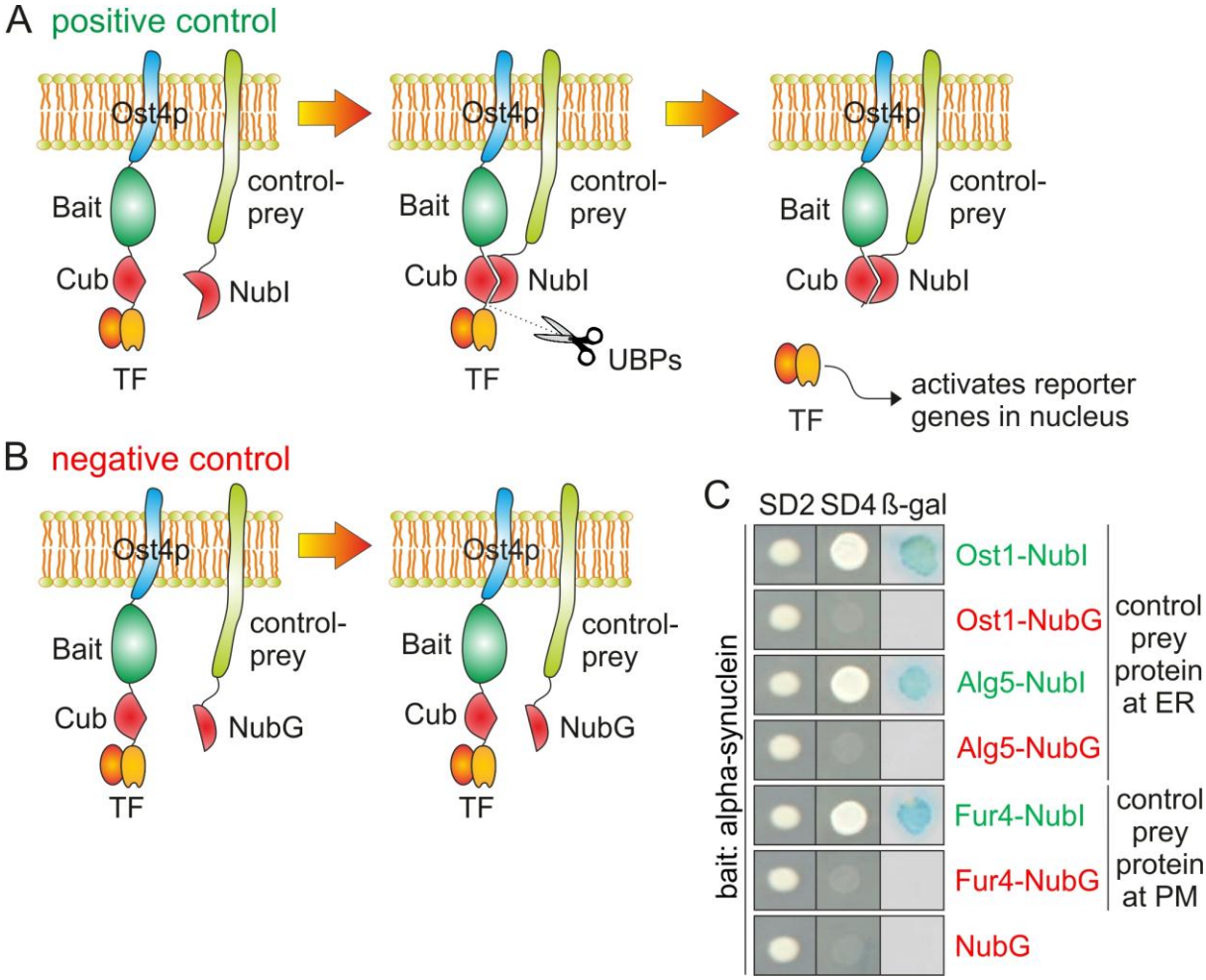

Figure 4-14: Demonstration of cytoY2H bait functionality using the NubG/NubI test. A: The positive controls for the NubG/NubI control test: The wild-type N-terminal half of ubiquitin is fused to yeast control prey proteins localized in the ER (Ost1p, Alg5p) or the plasma membrane (PM, Fur4p). The NubI-fusion proteins interact with any neighboring Cub fusion protein expressed in the same membrane, independent of the proteins fused to the ubiquitin-half. Formation of split-ubiquitin leads to cleavage by ubiquitin binding proteases (UBPs) and the release of the transcription factor (TF) with subsequent activation of reporter genes in the nucleus. Localization of a bait protein in the ER or PM, leading to the activation of the reporter genes, can therefore be monitored by growth on selective SD4 (-Leu-Trp-Ura-His) agar plates or colorimetric detection of active β-galactosidase (β-gal). B: The negative controls for the NubG/NubI control test: The mutated N-terminal half of ubiquitin (Ile13=>Glu) is fused to the same control prey proteins localized in the ER or the PM. The mutation decreases the affinity of the N- for the C-terminal ubiquitin half. Growth upon coproduction of baits with negative controls indicates bait auto-activation, which can be caused by bait overexpression, nonspecific cleavage of the bait protein or an interaction of the bait protein with either Ost1p, Alg5p or Fur4p. C: Yeast co-expressing wild-type alpha-synuclein as cytoY2H bait and positive (green) or negative (red) control preys or NubG alone were plated on SD2 (-Leu-Trp) agar plates selecting for the presence of both bait and prey plasmids. Subsequently, interactions were detected by growth and color change as described for A.

Only co-expression of the wild-type alpha-synuclein bait plasmid with the positive controls (green) but not with the negative controls (red) resulted in growth on selective SD4 agar plates and activation of the β-galactosidase gene (Figure 4-14 C). In addition, the alpha-synuclein baits carrying the A30P, E46K or A53T mutation were subjected to the NubG/NubI test and showed a similar growth pattern as the wild-type alpha-synuclein bait (see Supplementary Figure 1). However, the A30P and E46K

mutant baits of alpha-synuclein did not grow upon co-production with the positive control pFur4-NubI (localized at the PM), while the A53T mutant only showed weak growth when tested against this control. In contrast to the Y2H assay, in which the A53T mutant of alpha-synuclein showed auto-activating properties (see section 4.2.2), no auto-activation was detected for the cytoY2H bait generated from the A53T mutant isoform of alpha-synuclein. Taken together, these results indicate that the wild-type and mutant alpha-synuclein baits are produced in yeast and do not have auto-activating properties.

4.3.5 Synthesis of alpha-synuclein baits in yeast

Yeast cell fractionation and immunoblot analysis were used to confirm the synthesis and localization of wild-type alpha-synuclein as well as its mutant variants A30P, E46K and A53T (Figure 4-15). Therefore, the alpha-synuclein bait plasmids were transformed into the yeast strain DSY-6 (Dualsystems Biotech). This yeast strain is deleted for the vacuolar proteinase B (yscB), the vacuolar aspartyl protease (proteinase A) and the vacuolar carboxypeptidase Y (proteinase C). Due to these deletions, the strain is especially suitable for synthesis of recombinant proteins in yeast, as the degradation of synthesized proteins is reduced. Total cell lysates (T) were prepared from untransformed DSY-6 cells as well as cells transformed with the empty bait plasmid and cells transformed with plasmids encoding wild-type or mutant (A30P, E46K or A53T) alpha-synuclein bait proteins. In parallel, all yeast lysates were subjected to a two-step ultracentrifugation procedure to separate the cytosolic fraction (C) from the detergent-soluble membrane fraction (M). The cellular fractions were used for immunoblotting and detection of the bait proteins using an antibody specific for the LexA moiety of the transcription factor. Yeast fractionation was confirmed using antibodies against endogenous yeast proteins: The dolichol phosphate mannose synthase Dpm1p is a transmembrane protein localized in the yeast ER [273]. In contrast, 3-phosphoglycerate kinase Pgk1p is localized in the yeast cytoplasm [274].

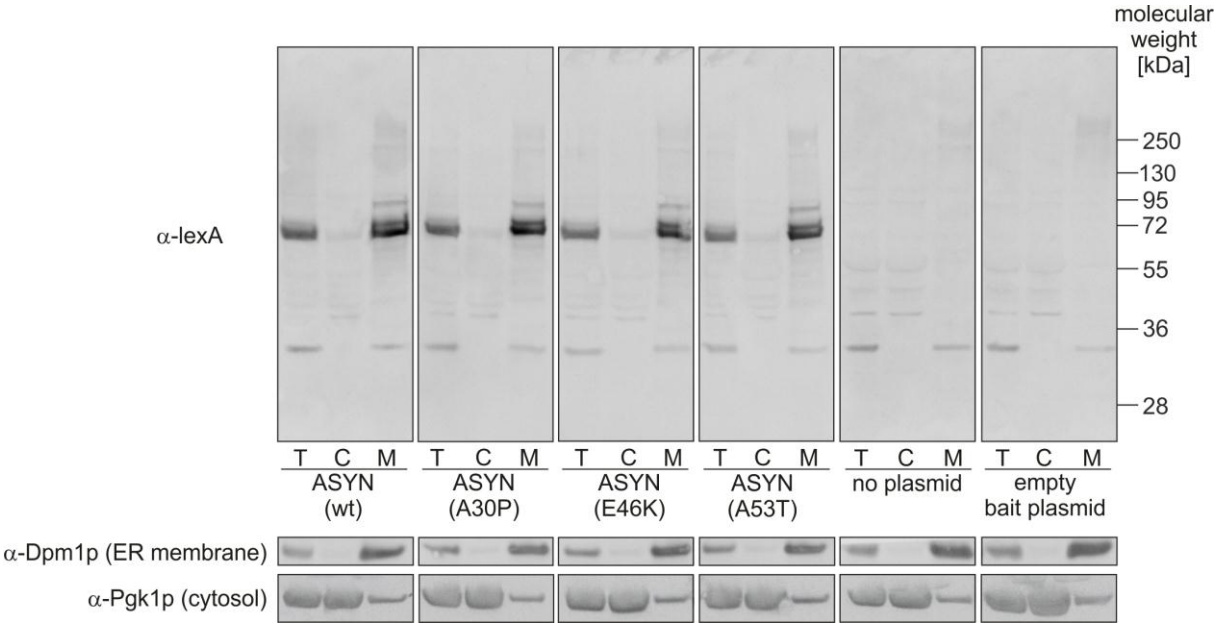

Figure 4-15: Investigation of alpha-synuclein bait synthesis in yeast cells. The empty cytoY2H bait plasmid and plasmids encoding wild-type or mutant (A30P, E46K or A53T) alpha-synuclein (ASYN) bait proteins were transformed into the yeast strain DSY-6. The resulting yeast transformants as well as the untransformed DSY-6 strain (no plasmid) were used to prepare total cell lysates (T). In parallel, all yeast lysates were subjected to two consecutive ultracentrifugation steps to separate the cytosolic fraction (C) from the detergent-soluble membrane fraction (M). The fractions were used for immunoblotting and detection of the bait proteins with an antibody specific for the LexA moiety of the transcription factor, which is fused to each cytoY2H bait protein. The separation of the fractions was confirmed using specific antibodies against the transmembrane ER protein Dpm1p and the cytosolic protein Pgk1p.

In all protein fractions prepared from yeast cells synthesizing wild-type or mutant alpha-sysnuclein, the transmembrane ER protein Dpm1p was detectable in the total and membrane fraction. The majority of the cytosolic protein Pgk1p was detectable in the total and cytosolic fraction. A low amount of Pgk1p could also be detected in the membrane fraction, probably due to cytosolic contaminations. These results indicate a separation of the cytosolic from the membrane fraction. For the wild-type as well as the mutant alpha-synuclein bait proteins, the LexA antibody showed a specific band in the total and in the membrane fractions. A predominant band of ~65 kDa was detected, while the theoretical size of alpha-synuclein with the cytoY2H tag (Ost1p-Cub-TF) is 56 kDa. This shows that the fusion proteins migrate slower than expected in SDS gels. One reason for this behavior could be that the protein is posttranslationally modified (e.g., glycosylation), which is commonly observed in yeast cells [275]. In addition, two faint bands at 72 (also visible in the cytosolic fraction) and 90 kDa were detected in the membrane fractions. These results confirm that wild-type and mutant alpha-synuclein proteins are localized in the membrane fractions of yeast cells. As the synthesized baits were positive in the NubG/NubI

genetic test and could be detected with an antibody specific for the LexA moiety, they were ready for high throughput cytoY2H interaction screening.

4.3.6 Summary of chapter 3

The vectors of the cytoY2H and MYTH system were successfully modified for high-throughput cloning and subsequent screening of PPIs. Correct function of the generated vectors was confirmed by reproducing published interactions between selected protein pairs. Subsequently, cytoY2H bait plasmids were generated from wild-type alpha-synuclein and its mutant isoforms A30P, E46K and A53T. The function of the generated bait proteins was confirmed using the genetic NubG/NubI test. In contrast to the classic Y2H system, the cytoY2H bait protein carrying the A53T mutation of alpha-synuclein did not have auto-activating properties. Finally, the correct synthesis and localization of all bait proteins was confirmed by immunoblot analysis that allowed the detection of alpha-synuclein in yeast membrane fractions.

4.4 Creating an alpha-synuclein interaction network based on cytoY2H and MYTH screening data

As alpha-synuclein is primarily located in the presynaptic terminals of neurons [276], the aim of these studies was to screen the generated alpha-synuclein cytoY2H baits for interactions against a prey matrix of synaptic proteins. Entry clones encoding soluble and membrane proteins were selected and used to generate the prey plasmids as well as additional bait plasmids. The MYTH system was used to screen for PPIs of membrane proteins, while the soluble proteins were tested in the cytoY2H system. Together with other bait proteins, the previously generated alpha-synuclein baits were then screened as part of a large PPI screen against the generated prey matrix, which also contained an alpha-synuclein prey protein.

4.4.1 Generating a prey matrix for cytoY2H and MYTH interaction screening

It has been published that alpha-synuclein is primarily located in the presynaptic terminals of neurons [261]. In order to get additional hints about the function of alpha-synuclein in the synapse, especially when it is recruited to membranes [261] by localization to the ER in the cytoY2H system, a list of genes encoding synaptic proteins was generated. The list of genes was created based on associated GO terms that described cellular components like “synapse”, “synaptic vesicle”, “postsynaptic membrane” and further synonyms of the term synapse. Genes encoding additional synaptic proteins were retrieved from the synapse protein

database SynDB [277]. To obtain more information on a potential role of alpha-synuclein in other neurodegenerative diseases [184], genes known to be involved in various neurodegenerative disorders were also added to the list, along with other genes of interest. Entry clones encoding the corresponding proteins were then used to generate a matrix of preys that could be screened for PPIs against cytoY2H baits generated from wild-type alpha-synuclein and its pathological mutants. For some proteins more than one entry clone encoding a protein was available. For example, these entry clones encoded different isoforms of a gene product. This is the reason why the number of unique proteins encoded by the entry clones is lower than the total number of selected entry clones: The prey plasmids were successfully generated from 297 entry clones encoding soluble proteins (222 unique proteins) and 193 entry clones encoding proteins with at least one transmembrane domain (172 unique proteins), resulting in 490 prey plasmids. The prey plasmids also included a prey plasmid generated from wild-type alpha-synuclein (clone CCSB_6120, Figure 4-4). All prey plasmids were generated by Gateway™ cloning using the vector pGPR4-Ns, which can be applied for interaction screening with both the cytoY2H and MYTH system. Previously performed experiments tested a defined set of interacting proteins fused to N-terminal and C-terminal cytoY2H and MYTH tags. In these experiments, most interactions could be detected with N-terminally tagged prey proteins expressed from the vector pGPR4-Ns. The identity of all prey plasmids was confirmed by restriction digestion and sequencing of the corresponding entry clones. Subsequently, the prey plasmids were transformed into the yeast strain L40ccua (MATa).

4.4.2 Generation of additional bait plasmids for cytoY2H and MYTH interaction screening

A common observation in classic Y2H assays is that many binary PPIs cannot be detected “bidirectionally”, meaning that an interaction can only be detected when protein X is used as bait protein and protein Y is a prey protein, but not vice versa. This can be due to steric hindrance or incorrect folding after synthesis of either the bait or prey proteins fused the tags, which allow the detection of PPIs [278, 279]. To avoid this problem in the interaction screen presented here, additional bait plasmids were generated from the entry clones encoding synaptic proteins (selected in section 4.4.2). As part of a large PPI screen, these bait proteins were subsequently tested for interaction against the proteins in the prey matrix, which also contained a wild-type

alpha-synuclein prey protein. Therefore, cytoY2H bait plasmids were generated from entry clones encoding soluble synaptic proteins. MYTH bait plasmids were generated from entry clones encoding transmembrane proteins. 207 entry clones encoding 186 unique proteins associated with the GO term “integral to membrane” were successfully Gateway™ cloned into the MYTH bait vectors pGBT5-Ns and pGBT5-Ste. 305 entry clones encoding 225 unique soluble proteins were successfully Gateway™ cloned into the cytoY2H bait vector pGDHB2. The identity of all bait plasmids was confirmed by restriction digestion of the expression plasmids and by sequencing the entry clones used to generate the bait plasmids. Confirmed plasmids were then transformed into the yeast strain L40ccα (MATα).

4.4.3 Perfoming the NubG/NubI interaction test in high-throughput format

To test the function of the generated cytoY2H and MYTH bait proteins, they were subjected to the NubG/NubI genetic test using a high-throughput format. Therefore, clones of the yeast strain L40ccα (MATα), each carrying a single cytoY2H or MYTH bait plasmid, were mixed with yeast clones (strain L40ccua, MATa) transformed with positive and negative control plasmids (for details see section 4.3.4) and mated on YPD agar plates. Subsequently, diploid clones were transferred onto SD4 (-Leu-Trp-Ura-His) agar plates for selection of bait and control prey protein interaction (Figure 4-16 A). In this high-throughput version of the NubG/NubI test, up to 72 bait proteins were tested for their function. Each bait protein was tested against each control prey protein in four repetitions and in eight repetitions against NubG alone, which was expressed from the empty prey plasmid (Figure 4-16 B).

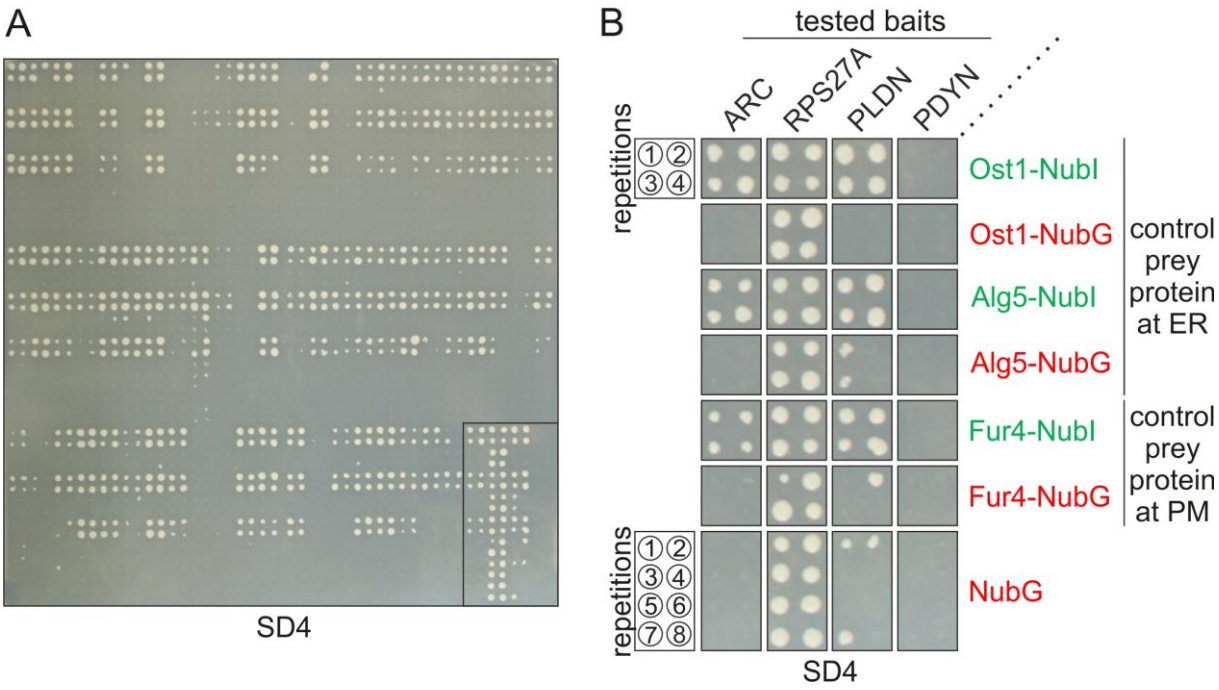

Figure 4-16: Functional test of cytoY2H and MYTH baits in high-throughput format using the NubG/NubI test. A: High-throughput functional test of baits. 72 cytoY2H and MYTH bait proteins were co-produced with control prey proteins in yeast and tested for growth on SD4 (-Leu-Trp-Ura-His) agar plates, selecting for the interaction of bait and prey proteins. B: Enlargement of the area marked in A. Four cytoY2H bait proteins were each tested against positive (green) and negative control prey proteins (red) localized to the ER or the plasma membrane (PM) in four repetitions. In addition, baits were tested in eight repetitions against NubG alone. Bait proteins like the activity regulated cytoskeleton associated protein (ARC), that only showed growth with positive controls, were classified as of "correct function" and used for screening. Bait proteins like the ribosomal protein S27a (RPS27A), that showed robust growth with all control prey proteins, were classified as a bait with "strong auto-activation" properties. Baits in this category were not used for screening. Bait proteins like Pallidin homolog (PLDN) showed robust growth when tested with positive control preys along with smaller colonies when tested with negative controls. This growth pattern was used to define "weak auto-activating" baits. Baits from this category were screened on selective medium containing 3 AT to inhibit growth due to autoactivation. Bait proteins like Prodynorphin (PDYN), that showed no growth at all, were not used for screening.

According to the resulting growth pattern, the bait proteins were grouped into four categories: "correct function", "strong auto-activation", "weak auto-activation" and "no growth". Figure 4-16 B showing only cytoY2H baits, gives an example for each category. The activity regulated cytoskeleton associated protein (ARC) showed growth only when tested with positive control preys, indicating the "correct function" of the bait [137]. Baits in this category, which had to interact with a positive control in at least 2 repetitions, but not with any negative control, were determined to be ready for cytoY2H and MYTH screening. Similar to the alpha-synuclein mutant bait proteins (Supplementary Figure 1), many baits only interacted with positive control preys localized in the ER (Ost-NubI and Alg-NubI), but not with control preys localized in the PM (Fur-NubI). In contrast, the ribosomal protein bait protein S27a (RPS27A) induced yeast growth in the presence of all control preys, indicating "strong auto-

activation" properties of the bait protein. RPS27A, a precursor of ubiquitin, contains a ubiquitin homolog domain (UBQ) [280] that might be recognized and cleaved by UBPs, freeing the transcription factor to activate the reporter genes in the nucleus and promoting growth on SD4 medium. Baits in this category were not used for screening. Other baits like the Pallidin homolog (PLDN) showed robust growth when tested with positive controls and smaller colonies with negative controls. This growth pattern was used to define baits with "weak auto-activating" properties. PLDN contains two coiled-coil (CC) domains [281] that could function as oligomerization domains [282] and thereby promote binding to the negative control preys. Yeast expressing bait plasmids from this category were tested again. This time the stringency of the selective medium was improved by the inclusion of 3-amino-1,2,4-triazole (3-AT). This compound is a competitive inhibitor of the *HIS3* gene product and therefore increases the threshold of selection. A titration of 1 to 30 mM 3-AT in the selection medium was tested and a concentration of 1 mM was found to be sufficient to inhibit most of the growth caused by auto-activating baits. However, some bait proteins still showed growth when co-produced with the negative control prey proteins and were not further used for screening. All subsequent interaction tests involving the constructs that successfully passed the repeated test were performed on SD4 agar plates containing 1 mM 3-AT. The last class of baits did not show any growth on SD4 plates at all, for example the Prodynorphin (PDYN) bait protein. PDYN contains an N-terminal signal peptide [283] that could lead to mistargeting and subsequent degradation of the gene product. Baits of this category were not used for screening. After passing the high-throughput NubG/NubI test, 76 MYTH baits were used for screening; 6 of these baits were screened on medium supplied with 3AT. In addition, 159 cytoY2H baits were also taken forward for screening; 27 of these baits required screening on 3AT supplied medium. Figure 4-17 shows the alpha-synuclein isoforms and the numbers of synaptic proteins that were screened as baits or preys, as well as their overlap.

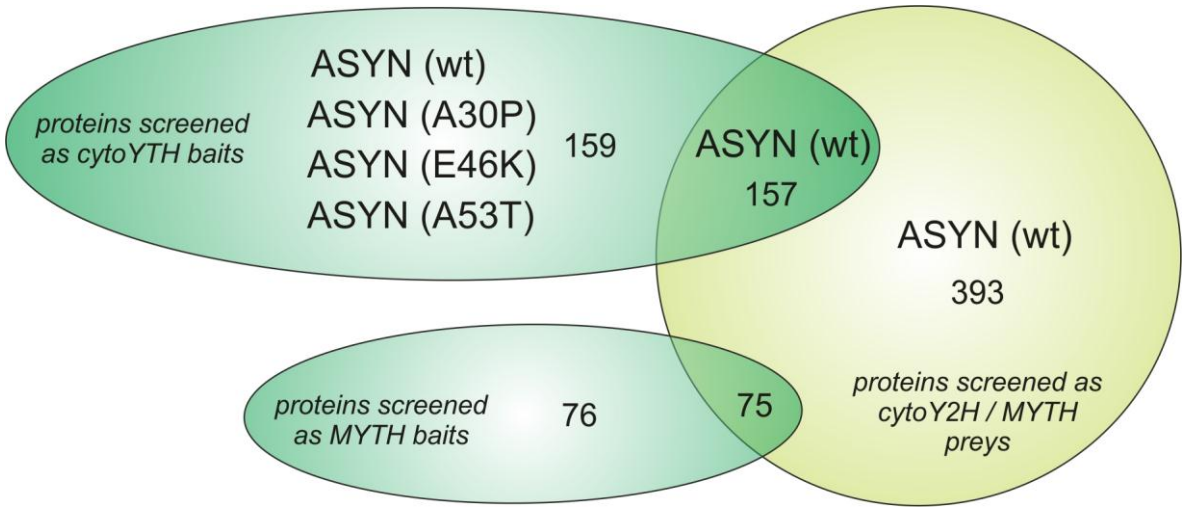

Figure 4-17: Alpha-synuclein isoforms and other synaptic proteins screened in the cytoY2H and MYTH system. The different isoforms of alpha-synuclein (wt, A30P, E46K and A53T) as well as the number of additional synaptic proteins (represented by numbers) that were screened in cytoY2H or MYTH are shown in a venn diagram. Only baits that successfully passed the NubG/NubI test were used for screening.

4.4.4 cytoY2H and MYTH screening procedures

Yeast transformants carrying a cytoY2H bait plasmid encoding wild type alpha-synuclein or its mutant isoforms (A30P, E46K and A53T) were united with transformants carrying the bait plasmids generated from additional synaptic proteins (see section 4.4.3) in pools of 16 baits each. These pools were screened against the cytoY2H / MYTH prey matrix of synaptic proteins (see section 4.4.1), which included a prey generated from wild-type alpha-synuclein. The pool screen and the subsequent backmating step were performed as described for the Y2H array screening approach (section 4.2.3 and 4.2.4). The pool screen was performed in four repetitions and all interactions of a prey with a bait pool containing an alpha-synuclein bait plasmid were analyzed in the backmating, even if the interaction could only be detected in one of the pool screen repetitions. Many biologically important interactions, for example those of various enzymes with their substrates, are often relatively weak and cannot be easily detected by Y2H assays [194]. In order to detect these weak interactions all PPIs of alpha-synuclein baits detected by cytoY2H in the backmating, including those that were only found once by growth on SD4 or in the β-gal assay, were taken into account. In the backmating step following the cytoY2H pool screen, each prey protein was tested for interactions against at least 16 bait proteins. See Supplementary Table 5 for detailed results. During the analysis of the cytoY2H results, the sizes of the growing yeast colonies and the size of the blue coloration from the β-galactosidase assay were categorized as small, medium or large. 1 point was awarded for a small colony / spot, 2 points for a medium colony /

spot and 3 points were awarded for a large colony / spot. For the final results ("result SD4" or "result lacZ" in Supplementary Table 5) the points from all four repetitions were added. This means that an interaction can get a maxium SD4 and lacZ score of 12 each (large colonies / spots in all 4 repetitions). Apart from identifying the specific bait or baits from a pool interacting with a prey, the PPI data generated in the backmating was also used for a "bait dependency testing" to ensure the identification of specific PPIs [137]. To test for bait dependency, the interaction spectrum of each prey protein that interacted with an alpha-synuclein bait protein was analyzed for interactions with unrelated control bait proteins. If a prey protein interacted with more than 50% of all bait proteins it was tested against, all interactions with that prey protein were considered unspecific. However, all tested interactions were found to be bait-dependent. In addition, interactions of the wild-type alpha-synuclein bait with 21 proteins, which were detected in the cytoY2H re-test of interactions detected by the subSEQ method (see section 4.5.12), were included in cytoY2H PPI dataset.

4.4.5 Results of the cytoY2H / MYTH screen

Surprisingly, the alpha-synuclein prey protein did not interact with any of the cytoY2H or MYTH bait proteins. Thus, as only the cytoY2H but not the MYTH screen detected PPIs with alpha-synuclein, the screening procedure will henceforth be referred to as "cytoY2H screen". In total, wild-type alpha-synuclein interacted with 251 prey proteins (254 clones). Only a small number of interactions was found for the mutant alpha-synuclein baits: 5 proteins (5 clones) interacted with the A30P mutant, while 4 proteins (4 clones) interacted with the E46K mutant. Interestingly, the interaction of 15 proteins (15 clones) with the A53T mutant bait of alpha-synuclein was detected in the cytoY2H screen. A PPI screen of this mutant protein was not possible in Y2H due to the autoactivating properties of the bait. The complete list of protein-protein interactions detected by cytoY2H can be found in Supplementary Table 5.

4.4.6 Confidence scoring of alpha-synuclein interactors detected by cytoY2H

The bioinformatic scoring system used previously to rank the detected Y2H interactions (see section 4.2.6) was applied to the interactions identified in the cytoY2H screen. 75% of the interactions with the wild-type bait were predicted to be low confidence (LC), while 3% were ranked as medium confidence (MC) and 22% were ranked as high confidence (HC) interactions. All interactions of the mutant alpha-synuclein isoforms ranked as low confidence.

4.4.7 Gene-term enrichment analysis of alpha-synuclein interactors detected by cytoY2H

In order to detect biological processes shared by interactors of alpha-synuclein detected in the cytoY2H screen, gene-term enrichment analysis was performed using the DAVID functional annotation tool [162, 163]. Thus, 55 high confidence interactors of wild-type alpha-synuclein were annotated. As were 2 published interactors of alpha-synuclein that were also detected by cytoY2H but were ranked as LC. In order to obtain high confidence results related to PD, only proteins surely co-expressed with alpha-synuclein in the human brain were selected. Therefore, expression data was obtained from HPRD [158] and 4 proteins not expressed in the human brain were removed. Interactions with proteins for which no expression information was available were kept in the list of interactors. After these selection steps, the genes encoding the remaining 53 proteins interacting with wild-type alpha-synuclein were subject for the enrichment analysis. Initially, the gene-term enrichment analysis was performed using the human genome as background list. Terms like the GO Biological Processes “synaptic transmission”,” transmission of nerve impulse” and “regulation of neurotransmitter levels” were found to be enriched with statistical significance (p-value <0.05). This was probably due to the composition of the proteins cytoY2H / MYTH prey matrix, which mainly consisted of synaptic proteins (see section 4.4.1). Therefore, the enrichment analysis was performed using the genes in the prey matrix as background. However, this analysis did not produce statistically significant results.

4.4.8 Interactors of wild-type alpha-synuclein detected by cytoY2H

Proteins interacting with wild-type alpha-synuclein in cytoY2H that were predicted as HC interactors are shown in Figure 4-18. The figure also includes published interactors of alpha-synuclein detected by cytoY2H that only ranked as LC. The official gene symbols are used to show the interacting proteins.

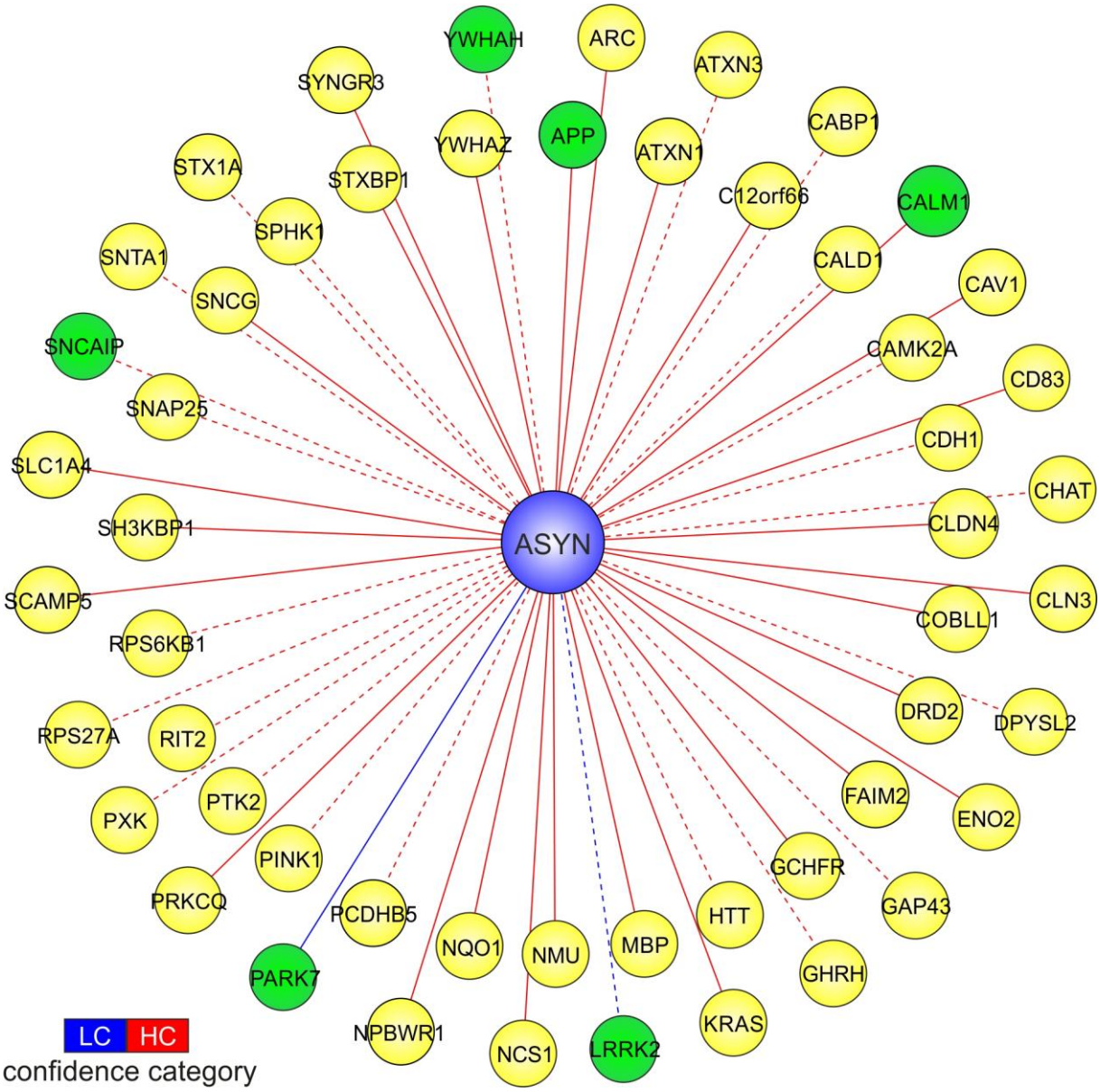

Figure 4-18: Interactors of wild-type alpha-synuclein detected by cytoY2H interaction screening. Predicted high-confidence and published interactors of wild-type alpha-synuclein detected by cytoY2H screening are shown. Published interactors are shown with a green node, while all other proteins are shown with yellow nodes. The edge color represents predicted low confidence (LC and high confidence (HC) interactions, as indicated in the scale bar. Bait-prey interactions activating one reporter gene are connected to alpha-synuclein with a dotted edge. Bait-prey interactions activating both reporters are connected with a solid edge.

The prey matrix used for the cytoY2H screen contained clones potentially expressing 12 published interactors of alpha-synuclein. In the cytoY2H array screen 6 of these proteins did interact with alpha-synuclein. The fact that published interactions could be identified with the cytoY2H system validates the method as a tool for the detection of novel interactors of alpha-synuclein. Interestingly, the interactions of alpha-synuclein with parkinson protein 7 (PARK7) and the alpha-synuclein interacting protein (SNCAIP) were only detected in the cytoY2H but not in the classic Y2H

screen. This indicates that classic Y2H and cytoY2H could be used in parallel to generate more comprehensive PPI networks.

Similar as the Y2H assay, cytoY2H detected the interaction of wild-type alpha-synuclein with several proteins that are known to be involved in other neurodegenerative disorders: APP and CALM1 are associated with Alzheimer's disease (AD) [216, 217] and ATXN1 and ATXN3 are associated with Spinocerebellar ataxias [213, 214]. Furthermore, CLN3 is involved in Batten disease [284] and HTT plays an important role in Huntington's disease (HD) [209]. The cytoY2H screen also detected several interactions of alpha-synuclein with proteins associated with cancer: CDH1, KRAS, NQO1, PIAS3, PTK2 and SNCG [221, 285-289]. There is a growing number of proteins that are involved in both cancer and neurodegenerative disorders [229]. With the CytoY2H system the reported alpha-synuclein interactions with the serine / threonine kinases CAMK2A, LRRK2, PINK1, PXK, PRKCQ and RPS6KB1 were detected. Furthermore, alpha-synuclein interacted with the tyrosine kinase PTK2 and, surprisingly, also with the lipid kinase SPHK1. Of these kinases, only LRRK2 is known to phosphorylate alpha-synuclein [232, 234]. The phosphorylation state of alpha-synuclein is important for its ability to form fibrils [72]. Moreover, the specific phosphorylation of serine [231] and tyrosine [232, 233] residues in alpha-synuclein has been demonstrated. In future experiments, the interacting kinases might be tested for their ability to phosphorylate alpha-synuclein and modulate its ability to form fibrils.

4.4.9 Interactions of wild-type and mutant alpha-synuclein detected by cytoY2H interaction screening

In addition to numerous interactions with wild-type alpha-synuclein, the cytoY2H screen also identified proteins interacting with the mutant isoforms of alpha-synuclein (A30P, E46K and A53T). In order to identify shared interactions or interactions specific for a certain mutant, the interacting proteins were grouped according to the alpha-synuclein isoforms. Only detected HC interactors of wild-type alpha-synuclein and all interactors of the mutant alpha-synuclein isoforms were taken into account. Furthermore, published interactors of wild-type alpha-synuclein detected in the cytoY2H screen but ranked as LC were included. Only proteins that are co-expressed with alpha-synuclein in the human brain were selected. Thus, expression data was obtained from HPRD [158] and proteins not expressed in the human brain were

removed. Proteins for which no expression information was available were kept in the list of interactors.

Along with 64 interactors of wild-type alpha-synuclein and 5 interactors of the A30P mutant, 4 interactors of the E46K mutant and 12 interactors of the A53T mutant isoform were arranged in groups (Figure 4-19). Group 1 contains 52 proteins that exclusively interacted with the wild-type alpha-synuclein bait protein. The second group summarizes 7 proteins, which interacted with the wild-type bait and the A30P mutant isoform. A third group contains 3 proteins that individually interacted with wild-type alpha-synuclein as well as its A30P and A53T mutant, while the 3 proteins in the last group 4 interacted with all alpha-synuclein isoforms. In addition, one interaction was found exclusively with the E46K mutant but not with other baits.

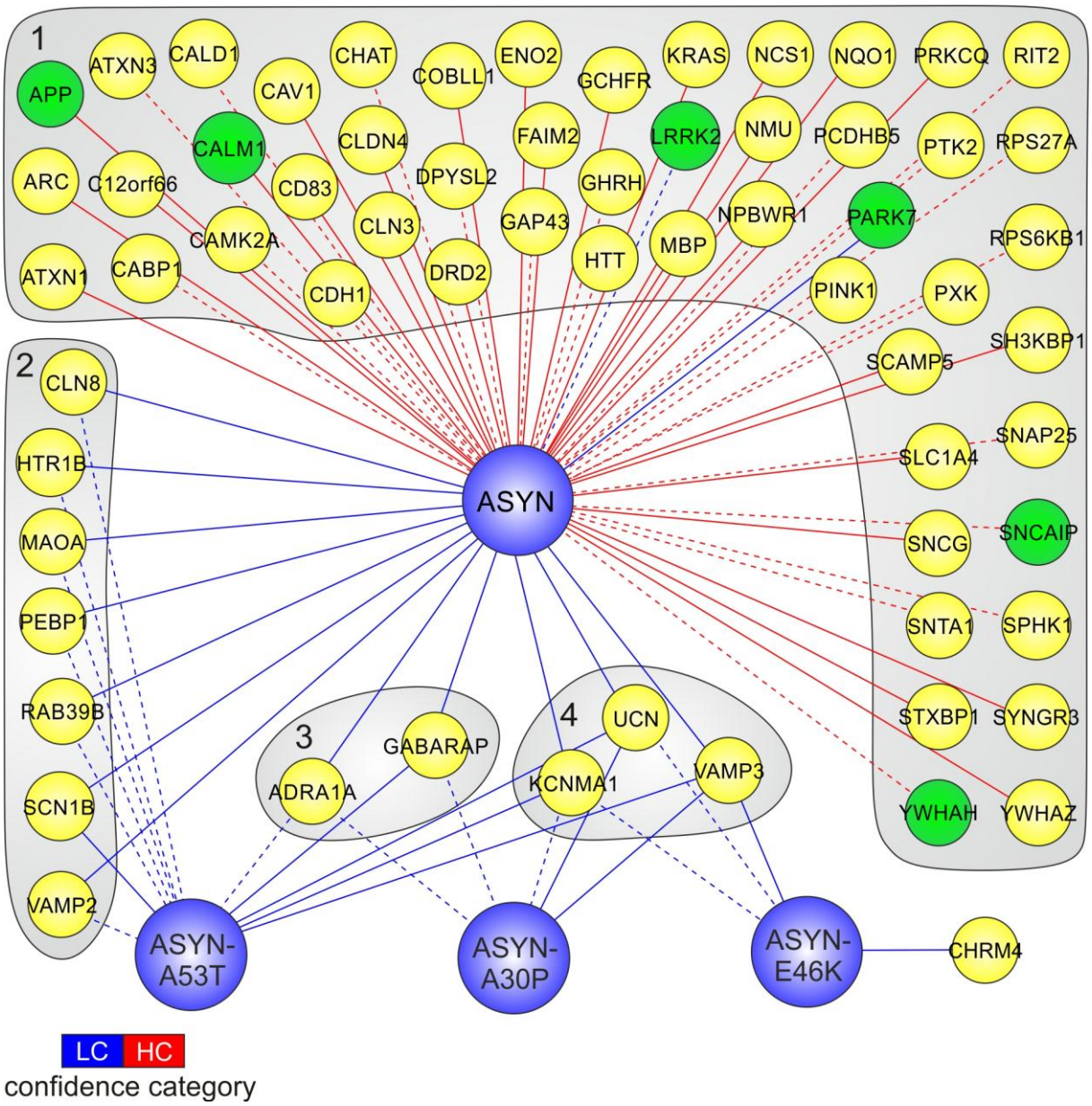

Figure 4-19: Interactors of wild-type and mutant alpha-synuclein detected by cytoY2H interaction screening. Interactors of wild-type and mutant alpha-synuclein were grouped according to their wild-type / mutant specificity, as indicated by the numbered grey outlines. For the wild-type bait, only predicted high confidence (HC) and published interactors were grouped. For the mutant baits, interactors of all confidence categories were taken into account. Published interactors are shown in green while all others are shown with yellow nodes. The edge color represents predicted low confidence (LC) and high confidence (HC) interactions, as indicated in the scale bar. Bait-prey interactions activating one reporter gene are connected to alpha-synuclein with a dotted edge. Bait-prey interactions activating both reporters are connected with a solid edge.

In contrast to the analysis of the Y2H interactions of wild-type and mutant alpha-synuclein proteins, most of the interactions identified in the cytY2H system were only detected with wild-type alpha-synuclein (Figure 4-19). In addition, only a few proteins interacted with two or even more alpha-synuclein baits. It is likely that the mutation of alpha-synuclein changes the binding properties of the bait protein, leading to an abnormal interaction spectrum of the mutant isoforms. In the cytoY2H screen, the

proteins in group 2 interacted with both wild-type alpha-synuclein as well as its A53T mutant. One protein from this group, the enzyme monoamine oxidase A (MAOA), is responsible for the degradation of amine neurotransmitters, for example dopamine [290]. The process of dopamine degradation is strongly associated with PD and inhibitors of both types of this enzyme (A and B) are currently being used as neuroprotective agents to treat neurodegenerative disorders [291]. Another protein in group 2, the vesicle-associated membrane protein 2 (VAMP2 / synaptobrevin 2), is part of the SNARE-complex, which is known to be involved in the docking and the fusion of synaptic vesicles with the presynaptic membrane [292]. Interestingly, alpha-synuclein has been shown to interact with components of the SNARE-complex and to promote complex assembly *in vivo* and *in vitro* [293]. Amongst other proteins, Urocortin (UCN) was found to interact with all isoforms of alpha-synuclein. Urocortin belongs to the corticotropin-releasing hormone (CRH) family of neuropeptides, that are involved in the regulation of stress responses [294]. Strikingly, the peptide has a protective effect on neurons against oxidative and excitotoxic cell death [295]. In addition, the benefits of Urocortin in PD could be demonstrated in two rodent models [296]. These examples demonstrate that the analysis of the mutant alpha-synuclein interactions can identify processes that are known to be associated with PD. Thus, the analysis can also be used to find detected novel PPIs associated with specific biological processes that could give hints on the function of alpha-synuclein in PD.

A potassium large conductance calcium-activated channel (KCNMA1) interacted with all isoforms of alpha-synuclein in the cytoY2H screen and was therefore associated with group 4 (Figure 4-19). Large potassium channels like KCNMA1 are fundamental to the control of smooth muscle tone and neuronal excitability [297]. Interestingly, KCNMA1 knockout mice show symptoms of cerebellar ataxias [298], creating an additional link between PD and other neurodegenerative diseases.

The vesicle-associated membrane protein 3 (VAMP3), which is also known as cellubrevin, interacted with all isoforms of alpha-synuclein. The v-SNARE protein VAMP3 is associated with autophagy [299], an intracellular degradation process that plays an important role in PD [300]. In addition, the protein levels of VAMP3 were significantly increased in dopaminergic cells after rotenone exposure [301]. By interacting with VAMP3, alpha-synuclein might impair autophagic processes.

The gamma-aminobutyric acid receptor-associated protein (GABARAP) interacted with wild-type, A30P and A53T mutant alpha-synuclein. GABARAP is associated with

autophagic processes [302]. A knockdown of GABARAP in a cell model of PD [107] could give further hints on the protein's role in PD. Furthermore, GABARAP deficient mice are phenotypically normal [303]. The neurotoxins MPTP or rotenone could be used to generate symptoms mimicking PD in these knockout mice and the effects could be compared with wild-type mice treated with these chemicals [21, 304].

4.4.10 Disease association and drug or compound availability for interactors detected by cytoY2H

The identification of interaction partners of alpha-synuclein with a known disease association might give additional hints on the role of alpha-synuclein in PD pathology. Therefore, the third analysis of the interacting proteins detected in the cytoY2H array screen focused on genetic diseases associated with the proteins and their possible amenability for available drugs or other small molecules. For this analysis, all predicted low, medium and high confidence interactors of wild-type and mutant alpha-synuclein were considered. Only proteins which are co-expressed with alpha-synuclein in the human brain were selected to get high confidence results that relevant to PD. Expression data was extracted from HPRD [158] to remove proteins expressed in other tissues than the human brain. Drug information was available from the DrugBank database [242], while disease association data was extracted from the OMIM database [241]. More information on both topics was retrieved from the GeneCards database [243]. Only interactions with disease associated proteins and / or where small molecules potentially targeting the interacting proteins were available were analyzed further.

A disease association was found for 51% of the interactors of wild-type alpha-synuclein. For 36% of the interaction partners compounds or small molecules targeting them were available. In total, 116 interactors of the wild-type bait were analyzed further. Interestingly, I found that 67% of the interactors of A53T alpha-synuclein were associated with a genetic disease and 47% of them are known targets for chemical compounds. 9 interactors of the A53T mutant isoform were used for further analysis. Only 2 proteins interacting with the A30P mutant and 2 proteins interacting with the E46K mutant of alpha-synuclein were found to have a disease association and were targets for small molecules. In Figure 4-20, the selected interactors of alpha-synuclein were grouped into one of four categories: receptors, ligands, ion channels or membrane transporters. The information used to categorize the interactors was obtained from the NCBI RefSeq summary linked for each

corresponding gene in the GeneCards database [243]. 30 interactors were grouped as receptors and 9 interactors were grouped as ligands. In addition, 9 proteins were assigned to the group of ion channels and 6 proteins were grouped as membrane transporters.

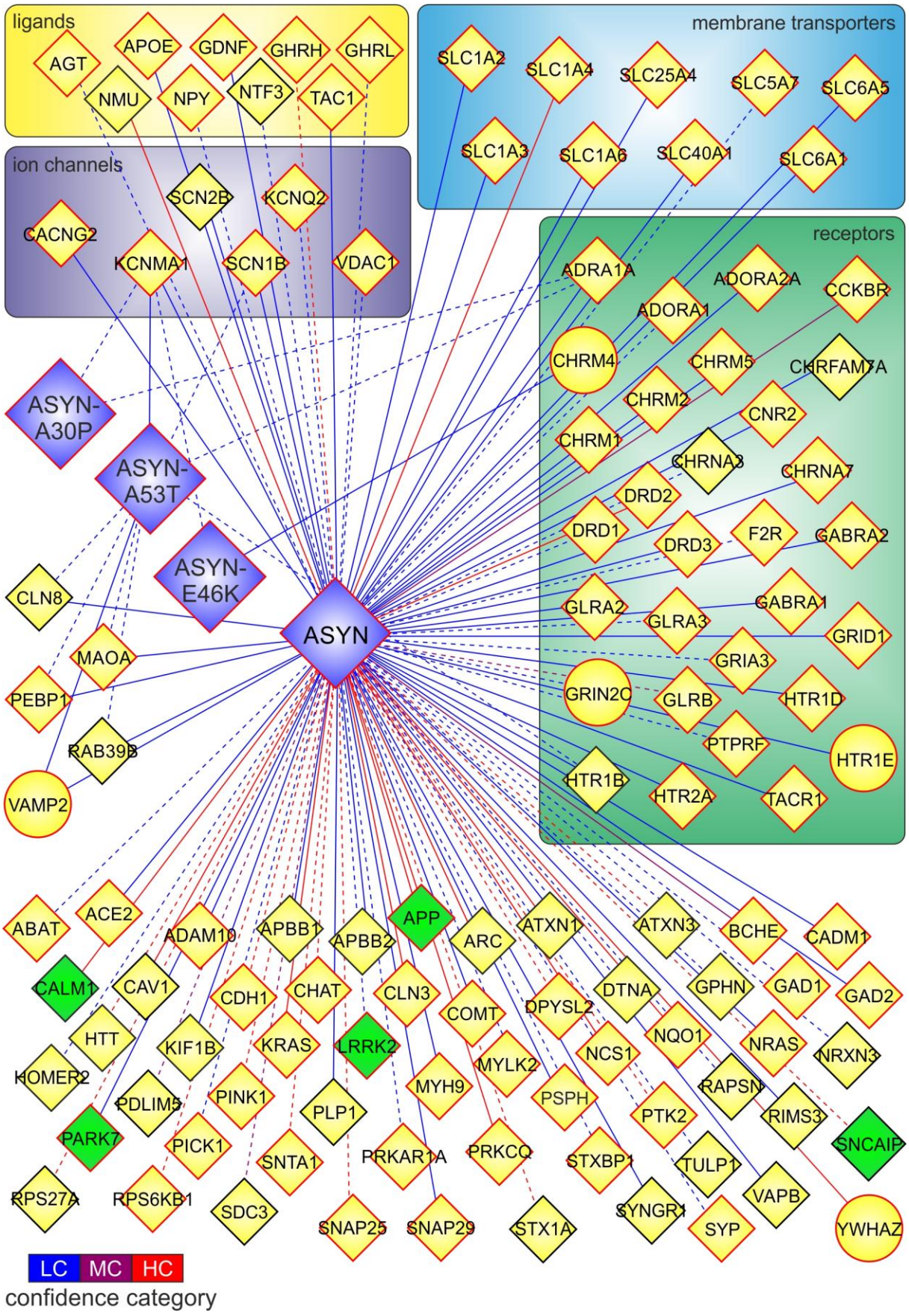

Figure 4-20: Disease association and compound availability for interactors detected by cytoY2H interaction screening. Proteins interacting with alpha-synuclein that had a disease association and / or where small molecules targeting the interacting protein are available were grouped according to one of the following categories: receptors, ligands, ion channels or membrane

Figure legend continued on next page.

transporters. Information was retrieved from OMIM, GeneCards and DrugBank databases. Interactors associated with genetic diseases are shown as a diamond. If interacting proteins were known compound targets, the border color of the node was changed from black to red. Published interactors are shown in green while all others are shown with yellow nodes. The edge color represents predicted low confidence (LC), medium confidence (MC) and high confidence (HC) interactions, as indicated in the scale bar. Bait-prey interactions activating one reporter gene are connected to alpha-synuclein with a dotted edge. Bait-prey interactions activating both reporters are connected with a solid edge.

The cytoY2H screen detected interactions of wild-type alpha-synuclein with three subtypes of the dopamine receptors (DRD1, DRD2 and DRD3). Defects in all dopamine receptor subtypes have been associated with schizophrenia [305-307]. There are various lines of evidence suggesting that alpha-synuclein influences dopamine receptors [308-310], yet so far no direct interaction has been demonstrated. Selective agonists and antagonists for all three subtypes that were found to interact with alpha-synuclein are available. The dopamine D3 receptor appears to play an important role in neural development [311] and the delivery of a specific receptor agonist led to neurogenesis and recovery of locomotor function in a PD mouse model [312]. An additional trans-membrane protein, the adrenergic, alpha-1A-, receptor (ADRA1A), was found to interact with all isoforms of alpha-synuclein. Interestingly, the number of these receptors was found to be increased in PD patients [313]. The ADRA1A antagonist Idazoxan improves the anti-parkinsonian actions of the dopamine precursor L-DOPA and reduces its dyskinesia side-effects in a primate model of Parkinson's disease [314]. The cytoY2H screen detected a previously unknown PPI of wild-type alpha-synuclein with the extraneural DA degradation enzyme catechol-ortho-methytransferase (COMT). COMT is an enzyme degrading dopamine and other catecholamimes [315]. A role of COMT in schizophrenia has been implicated [316]. Interestingly, COMT is transcriptionally downregulated in mice expressing the A53T mutant of alpha-synuclein [309]. In addition, COMT has been suggested as a drug target in PD, and specific inhibitors of the enzyme are used in combination with L-DOPA in the drug therapy of the disease [317]. Alpha-synuclein also interacted with the glial cell derived neurotrophic factor (GDNF). This factor enhances the survival and morphological differentiation of dopaminergic neurons and increases their high-affinity dopamine uptake [318]. Clinical trials with PD patients have shown a beneficial effect of GDNF on disease progression [319, 320].

The previous examples demonstrate that the current analysis can identify disease-associated proteins with a published role in PD. Targeting these proteins with chemical compounds or administration of the proteins themselves produces positive effects in models of PD. Administration of the compounds or proteins is even used as

therapeutic approach to treat PD patients. The analysis can thus be used to identify new potential therapeutic targets for PD. Agonists or antagonists of these targets could be tested for possible effects in PD models.

The cytoY2H screen detected an interaction of alpha-synuclein with Tachykinin (TAC1) and its receptor (TACR1). Tachykinin, which is also known as substance P, is involved in the regulation of neuronal survival and degeneration [321]. A role of Tachykinin and its receptor in neurodegenerative disorders has been suggested [322]. TACR1 antagonists prevent degeneration of neurons induced by methamphetamine [323]. These chemicals and could be tested in cell [107] and animal models [258] of PD.

Alpha-synuclein also interacted with the protein interacting with PRKCA (PICK1). A role of PICK1 in schizophrenia [324] and cancer [325] has been suggested. It has been demonstrated that PICK1 interacts with dopamine transporters (DAT) [326]. Interestingly, binding of alpha-synuclein to DAT leads to increased cellular dopamine uptake and dopamine-induced cellular apoptosis [327], and PICK1 might mediate this interaction or play a regulatory role. PICK1 can be inhibited by the small-molecule FSC231 and a possible therapeutic effect could be tested in a cell model of the disease [107].

CytoY2H also detected an interaction of alpha-synuclein with the protein tyrosine phosphatase, receptor type, F (PTPRF). Knock-down of this protein tyrosine phosphatase induces insulin resistance in HEK cells [328] and insulin signaling was found to be defective in a PD mouse model [329]. Along with other evidence, these findings indicate that PTPRF might be a possible link between the diseases. Systemic treatments with LAR-targeting peptides that inhibit protein-tyrosine kinase function (LAR wedge Tat peptides) showed survival- and neurite-promoting effects in PC12 cells [330] and these peptides could be tested for an effect in PD cell [107] or mouse models [258] of PD.

4.4.11 Summary of chapter 4

A cytoY2H screen of alpha-synuclein against an array of synaptic prey proteins was performed. The screen detected 6 published (50% of the interactions that could potentially have been detected) as well as 245 previously unknown PPIs of wild-type alpha-synuclein. 4 of the published and 23 of the novel alpha-synuclein interactions detected by cytoY2H had also been found in the previously performed Y2H screen. Consistent with the Y2H data, the cytoY2H screen detected interactions of wild-type

alpha-synuclein and several proteins associated with other neurodegenerative disorders like Alzheimer's and Huntington's disease, further supporting the hypothesis that similar pathological mechanisms are underlying these disorders [184]. Wild-type alpha-synuclein interacted with numerous proteins involved in cancer, increasing the evidence for common molecular mechanisms of neurodegenerative diseases and cancer [229]. The screen also identified interactions of alpha-synuclein with several kinases, which might phosphorylate alpha-synuclein and thereby modulate its aggregation properties [72]. In contrast to the Y2H screen, cytoY2H assays allowed the screening of the A53T mutant and other mutant isoforms of alpha-synuclein. The analysis of these interactions highlighted several proteins that are involved in processes like apoptosis, which might be altered upon mutation of the protein and thereby influence disease progression. The disease association analysis identified proteins involved in other known genetic diseases. Chemical compounds targeting these proteins are used as a therapeutic approach for PD and have been tested both in disease models as well as PD patients. In addition, the analysis identified new therapeutic targets of PD as well as compounds targeting these proteins, which could be tested in PD cell or animal models.

4.5 Identification of alpha-synuclein PPIs using the subSEQ method

The generation of a cytoY2H and MYTH prey matrix is very laborious and expensive. Although the cDNA clone collection available for this thesis contains clones of a large number of genes, it still does not cover all genes of the human genome. Therefore, the aim of this chapter was to perform a cytoY2H / MYTH screen against a human brain derived cDNA prey library and to identify the proteins interacting with alpha-synuclein by next-generation sequencing (NGS). Subsequently, interactions of alpha-synuclein detected by this novel method were validated using the cytoY2H system.

4.5.1 Description of the subSEQ method

The method described combines a cytoY2H / MYTH library screen with Illumina Solexa sequencing to identify the prey proteins interacting with a specific bait protein. The method was named subSEQ, which is derived from the terms split-ubiquitin and SEQuencing. The procedure allows the interaction-analysis of up to 56 baits in parallel. Both cytoY2H and MYTH baits can be used for PPI screening in parallel. The cytoY2H bait vector is used to identify interactions of soluble proteins while the MYTH bait vectors are used for the analysis of membrane proteins.

4.5.2 Principle of Illumina Solexa sequencing

The Illumina solexa system utilizes a sequencing-by-synthesis (SBS) approach with reversible terminator chemistry [331] as depicted in Figure 4-21 and Figure 4-22. The “libraries”, DNA fragments of interest ligated to specific sequencing DNA adapters, are immobilized by binding to primers on the surface of the proprietary “flow cell” (Figure 4-21 A). Bridge amplification, a solid-phase PCR with unlabeled nucleotides, creates clusters of up to 1,000 identical copies of each single template DNA molecule in close proximity (Figure 4-21 B). A final denaturation step leaves single stranded molecules remaining on the flow cell.

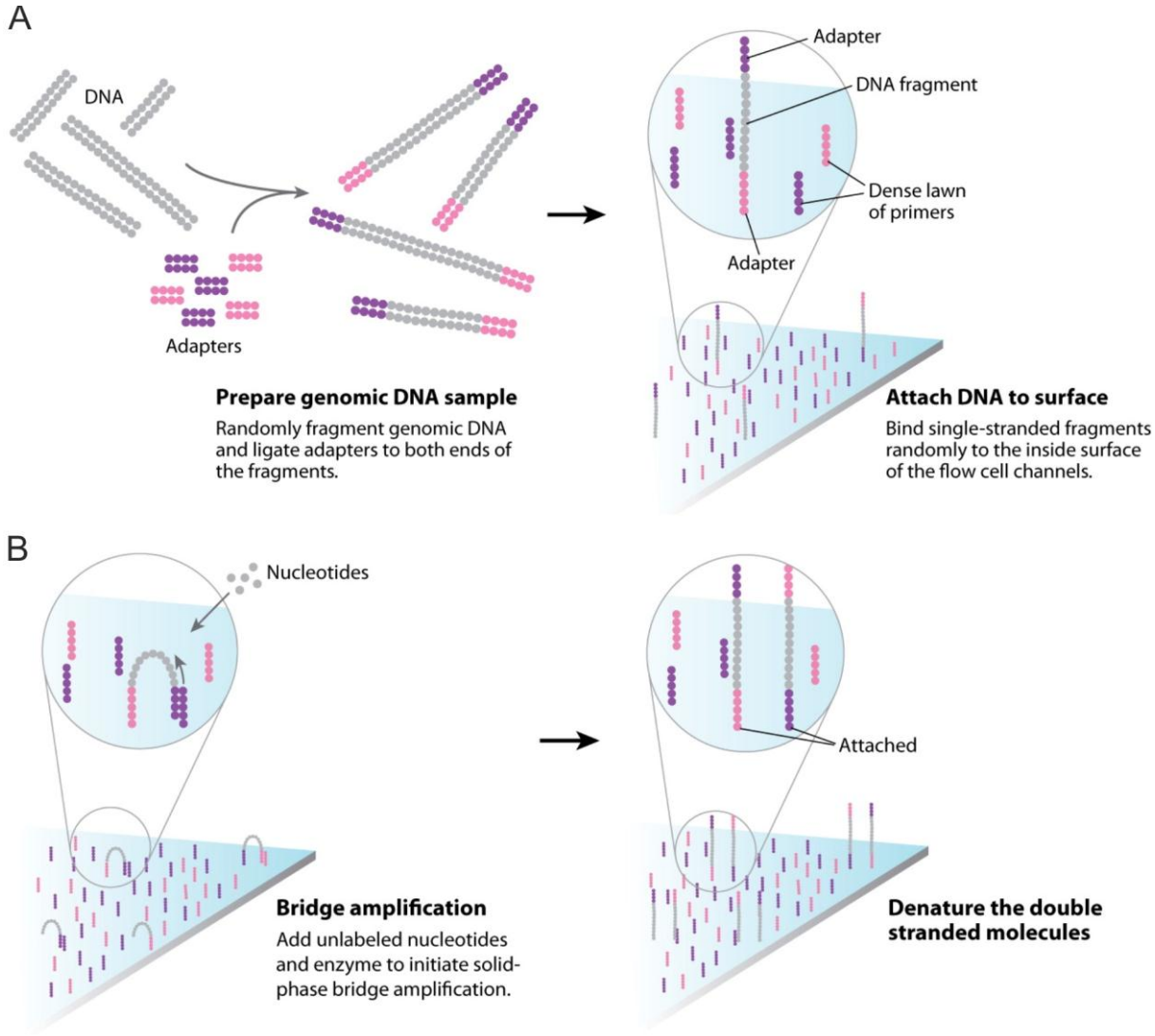

Figure 4-21: The Illumina sequencing-by-synthesis approach: cluster generation. A: DNA fragments of interest are ligated to specific adapters, which can bind to primers attached to the flow cell surface. B: PCR bridge amplification with unlabeled nucleotides generates clusters of fragments, each containing ~1000 copies of the DNA sample. A final denaturing step leaves single-stranded DNA on the flow-cell. Modified from Mardis [332].

For the subsequent PCR reaction, fluorescently labeled nucleotides, primers and a polymerase are added to the flow cell. Each nucleotide is covalently bonded to a different fluorophore, which also serve as a terminator for polymerization. Therefore, after each nucleotide incorporation step, the fluorescence can be imaged to identify the first base in the cluster (Figure 4-22 A). The fluorescent label is then cleaved in a chemical reaction to allow the incorporation of the next labeled nucleotide. These steps are repeated for a specific number of cycles, resulting in read lengths of 36 bases (Figure 4-22 B).

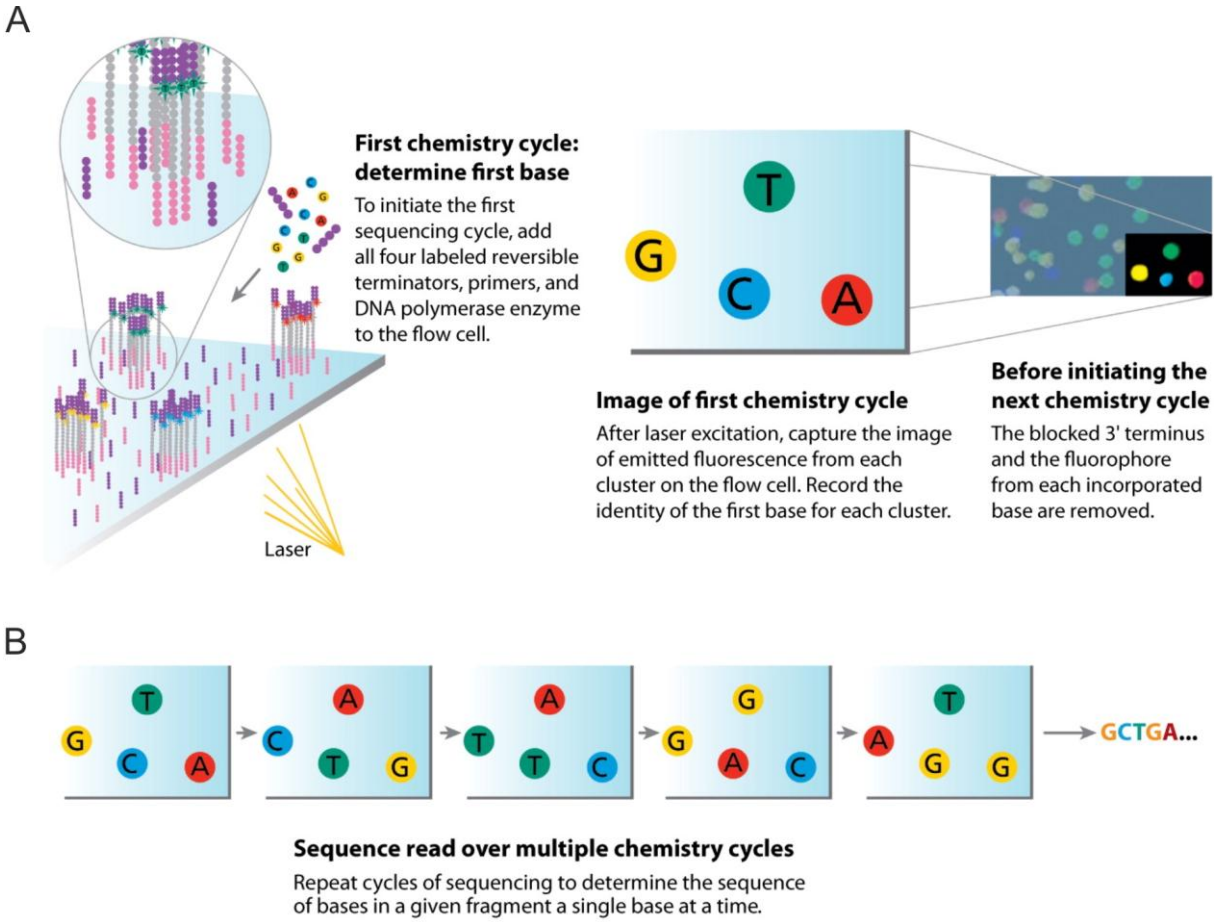

Figure 4-22: The Illumina sequencing-by-synthesis approach: sequence determination. A: Cluster strands created by bridge amplification are primed and all four fluorescently labeled nucleotides and a DNA polymerase are added to the flow cell. The nucleotide label serves as a terminator for polymerization, so after each dNTP incorporation, the fluorescence is imaged to identify the base. The label and the base are then cleaved to allow incorporation of the next nucleotide. B: The sequencing cycles are repeated to determine the identity of up to 36 base pairs of the analyzed DNA fragments. Modified from Mardis [332].

4.5.3 Modification for multiplexing

The flow cells used for Illumina Solexa sequencing with the Genome Analyzer II (llumina) contain eight channels, so-called lanes, which can each be loaded with separate libraries. One of the lanes is reserved for quality control. For the subSEQ library preparation, eight different multiplexing adapters were used instead of the standard Illumina adapters. Each of the adapters contains a unique degenerate six-base index [333], which adds a “bar-code” to the DNA-fragments to be sequenced. With this optimization, up to 8 libraries can be pooled and loaded onto a single lane, allowing the analysis of 56 different libraries on one flow cell.

4.5.4 Selective enrichment of prey plasmids encoding interacting prey proteins

In the first part of the subSEQ sample preparation process, plasmid DNA encoding prey proteins that interact with a specific bait protein (Figure 4-23) is enriched and isolated from yeast. Bait plasmids for selective enrichment were generated by Gateway™ cloning into cytoY2H or MYTH bait vectors (see section 4.3.2). The wild-type alpha-synuclein cytoY2H bait plasmid was taken for a proof of concept experiment. Additional bait plasmids were generated from entry-clones encoding 4 different fragments of the Huntingtin (HTT) protein. The sequences of the fragments varied in length (513 or 586 amino acids) and contained short (17 or 25 amino acids) or long (68 or 73 amino acids) polyglutamine stretches. In addition, cytoY2H bait plasmids were generated from entry-clones encoding the Spectinomycin resistance gene (SpecR), cyan fluorescent protein (CFP) or yellow fluorescent protein (YFP). Interaction data obtained from these bait proteins was used to identify non-specific interactions of baits screened in the assay. After confirmation by restriction digest and sequencing, the generated bait plasmids were transformed into the yeast strain L40ccα (MATα). The expression of all bait proteins was confirmed by the genetic NubG/NubI test (see section 4.3.4) and / or by immunoblotting (as in results section 4.3.5).

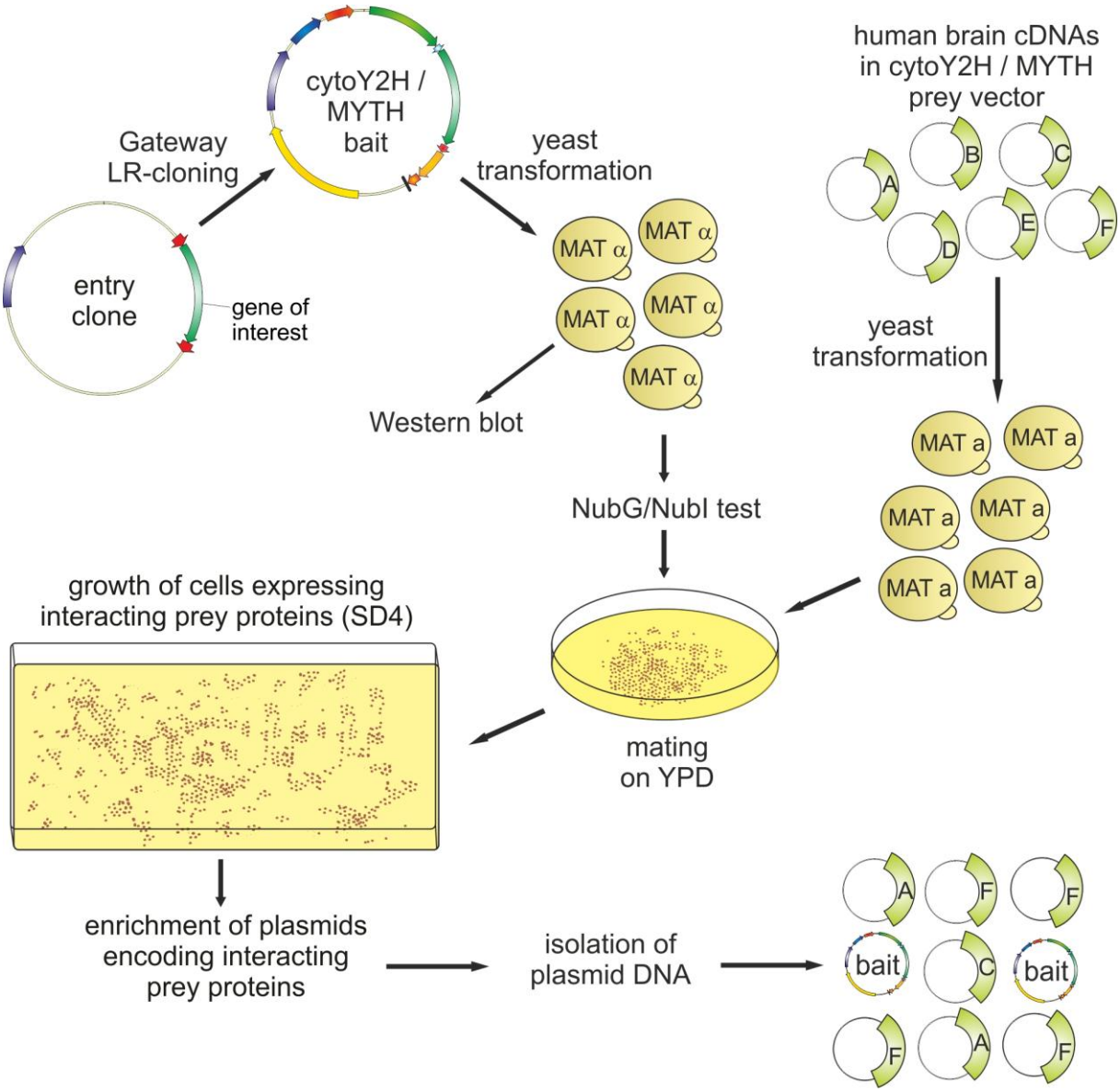

Figure 4-23: Selective enrichment of prey plasmids encoding proteins interacting with a bait protein. A: cytoY2H or MYTH bait plasmids generated by Gateway™ cloning were transformed into the yeast strain L40ccα (MATα). Expression of the bait proteins was confirmed by western blot and / or genetic NubG/NubI test. A cDNA prey library derived from human adult brain tissue was transformed into the yeast strain L40ccua (MATa). Transformants of both yeast strains were plated on rich medium (YPD) to allow mating. A defined amount of cells of resulting diploid cells was then transferred to SD4 (-Leu-Trp-Ura-His) agar plates selecting for interaction of bait and prey. It was assumed that only cells containing plasmids that encode prey proteins interacting with a bait protein would be able to grow, leading to an enrichment of plasmids encoding interacting prey proteins. Bait and prey plasmids were isolated from a defined amount of cells.

In parallel to the bait plasmid generation, a cDNA prey library derived from human adult whole brain tissue (P12221, Dualsystems) was transformed into the yeast strain L40ccua (MATa). The complexity of the library was 2.8E+06 independent plasmid clones with an average insert size of 1.6 kb. The size range of the inserts was 0.5 - 8.0 kb. The prey vector used to generate the prey library plasmids (pPR3-N) fuses the N-terminal half of ubiquitin (NubG) to the N-terminus of the proteins encoded by the different cDNAs. To generate a large number of yeast clones each carrying a

different plasmid, 28 µg library DNA, the amount recommended for a single library screen, were transformed into the yeast strain L40ccua (MATa). Yeast transformants were plated onto SD-t/hul (-Trp) agar plates, only allowing the growth of yeast transformants carrying a prey plasmid. After 48 h incubation at 30°C, the growth of small yeast colonies was visible. The colonies were washed off the plate with NBG medium, mixed well, aliquotted and frozen. To allowing mating, yeast clones (strain L40ccα) carrying a single bait plasmid were mixed with yeast transformed with the library (thawed aliquots) and plated on YPD agar plates. The mating and all subsequent work steps were performed in duplicates for each bait. After 48 h incubation at 30°C, 40 OD600 resulting diploid yeast cells were transferred to SD4 medium (-Leu-Trp-Ura-His) to select for interactions between bait and prey proteins. It was assumed that only cells containing a prey plasmid encoding a prey protein that interacts with the bait protein would be able to grow. Growth of these colonies leads to a multiplication and selective enrichment of the prey plasmids containing cDNAs that encoded interacting prey proteins. The cells were washed off the plate with sterile water and plasmid DNA (including the baits) was isolated from 20OD cells.

4.5.5 PCR amplification of cDNAs from isolated plasmids

To amplify the cDNA sequences from the isolated prey plasmids, 100 ng of each plasmid DNA preparation were used as a template for a PCR reaction with primers annealing up- and downstream of the SfiI restriction sites. These restriction sites had been used to insert the human brain derived cDNAs into the prey vector. Previously, it was verified that the primers do not to anneal to any other region of the prey-vector or the bait-vectors. In a test PCR using a single prey or bait plasmid as a template, a specific band was detected only for the prey plasmid but not for the bait plasmid. As a proof of concept experiment, used templates were the untransformed cDNA prey library (library) as well as the prey library, which was transformed into and subsequently isolated from yeast (pool). Additional templates were plasmid preparations selected against alpha-synuclein, different HTT-fragments and unspecific baits (SpecR, CFP or YFP, see section 4.5.4). After PCR amplification of the cDNAs from these plasmid preparations, the amplification products were visualized on an agarose gel (Figure 4-24 A).

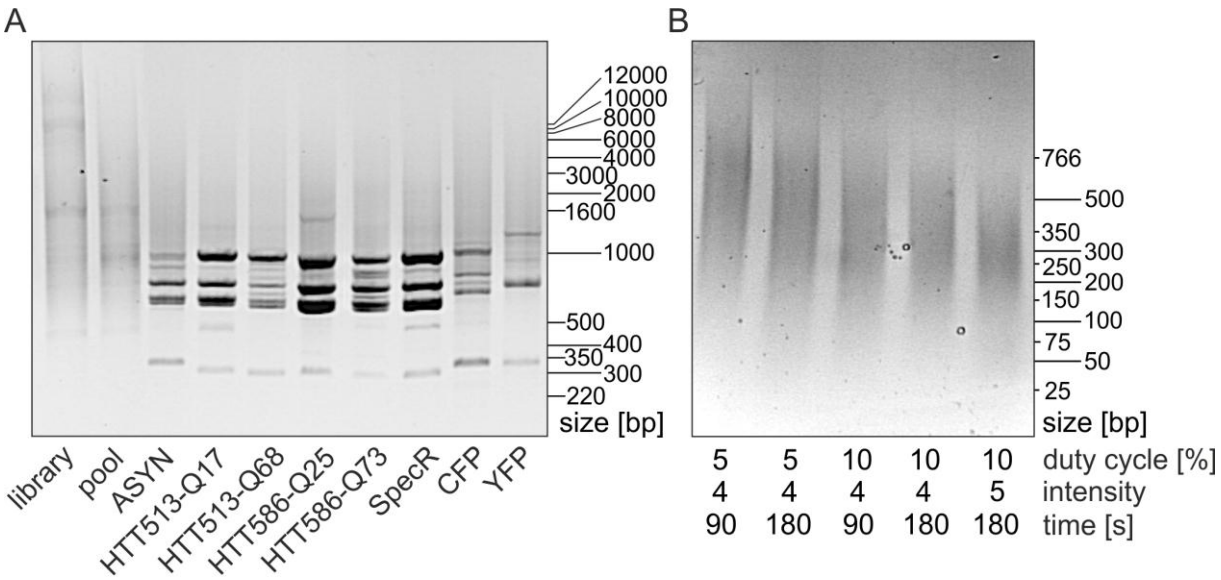

Figure 4-24: Optimization of subSEQ library preparation process. A: PCR amplification of cDNA sequences. Different plasmid preparations obtained after selective enrichment were used as templates for the PCR amplification of the cDNA insert sequences with primers annealing up- and downstream of each cDNA. As templates I used the untransformed cDNA prey library (library), the cDNA prey library which was transformed into and subsequently isolated from yeast (pool), as well as libraries selected against specific and unspecific (CFP, YFP, SpecR) baits. The bait proteins used for selection were generated from wild-type alpha-synuclein (ASYN) as well as Huntingtin (HTT) fragments of different lengths (513 or 586 amino acids) with a short (17 or 25 amino acids) or a long (68 or 73 amino acids) polyglutamine stretch. The PCR products were visualized on an agarose gel. B: Optimization of DNA fragmentation settings. The PCR products resulting from a cDNA amplification reaction as shown in A were fragmented by acoustic DNA shearing and visualized on an agarose gel. The correct parameters (duty cycle, intensity, time) to obtain DNA fragments with an average size of ~300 bp were determined (lane 5).

The PCR reaction using the “library” template produced a smear of DNA on the gel. A DNA smear with a smaller size range was visible in the products of the PCR reaction using the “pool” template. It is possible that the transformation of the library into yeast is a first selection step and that the prey plasmids containing inserts of large size might not be present in the yeast pool. However, this will need further investigation as this ovservation might also be due to technical problems with sample preparation. When plasmid preparations selected against specific and unspecific bait proteins were used as template, the PCR reaction generated a smear of DNA containing various defined bands. The fact that the observed band patterns were unique for each bait indicates a bait-dependent enrichment of the plasmids.

4.5.6 Accoustic fragmentation of PCR products

The modifications to the standard protocol described in the Genomic DNA Sample Preparation Guide (available from the Illumina website) in the current and the following results section were inspired by published modifications [334]. After amplification, the obtained PCR products were fragmented by acoustic DNA shearing (AFA technology, Covaris). In this process, various parameters can be changed to

allow precise regulation of the mechanical force applied to the DNA. Different settings were tested on PCR products amplified from a plasmid preparation selected against the wild-type alpha-synuclein cytoY2H plasmid. The resulting DNA fragments were visualized on an agarose gel (Figure 4-24 B). The required average fragment size of ~300 bp was obtained with the following settings: duty cycle: 10%, intensity: 5, time: 180 s.

4.5.7 SubSEQ library preparation process

The working steps required for the library preparation after selective enrichment of plasmid DNA are depicted in Figure 4-25. After each step, samples were purified using the QIAEX II Gel Extraction Kit.

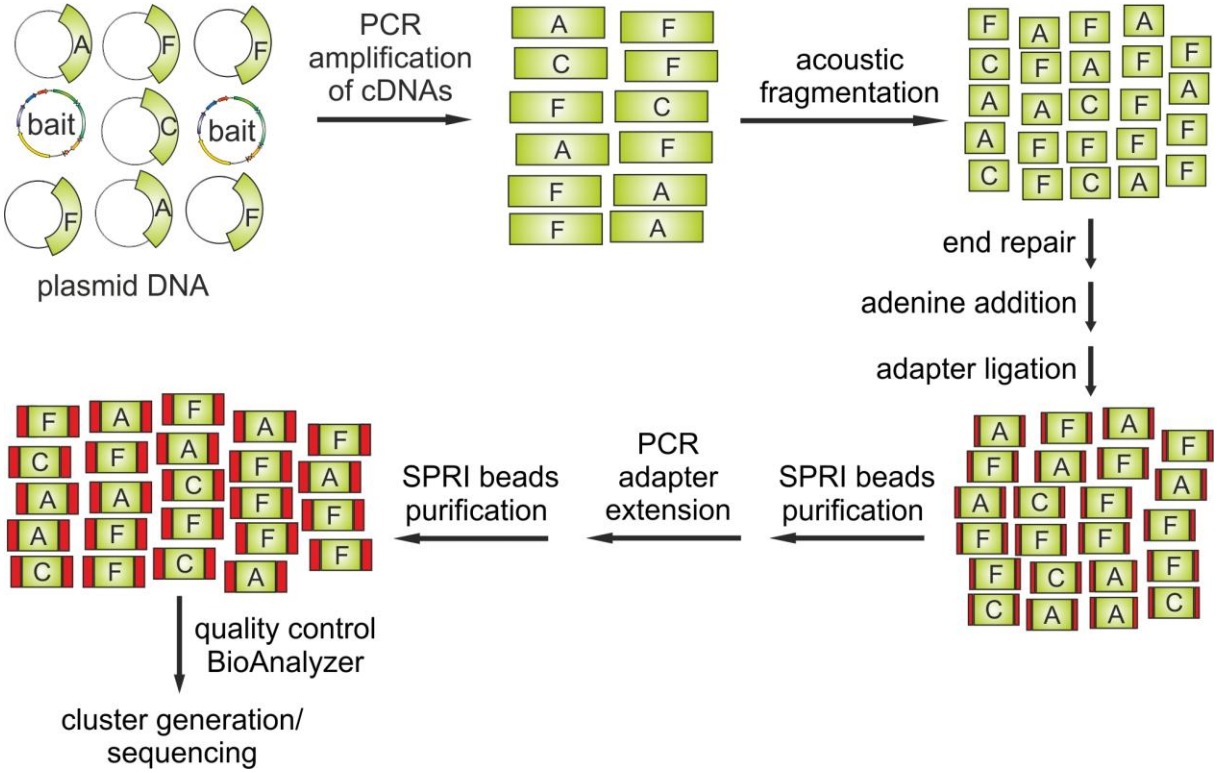

Figure 4-25: SubSEQ library preparation process. cDNA sequences were PCR amplified from prey plasmids isolated after selective enrichment against different bait proteins. The resulting PCR products were fragmented by acoustic DNA shearing (Covaris). Subsequently, single-stranded overhangs were removed from the fragments (end repair) and a single overhanging adenine nucleotide was added to allow the subsequent ligation of multiplexing adapters to the DNA fragments. After sample purification with SPRI beads (see text below), the adapters were extended with a PCR reaction. Final samples were purified again and the sample quality was assessed by chip-based capillary electrophoresis on a BioAnalzyer (Agilent). Verified libraries were used for cluster generation followed by the sequencing run.

The generation of DNA fragments by acoustic force generates overhanging single-stranded DNA ends, which were removed with a blunting enzyme (end repair) to allow subsequent addition of a single overhanging adenine (A) nucleotide to the 3' end of the fragments (adenine addition) using Klenow fragment. Afterwards, one of eight unique multiplexing adapters (see section 4.5.3) containing a 3′ thymine (T) overhang was ligated to the fragments using ultrapure T4 DNA Ligase. The minimum required amount of adapters was used to avoid the formation of adapter dimers. The amount of adapter dimers should be as low as possible, as they can form clusters on the flow cell that are sequenced instead of clusters formed from adapters ligated to DNA fragments. This way, adapter dimers waste the sequencing capacity of the flow cell (source: seqanswers.com). After adapter ligation, a subsequent purification and size selection step was performed with AMPure XP beads. Using the Solid Phase Reversible Immobilization (SPRI) principle [335], these paramagnetic beads allowed the purification of DNA with minimal sample loss. Unligated adapter molecules and other contaminants from the ligation reaction were removed in this purification procedure. A final PCR step was performed to extend the multiplexing adapters including the DNA fragments ligated to them (PCR adapter extension). Extension of the adapter sequences allowed the binding of the adapters (including the DNA fragments ligated to them) to primers on the surface of the flow cell. The parameters of this crucial step were optimized as shown Figure 4-26 A. The enzymes Platinum *Pfx* DNA Polymerase (Invitrogen) and Phusion High-Fidelity DNA Polymerase (NEB) were tested with different templates and different amounts of template DNA. Optimal results were obtained using Platinum *Pfx* DNA Polymerase and 4 ng of template DNA.

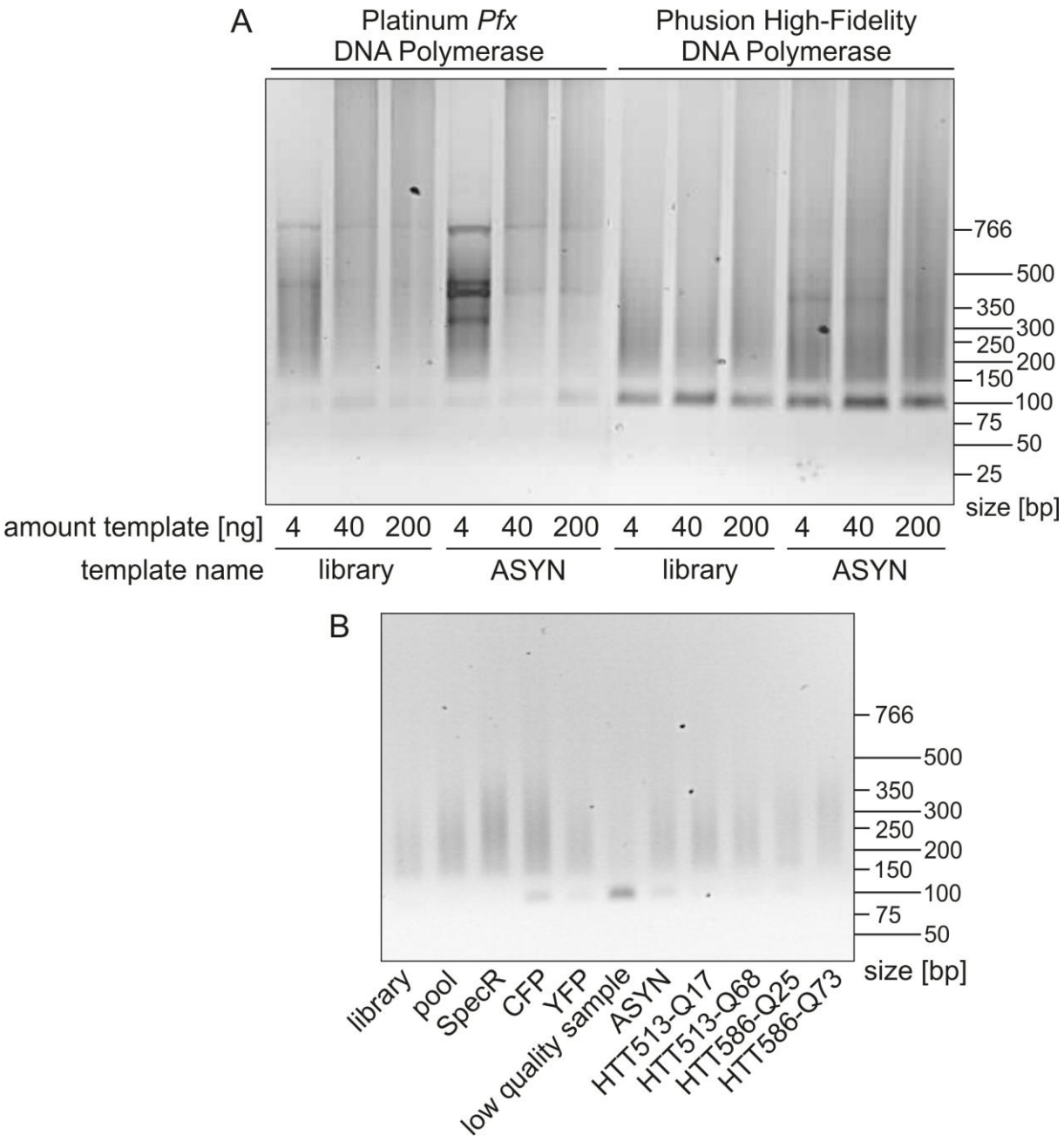

Figure 4-26: Optimization of adapter extension PCR and library quality control. A: Platinum *Pfx* DNA Polymerase (Invitrogen) and Phusion High-Fidelity DNA Polymerase (NEB) were tested with different amounts of template DNA to determine optimal conditions for the adapter extension PCR. The resulting PCR products were visualized on an agarose gel. Best results were obtained with Platinum *Pfx* DNA Polymerase and 4 ng of template DNA. B: Generated DNA libraries were visualized on an agarose gel. A low quality sample was loaded in comparison.

A last purification step was performed using SPRI beads. The final products of the sample preparation process are called libraries. All generated libraries were visualized on an agarose gel as shown in Figure 4-26 B. Most of the libraries had an average fragment size of ~200 bp and were used for sequencing after quality control by chip-based capillary electrophoresis [336] on a BioAnalzyer (Agilent). An additional library was prepared according to a standard protocol without the previously described modifications. In the lane loaded with this “low quality sample”,

a prominent band of 100 bp was visible on the agarose gel. It was assumed that this band represents adapter dimers that were generated after the ligation step. Furthermore, only a small amount of DNA of the expected average size of 200 bp was visible. These results indicate that the optimized library preparation protocol does increase the quality of the library. Cluster generation and the final sequencing run were performed according to manufacturer's protocols. All worksteps of the subSEQ library preparation process, including the modifications to the standard protocol, are summarized in Table 4-4.

Table 4-4: subSEQ library preparation steps.

Step	Description of workstep	Modification
1	bait generation	
2	expression- and localization-test of baits	
3	mating and enrichment of prey plasmids	
4	plasmid isolation	
5	PCR amplification of cDNA inserts	Phusion High-Fidelity polymerase
6	fragmentation of PCR products	optimized acoustic fragmentation settings
7	end repair	
8	addition of A overhang	
9	ligation of multiplexing adapters	ultrapure ligase
10	size selection and purification	SPRI paramagnetic beads
11	adapter extension PCR	Platinum *Pfx* polymerase with optimal amount of template, SPRI bead purification
12	quality control with BioAnalyzer	
13	cluster generation / sequencing	

4.5.8 Processing of obtained sequencing data

The raw image data obtained from the optical detection of the fluorescently labeled nucleotides in the sequencing run was converted into DNA sequences. This "base calling" step was performed using the Real Time Analysis (RTA) software, which is part of the Illumina Sequence Control Software (SCS, Version 1.5). The resulting short sequences, each of them 36 bp long, are called reads. As a different adapter with a unique multiplexing tag (see results 4.5.3) was ligated to the 8 libraries to be sequenced on one lane, the reads could be assigned to the specific bait that was used for selective plasmid enrichment. Using a Perl script (developed by J. Russ), the obtained reads were assigned to their corresponding baits and further analyzed seperately for each bait (done by J. Russ). In parallel, the multiplexing tags, each 6 bp long, were removed from the sequence of the reads. Subsequently, the program MosaikAligner (MOSAIK 1.1.0014, bioinformatics.bc.edu/marthlab/Mosaik) was used

to produce short pairwise sequence alignments for the obtained reads against a reference sequence library (done by J. Russ). The DNA insert sequences of all entry clones available for this thesis were used as reference set. In total, a reference set of 13.885 sequences was downloaded from the NCBI GenBank database [337] using a self-developed Perl script [173] (done by J. Russ). MosaikAssembler assigned each aligned read to one of two groups – unique or multi reads. Unique reads could be aligned to a single reference sequence, while multi reads were aligned to several reference sequences. With another Perl script (developed by J. Russ) the number of unique and multi reads, which could be aligned to a certain reference sequence, were counted. As multi reads were counted for several reference sequences, only the unique read values were considered for the following analysis. After sequence alignment, the refSEQ accession numbers were converted to Gene IDs using the tool IDconverter [174]. In order to make the reads obtained from the libraries comparable to each other, the read number was normalized to the sample quality, which is represented by the number of total reads obtained from a library. For normalization, the unique reads obtained for each Gene ID were each multiplied by a quality factor, which was calculated separately for each library. Using this quality factor, the reads for each library were normalized to the library with the lowest number of reads (HTT513-Q17, 1.135.495 reads). Therefore, the quality factor for a specific library was obtained by dividing the number of total reads of that library by 1.135.495. After quality normalization, values from the duplicates prepared for each library were used to calculate the arithmetical mean of the obtained number of reads for each gene. Subsequently, non-specific interactions were removed from the dataset. Therefore, unique reads obtained for each Gene ID from a library were corrected by subtracting the arithmetic mean of the unique reads of the same Gene ID obtained from the libraries selected against CYP, YFP and SpecR.

4.5.9 Detection of published interactors of alpha-synuclein using subSEQ

To assess if the subSEQ method generates physiologically relevant data, it was determined how many published interactors of alpha-synuclein were detected using the method. In total, unique reads were aligned to the sequences of 16 published interactors of alpha-synuclein (Supplementary Table 6). The lowest number of unique reads detected for published interactors of alpha-synuclein was 5, which was used as a threshold: 5 unique reads had to be aligned with a gene in order to qualify as possible interaction partner of alpha-synuclein. As subSEQ detected the interactions

of alpha-synuclein with 38% of its published interactors, it was assumed that this technique could also be used to predict novel interactors of alpha-synuclein. Using 5 unique reads as threshold, the subSEQ method predicted 1919 potential interactors of wild-type alpha-synuclein. The highest number of unique reads was obtained for the gene FBXW7 with 17733 unique reads mapped to its sequence. See http://141.80.164.19/koenn/ for detailed results.

4.5.10 The enrichment of prey plasmids in subSEQ is bait specific

It was further assessed whether the selection step of the subSEQ method led to bait-specific plasmid enrichment. Thus, the interactions predicted for the alpha-synuclein library were compared with the library selected against a Huntingtin fragment (Htt513-Q17). The analysis of the Htt sample predicted 1093 proteins (with 5 or more reads aligned to their corresponding genes) as potential Huntingtin interactors. 699 of these interactions were overlapping with the alpha-synuclein library, which equals 36% of the total interactions predicted for alpha-synuclein by subSEQ. However, only 2 of the interactors detected in both samples (APP and YWHAE) are known interactors of alpha-synuclein. Furthermore, the protein F-box/WD repeat-containing protein 7 (FBXW7), which was predicted to interact with alpha-synuclein with 17733 unique reads, did not obtain any reads in the library selected against Htt513-Q17. Taken together, these results indicate that the enrichment of prey plasmids in the subSEQ method is bait specific.

4.5.11 Confidence scoring of alpha-synuclein interactions predicted by subSEQ

To rank the interactions of alpha-synuclein predicted by subSEQ and estimate their likeliness to occur *in vivo*, a bioinformatic scoring system was applied. This system was used previously used to rank the detected Y2H and cytoY2H interactions. 1919 predicted interactors of alpha-synuclein were ranked as following: 1392 (72%) ranked as low confidence, 54 (3%) ranked as medium confidence and 472 (25%) ranked as high confidence (HC).

4.5.12 cytoY2H validation of subSEQ predicted alpha-synuclein interactions

To determine whether alpha-synuclein interactions predicted by subSEQ could be validated by other PPI detection methods, selected interactions were reconstructed using the cytoY2H system. Therefore, 48 proteins that were predicted as interactors of alpha-synuclein by subSEQ were chosen based on the number of unique reads assigned to an interaction: Some proteins with low, some with medium and some

proteins with a high number of unique read numbers were selected. The number of unique reads assigned to the selected interactors ranged from 5 to 16342. ORFs encoding the selected putative interaction partners were Gateway™ cloned into the prey vector pGPR4-Ns. The resulting prey plasmids were transformed into the yeast strain L40ccua (MATa) and tested for interaction with wild-type alpha-synuclein and unrelated cytoY2H baits as described previously (section 4.4.4). Bait and prey proteins were tested for an interaction in five repetitions in 96 well format. An interaction was only counted when both the *HIS3* and *lacZ* reporter gene were activated in at least one repetition. In total, the cytoY2H assay detected the interaction of alpha-synuclein with 21 proteins (Supplementary Table 7). These interactions were considered bait-specific, as no interaction with unspecific baits was detected. The subSEQ predicted interactors of alpha-synuclein confirmed by cytoY2H are shown in a pictorial representation in Figure 4-27. As 44% of the tested interactions that were predicted by subSEQ could be confirmed using the cytoY2H system, it was concluded that the subSEQ system can be used to identify novel interactors of alpha-synuclein. This hypothesis was supported by the finding that subSEQ predicted interactions could also be validated in mammalian cells (section 4.6.2).

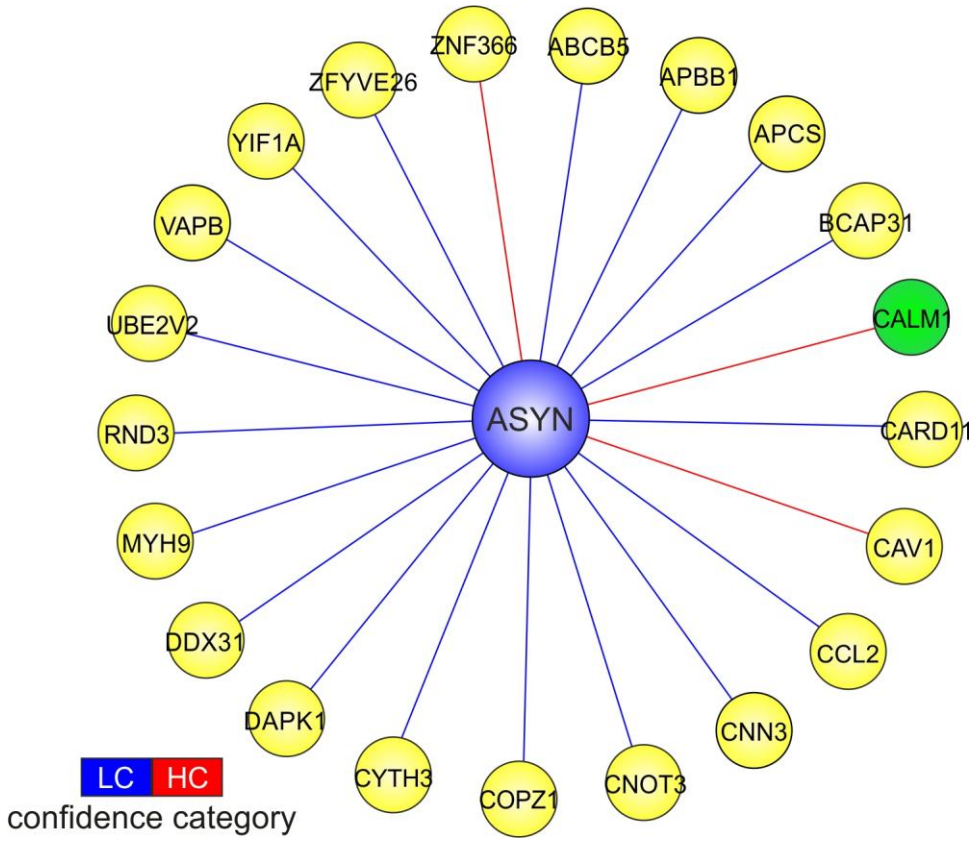

Figure 4-27: cytoY2H validation of subSEQ predicted alpha-synuclein interactions. Alpha-synuclein interactions predicted by the subSEQ method were reconstructed using the cytoY2H system. The green node indicates a published interactor of alpha-synuclein, while all other prey proteins are shown with yellow nodes. The edge color represents predicted low confidence (LC) and high confidence (HC) interactions, as indicated in the scale bar.

4.5.13 Literature based analysis of selected interactors confirmed by cytoY2H

The cytoY2H assay confirmed the subSEQ predicted interaction between alpha-synuclein and caveolin 1 (CAV1). This scaffolding protein is involved in various cellular processes, for example signal transduction and vesicular transport [338]. The interaction between alpha-synuclein and CAV1 has previously been reported, and overexpression of alpha-synuclein increases the protein levels of CAV1 [339]. The authors suggested that CAV1 might regulate alpha-synuclein induced cell death. Furthermore, alpha-synuclein interacted with the amyloid beta (A4) precursor protein-binding, family B, member 1 (APBB1). Mutations in the gene have been associated with an increased risk for early-onset Alzheimer's disease [340]. This interaction supports the view that both diseases are linked [184].

The cytoY2H assay also confirmed the interaction of alpha-synuclein and the VAMP-associated protein B (VAPB). A mutation in VAPB causes late-onset amyotrophic lateral sclerosis and spinal muscular atrophy [341], creating an additional link between PD and other neurodegenerative diseases.

Alpha-synuclein also interacted with the death-associated protein kinase 1 (DAPK1), a pro-apoptotic serine–threonine protein kinase [342]. Several studies demonstrated that apoptosis may play a critical role in PD [343] Various specific inhibitors for DAPK1 are available, and they could be tested in cell [107] and animal models [258] of PD.

4.5.14 Summary of chapter 5

The novel subSEQ method, which combines a cytoY2H or MYTH screen with next-generation sequencing, was used to predict interactors of alpha-synuclein. SubSEQ allows the selective enrichment of plasmids from a human brain derived prey library that encode proteins interacting with a tested bait protein. Subsequently, the genes carried by plasmids are identified by next-generation sequencing. The subSEQ method detected 38% of the published interactors of alpha-synuclein. In addition, the method was used to predict novel interaction partners of wild-type alpha-synuclein. Selected predicted interactions were investigated in cytoY2H assays and 44% of these interactions could be confirmed. The confirmed interaction partners supported a role of alpha-synuclein in apoptosis, unfolded protein response and cytoskeletal organization.

4.6 Validation of detected alpha-synuclein PPIs using the LUMIER assay

To increase the experimental support for the protein-protein interaction data obtained with the Y2H, cytoY2H and subSEQ methods, the aim of this chapter was to validate detected interactions of wild-type and mutant alpha-synuclein. Therefore, selected interactions were to be reconstructed with a high-throughput version of the LUMIER co-immunoprecipitation assay, which allows the detection of PPIs in mammalian HEK cells.

4.6.1 Principle of LUMIER co-immunoprecipitation assay

The modified version of the LUMIER assay (luminescence-based mammalian interactome mapping) [149] is a high-throughput technique that allows the detection of protein-protein interactions in mammalian cells. This assay was used to validate interactions of wild-type and mutant alpha-synuclein that were previously detected with the Y2H, cytoY2H and subSEQ methods. All alpha-synuclein interactions were tested bidirectionally in the LUMIER assay: To test the interaction between alpha-

synuclein (A) and a putative interaction partner (B), A was used as a bait protein, while B was used as prey protein in the first experiment. In the second experiment, B was used as bait protein while A was used as prey protein. Each bait protein, which was fused to protein A (PA) and Renilla luciferase (RL), was co-produced in HEK293 cells with a prey protein fused to Firefly luciferase (FL) (Figure 4-28).

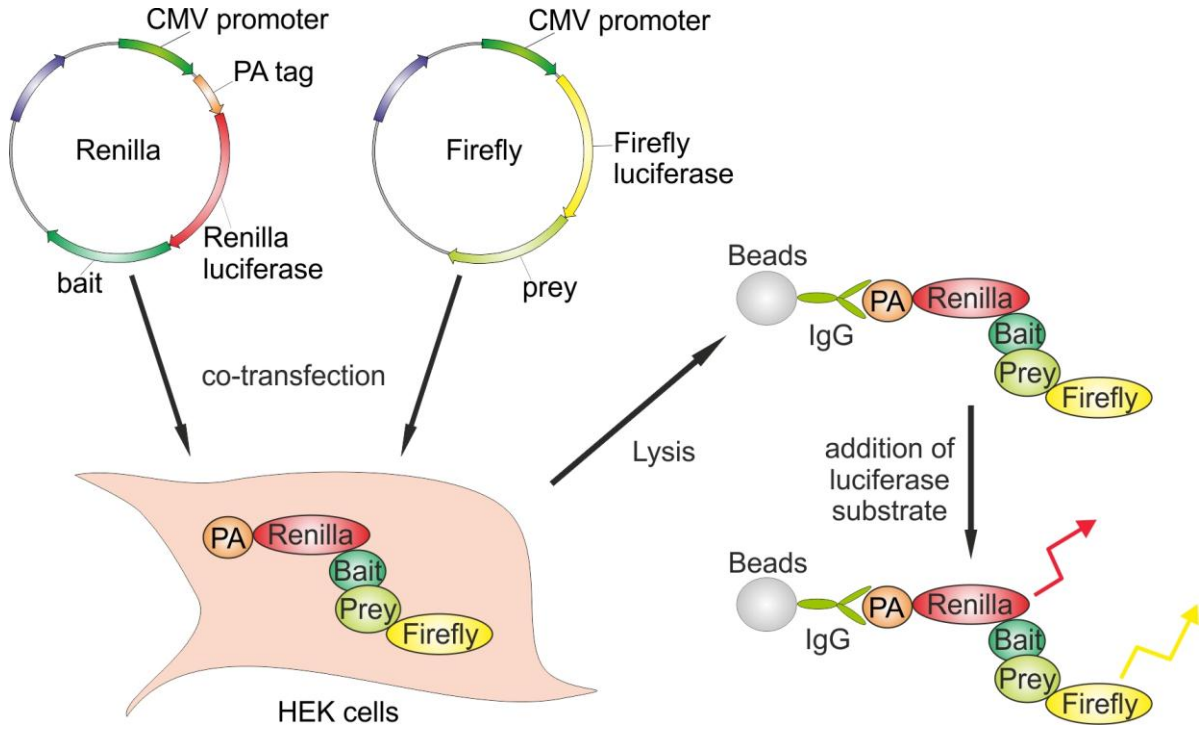

Figure 4-28: Schematic representation of a LUMIER co-immunoprecipiation assay. Protein A (PA)-Renilla luciferase-tagged bait proteins and Firefly luciferase-tagged prey fusion proteins were co-produced in HEK293 cells. After co-immunoprecipitation from cell lysates, the interactions between bait and prey proteins were monitored by quantification of Firefly luciferase activity of prey proteins in protein complexes. Successful immunoprecipitation of bait proteins was examined by quantification of Renilla luciferase activity.

All Renilla and Firefly plasmids were generated by Gateway™ cloning. Subsequently, the generated plasmids were co-transfected into HEK cells in 96-well plates. After incubation, the cells were lysed and protein complexes were co-immunoprecipitated with IgG coated magnetic beads, which bind to the PA tag fused to the bait proteins. The successful immunoprecipitation of the bait proteins was confirmed by measuring the Renilla luciferase activity in a luminescence plate reader using the Dual-Glo Luciferase Assay System. The interaction between the RL-tagged bait and FL-tagged prey proteins was determined by quantification of the Firefly luciferase activity [153]. For each tested interaction, 3 different parallel co-immunoprecipitation experiments were performed to assess the specificity of an interaction. To examine background protein binding, Renilla and Firefly luciferase activity was determined in lysates of cells transfected with a bait plasmid (encoding a putative interaction partner or alpha-

synuclein itself) and an empty prey plasmid (containing the Gateway™ ccdB sequence), as well as cells transfected with the empty bait vector and the prey vector. See section 3.11 for details of the calculation. http://141.80.164.19/koenn/ for detailed results.

4.6.2 LUMIER assay validates Y2H, cytoY2H and subSEQ interaction data

The LUMIER assay was used to validate interactions of alpha-synuclein detected by the Y2H, cytoY2H and subSEQ methods. 67 interactions of wild-type alpha-synuclein detected in the Y2H screen were tested in the LUMIER assay, and 36 of the interactions could be confirmed (validation rate: 54%). In addition, 32 out of 62 interactors of the A30P isoform of alpha-synuclein detected by Y2H could be reproduced (validation rate: 52%). Out of 9 interactions of the E46K mutant isoform of alpha-synuclein detected by Y2H, 3 interactions could be validated using the LUMIER assay (validation rate: 33%). Subsequently, it was determined that the LUMIER assay could validate 20 out 40 interactions that were detected by cytoY2H assays (validation rate: 50%). Furthermore, the LUMIER assay was used to validate alpha-synuclein interactions predicted by the subSEQ method. Therefore, 42 interactors of wild-type alpha-synuclein identified by a least 5 unique reads in subSEQ were selected. Out of these interactions, 19 could be validated using the LUMIER assay (validation rate: 45%). The validation rate could be increased by selecting interactions found in cytoY2H and Y2H: out of 18 interactions of wild-type alpha-synuclein detected by both 2H methods, 12 could be validated using the LUMIER assay (validation rate: 67%). The highest validation rate was achieved when selecting interactions detected in Y2H, cytoY2H and subSEQ: with these criteria, the LUMIER assay validated 4 out of 5 selected interactions (validation rate: 80%). A large fraction of the interactions detected by Y2H, cytoY2H and the subSEQ method could be validated in mammalian cells using the LUMIER assay. Furthermore, the probability to reproduce an interaction using the co-immunoprecipitation assay can be increased be selecting interactions that were detected by two or even all 3 PPI detection methods.

4.6.3 LUMIER assay validates PPIs of wild-type and mutant alpha-synuclein

Using the high-throughput LUMIER assay, 115 proteins (128 different clones) were tested in total for an interaction with wild-type alpha-synuclein. 60 of these interactions could be validated in the LUMIER assay (validation rate: 52%). Furthermore, 64 proteins were tested for an interaction with the A30P mutant isoform of alpha-synuclein. 33 of these interactions could be confirmed with the LUMIER assay (validation rate: 52%). In addition, the interaction of 12 proteins with the E46K mutant isoform of alpha-synuclein was tested and 5 of them could be confirmed (validation rate: 42%).

4.6.4 Alpha-synuclein interactors validated with the LUMIER assay

In order to identify shared interactions or interactions specific for a certain mutant variant, the proteins tested for interaction with wild-type, A30P or E46K isoforms of alpha-synuclein were grouped according to the baits they were tested against (Figure 4-29). Green edges indicate successfully confirmed interactions, while red edges indicate interactions that could not be reproduced using the LUMIER assay. 33 proteins that exclusively interacted with wild-type alpha-synuclein were assigned to group 1, while 17 proteins exclusively interacting with the A30P isoform of alpha-synuclein were assigned to group 2. Group 3 contains 16 proteins that were tested for interaction with wild-type alpha-synuclein and its A30P mutant isoform. The proteins in group 4 were tested for interaction with wild-type alpha-synuclein and its E46K mutant, while the proteins in group 5 were tested for interaction with the A30P and the E46K mutant isoform. Group 6 contains 6 proteins that were tested against wild-type and all mutant isoforms of alpha-synuclein.

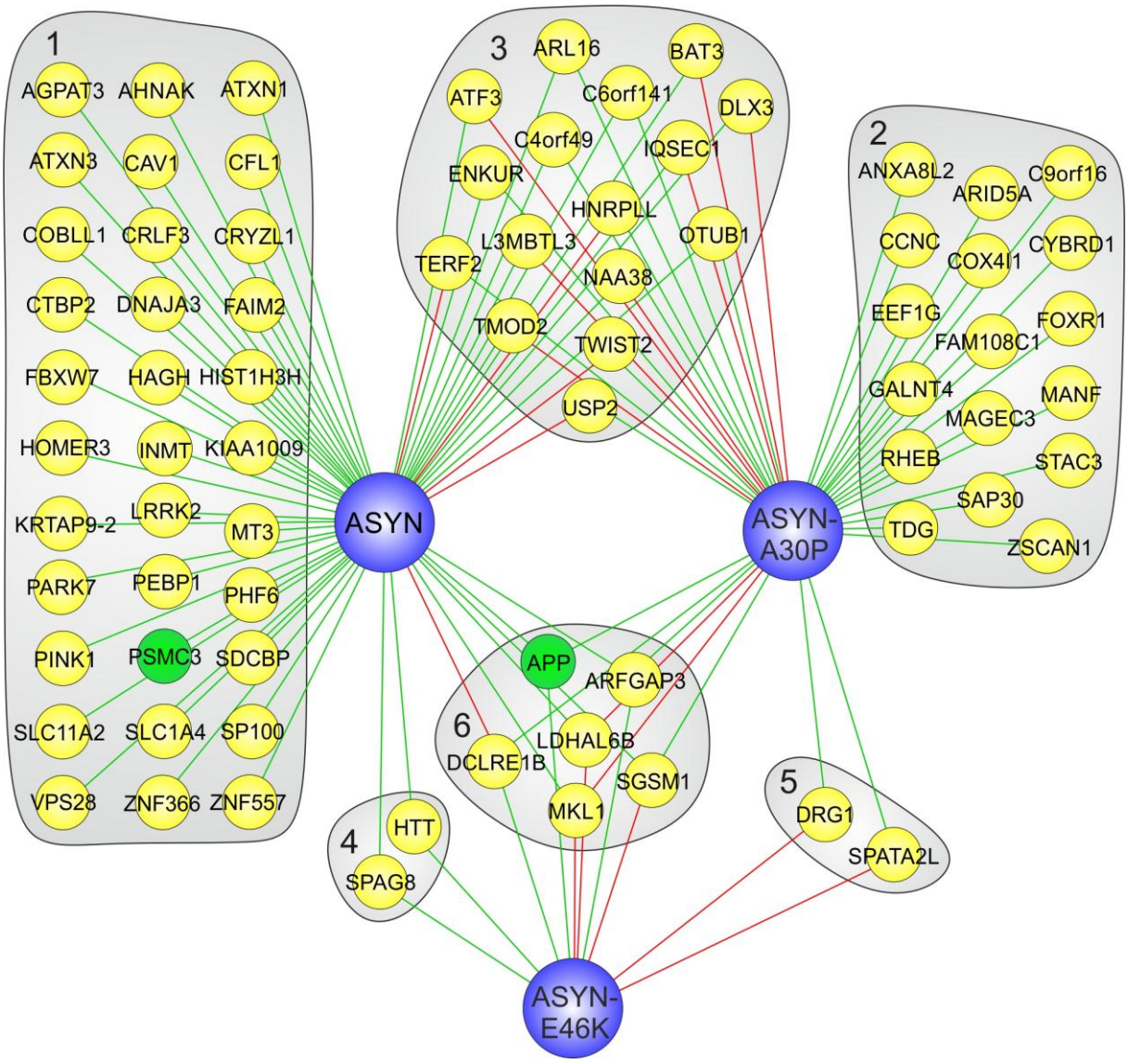

Figure 4-29: Validation of alpha-synuclein interactions with LUMIER co-immunoprecipiation assay. Protein-protein interactions of wild-type and mutant alpha-synuclein previously detected by Y2H, cytoY2H or subSEQ were validated using the LUMIER assay. Proteins were grouped according to the alpha-synuclein baits they were tested against, as indicated but the numbered grey outlines. Validated interactions are shown with green edges, while interactions drawn with red edges could not be reproduced in the LUMIER assay. Known interactors of alpha-synuclein are shown with green nodes while all other proteins are shown with yellow nodes.

4.6.5 Literature based analysis of selected interactors confirmed by LUMIER

The LUMIER assay validated an interaction between the Sin3A-associated protein SAP30 and the A30P mutant of alpha-synuclein, which was detected previously using the Y2H assay. The Sin3A-associated protein is part of the histone deacetylase complex [344]. The A30P mutation of alpha-synuclein leads to increased nuclear targeting of the protein, where it inhibits histone acetylation and promotes neurotoxicity in both cell culture and transgenic flies [103]. Alpha-synuclein might cause these effects by its direct interaction with SAP30. An interaction between wild-type alpha-synuclein as well as its A30P mutant isoform with the ubiquitin specific

peptidase 2 (USP2) was previously detected in the Y2H interaction screen. However, the LUMIER assay only confirmed the interaction with the A30P isoform but not with wild-type alpha-synuclein. USP2 is a de-ubiquitinating enzyme that promotes the activation of the NF-κB pathway and protects cells against TNF-induced cell death [345]. Furthermore, USP2 acts as regulator of the p53 pathway by the E3 ubiquitin ligase Mdm2 [346]. By its direct interaction with USP2, the A30P isoform of alpha-synuclein might promote the death of dopaminergic neurons by misregulating the NF-κB and p53 pathway. Another protein that interacted with the A30P isoform of alpha-synuclein both in Y2H and in the LUMIER assay is the mesencephalic astrocyte-derived neurotrophic factor (MANF). Interestingly, it has been demonstrated recently that this factor can protect neurons from apoptotic cell death and is able to reverse disease-like symptoms in a PD rat model [347]. By binding to the protein, alpha-synuclein might interfere with the positive effects of MANF.

4.6.6 Summary of chapter 6

A high-throughput version of the LUMIER assay was used to validate protein-protein interactions of alpha-synuclein previously detected using the Y2H, cytoY2H and subSEQ method. The LUMIER interaction data validated all three methods as suitable tools to detect novel protein-protein interactions of alpha-synuclein. Specifically, the assay confirmed 52% of the tested interactions of wild-type alpha-synuclein, 52% of the interactions detected with its A30P and 42% of the interactions of its E46K mutant isoforms. The detailed analysis of the validated interactors suggested possible roles of alpha-synuclein in the regulation of histone-deacetylation, the NF-κB and the p53 pathway.

4.7 Generation of a high-confidence interaction network for alpha-synuclein

To obtain interaction data with strong experimental support, the aim of this chapter was to combine all protein-protein interactions detected by two or more experimental procedures into a high-confidence interaction network for alpha-synuclein. A detailed analysis of its interaction partners was performed to obtain additional hints on potential functional roles of alpha-synuclein in PD.

4.7.1 A high-confidence interaction network for alpha-synuclein

Interaction data of wild-type alpha-synuclein and its mutant isoforms obtained by the Y2H, cytoY2H, subSEQ or LUMIER assays was integrated to obtain a high-confidence interaction network. Only interactions of wild-type or mutant alpha-synuclein detected in at least 2 of the assays were integrated into this network. Interactions excluded in the previous analyses, as profiling data suggested the proteins might not be expressed in the human brain, were also included into the high-confidence interaction network. In addition, the network includes interactions that were predicted as low confidence by bioinformatic scoring.

In total, 135 interaction partners of wild-type alpha-synuclein were integrated into the high-confidence network. 4 of these interactions were identified by all 4 applied PPI detection methods. 18 interactions were detected by 3 methods, and 113 interactions were only detected by 2 methods. 32 interactions of the A30P mutant of alpha-synuclein were also integrated; all of them detected by 2 PPI detection methods. Furthermore, 3 interactions of E46K alpha-synuclein were taken into account, which were all detected by 2 methods. Interactions of the A53T mutant isoform of alpha-synuclein were not integrated, as it was only screened for interactions in the cytoY2H assay. The high-confidence interactors of wild-type and mutant alpha-synuclein were grouped according to the alpha-synuclein isoforms they interacted with (Figure 4-30). In total, the high-confidence network contains 8 known interactors of alpha-synuclein. 125 proteins that only interacted with wild-type alpha-synuclein are summarized in group 1, while group 2 contains 22 proteins that exclusively interacted with the A30P isoform. Group 3 summarizes 8 proteins that interacted with both wild-type and A30P alpha-synuclein. A single protein interacted with the wild-type and the E46K isoform, while another protein exclusively interacted with the E46K isoform of alpha-synuclein. Finally, one protein interacted with all three alpha-synuclein isoforms.

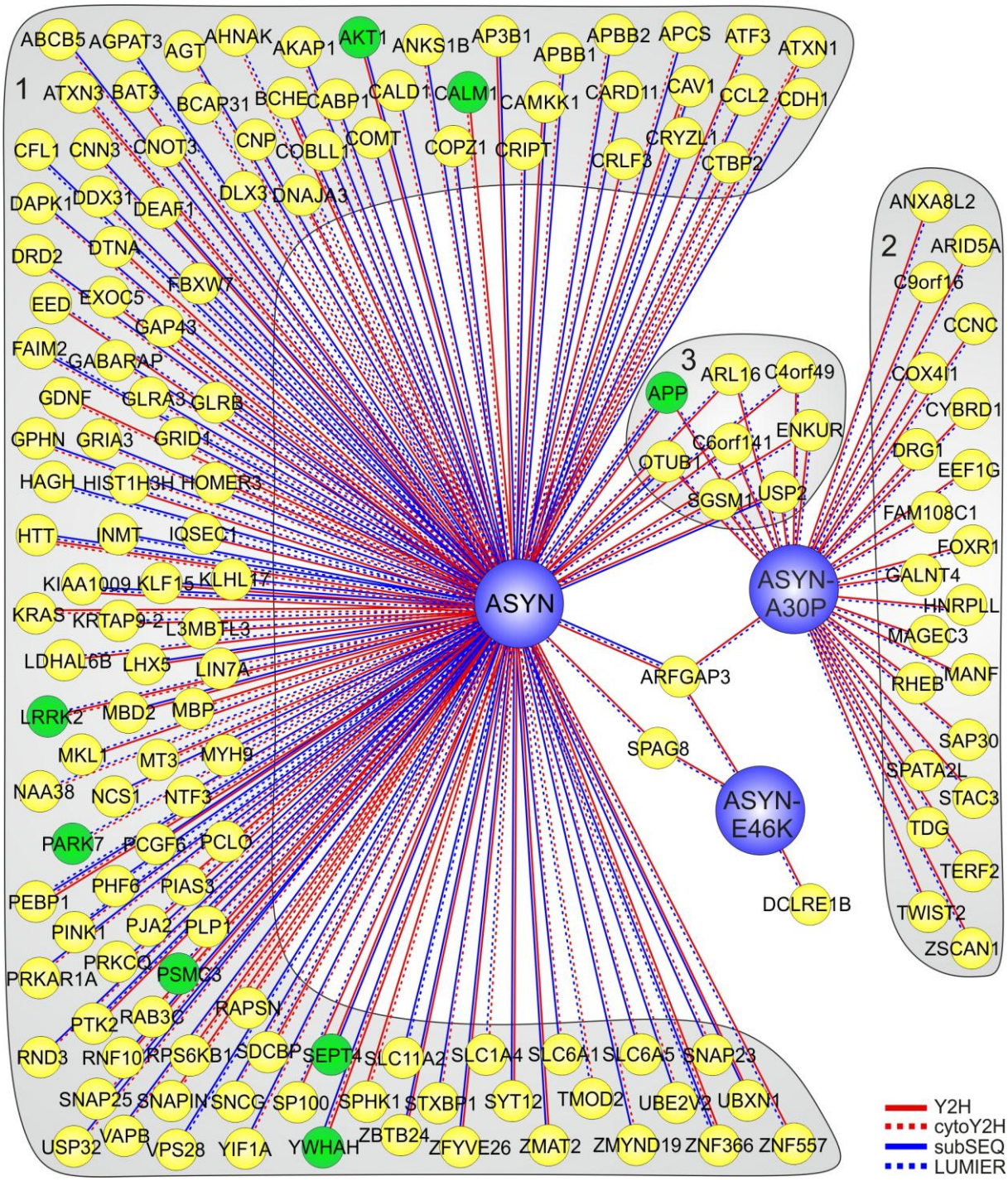

Figure 4-30: High-confidence interaction network of alpha-synuclein. Proteins interacting with alpha-synuclein in at least two PPI detection methods were grouped according to the alpha-synuclein isoform they interacted with, as indicated by the numbered grey outlines. The methods reporting an interaction are represented by edges as explained in the legend. Published interactors of alpha-synuclein are shown with green nodes, while all other proteins are shown with yellow nodes.

4.7.2 Literature based analysis of selected high-confidence interactors

An interaction between the Ras homolog enriched in brain (RHEB) and the A30P isoform of alpha-synuclein was detected by Y2H and confirmed in the LUMIER assay. The protein is vital for the regulation of growth and cell cycle progression due to its regulatory role in the insulin/TOR/S6K signaling pathway [348]. Strikingly,

expression of a constitutively active form of RHEB protects dopaminergic neurons from neurodegeneration and mediates axon regrowth [349]. This example indicates that the literature based functional analysis of alpha-synuclein interactors detects known proteins and could also help to identify novel potential therapeutic targets for PD.

The interaction of wild-type alpha-synuclein with the Fas apoptotic inhibitory molecule 2 (FAIM2) was detected by cytoY2H and subSEQ and could be further validated in the LUMIER assay. FAIM2 can inhibit FAS mediated apoptosis [350] and reduction of the FAIM2 protein levels by RNAi knockdown sensitizes neurons to FasL-induced (ligand of the FAS receptor) cell death and caspase-8 activation [351]. Potential beneficial effects of FAIM2 in PD could be assessed by overexpression of the protein in a cell model [107] of the disease.

Y2H, cytoY2H and subSEQ interaction methods detected the interaction of wild-type alpha-synuclein with the phosphatidylethanolamine binding protein 1 (PEBP1). In addition, the interaction was confirmed with the LUMIER assay. PEBP1 inhibits NF-κB signaling [352] and inhibition of this pathway reduces the loss of dopaminergic neurons in a PD mouse model [353]. Alpha-synuclein might influence the NF-κB pathways by binding to PEBP1. An effect of PEBP1 on the disease could be tested by overexpression of the protein in a mouse model of PD [258].

Alpha-synuclein localizes to pre-synaptic terminals and is thought to regulate synaptic vesicle formation and neurotransmitter release [202, 203], both crucial processes for the transmission of nerve impulses. Strikingly, the high-confidence interaction network includes several presynaptic proteins involved in vesicle trafficking, specifically endocytosis and exocytosis. These proteins include the synaptosomal-associated proteins 23 and 25 (SNAP23, SNAP25), the SNAP-associated protein (SNAPIN), synaptotagmin XII (SYT12), the presynaptic cytomatrix protein piccolo (PCLO) and RAB3C, a member of the RAS oncogene family. All of these proteins interacted with wild-type alpha-synuclein, further supporting a role of alpha-synuclein in vesicle trafficking. Alpha-synuclein, especially in a misfolded or aggregated form, might sequester presynaptic proteins involved in vesicle trafficking, and thereby disturb this essential process, eventually leading to neuronal death.

4.7.3 Gene-term enrichment analysis of high-confidence interactors of wild-type alpha-synuclein

To identify specific biological functions associated with the high-confidence interactors of alpha-synuclein, gene-term enrichment was performed using the DAVID functional annotation tool [162, 163]. The tool was used to compare the terms enriched among the high-confidence interactors of wild-type alpha-synuclein with the terms enriched among the possible interactors of alpha-synuclein. The list of possible interactors contains all genes encoding proteins that could have interacted with alpha-synuclein in the subSEQ screen and at least one other PPI detection method (Y2H, cytoY2H, LUMIER). Only results with a p-value <0.05 were considered as statistically significant. Figure 4-31 compares the results of the analysis with the terms enriched among the published interactors of alpha-synuclein. See Supplementary Table 8 for the exact numbers and the corrected p-values behind the gene-term enrichment analysis. It was also attempted to detect terms enriched among the proteins exclusively interacting with the A30P isoform (Group 2 in Figure 4-30) or the shared interactors of wild-type and A30P alpha-synuclein (Group 3 in Figure 4-30). However, no statistically significant results were detected for these groups of alpha-synuclein interactors.

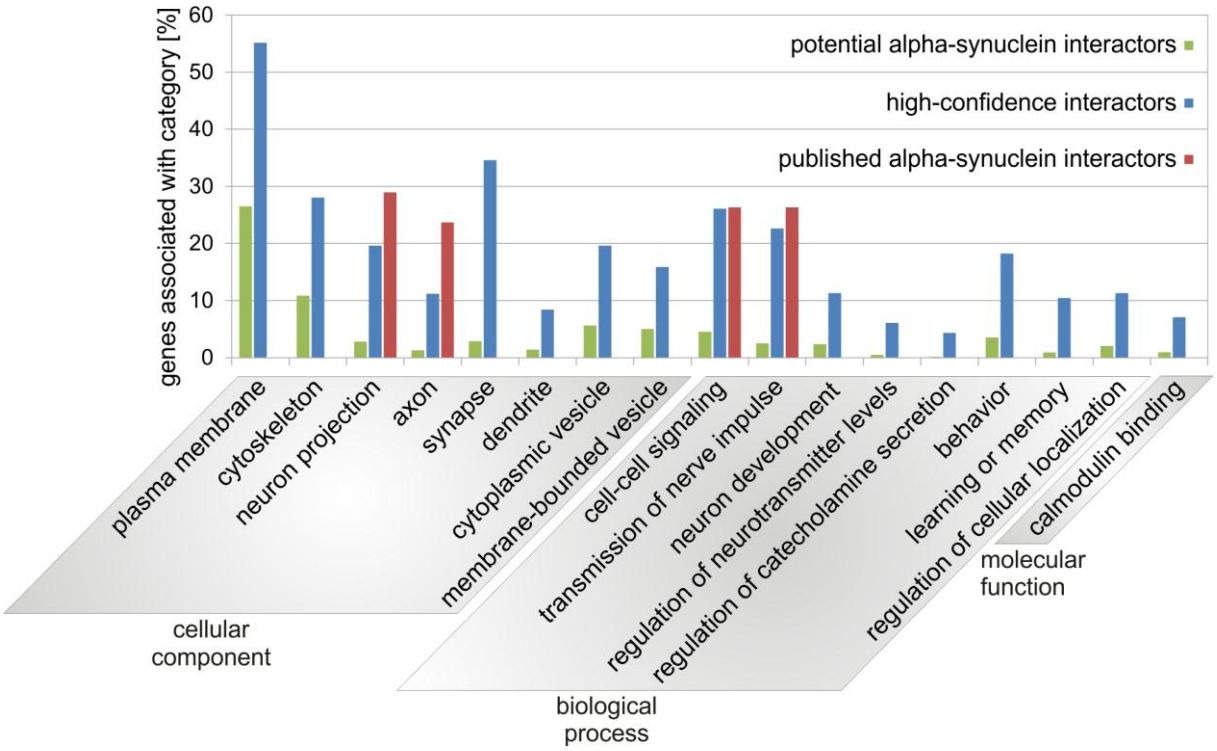

Figure 4-31: Gene-term enrichment analysis of high-confidence interactors of alpha-synuclein. Interactors of wild-type alpha-synuclein from the high-confidence network were analyzed for gene-term enrichment compared to all possible interactors (see text) and published interactors of alpha-synuclein using the DAVID Functional Annotation Tool. Only statistically significant results (P<0.05, Bonferroni correction) were taken into account.

The terms “neuron projection” and “axon” (GO cellular components), as well as the terms “cell-cell signaling” and “transmission of nerve impulse”, (GO biological processes) enriched among the high-confidence interactors were also found among the published interactors of alpha-synuclein. The fact that the gene-term enrichment analysis of the high-confidence interactors of alpha-synuclein detected terms enriched among the published interactors validates the analysis as a tool to identify new biologically relevant terms. A large fraction of the high-confidence interactors were localized to the plasma membrane (55.1% of interactors associated) or were part of the cytoskeleton (28% of interactors associated). The enrichment analysis also identified a localization of the interactors in the neuron projection (19.6% of interactors associated), more specifically to the axon (11.2% of interactors associated) and the synapse (34.6% of interactors associated). As alpha-synuclein is a protein localized to the pre-synaptic nerve terminals [56], these terms further underline the biological relevance of the detected interactions. Furthermore, the interactors were localized to the dendrite (8.4% of interactors associated) and associated with cytoplasmic (19.6% of interactors associated) or membrane-bounded vesicles (15.6% of interactors associated), all terms previously associated with alpha-synuclein. Biological processes associated with the high-confidence interactors were “cell-cell signaling” (26.1% of interactors associated), in particular “transmission of nerve impulse” (21.6% of interactors associated). Alpha-synuclein localizes to pre-synaptic terminals and is thought to regulate synaptic vesicle formation and neurotransmitter release [202, 203], both are crucial processes for the transmission of nerve impulses. Interestingly, the high-confidence interactors were also associated with the terms “regulation of neurotransmitter levels” (6.1% of interactors associated), especially the “regulation of catecholamine secretion” (4.3% of interactors associated). Catecholamines include the neurotransmitter dopamine and alpha-synuclein overexpression has been shown to inhibit catecholamine release in different cell models [354]. Other associated terms described biological processes like “neuron development” (11.3% of interactors associated), “behavior” (18.3% of interactors associated) and “learning or memory” (10.4% of interactors associated). It is published that alpha-synuclein can affect synaptic plasticity during learning [55]. The analysis also suggested a role of the interactors in the “regulation of cellular localization” (11.3% of interactors associated). A GO molecular function associated with the high-confidence alpha-synuclein interactors was “calmodulin binding” (7.1%

of interactors associated). Alpha-synuclein itself has been shown to bind calmodulin and this interaction reduces its propensity to interact with membranes [355]. In summary, the gene-term enrichment analysis did not detect any terms that had not been previously associated with alpha-synuclein. However, the detection of terms with a known association to PD of alpha-synuclein indicates that the high-confidence PPI network contains physiologically relevant interaction data.

4.7.4 Summary of chapter 7

Protein-protein interaction data obtained from the previous experiments was integrated into a high-confidence interaction network of alpha-synuclein. Only proteins that interacted with alpha-synuclein in two of the applied PPI detection methods (Y2H, cytoY2H, subSEQ, LUMIER) were included in the network. The network contained 8 published interactors of alpha-synuclein, indicating that the integration of PPI data into a high-confidence network could also identifiy biologically relevant, previously unknown interactors of alpha-synuclein. The analysis of selected interactors supported the hypothesis that alpha-synuclein plays an important role in vesicle trafficking. It also highlighted a possible regulatory role of alpha-synuclein in the insulin/TOR/S6K and NF-κB signaling pathways and in FAS mediated apoptosis. Physiological relevance of the interactions in the high-confidence network was also suggested by a gene-term enrichment analysis that identified terms with a known association with alpha-synuclein or PD.

4.8 Modifiers of alpha-synuclein induced toxicity

Studies in *S. cerevisiae* and the nematode *C. elegans* have identified many genes and proteins that modulate alpha-synuclein induced toxicity. The interaction studies presented in the previous chapters identified several interactors of alpha-synuclein that are human orthologs of the modulators proteins identified in yeast and in worms. The aim of this chapter was to test the ability of some of these interacting human proteins to modulate alpha-synuclein toxicity in a yeast model of PD.

4.8.1 Published modifiers of alpha-synuclein induced toxicity

Alpha-synuclein induced toxicity can be enhanced or suppressed by other genes and proteins [100]: Many of these toxicity modifiers were identified in studies using *S. cerevisiae* knockout strains producing alpha-synuclein [356] or in yeast strains

coproducing alpha-synuclein with other gene products [100, 357]. In addition, RNAi knockdown screens in the nematode *C. elegans* identified additional modifiers of alpha-synuclein induced toxicity [358, 359]. These modifiers of alpha-synuclein induced toxicity will be referred to as “modifiers” or “toxicity modifiers” henceforth. Modifier genes were retrieved from these publications and their corresponding human orthologs were identified using the HomoloGene database [360]. In many cases, more than one human ortholog of a modifier gene was identified. In total, 207 orthologous genes encoding known modifiers were found. 23 of these orthologous genes were identified as toxicity modifiers in 2 of the publications, while the 2 orthologous genes were even found in 3 publications. Interestingly, 57 of the orthologous genes encoded proteins were found to interact with alpha-synuclein in the Y2H, cytoY2H and subSEQ interaction studies. See http://141.80.164.19/koenn/ for detailed results.

4.8.2 Expression of human modifier proteins in a yeast model of PD

To test whether the toxicity modifier orthologs interacting with alpha-synuclein can also modify alpha-synuclein induced toxicity, I randomly selected 37 genes (for which entry clones were available) from the list of orthologs. 5 of the selected genes were found to encode suppressors of alpha-synuclein induced toxicity in the *C. elegans* PD model. 31 of the genes encoded toxicity modifiers identified in yeast, where 23 of the proteins suppressed and 8 enhanced toxicity. One gene was identified in both yeast and worm models and encoded a toxicity suppressor. Entry-clones encoding the 8 putative enhancers and 29 suppressors of alpha-synuclein toxicity were selected (Table 4-5). See Supplementary Table 9 for details about the tested proteins. The sequences of the putative modifiers were Gateway™ cloned into the yeast expression vector pAG425-FLAG. This vector fuses the FLAG-tag (1012 Da) to the N-terminus of the toxicity modifiers, which are expressed under control of an inducible GAL promoter. The generated plasmids as well as the empty pAG425-FLAG vector were transformed into W303-1A yeast strains. These strains expressed either two copies of GFP, GFP-tagged wild-type or GFP-tagged A53T alpha-synuclein [108]. All constructs were integrated into the yeast genome and are under control of an inducible GAL promoter. Liquid cultures were normalized for OD600 and serial dilutions of yeast cells were spotted onto SD-ltu/ha (-Leu-Trp-His) agar plates containing glucose or galactose. Growth on glucose medium represses the expression of the alpha-synuclein as well as the modifiers, while growth on

galactose medium strongly induces their expression. All experiments were performed in triplicates.

4.8.3 Human proteins co-produced with alpha-synuclein modulate its toxicity

As reported previously [108], co-expression of the FLAG-tag (without a modifier protein) with wild-type alpha-synuclein (Figure 4-32 A), but even more with the A53T mutant isoform (Figure 4-32 B), was toxic for yeast cells and led to reduced growth in comparison to the control strain without GFP expression (Figure 4-32 C). The growth of these three yeast strains expressing different potential modifiers was compared to the growth of yeast cells that only express the FLAG tag from the empty pAG425-FLAG vector (vector). According to the resulting growth patterns, the tested modifier proteins were assigned to one of the following categories: no effect, enhancer or suppressor of toxicity.

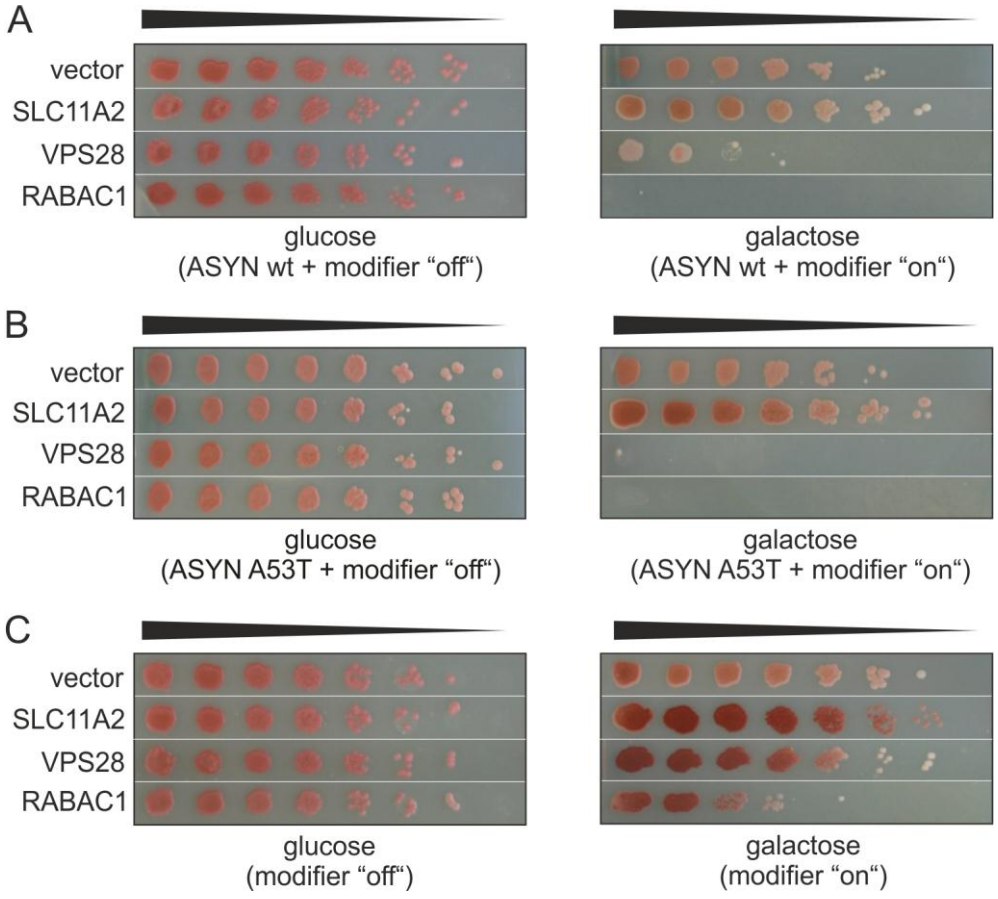

Figure 4-32: Human proteins modulate alpha-synuclein induced toxicity in yeast. Modifiers of alpha-synuclein induced toxicity were synthesized as FLAG-tag fusion proteins in yeast strains expressing wild-type alpha-synuclein (A), the GFP-tagged A53T mutant of alpha-synuclein (B) or GFP alone (C). Serial dilutions of yeast cells were spotted onto medium containing glucose (repressing alpha-synuclein / GFP and modifier expression) or galactose (inducing alpha-synuclein / GFP and modifier expression). Growth of strains expressing alpha-synuclein (or GFP) and the FLAG tag alone (vector) was compared to the growth of strains expressing FLAG-tagged modifier proteins. Analysis of the resulting growth patterns revealed modifier proteins that suppressed (SLC11A2) or enhanced (VPS28, RABAC1) alpha-synuclein incuded toxicity in yeast. Some modifiers (RABAC1) were already toxic when expressed without alpha-synuclein (C).

Enhancers of toxicity reduced yeast growth in comparison to the vector control (no modifier expressed). Upon co-expression with alpha-synuclein, some of the enhancers showed minimal growth (e.g. VPS28), while others completely inhibited yeast growth (e.g. RABAC1). Interestingly, some modifier proteins (e.g. VPS28) enhanced toxicity much stronger in the yeast strain expressing the A53T isoform than in the strain expressing wild-type alpha-synuclein. Suppressors of toxicity (e.g. SLC11A2) allowed growth similar to the yeast strain expressing GFP alone. In total, 3 human orthologs had a suppressive, 30 had an enhancing and 4 had no effect on alpha-synuclein induced toxicity when overexpressed in yeast. Interestingly, 9 of the proteins enhancing toxicity were also slightly toxic in the control strain (e.g. RABAC1 in Figure 4-32 C), while the expression of 9 other strong enhancers only allowed marginal or no growth of the control strain. These results indicate that, independent of alpha-synuclein induced toxicity, overexpression of some of the modifier proteins alone is already toxic for yeast cells.

Table 4-5: Tested modifiers of alpha-synuclein induced toxicity.

Modifier symbol (species)	Publ.	study type	effect in study	Gene symbol human ortholog	interaction with alpha-synuclein identified by	Growth control strain (no ASYN)	Growth ASYN wt strain	Growth ASYN A53T strain	Modifier effect
GLO3 (S. c.)	[357]	overex	enh	ARFGAP3	subSEQ	--	---	---	enh
SEC28 (S. c.)	[357]	overex	sup	COPE	subSEQ	0	--	---	enh
CAX4 (S. c.)	[357]	overex	enh	DOLPP1	subSEQ	0	--	--	enh
YCR026C (S. c.)	[356]	del	sup	ENPP5	subSEQ	-	---	---	enh
C35D10.2 (*C. e.*)	[358]	RNAi	sup	GIPC1	cytoY2H	0	---	---	enh
GLO4 (S. c.)	[356]	del	sup	HAGH	subSEQ	0	---	---	enh
HBS1 (S. c.)	[356]	del	sup	HBS1L	subSEQ	-	--	---	enh
IME2 (S. c.)	[357]	overex	sup	ICK	subSEQ	0	0	0	no effect
FZF1 (S. c.)	[357]	overex	sup	KLF15	Y2H	0	--	--	enh
lit-1 (*C. e.*)	[359]	RNAi	sup	NLK	subSEQ	0	0	0	no effect
NRG1 (S. c.)	[100]	overex	enh	NRG1	subSEQ	-	---	---	enh
PDE2 (S. c.)	[357]	overex	sup	PDE1C	subSEQ	0	-	--	enh
PDE2 (S. c.)	[357]	overex	sup	PDE4C	subSEQ	0	0	0	no effect
PDE2 (S. c.)	[357]	overex	sup	PDE4D	subSEQ	-	-	-	enh
PDE2 (S. c.)	[357]	overex	sup	PDE6B	subSEQ	--	--	---	enh
OPI3 (S. c.)	[356]	del	sup	PEMT	subSEQ	0	-	--	enh
pink-1 (*C. e.*)	[358]	RNAi	sup	PINK1	cytoY2H / subSEQ	0	-	--	enh
CUP9 (S. c.)	[357]	overex	sup	PKNOX1	subSEQ	0	+	+	sup
PPZ1 / PPZ2 (S. c.)	[357]	overex	enh	PPP1CA	subSEQ	--	---	---	enh

Table continued on next page.

Modifier symbol (species)	Publ.	study type	effect in study	Gene symbol human ortholog	interaction with alpha-synuclein identified by	Growth control strain (no ASYN)	Growth ASYN wt strain	Growth ASYN A53T strain	Modifier effect
PTK2 (S. c.)	[356]	del	sup	PTK2	cytoY2H / subSEQ	0	0	-	enh
PTP2 (S. c.)	[357]	overex	sup	PTPRE	subSEQ	-	---	---	enh
YPT1 (S. c.)	[357]	overex	sup	RAB13	subSEQ	0	---	---	enh
YIP3 (S. c.)	[357]	overex	enh	RABAC1	cytoY2H	--	---	---	enh
RPS31 (S. c.)	[100]	overex	sup	RPS27A	cytoY2H	0	--	--	enh
SEC31 (S. c.)	[357]	overex	enh	SEC31A	subSEQ	0	0	0	no effect
SEC31 (S. c.)	[357]	overex	enh	SEC31B	subSEQ	0	+	0	sup
smf-1 (*C. e.*)	[358]	RNAi	sup	SLC11A2	subSEQ	0	+	+	sup
SLY41 (S. c.)	[100] [357]	overex	enh	SLC35E1	subSEQ	0	-	-	enh
AVT4 (S. c.)	[357]	overex	sup	SLC36A2	subSEQ	---	---	---	enh
DIP5 (S. c.)	[357]	overex	sup	SLC7A1	subSEQ	-	---	---	enh
DIP5 (S. c.)	[357]	overex	sup	SLC7A14	subSEQ	-	---	---	enh
DIP5 (S. c.)	[357]	overex	sup	SLC7A3	subSEQ	--	---	---	enh
ERV29 (S. c.) / sft-4 (C. e.)	[100] [357] [358]	overex / RNAi	sup	SURF4	subSEQ	--	---	---	enh
CUP9 (S. c.)	[357]	overex	sup	TGIF1	subSEQ	0	--	---	enh
ubc-9 (*C. e.*)	[359]	RNAi	sup	UBE2I	subSEQ	-	--	---	enh
VPS28 (S. c.)	[356]	del	sup	VPS28	subSEQ	0	--	---	enh
YDR374C (S. c.)	[357]	overex	sup	YTHDF3	subSEQ	--	---	-	enh

Abbreviations: *S. c.*: *Saccharomyces cerevisiae*; *C. e.*: *Caenorhabditis elegans*; RNAi: RNAi knockdown study in *C. elegans*; overex: yeast overexpression study; del: yeast deletion strain study; sup: suppressor; enh: enhancer; +: increased growth; 0: no influence on growth; -: slightly reduced growth; --: strong growth reduction; ---: marginal or no growth.

4.8.4 Modifier screen includes human proteins with known PD association

Several of the human proteins tested in the toxicity essay have a published association with PD: Similar to its yeast ortholog [100], overexpression of human neuregulin (NRG1) increased alpha-synuclein induced toxicity in yeast. In contrast, administration of the neurotrophic factor neuregulin in a PD mouse model protects dopaminergic neurons against the disease phenotype [361].

The ortholog of the PTEN-induced putative kinase 1 (PINK1) was identified as a suppressor of alpha-synuclein induced toxicity in a RNAi knockdown screening in *C. elegans* [358]. Consistent with these findings, overexpression of its human ortholog in yeast enhances alpha-synuclein induced toxicity. In contrast, the

D. melanogaster ortholog of PINK1 is known to modulate alpha-synuclein toxicity in flies, where its overexpression rescues the PD disease phenotype [362].

An RNAi knockdown screen in *C. elegans* [358] identified the ortholog of the divalent metal transporter 1 (DMT1) as a suppressor of alpha-synuclein induced toxicity. Its human ortholog, which is encoded by the SLC11A2 gene, suppressed alpha-synuclein induced toxicity. In contrast, overexpression of the transporter in a mouse PD model increased disease symptoms like oxidative stress, and dopaminergic cell loss [363].

As the toxicity assays included human orthologs of known modulators of alpha-synuclein induced toxicity with known PD association, it was assumed that the assay could also identify new toxicity modulators.

4.8.5 Modifier screen identifies human proteins as novel modulators of alpha-synuclein induced toxicity

Several of the human proteins that modulated alpha-synuclein induced toxicity have not previously been associated with PD. The ADP-ribosylation factor GTPase-activating protein 3 (ARFGAP3) associates with the Golgi apparatus and has a regulatory function in the early secretory pathway of proteins [364]. Its yeast ortholog was identified as an enhancer of alpha-synuclein induced toxicity by a protein overexpression screen in yeast [357]. In a similar way, overexpression of its human ortholog enhanced alpha-synuclein induced toxicity in the yeast assay, but overexpression of the protein was slightly toxic in the control strain (not expressing alpha-synuclein). ARFGAP3 has been described as a toxicity modulator of leucine-rich repeat kinase 2 (LRRK2) [365], a protein that is associated with autosomal-dominant parkinsonism [366]. ARFGAP3 might also interact with alpha-synuclein and thereby stimulate its propensity to form aggregates as well as induce toxicity.

The transcription factor encoded by the yeast gene CUP9 was identified as suppressor of alpha-synuclein induced toxicity in a yeast overexpression screen [357]. In accordance with these results, overexpression of its human ortholog PKNOX1, encoding the PBX-regulating protein-1 (Prep1), also suppressed toxicity in the current yeast screen. Interestingly, the homeodomain transcription factor Prep1 can directly regulate apoptotic pathways by controlling the levels of the antiapoptotic Bcl-XL protein [367], and several studies have demonstrated that apoptosis may play a critical role in PD [343]. Aggregated alpha-synuclein might sequester Prep1 and thereby decrease the levels of Bcl-XL, leading to induction of apoptosis.

In general, the localization and aggregation of alpha-synuclein in the presence of the identified human modifier proteins could be monitored in yeast, as the GFP tag fused to alpha-synuclein can be visualized by fluorescence microscopy *in vivo*. Furthermore, the modifiers could be tested in cell [107] and animal models [258] of PD, both by knockout or overexpression studies. In addition, small molecules or peptide inhibitors targeting the modifier proteins could be tested for possible effects in PD models.

4.8.6 Gene-term enrichment analysis of toxicity modifiers

One-third of the genes that enhanced alpha-synuclein toxicity in a genome-wide yeast screen are functionally related to vesicle trafficking and lipid metabolism [356]. To identify biological processes or signaling pathways associated with the modifiers tested in the current work, gene-term enrichment analysis was performed using the DAVID functional annotation tool [162, 163]. Thus, the tool was used to quantify gene-terms associated with all 207 human orthologous genes encoding published modifiers (toxicity modifiers) of alpha-synuclein toxicity in comparison to the human genome. In Figure 4-33, the results were compared to the terms enriched among the 57 modifier orthologs interacting with alpha-synuclein. See Supplementary Table 10 for the exact numbers and the corrected p-values behind the gene-term enrichment analysis. Only results with a p-value <0.05 were considered as statistically significant. In addition, gene-terms enriched among the proteins enhancing or suppressing toxicity in the performed assays were identified and compared to the enrichment of all tested modifier proteins. However, these results were not statistically significant.

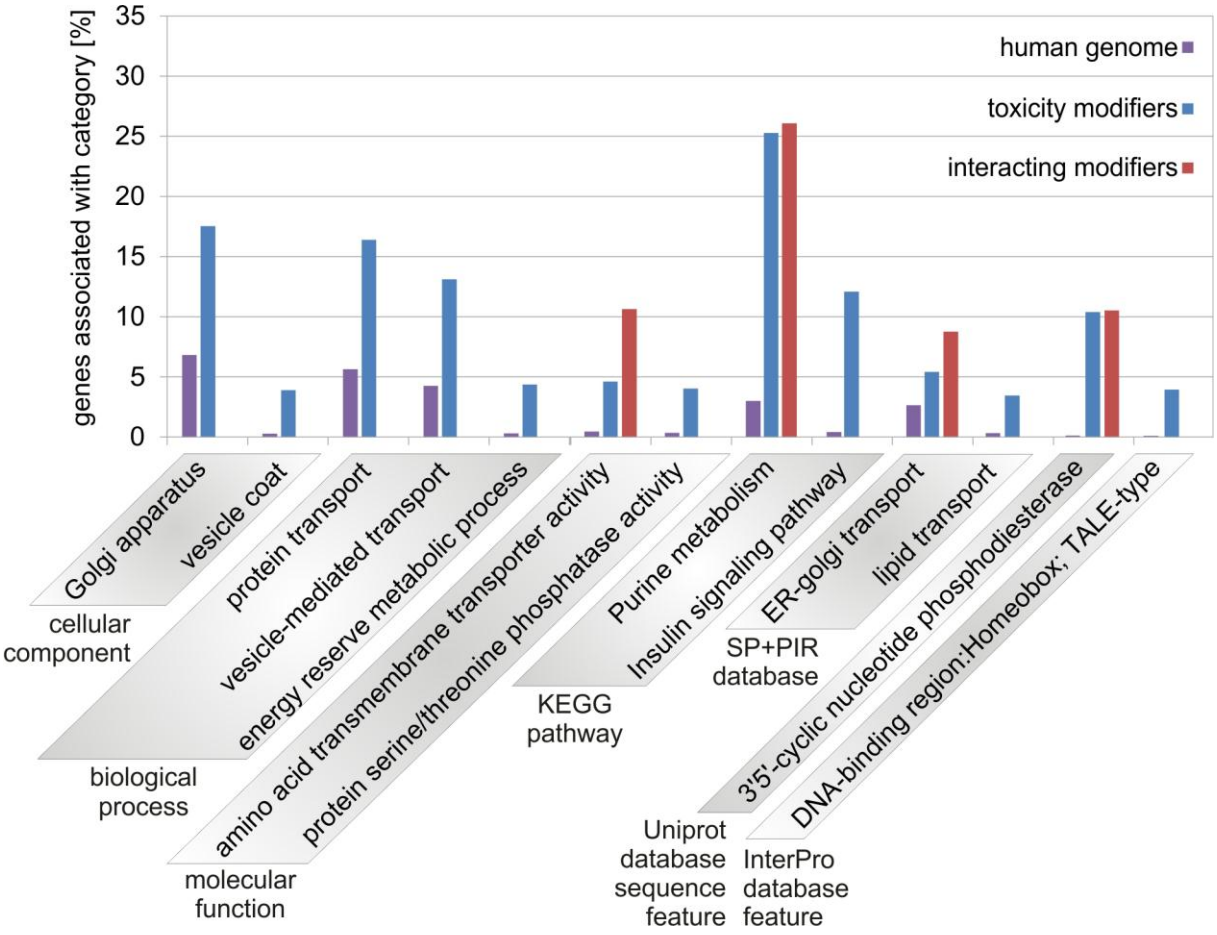

Figure 4-33: Gene-term enrichment analysis of toxicity modifiers. Human orthologues of published modifiers of alpha-synuclein induced toxicity (toxicity modifiers) and orthologues interacting with alpha-synuclein (interacting modifiers) were analyzed for gene-term enrichment compared to the human genome using the DAVID Functional Annotation Tool. Only statistically significant results (P<0.05, Bonferroni correction) were taken into account. SP+PIR database: SwissProt and Protein Information Resource database (SP_PIR_KEYWORDS). Uniprot database sequence feature: Uniprot database (UP_SEQ_FEATURE), InterPro database feature: InterPro database (INTERPRO).

The gene-term enrichment analysis identified several biological processes and functions associated with the modifiers of alpha-synuclein induced toxicity. Many of the proteins are involved with transport processes, specifically the transport of proteins (GO biological process: protein transport, 16.4% associated), amino acids (GO molecular function: amino acid transmembrane transporter activity, 4.6%) and lipids (SP_PIR_KEYWORD: lipid transport, 3.4%). Some of these transport processes might be associated with vesicles (GO cellular component: vesicle coat, 3.9%; GO biological process: vesicle mediated transport, 13.1%), in particular the Golgi apparatus (GO cellular component: Golgi apparatus, 17.5%; SP_PIR_KEYWORD: ER-golgi transport, 5.4%). Several lines of evidence suggest that alpha-synuclein is involved in the control of vesicle trafficking, most likely by lipid binding or association with membranes [100, 357, 368]. In addition, overexpression of alpha-synuclein specifically blocks ER-Golgi traffic [100]. According to the gene-

term enrichment analysis, the modifier proteins are also involved in nucleotide (KEGG pathway: Purine metabolism, 25.3%; UP_SEQ_FEATURE: 3'5'-cyclic nucleotide phosphodiesterase, 10.4%) and energy metabolism (GO biological process: energy reserve metabolic process, 4.4%). These terms have not been associated with alpha-synuclein or PD previously. Other modifier proteins function as phosphatases (GO molecular function: protein serine/threonine phosphatase activity, 3.9%) or transcription factors (INTERPRO: DNA-binding region: Homeobox; TALE-type, 3.9%). Furthermore, the gene-term enrichment analysis suggested a role of some modifier proteins in Insulin signaling (KEGG pathway: Insulin signaling pathway, 12.1%). Insulin signaling was found to be defective in a PD mouse model [329].

4.8.7 Summary of chapter 8

A yeast model of PD was used to test the effect of 37 human proteins on alpha-synuclein induced toxicity. Orthologs of these proteins had previously been identified as modifiers of alpha-synuclein induced toxicity in *S. cerevisiae* and *C. elegans*. In addition, all of these proteins interacted with alpha-synuclein in previously performed interaction studies. 81% of the tested proteins had an enhancing, while only 8% had a suppressing effect on alpha-synuclein induced toxicity when overexpressed in yeast. 11% of the tested proteins did not modify toxicity. Testing alpha-synuclein-interacting proteins for their ability to influence alpha-synuclein induced toxicity in yeast identified known and novel modulator proteins. The effects of the novel modulator proteins could be tested further in other PD model systems. In addition, the effects of small molecules or peptide inhibitors that target the modifier proteins could also be assessed. A gene-term enrichment analysis indicated that the toxicity modifiers physically interacting with alpha-synuclein are involved in vesicular transport processes, further supporting a role of alpha-synuclein in this vital process.

5 Discussion

Parkinson's disease (PD) and other progressive neurological disorders like dementia with Lewy bodies and multiple systems atrophy belong to the group of synucleinopathies. The two major pathological features of PD are the death of dopaminergic neurons and diffuse accumulation of the alpha-synuclein protein in intracellular aggregates of surviving neurons. These aggregates are known as Lewy bodies and Lewy neurites [369]. Additional evidence for a role of alpha-synuclein in the pathogenesis of familial PD is provided by the identification of three point mutations in the SNCA gene that have been linked to early onset PD [42-44]. Furthermore, duplication and triplication of the SNCA locus have been found in families with dominant PD [45, 46]. A role of alpha-synuclein in the pathogenesis of sporadic PD is implicated by single nucleotide polymorphisms in the SNCA gene that are associated with increased PD risk [49, 50, 370]. Even though a lot of research effort has been devoted to the identification of the precise role of alpha-synuclein in PD pathology, the exact disease mechanism has not been identified yet. A well-established method for determining the function of a protein of interest is the study of interacting proteins. For example, if a protein is found to interact with known components of the proteasome, it is quite likely that it also plays a role in ubiquitin-mediated protein degradation. Although the interaction of alpha-synuclein with numerous proteins has been described in literature, studies to create a comprehensive protein-protein interaction (PPI) network have not been published. To find out more about the role of alpha-synuclein in the pathogenesis of PD, a high-confidence PPI network was generated by combining the interaction data obtained by different PPI detection methods. Therefore, two methods that are commonly used in our workgroup to generate PPI networks, the Y2H and the LUMIER co-immunoprecipitation assay, were applied. Furthermore, two additional methods for PPI detection were developed and applied: the cytosolic yeast two-hybrid (cytoY2H) system modified for high-throughput application detects interactions of a membrane-recruited bait protein with an array of prey proteins in the yeast cytoplasm. The subSEQ method combines a cytoY2H cDNA library screen with next-generation sequencing (NGS) to identify prey proteins interacting with baits. Several human proteins that interacted with alpha-synuclein were orthologs of alpha-synuclein toxicity modifiers identified in yeast and worms. These human proteins were tested for their ability to modify alpha-synuclein toxicity when overexpressed in yeast.

5.1 An alpha-synuclein interaction network based on published data

Using PPI database mining and manual literature curation, published information on proteins interacting with alpha-synuclein was collected. The generated network based on published data was used to get a detailed overview of the current knowledge on alpha-synuclein. In addition, the set of published interactors was used to validate the interaction data obtained from the PPI detection methods applied in this thesis. To select only interactors with high experimental support, it was decided that at least two independent experiments had to support an interaction to qualify it as high-confidence (HC). Initially, PPI data was collected using the HIPPIE database (Human Integrated Protein-Protein Interaction rEference) [171], which integrates datasets from other PPI databases and provides a confidence score for each interaction. This confidence score is based on the experimental data supporting the reported interactions. However, additional PPI database searches and manual literature curation were necessary, as 38% of the proteins defined as high-confidence interactors of alpha-synuclein were not included in the HIPPIE database. Additional manual curation of all publications associated with an interaction listed in the HIPPIE database was necessary as some of the presented experiments demonstrated the absence of a specific interaction. The high stringency of two independent experiments required for the selection as a high-confidence interaction partner also led to the exclusion of some interactors like the protein-tyrosine kinases FYN and LYN. Published work only demonstrated *in vitro* phosphorylation of alpha-synuclein by these kinases [232, 233], but provided no additional evidence for a direct interaction. However, phosphorylation requires a physical interaction of the kinase and its substrate. Interestingly, the Y2H screen performed for this thesis provided experimental support for a direct interaction between alpha-synuclein and both of the kinases. In total, 42 proteins were defined as HC interactors of alpha-synuclein. In order to detect shared functions and biological themes associated with the high-confidence set of interactors, a gene-term enrichment analysis was performed. In accordance with published localization data of alpha-synuclein in presynaptic nerve terminals [371], its interacting proteins were also associated with gene-terms describing a localization to neurons, more specifically to the axon. Several biological processes like “regulation of programmed cell death”, “transmission of nerve impulse”, more specifically “dopaminergic synaptic transmission” were also associated with the published interactors. There are various lines of evidence

suggesting that the activation of programmed cell death pathways may lead to neurodegeneration in PD, specifically the degeneration of dopaminergic neurons in the substantia nigra pars compacta (SNpc) [199]. Furthermore, an association of the published interactors with the KEGG pathways **“**Parkinson's disease” and “Alzheimer's disease” were found. This finding is in accordance with the view that there are common molecular mechanisms underlying different neurodegenerative disorders [372]. As described in the results section, all gene-terms enriched among the published interactors of alpha-synuclein had a known association with PD; no novel terms were identified. This is likely due to the fact that only published interactors were chosen for the analysis.

5.1.1 Physiological and pathological roles of alpha-synuclein suggested by literature

Several functional roles of alpha-synuclein, especially in the pathogenesis of PD, are currently being proposed by literature. An initial hint on the function of a protein can often be obtained by phenotype characterization of knockout models, for example mice. Mice lacking alpha-synuclein are viable and do not show morphological abnormalities. However, they display a reduction in total striatal dopamine levels [373]. The authors suggested that alpha-synuclein might act as negative regulator of the readily releasable pool of dopaminergic synaptic vesicles. In contrast, another group could not reproduce these findings and suggested that alpha-synuclein regulates the size of the reserve/resting pool of dopaminergic synaptic vesicles. Alpha-synuclein might thus control the refilling of the readily releasable vesicle pool [203].

Additional functions of alpha-synuclein are implied by its interaction with proteins involved in dopamine homeostasis. For example, alpha-synuclein interacts with tyroxine hydroxylase (TH) [113], the rate-limiting enzyme in dopamine biosynthesis. Cells overexpressing alpha-synuclein had significantly reduced TH activity [113]. As expected, dopamine synthesis was reduced in these cells, suggesting that alpha-synuclein plays a regulatory role in dopamine biosynthesis by influencing the activity of TH. This concept is supported by an increased TH activity after alpha-synuclein suppression in cell culture models [114]. In addition, alpha-synuclein interacts with the presynaptic human dopamine transporter (hDAT), which mediates the reuptake of dopamine released from presynaptic terminals of substantia nigra neurons [374-376]. The interaction with alpha-synuclein leads to membrane clustering of hDAT, which in

turn increases cellular dopamine uptake and eventually leads to dopamine-induced cellular apoptosis [327, 377, 378]. Furthermore, alpha-synuclein interacts and selectively inhibits phospholipase D (PLD) [379-381], an enzyme involved in lipid signaling cascades and vesicle trafficking. It was suggested that alpha-synuclein regulates the content of monoaminergic vesicles and the storage of dopamine in synaptic nerve terminals by binding to PLD. In general, dopamine has been reported to induce neurotoxicity [382, 383], indicating that the misregulation of any process involved in dopamine homeostasis can lead to elevated cytoplasmic dopamine levels, leading to the death of dopaminergic neurons [384].

Alpha-synuclein also directly binds to lipid membranes [75] and forms an extended helical structure on small unilamellar vesicles [385]. By binding to lipid membranes, alpha-synuclein alters the bilayer structure which leads to the formation of small vesicles [386]. Alpha-synuclein is also able to bend membranes of large phospholipid vesicles and stimulate the formation of tubules [387]. Furthermore, the binding of alpha-synuclein to membranes is modulated by its interaction with calmodulin [355]. Taken together, the membrane binding properties of alpha-synuclein further support its role in vesicle trafficking, which is impaired in several PD model systems [388]. Additional studies have also suggested an antioxidant activity of alpha-synuclein in the membrane: monomeric but not fibrillar alpha-synuclein prevents lipid oxidation, and this function of alpha-synuclein might be impaired in PD [389].

A function of alpha-synuclein as a molecular chaperone has been suggested as it shares structural homology and interacts with 14-3-3 proteins and several of their ligands [177, 390]. 14-3-3 proteins constitute a family of protein chaperones that bind to ligands at sites containing phospho-serine residues and are present abundantly in neurons [391]. Additional evidence for a role of alpha-synuclein as a chaperone is provided by its interaction with the heat shock 70 kDa protein 1 [392]. Furthermore, alpha-synuclein functions as a nonclassical chaperone that is required for the continuous maintenance of presynaptic SNARE-complex assembly [293, 393]. SNARE complexes are crucial for the release of neurotransmitters at the neuronal synapse, vesicle recycling, and synaptic integrity [394].

Other publications suggest a role in protein degradation, as alpha-synuclein interacts with components of the proteasome [235]. Impaired ubiquitin-proteasome activity is believed to be an important factor in PD pathogenesis, partially as it causes aggregation of alpha-synuclein [395]. Aggregation of alpha-synuclein is also

enhanced after its ubiquitination by Siah-1, which promotes apoptotic cell death [118]. Apoptotic cell death is induced by the release of toxic factors from mitochondria, a process that might me induced by the interaction of the mitochondrial cytochrome C oxidase with alpha-synuclein [396].

Alpha-synuclein might also function as microtubule-associated protein similar to tau [87], which is supported by its interaction with tubulin [182, 183] and the Tubulin Polymerization Promoting Protein (TPPP) [397, 398]. It was shown that alpha-synuclein is able to cause microtubule instability and thereby can induce loss of dopaminergic neurons in PD brain [399].

Furthermore, it was demonstrated that alpha-synuclein interacts with histones in the nucleus, inhibits their acetylation and thereby promotes neurotoxicity [400]. The protein also plays a role in glial cells: Isolated cells lacking the protein secrete elevated levels of proinflammatory cytokines, such as TNF-α (tumor necrosis factor α) and IL-6 (interleukin-6). In addition, the phagocytic abilities of the cells were impaired [401], suggesting that also microglia contribute to the pathophysiology of PD.

Taken together, several functions of alpha-synuclein are suggested by published literature, however its exact role in PD pathogenesis remains unclear.

5.2 An alpha-synuclein interaction network based on Y2H screening data

To get additional hints on the function of wild-type and mutant alpha-synuclein, a semi-automated, robot-assisted Y2H array screen was performed. The Y2H system is a powerful tool for the identification of PPIs. When applied in a high-throughput format, it can be used to detect interactions across the entire proteome of an organism. Proteome-wide studies have generated large Y2H interaction maps for model organisms such as *S. cerevisiae* [121, 402], *C. elegans* [122], and *D. melanogaster* [123]. The generated PPI networks can be used to ask specific biological questions. These can be answered them by performing detailed experiments based on the PPI data. The screening procedure is well established in our workgroup. It has been used to generate large interaction maps for human proteins [125] or interaction maps focused on specific disorders like Huntington's disease [124]. Y2H bait plasmids encoding wild-type alpha-synuclein and its mutant isoforms (A30P, E46K and A53T) were generated by Gateway™ cloning. However, the A53T alpha-synuclein bait failed the subsequent auto-activation test and thus

could not be used for interaction screening. The baits were tested for interactions against an existing prey matrix generated from 16098 ORFs.

5.2.1 Y2H identifies known and novel interactors of alpha-synuclein

In total, the screen detected 200 PPIs of wild-type alpha-synuclein, 146 PPIs of the A30P and 46 PPIs of the E46K isoform. The prey matrix used for the screen contained clones potentially expressing 36 known interacting proteins. 18 of these proteins did interact with wild-type and mutant alpha-synuclein proteins in the Y2H assay. Surprisingly, the rate of detected published interactors in this Y2H screen (50%) was much higher than the detection rate of known interactions in a publication benchmarking the Y2H method [403]. The authors were able to reproduce 25% of the interactions from a reference set of published interacting protein pairs [403]. The fact that published interaction partners of alpha-synuclein were detected in the Y2H assay indicates that the screen generated biologically relevant data. It also validates the technique as a tool to detect novel interactors of alpha-synuclein.

5.2.2 Alpha-synuclein interacts with a large number of proteins

The number of 200 PPIs of wild-type alpha-synuclein detected by Y2H was surprisingly high. The performed cytoY2H screen detected a similar large number of 251 PPIs. A reason for these relatively high number of detected interactions could be the fact that alpha-synuclein is a natively unfolded protein [58]. This class of proteins lacks a stable tertiary structure and it is assumed that more than 30% of all eukaryotic proteins contain disordered regions greater than 50 consecutive residues [404]. Natively unfolded proteins are able to bind to several different targets as they only fold upon binding to a target protein [405]. Furthermore, intrinsically disordered regions are often hotspots of posttranslational modifications [404]. In accordance with these observations, alpha-synuclein is subject to several posttranslational modifications like phosphorylation, oxidation and sumoylation [62].

5.2.3 Correlation between Y2H reproducibility and HIPPIE score

A possible correlation between the experimental support for a published interaction (indicated by the HIPPIE score) and the reproducibility of the interaction in Y2H assays was examined. In total, the Y2H assay detected 11 published alpha-synuclein PPIs annotated in the HIPPIE database. 6 of these interactions with a HIPPIE score lower than 0.3 were identified by the activation of one reporter gene that was only detected in one replicate. In contrast, 4 out of 5 PPIs with a HIPPIE score higher than

0.3 activated both reporter genes and were found in 2 or more replicates. These results indicate that it is more likely to reproduce PPIs with a higher HIPPIE score using the Y2H assay.

5.2.4 Correlation between LUMIER validation and bioinformatic confidence scoring

A bioinformatic scoring system was used to rank the interactions identified in the Y2H screen according to their likeliness to occur *in vivo*. The scoring system ranked the interactions as low confidence (LC), medium confidence (MC) or high-confidence (HC). In addition, the LUMIER co-immunoprecipitation assay was used to validate the Y2H PPI data. A possible correlation between the confidence score calculated for an interaction and its reproducibility in the LUMIER assay was determined. 42 of the interactions of wild-type alpha-synuclein tested in the LUMIER assay were predicted as low-confidence (LC) and 45% of them could be validated in mammalian cells. In contrast, the assay validated 57% of the 23 interactions that were predicted as high-confidence (HC). These results show that HC interactions are more likely to be reproduced in the LUMIER assay.

5.2.5 Gene-term enrichment analysis indicates biological relevance of Y2H PPI data

A gene-term enrichment analysis was performed using the DAVID functional annotation tool [21, 22] to identify shared biological processes for alpha-synuclein interactors detected by Y2H assays. Identified gene terms could have revealed new, previously not described biological functions or pathway associations of alpha-synuclein. However, the analysis only identified terms associated with known alpha-synuclein functions or with processes known to be associated with PD. In particular, the gene-term enrichment analysis of the alpha-synuclein interactors detected by Y2H led to the identification of biological processes like “regulation of programmed cell death” and “transmission of nerve impulse”, which were also enriched among the published interactors of alpha-synuclein. Taken together, these results suggest that the Y2H screen generated biologically relevant data. Therefore, the PPI dataset can also be used to find novel interactors of alpha-synuclein.

5.2.6 Y2H studies identify connections between Parkinson's disease and other neurodegenerative diseases

The Y2H assay identified several interaction partners of wild-type alpha-synuclein that are known to be involved in other neurodegenerative disorders like Alzheimer's disease (AD), amyotrophic lateral sclerosis (ALS), Huntington's disease (HD), spinocerebellar ataxias (SCA) and prion diseases. It has been described previously that alpha-synuclein also plays a role in other neurodegenerative disorders [54]. In addition, there are several lines of evidence suggesting that there are common cellular and molecular mechanisms between PD and other neurodegenerative disorders [220]. These similarities include protein aggregation and inclusion body formation. These aggregates are formed by protein fibers, which mainly consist of misfolded protein arranged in a β-sheet conformation, termed amyloid [406]. The probably best-characterized amyloid structure is formed by the β-amyloid (Aβ) peptide, which is implicated in AD pathogenesis [407]. Chemical cross-linking, solid phase binding assays and *in situ* staining in AD patient brains have confirmed an interaction and the exact binding region between alpha-synuclein and the Aβ peptide [408]. Interestingly, the Y2H assay detected an interaction of the two major isoforms (695 and 770 amino acids) of the Aβ precursor protein APP with alpha-synuclein (not indicated in Figure 4-8). These findings are supported by the detection of this interaction in the cytoY2H assay (see section 4.4.8), the subSEQ assay (Supplementary Table 6) and subsequent validation with the LUMIER assay (see section 4.6.4). However, it is known that APP is processed by proteases when expressed in yeast [409, 410] and in HEK cells [411]. Therefore, it is possible that not the full-length protein, but rather protease-cleaved fragments of APP interact with alpha-synuclein. This hypothesis could be tested by immunoblot analysis of yeast cell extracts using an antibody specific for the HA tag fused to the prey protein.

5.2.7 Y2H assays identify connections between Parkinson's disease and cancer

Furthermore, the Y2H array screen identified the interaction of alpha-synuclein with various proteins associated with cancer. The expression of alpha-synuclein has previously been demonstrated in a variety of brain tumors [412, 413] as well as other cancers, including ovarian, breast [414] and colorectal tumors [415] and melanomas [416]. It has been suggested that the activation of cell cycle components induces neuronal loss in neurodegenerative diseases [230]. Activation of the cell cycle machinery may result in proliferation of cancer cells, whereas reactivation of cell

cycle components in post mitotic neurons may lead to apoptosis [230]. This hypothesis is supported by the expression of oncogenes in neurons, which causes cell death rather than cell proliferation [417]. Current research is revealing a growing number of proteins that are involved in both cancer and neurodegenerative disorders [229].

5.2.8 Y2H studies identify multiple kinases interacting with alpha-synuclein

Several protein kinases were found to interact with alpha-synuclein in the Y2H assays. It is known that the phosphorylation state of alpha-synuclein is important for its ability to form fibrils [72]. Interestingly, 90% of insoluble alpha-synuclein in DLB (dementia with Lewy bodies) brains is phosphorylated at serine 129 [72, 418]. In healthy brains only 4% of total alpha-synuclein is phosphorylated at this residue, suggesting that extensive alpha-synuclein phosphorylation is an important pathogenetic event [72]. Therefore, it is interesting to find new kinases that interact with and phosphorylate alpha-synuclein. Among others, the Y2H screen identified the interaction of alpha-synuclein with the serine/threonine kinases protein kinase C epsilon type (PRKCE), and the ribosomal protein S6 kinase (RPS6KB1), which could both be tested for their ability to phosphorylate alpha-synuclein *in vitro*. Furthermore, the effect of a possible phosphorylation on the aggregation properties of alpha-synuclein could be assessed. Surprisingly, the lipid kinase SPHK1 interacted with alpha-synuclein in the Y2H assay. This interaction could also be reproduced by the cytoY2H assay. It is unlikely that alpha-synuclein is phosphorylated by this kinase. However, alpha-synuclein could regulate the activity of SPHK1, which is involved in TNF-alpha signaling [419] and the NF-kappa-B activation pathway, which play important roles in inflammatory, antiapoptotic and immune processes. Misregulation of these processes in neurons might lead to the degeneration of these cells. Alpha-synuclein also interacts with the calcium/calmodulin-dependent protein kinase kinase 1 (CAMKK1). This kinase promotes cell survival by phosphorylating AKT1, which in turn inhibits the pro-apoptotic BAD/Bcl2-antagonist of cell death [420]. Elevated levels of alpha-synuclein might lead to the inhibition of CAMKK1 and thereby promote apoptotic cell death, which has been described as possible cause for the degeneration of dopaminergic neurons in PD [180].

5.2.9 Alpha-synuclein interacts with components of the ubiquitin proteasome system

Alpha-synuclein is degraded by both autophagy and the proteasome [78]. However, aggregated and monomeric alpha-synuclein are both able to bind subunits of the proteasome complex and impair its function [235]. Furthermore, proteasomal degradation of alpha-synuclein can be inhibited upon its binding to synphilin-1 (SNCAIP) [421]. Also, ubiquitination of alpha-synuclein does not necessarily target the protein for degradation. Ubiquitination of alpha-synuclein by Siah-1 promotes alpha-synuclein aggregation, leading to apoptotic cell death [421]. Taken together, these findings indicate that the identification of new components of the UPS interacting with alpha-synuclein might lead to a better understanding of its degradation and aggregation pathway. The Y2H assay detected published as well as previously undescribed interactions of alpha-synuclein with subunits of the UPS. These novel components were the E3 ubiquitin-protein ligase RNF168 as well as the von Hippel-Lindau tumor suppressor protein (VHL). This protein is member of the E3 ubiquitin ligase complex [95] and possesses E3 ubiquitin ligase activity [395]. Mutations in the VHL gene cause von Hippel-Lindau disease, an autosomal dominant genetic condition associated with tumors of the central nervous system [82]. VHL controls the levels of vascular endothelial growth factor (VEGF) in human renal carcinoma cells [396]. Interestingly, VEGF showed neuroprotective effects upon dopaminergic neurons in a PD animal model [397]. VHL and RNF168 could be further tested for their ability to ubiquitinate alpha-synuclein *in vitro*. Subsequently, an effect of the post-translational modification of alpha-synuclein for degradation or its tendency to form aggregates could be assessed.

5.2.10 Y2H identifies possible disease mechanisms of mutant alpha-synuclein

Several interaction partners of A30P and E46K mutant alpha-synuclein were identified in Y2H interaction screens. The number of interactions for wild-type alpha-synuclein was significantly higher than for its mutant isoforms. This is probably due to the baits used in the Y2H screen: Only one bait was screened for each mutant isoform, whereas two different baits were screened for wild-type alpha-synuclein.

It is known that the pathological mutations of alpha-synuclein change the conformation of the protein [71, 422], which leads to altered membrane binding properties [423-425]. The A30P mutation disrupts the first α-helical domain of alpha-synuclein and thereby reduces its affinity for phospholipids [426]. Furthermore, *in*

vitro experiments demonstrated that this mutation reduces amyloid formation [427]. The E46K mutation increases the binding of alpha-synuclein to anionic phosopholipids [428]. Binding might induce toxicity as the hydrophobic surfaces of alpha-synucelin are exposed for aberrant interactions [428]. The A53T mutation destabilizes the α-helical domain between residues 51 and 66. The hydrophobic domain is thereby extended from 11 to 30 amino acids [429]. Extended hydrophobic regions might increase the ability of the protein to adopt a β-sheet structure, which is required for the formation of oligomeric alpha-synuclein species [430-432].

The Y2H results demonstrate that conformational changes in mutant alpha-synuclein also lead to an altered protein interaction spectrum. Only 33% of the publications that were selected to generate the list of published alpha-synuclein interactors (see section 4.1.1) presented evidence for interactions with the mutant protein. In addition, none of these publications investigated in aberrant interactions of E46K alpha-synuclein. Thus, the Y2H results presented in the current study gives a more detailed insight into the PPI spectrum of mutant alpha-synuclein. Thereby, they might help to better understand the disease mechanisms underlying familial PD and identify new therapeutic targets.

The screen identified casein kinase 2 (CSNK2A1), a serine / threonine protein kinase, as interaction partner of A30P alpha-synuclein. Among several other described functions, casein kinase 2 is associated with regulation of apoptosis [238] and the cell cycle [433]. It is known that casein kinase 2 can phosphorylate wild-type alpha-synuclein at serine residue 129 [434]. Overexpression of alpha-synuclein in HEK cells can inhibit protein kinase C activity, possibly by blocking the catalytic site of the kinase [177]. A30P mutant alpha-synuclein might bind and inhibit casein kinase 2 and thereby influence the regulation of apoptosis in the familial forms of PD. This hypothesis could be tested in future experiments using a cell model expressing A30P mutant alpha-synuclein.

The Bcl2 modifying factor (BMF), which is associated with the regulation of apoptosis [239], was also identified as interaction partner of A30P alpha-synuclein. BMF binds to BCL2 proteins and functions as an apoptotic activator [239]. In healthy cells, the protein is bound to components of the cytoskeleton [240]. Wild-type alpha-synuclein binds actin and accelerates its depolymerization [240]. In contrast, A30P alpha-synuclein accelerates actin depolymerization and disrupts the cytoskeleton during reassembly of actin filaments [240]. As a result, cytoskeleton-dependent processes,

such as cell migration, are inhibited in cells expressing A30P alpha-synuclein [240]. Mutant alpha-synuclein might induce instability of the cytoskeleton, thereby release BMF and promote neuronal apoptosis in familial PD. However, several additional experiments will be necessary to follow up on this hypothesis.

5.2.11 Disease association analysis identifies new potential therapeutic targets for PD

Currently, there are several approaches to develop disease-modifying therapies for PD. A primary target for drug development is the inhibition of alpha-synuclein aggregation and several peptide-based and small-molecule inhibitor of alpha-synuclein aggregation have been developed [435-437]. Other approaches are the upregulation of cellular heat shock proteins (HSPs) [438]. For example, induction of HSPs with geldanamycin protects transgenic flies expressing alpha-synuclein from its toxicity [438]. Furthermore, cellular protein degradation mechanisms like the UPS and the autophagic system could be stimulated to counteract the accumulation of misfolded alpha-synuclein [79].

It has been demonstrated that alpha-synuclein interacts with several proteins involved in genetic diseases, for example other neurodegenerative disorders [54] and cancer, the most common human genetic disease [229]. Interacting proteins might influence the cellular function as well as the aggregation properties of alpha-synuclein. Thus, identifying interaction partners of alpha-synuclein with a known disease association might give hints on the role of alpha-synuclein in PD pathology. Proteins identified as interactors of alpha-synuclein were assessed for disease association and compounds or small molecules targeting the interacting proteins were identified. These substances could be tested for an effect in PD disease models.

Among the proteins that are targeted by small molecules as a therapeutic approach for PD, the analysis of Y2H interactors identified several new potential therapeutic targets.

Wild-type, A30P and E46K alpha-synuclein interacted with the baculoviral IAP repeat containing protein 5 (BIRC5), which is also known as apoptosis inhibitor survivin. The protein plays an important role in the control of apoptosis and the mitotic spindle checkpoint [255]. Survivin is associated with various types of cancer and has been suggested as a cancer therapeutic target [256]. There are various connections between PD and cancer, for example enhanced tumor growth and increased

proliferation caused by alpha-synuclein expression in mouse models [439]. Survivin is a target for the compound Paclitaxel (trade name Taxol, Bristol-Myers Squibb), a mitotic inhibitor which stabilizes microtubules and induces the expression of survivin in cancer cells [440]. Both alpha-synuclein and survivin associate with microtubules in mammalian cells [87, 255]. Strikingly, mitosis-like signals, which mediate neuronal death in experimental models of PD, are activated in mature dopaminergic neurons in PD patients [257]. It has been published that Paclitaxel might be beneficial for AD as it restores nerve function in a tauopathy animal model [441]. A possible effect of Paclitaxel on PD disease progression could be tested in animal models mimicking the disease [258].

Among several kinases, the non-receptor tyrosine kinase FYN (oncogene related to SRC, FGR, YES) interacted with both wild-type and A30P alpha-synuclein. The subcellular localization of FYN might influence neurofibrillary pathology and synapse loss in AD [260], making FYN a potential pharmacological target in this neurodegenerative disease [259]. Interestingly, FYN is known to phosphorylate alpha-synuclein at tyrosine residue 125 [232]. The kinase can be inhibited by the Src family tyrosine kinase inhibitor Dasatinib (trade name Sprycel, Bristol-Myers Squibb), which is used for the treatment of leukemia [442]. This small molecule inhibitor can be administered orally and its possible effect on PD could be tested in animal models mimicking the disease [258]. However, it should be noted that phosphorylation of the tyrosine residue 125 protects cells from alpha-synuclein neurotoxicity in a *Drosophila* model of Parkinson disease [443].

5.3 Successful adaptation of cytoY2H for high-throughput PPI screening

Although alpha-synuclein was discovered as a nuclear protein [56], the protein is predominantly found in presynaptic termini, both in a free and a membrane bound form [261]. However, the classic Y2H system requires both the bait and the prey protein to translocate to the nucleus to detect their interaction [119]. In contrast, the cytoY2H system detects PPIs in the yeast cytoplasm [141]. Fusion to the small yeast ER integral membrane protein Ost4p anchors the cytoY2H bait protein to the ER membrane and thereby prevents its translocation to the nucleus [141]. Thus, it was assessed whether the cytoY2H system delivers different interaction spectra for alpha-synuclein than classic Y2H assays. The cytoY2H system can be used for the detection of bait protein interactions with transmembrane prey proteins, as their hydrophobic nature prevents their translocation into the yeast nucleus. The fact that a

synapse contains a large fraction of membrane proteins makes the cytoY2H system especially suitable to detect PPIs in this projection of a nerve cell. In addition, the MYTH system was used to determine interactions of an alpha-synuclein prey protein with synaptic membrane-bound bait proteins. The MYTH system detects interactions between full-length integral membrane proteins and their putative interaction partners [137] and has been used to detect PPIs between yeast [138], plant [139] and human proteins [140].

The cytoY2H and MYTH bait vectors as well as the prey vectors, which are compatible with both systems, were modified for high-throughput cloning with the Gateway™ system. In addition, the *E. coli* selection marker of the bait vectors was exchanged from a Kanamycin to Tetracycline resistance gene to ensure compatibility with all entry clones from the available collection.

The correct function of the modified vectors was successfully demonstrated by using both PPI detection systems to reconstruct published interactions between defined protein pairs. The interactions of IκB-α with p65, S100A1 with S100B and PTPLB with BAP31 have been demonstrated previously using the cytoY2H [141] and MYTH system [268].

5.3.1 Production of alpha-synuclein bait proteins in yeast

CytoY2H bait plasmids encoding wild-type alpha-synuclein and its mutant isoforms A30P, E46K and A53T were generated and the production of the bait proteins was confirmed using the genetic NubG/NubI test. In contrast to the classic Y2H system, the cytoY2H bait protein carrying the A53T mutation of alpha-synuclein did not have auto-activating properties and thus could be used for subsequent PPI screening experiments. Interestingly, wild-type alpha-synuclein, which should be targeted to the ER, interacted with the positive Fur4p control prey protein, which is localized to the plasma membrane. It is possible that the bait and the control prey protein already interact in the secretory pathway and thereby promote yeast growth.

In addition, the correct synthesis and localization of all bait proteins was confirmed by immunoblot analysis that detected alpha-synuclein in yeast membrane fractions. Specific antibodies detected a low amount of the cytosolic yeast protein Pgk1p in the membrane fraction, which could be due to cytosolic contamination. However, specific antibodies against the transmembrane ER protein Dpm1p demonstrated a separation of the membrane fraction from the cytosolic fraction. All cytoY2H bait proteins migrated slower than expected in the SDS gel. A reason for this observation could be

posttranslational modifications of the bait proteins, for example glycosylation, a commonly observed post-translation modification in yeast [275] and higher organisms [444]. Interestingly, the E3 ubiquitin ligase parkin (encoded by the PARK2 gene) is known to interact with and ubiquitinate a glycosylated form alpha-synuclein (size: 22 kDa) [445], and this interaction was detected in the Y2H screen. Wild-type alpha-synuclein has a theoretical molecular weight of 14.5 kDa. Thus, different glycosylation of alpha-synuclein in yeast could be an explanation for the observed ~9 kDa difference between the theoretical size of the bait proteins and the size observed in SDS gels.

Taken together, these experiments clearly demonstrate the correct expression of the bait proteins in yeast, which was further confirmed by the detection of published alpha-synuclein interactors in PPI screens.

5.3.2 High-throughput NubG/NubI test ensures synthesis and localization of screened bait proteins

In addition to 207 MYTH and 305 cytoY2H bait plasmids, a matrix of 490 prey plasmids was generated. As the encoded proteins are expressed ectopically and tagged, they may not always be properly folded. Therefore, all encoded bait proteins were tested in a high-throughput version of the NubG/NubI genetic test before screening. The NubG/NubI genetic test assesses the synthesis, the localization as well the auto-activation properties of a bait protein. Thus, only proteins that are synthesized and localized to the yeast ER membrane are screened, thereby saving resources. Functionally validated, non-auto-activating cytoY2H and MYTH bait proteins were finally screened in pools of 16 baits each, as described for the Y2H method. Subsequently, pairwise PPIs were identified in the backmating step as in the Y2H method.

5.3.3 Future modifications to the cytoY2H and MYTH screening procedure

In the backmating step following the cytoY2H pool screen, each prey protein was tested for interactions against at least 16 bait proteins. The PPI data generated in the backmating was used for a “bait dependency test” to ensure the identification of specific PPIs [137]. To test for bait dependency, the interaction spectrum of each prey protein that interacted with an alpha-synuclein bait protein was analyzed for interactions with unrelated control bait proteins. However, all tested interactions were found to be bait-dependent. For future screens, it will be useful to generate a list of “sticky” prey proteins that interact with an unusual large number of bait proteins.

These proteins are likely to generate false positive results and a database containing sticky prey proteins has already been generated for the classic Y2H system, which was also applied in this study.

5.3.4 CytoY2H and Y2H assays detect different alpha-synuclein interaction partners

In total, the cytoY2H screen detected 251 PPIs of wild-type alpha-synuclein, but only 5 PPIs of the A30P and 4 PPIs of the E46K isoform. In addition, the screen detected 15 PPIs of the A53T isoform of alpha-synuclein, which could not be screened in classic Y2H assays due to auto-activation properties of the bait protein. All interactions were detected with alpha-synuclein bait proteins. The prey matrix used for the cytoY2H screen contained clones potentially expressing 12 known alpha-synuclein interacting proteins. 6 of these proteins interacted with alpha-synuclein in the cytoY2H assay. Interestingly, the interactions of alpha-synuclein with parkinson protein 7 (PARK7) and the alpha-synuclein interacting protein (SNCAIP) were only detected in the cytoY2H but not in the classic Y2H screen. This indicates that classic Y2H and cytoY2H assays should be used in parallel to generate more comprehensive PPI networks. In addition, the fact that published alpha-synuclein interaction partners were detected in the cytoY2H assay demonstrates that the screen generated biologically relevant data. The results also validate the cytoY2H technique as a tool to detect novel interactors of alpha-synuclein.

5.3.5 Overlap between cytoY2H and Y2H data

The overlap of the PPIs of wild-type alpha-synuclein detected in the cytoY2H and the Y2H assay was calculated. Only 11% of the interactions were detected by both methods. However, a suitable benchmarking the two systems based on the current data is not possible, as the cytoY2H prey matrix only contained 490 different synaptic prey proteins. In contrast, the Y2H prey matrix consisted of 16098 prey proteins, which also included proteins that are expressed in other tissues than the brain.

5.3.6 CytoY2H PPI data can be reproduced in HEK cells

The LUMIER co-immunoprecipitation assay was used to validate the interactions of wild-type alpha-synuclein detected by cytoY2H. 20 of 40 tested interactions could be confirmed (validation rate: 50%). The validation rate clearly demonstrates that PPIs detected by cytoY2H assays can be reproduced in HEK293 cells and that they are no technical artifacts of the yeast assay.

5.3.7 CytoY2H assays identify connections between PD and other neurodegenerative diseases

Similar to the Y2H assay, the cytoY2H system identified several interaction partners of wild-type alpha-synuclein that are known to be involved in other neurodegenerative disorders like Alzheimer's disease (AD), Huntington's disease (HD) and spinocerebellar ataxias (SCA). Interestingly, alpha-synuclein interacted with the protein ceroid-lipofuscinosis, neuronal 3 (CLN3), which plays a role in Batten disease [284]. Batten disease is caused by the buildup of so called lipofuscins, deposits containing fats and proteins, in the human body's tissues [446]. Increased levels of lipofuscins have been observed in PD patients [447]. It was suggested that CLN3 is involved in synaptic vesicle transport and synaptic transmission [448]. Furthermore, CLN3 is required for the response to oxidative stress [449]. Oxidative stress contributes to the degeneration of dopaminergic neurons in PD [450]. However, a direct connection between PD and Batten disease has not been described previousely and could be further investigated in the future.

5.3.8 CytoY2H identifies parallels between Parkinson’s disease and cancer

The cytoY2H screen detected the interaction of alpha-synuclein with 6 proteins (CDH1, KRAS, NQO1, PIAS3, PTK2 and SNCG) that are associated with cancer. Current research is revealing a growing number of proteins that are involved in both cancer and neurodegenerative disorders [229], and the combination of Y2H and cytoY2H methods can be used to identify additional links between these diseases.

5.3.9 CytoY2H identifies kinases interacting with alpha-synuclein

Several interacting kinases identified by cytoY2H were not detected in the Y2H screen. These kinases included the PTEN-induced putative kinase 1 (PINK1), the PX domain containing serine/threonine kinase PXK and the protein kinase C theta type (PRKCQ). The interaction with PINK1 was also detected by the subSEQ method and further confirmed with the LUMIER assay. Mutations in the mitochondrial serine / threonine kinase PINK1 cause an autosomal recessive form of PD [451]. Mutant PINK1 impairs mitochondrial function and induces proteasomal malfunction [452]. Strikingly, the aggregation of alpha-synuclein is increased in cell culture models of PD upon mutation of PINK1 [452]. In addition, mitochondrial fragmentation induced by expression of alpha-synuclein can be rescued by co-expression of wild-type PINK1 but not by its known mutants [453]. In contrast, overexpression of PINK1

enhanced alpha-synuclein induced toxicity in the yeast assays presented in this thesis.

An association of PXK and PRKCQ with PD has not been previousely described. PXK is a protein involved in epidermal growth factor receptor trafficking and PXK expression in COS7 cells accelerates the degradation of epidermal growth factor receptors [454]. Interestingly, the protein levels of the ligand EGF are decreased in PD patients [455]. In accordance with these findings, EGF supplementation in the striatum of a PD mouse model prevented dopaminergic neurodegeneration [455]. The detected interaction of alpha-synuclein with PXK might be a link between alpha-synuclein and impaired neurotrophic support of neurons in PD and should be further investigated. The interaction of alpha-synuclein with PRKCQ was further confirmed using the LUMIER assay.

5.3.10 CytoY2H assays identify possible disease mechanisms of mutant alpha-synuclein

Several interaction partners of A30P, E46K and A53T mutant alpha-synuclein were identified in the cytoY2H screen. A role of several of these proteins like monoamine oxidase A (MAOA), the vesicle-associated membrane protein 2 (VAMP2 / synaptobrevin 2) and Urocortin (UCN) has already been identified. This indicates that the analysis of the mutant alpha-synuclein interactions can identify processes that are known to be associated with PD. Thus, the analysis can also be used to find novel PPIs associated with specific biological processes that could give hints on the function of alpha-synuclein in PD.

The vesicle-associated membrane protein 3 (VAMP3, cellubrevin) interacted with all isoforms of alpha-synuclein. Protein levels of VAMP3 were significantly increased in dopaminergic cells after rotenone exposure [301], a pesticide that inhibits the mitochondrial complex I and promotes the loss of nigral dopaminergic neurons in PD [456]. Furthermore, VAMP3 is associated with autophagy [299], an intracellular degradation process that might play an important role in PD [300]. In addition, VAMP3 is involved in the degradation of the extracellular cell matrix [457], a process that might contribute to the degeneration of dopaminergic neurons in PD. Alpha-synuclein is known to be degraded by autophagy [78] and it might reduce its own degradation by interacting with VAMP3 by and thereby impairing autophagy. However, several additional experiments will be necessary to follow up on this hypothesis.

The gamma-aminobutyric acid receptor-associated protein (GABARAP) interacted with wild-type alpha-synuclein and its A30P and A53T mutant isoforms. A role of GABARAP in intracellular transport events was suggested. Furthermore, a publication demonstrated an association of the protein with autophagic processes [302]. GABARAP also functions as a tumor suppressor [458], creating an additional link between PD and cancer. Another study identified the proapoptotic protein Nix/Bnip3L as be a potential GABARAP ligand, linking the protein to apoptosis [459]. A knockdown of GABARAP in a cell model of PD [107] could reveal a possible role of the protein in the pathogenesis of PD. As GABARAP deficient mice are phenotypically normal [303], MPTP or rotenone could be used to generate symptoms mimicking PD in these knockout mice and the effects could be compared with wild-type mice treated with these chemicals [21, 304].

5.3.11 Disease association analysis identifies new potential therapeutic targets for PD

To identify parallels between PD and other genetic diseases and get additional hints on the role of alpha-synuclein in PD pathology, its interacting proteins were analyzed for disease association. Interestingly, this analysis identified proteins associated with other genetic diseases that are also therapeutic targets for PD. Targeting these proteins with chemical compounds or administration of the proteins themselves produces positive effects in models of PD. Administration of some of these compounds or proteins is even used as a therapeutic approach to treat PD patients. Therefore, it was assumed that the analysis could be used to identify new potential therapeutic targets for PD.

The cytoY2H screen identified Tachykinin (TAC1) and its receptor (TACR1) as interactors of alpha-synuclein. TAC1, which is also known as substance P, is involved in the regulation of neuronal survival and degeneration [321]. Tachykinin has been shown to stimulate neurons in rats [460]. A role of TAC1 and its receptor in neurodegenerative disorders has been suggested previously [322], and the number of tachkinin receptors is decreased in PD patients [461]. Furthermore, the Tachykinin receptor has been suggested as a potential drug target in cancer [462]. TACR1 antagonists have been found to prevent dopaminergic terminal degeneration of nigrostriatal neurons induced by methamphetamine [323] and could be tested in cell [107] and animal models [258] of PD.

Alpha-synuclein also interacted with PICK1, the protein interacting with PRKCA 1. A role of PICK1 in schizophrenia [324] and cancer [325] has been suggested. PICK1 has been shown to interact with PRKCA [463]. Furthermore, PICK1 is ubiquinated by the E3 ubiquitin ligase parkin (PARK2) [464] and interacts with dopamine transporters (DAT) [326]. Interestingly, alpha-synuclein also interacts with both PARK2 [465, 466] and the carboxyl-terminal tail of DAT [327]. Binding of alpha-synuclein to DAT leads to increased cellular dopamine uptake and dopamine-induced cellular apoptosis [327]. Despite these multiple lines of evidence of a role of PICK1 in PD, known inhibitors of PICK1, like the small-molecule FSC231, have not yet been tested for an influence on PD. A possible therapeutic effect could be tested in a cell model of the disease [107].

The cytoY2H screen also detected an interaction of alpha-synuclein with the protein tyrosine phosphatase, receptor type, F (PTPRF). Knock-down of this protein, which is also known as leukocyte common antigen-related (LAR), induces insulin resistance in HEK cells [328]. It was shown that PTPRF is important for the development as well as the maintenance of excitatory synapses in hippocampal neurons [467]. Interestingly, insulin signaling was found to be defective in a PD mouse model [329]. These findings indicate that PTPRF might be a possible link between the diseases. Systemic treatments with LAR-targeting peptides that inhibit protein-tyrosine kinase function (LAR wedge Tat peptides) showed survival- and neurite-promoting effects in PC12 cells [330]. The treatment also promoted locomotor functional recovery in mice with thoracic spinal cord transection injuries [468]. These peptides could be tested for an effect on PD cell [107] or mouse models [21] of PD.

5.4 Development of a novel method for PPI detection

A cytoY2H screen of alpha-synuclein against a human brain derived cDNA prey library was performed and proteins interacting with alpha-synuclein were identified by next-generation sequencing (NGS) using the Illumina Solexa system. The method was named subSEQ, which is derived from the terms split-ubiquitin and SEQuencing. The NGS technologies developed during the past decade enabled large-scale sequencing to identify millions of base-pairs in a single sequencing run, allowing cost-effective genome-scale sequencing projects [332]. So far, NGS has been used for interactome network mapping only once [469]. However, this method requires additional PCR steps to amplify each pair of open reading frames to be tested for

interaction in the subsequent assay. Currently, other projects combining classic Y2H screening with NGS are being developed [470].

For the subSEQ interaction screen, a yeast strain carrying a single bait plasmid was mated with yeast clones transformed with a human brain derived cDNA prey library. It was assumed that only cells containing plasmids encoding a prey protein that interacts with the bait protein would be able to grow on selective medium. This would lead to an enrichment of plasmids encoding interacting prey proteins. Plasmid DNA was isolated from the yeast cells and cDNA sequences were PCR amplified from the plasmids. The PCR products were fragmented and their identity was determined using the Illumina Solexa NGS system.

The subSEQ method allows the interaction-analysis of up to 56 baits in parallel. Both cytoY2H and MYTH baits can be used for PPI screening in parallel. The cytoY2H bait vector is used to identify interactions of soluble proteins while the MYTH bait vectors are used for the analysis of membrane proteins.

5.4.1 SubSEQ detects bait specific interactions

The subSEQ method predicted 1919 proteins as interactors of alpha-synuclein. To assesses whether these interactions were bait specific, it was determined whether they are also identified as interactors of a different protein (selected against a Huntingtin fragment, Htt513-Q17). 36% of the total interactions predicted for alpha-synuclein were also detected in the Htt sample. A possible reason for this overlap might be “sticky” proteins that interact with all bait proteins used for the plasmid enrichment. Interacting proteins might also bind to the C-terminal half of ubiquitin or the transcription factor fused to it. DNA bands of identical size detected in all samples after PCR amplification of the cDNA inserts (Figure 4-24) further support these hypotheses. After completion of additional subSEQ interaction screens, a database with interaction data from all samples should be created to allow the identification of false positive interactions. However, only 2 of the overlapping interactors from the analyzed libraries are known interactors of alpha-synuclein. In addition, the protein FBXW7 (F-box/WD repeat-containing protein 7), which was predicted as alpha-synuclein interactor with 17733 unique reads, was not identified in the Htt library. Taken together, these results indicate that the enrichment of prey plasmids and their identification with the subSEQ method is bait specific.

5.4.2 SubSEQ detects known interactors of alpha-synuclein

The subSEQ method detected 38% of the published interactors of alpha-synuclein. This indicates that the method generates physiologically relevant data and can also be used to predict novel interaction partners of alpha-synuclein.

5.4.3 CytoY2H and LUMIER assays validate interactions predicted by the subSEQ method

The cytoY2H assay was used to validate selected interactions of alpha-synuclein. 44% of the tested interactions could be reconstructed in the cytoY2H assay with full-length proteins. In addition, subSEQ predicted interactions of alpha-synuclein were validated in mammalian cells. 45% of the tested interactions could be confirmed in the LUMIER assay. However, only 4 interactions were tested by both assays. 2 of them were confirmed in both assays, whereas the remaining 2 interactions could either be reconstructed by the LUMIER or the cytoY2H method. Taken together, the results validate subSEQ as a method to identify novel interactors of alpha-synuclein.

5.4.4 SubSEQ and cytoY2H methods identify potential therapeutic targets for PD

The cytoY2H assay confirmed the subSEQ predicted interaction of alpha-synuclein with the amyloid beta (A4) precursor protein-binding, family B, member 1 (APBB1). Mutations in the gene have been associated with an increased risk for early-onset Alzheimer's disease [340]. This protein functions as co-activator of the amyloid precursor protein intracellular domain (AICD), and induction of both proteins disturbs organized filamentous actin structures within cells, leading to malfunction of mitochondria [471]. Aggregated alpha-synuclein might sequester APBB1 and thereby impair mitochondrial function, which is a possible cause of parkinsonism and other neurodegenerative diseases [472].

Furthermore, the cytoY2H assay confirmed the interaction of alpha-synuclein and the VAMP-associated protein B (VAPB). This vesicle-trafficking protein plays a critical role in unfolded protein response, a physiological reaction of cells to conquer ER stress [473]. A mutation in VAPB causes late-onset amyotrophic lateral sclerosis and spinal muscular atrophy [341], creating an additional link between PD and other neurodegenerative diseases.

Alpha-synuclein also interacted with the death-associated protein kinase 1 (DAPK1), a pro-apoptotic serine–threonine protein kinase [342]. DAPK1 is known to act rather early in the apoptosis pathways, even before the cell is committed to death [474,

475]. The ability of DAPK1 to phosphorylate alpha-synuclein *in vitro* could be tested. In addition, the influence of this putative phosphorylation on the aggregation properties of alpha-synuclein could be assessed. Furthermore, various specific inhibitors of DAPK1 are available, and these could be tested in cell [107] and animal models [258] of PD.

5.5 Generation of a high-confidence interaction network for alpha-synuclein

To obtain interaction data with strong experimental support, interaction data of wild-type alpha-synuclein and its mutant isoforms obtained by the Y2H, cytoY2H, subSEQ and LUMIER assays was integrated to form a high-confidence interaction network. Only interactions of wild-type or mutant alpha-synuclein detected in at least 2 of the assays were taken into account.

Although PD is considered a degenerative brain condition and most of its symptoms are caused by loss of movement-regulating neurons near the brainstem, additional symptoms and effects in other parts of the nervous system have been described. These include autonomic and gastrointestinal dysfunction, which are associated with pathological changes outside the CNS [476]. Strikingly, administration of low-dose rotenone to the stomach of mice induced alpha-synuclein aggregate formation in the enteric nervous system [477]. After extended rotenone exposure, these mice also developed lesions in brains regions normally affected in PD [477]. Strikingly, similar abnormalities in the enteric nervous system (ENS) including alpha-synuclein aggregates could be reproduced by expressing A30P or A53T mutant alpha-synuclein including its endogenous regulative elements in mice [478]. In the previous chapters, several interactions were excluded as gene expression profiling data suggested the proteins might not be expressed in the human brain. However, these interactions were included into the high-confidence interaction network.

Furthermore, several interactions identified by the individual assays were ranked as low confidence by bioinformatic scoring. As several of these interactions could be reproduced in more than one assay, they were also included into the high-confidence interaction network.

The biological relevance of the interactions in the high-confidence PPI network was indicated by a gene-term enrichment analysis. Among the alpha-synuclein interactors, this analysis detected gene-terms describing cellular components, biological processes and molecular functions with a known association with alpha-synuclein or PD.

5.6 The high-confidence alpha-synuclein PPI network suggests potential therapeutic targets for PD

An interaction between the Ras homolog enriched in brain (RHEB) and the A30P isoform of alpha-synuclein was detected by Y2H assays and confirmed in the LUMIER assay. RHEB plays an important regulatory role in the insulin/TOR/S6K signaling pathway, and is therefore vital for the regulation of growth and cell cycle progression [348]. RHEB is highly expressed in some human lymphomas as well as other cancers [479]. Furthermore, the protein can control misfolded protein metabolism by inhibiting autophagy and the formation of aggresomes [480]. Although no direct interaction between alpha-synuclein and RHEB has been published yet, it has been demonstrated that expression of a constitutively active form of RHEB by adenoassociated virus (AAV)-mediated transduction protects dopaminergic neurons from neurodegeneration and mediates axon regrowth after neurotoxin lesion [349]. This example indicates that the literature-based functional analysis of alpha-synuclein interactors detects known and could help to identify novel potential therapeutic targets for PD.

The interaction of wild-type alpha-synuclein with the Fas apoptotic inhibitory molecule 2 (FAIM2) was detected by the cytoY2H and subSEQ methods and could be further validated in the LUMIER assay. This anti-apoptotic protein is also known as protein lifeguard. Nigrostriatal neuron degeneration has been associated with two apoptosis pathways, the p53–glyceraldehyde-3-phosphate dehydrogenase (GAPDH)–BAX and the FAS receptor–FADD–caspase 8–BAX pathway. Strikingly, FAIM2 is able to inhibit FAS mediated apoptosis [350]. Consistent with these findings, reduction of the FAIM2 protein levels by RNAi knockdown sensitizes neurons to FasL-induced (ligand of the FAS receptor) cell death and caspase-8 activation [351]. Interestingly, a role of FAS mediated apoptosis in PD has been suggested [481]. Potential beneficial effects of FAIM2 in PD could initially be tested by overexpressing the protein in a cell model [107] or in animal models of the disease [258].

Y2H, cytoY2H and subSEQ methods detected the interaction of wild-type alpha-synuclein with the phosphatidylethanolamine binding protein 1 (PEBP1). In addition, the interaction was confirmed in mammalian cells using the LUMIER assay. PEBP1, also known as RKIP (Raf-1 Kinase Inhibitor Protein), has been shown to inhibit NF-κB signaling pathways [352]. It is well established that NF-κB signaling is important for neuron survival and plasticity [482]. Strikingly, the selective inhibition of this

pathway by a peptide reduces the loss of dopaminergic neurons in a PD mouse model [353]. By binding to PEBP1, alpha-synuclein might influence the NF-κB pathways. This effect might be even stronger upon increased alpha-synuclein protein levels. An effect of PEBP1 overexpression could first be tested in a cell model [107] and further assessed in mouse model of PD [258].

5.7 The high-confidence PPI network supports a role of alpha-synuclein in vesicle trafficking

Alpha-synuclein localizes to pre-synaptic terminals and is thought to regulate synaptic vesicle formation and neurotransmitter release [202, 203], Interestingly, mutant or over-expressed alpha-synuclein interferes with neuronal membrane trafficking by Rab GTPases and soluble N-ethylmaleimide–sensitive factor attachment protein receptors (SNAREs) [101, 483]. Rab GTPases regulate lipid and protein traffic between the intracellular membrane system of eukaryotic cells [484]. The primary role of SNARE proteins is to mediate vesicle fusion [485]. The synaptic co-chaperone protein cystein-string protein α (CSPα) is essential for the assembly of SNARE complexes [486]. Strikingly, transgenic expression of alpha-synuclein counters the lethality and neurodegeneration caused by a deletion of CSPα [393]. Furthermore, alpha-synuclein modulates SNARE complex formation indirectly by sequestering arachidonic acid, a polyunsaturated fatty acid, which stimulates SNARE complex formation [487]. Alpha-synuclein co-immunoprecipitates components of the presynaptic SNARE complex from cell as well as mouse brain extracts [293]. Strikingly, the high-confidence interaction network includes several presynaptic proteins involved in vesicle trafficking, specifically endocytosis and exocytosis. These proteins include the SNARE proteins 23 and 25 (SNAP23, SNAP25), the SNAP-associated protein (SNAPIN), synaptotagmin XII (SYT12) and the presynaptic cytomatrix protein piccolo (PCLO) and RAB3C, a member of the RAS oncogene family. So far, there is little is evidence of direct interactions of alpha-synuclein with SNARE complex proteins. Experiments based on these findings could help to better understand the role of alpha-synuclein in vesicle formation under physiological or pathological conditions. All these proteins interacted with wild-type alpha-synuclein, further supporting a role of alpha-synuclein in vesicle trafficking. Alpha-synuclein, especially in a misfolded or aggregated form, might sequester presynaptic proteins involved in vesicle trafficking, and thereby disturb this essential process, eventually leading to neuronal death.

5.8 Proteins interacting with alpha-synuclein modulate its toxicity

Studies in yeast and worms have identified several genes and proteins that modulate alpha-synuclein induced toxicity. The interaction studies presented in the previous chapters identified numerous interactions partners of alpha-synuclein that are human orthologs of these modulator proteins identified in yeast and worms. A well-established yeast model of PD [108] was used to test a possible effect of these proteins on alpha-synuclein induced toxicity. The utilized yeast strains express two copies of GFP-tagged wild-type, A53T alpha-synuclein or GFP alone. In these strains, alpha-synuclein associates with the plasma membrane and forms cytoplasmic inclusions through a concentration-dependent, nucleated process. Alpha-synuclein inhibits phospholipase D, induces lipid droplet accumulation and affects vesicle trafficking. Thus, this disease model is a convenient tool to dissect the molecular pathways underlying normal alpha-synuclein biology and to study the pathogenic consequences of protein misfolding [108]. For example, the model helped to identify various yeast genes enhancing alpha-synuclein toxicity that were functionally related to vesicle trafficking and lipid metabolism [356]. For the current work, FLAG-tagged putative modifier proteins were co-expressed with alpha-synuclein and tested for their ability to modulate toxicity in yeast.

5.8.1 The majority of modifier proteins enhances toxicity

The alpha-synuclein yeast strains grew on selective plates as reported previously [110], as expression of wild-type alpha-synuclein led to reduced growth, while growth was even more affected by expression of A53T alpha-synuclein. In total, 3 human orthologs had a suppressive, 30 had an enhancing and 4 had no effect on alpha-synuclein induced toxicity when overproduced in yeast. Notably, 49% of the proteins also decreased the growth of the control strain that does not express alpha-synuclein. This indicates that, independent of alpha-synuclein induced toxicity, overexpression of some of the modifier proteins alone is toxic for yeast cells. However, no common biological function among these proteins could be identified.

5.8.2 Modifier screens identify human modulator proteins with known PD association

Several of the human proteins tested in the toxicity assay had a published association with PD, among them neuregulin (NRG1), the PTEN-induced putative kinase 1 (PINK1) and the divalent metal transporter 1 (DMT1). As the toxicity assays

included human orthologs of known modulators of alpha-synuclein, it was assumed that the assay could also identify novel toxicity modulators.

5.8.3 Novel modulators of alpha-synuclein induced toxicity

Several of the human proteins that were tested for their ability to modulate alpha-synuclein induced toxicity have not been associated with PD yet. The yeast protein glo3p is involved in the retrograde transport of proteins from the Golgi to the endoplasmic reticulum [488] and was identified as an enhancer of alpha-synuclein induced toxicity when overexpressed in yeast [357]. Its human ortholog, the ADP-ribosylation factor GTPase-activating protein 3 (ARFGAP3), also enhanced alpha-synuclein induced toxicity when overexpressed in yeast. However, overexpression of the protein was slightly toxic in the control strain (not expressing alpha-synuclein). The protein associates with the Golgi apparatus and has a regulatory function in the early secretory pathway of proteins [364]. Specifically, the small GTPase ARFGAP3 associates with organellar membranes and triggers the formation of coated carrier vesicles, e.g. coat protein I (COPI)-coated vesicles [489]. These vesicles mediate retrograde transport from the cis-Golgi or ER-Golgi intermediate compartment to the ER [489]. Furthermore, ARFGAP3 is involved in maintaining Golgi organization [489]. These findings are in accordance with the fact that many genes enhancing alpha-synuclein toxicity in yeast are functionally related to vesicle trafficking [356]. Interestingly, ARFGAP3 directly interacts with and modulates toxicity induced by the leucine-rich repeat kinase 2 (LRRK2) [365], a protein that is associated with autosomal-dominant parkinsonism [366] and physically interacts with alpha-synuclein [490, 491]. Similar to alpha-synuclein, LRRK2 is also able to form aggregates [492]. Thus, ARFGAP3 might also interact with alpha-synuclein and thereby modulate its propensity to form aggregates and / or to induce toxicity. A possible follow up study is the monitoring of GFP-tagged alpha-synuclein localization in yeast by fluorescence microscopy. In parallel, ARFGAP3 localization could be assessed using a FLAG-specific antibody. Furthermore, a modulatory effect of ARFGAP3 could be tested by overexpression or knockdown of the protein in cell models of PD [107].

The transcription factor encoded by the yeast gene CUP9 was identified as suppressor of alpha-synuclein induced toxicity in a yeast overexpression screen [357]. In accordance with these results, overexpression of its human ortholog PBX/knotted 1 homeobox 1 (PKNOX1), which encodes the PBX-regulating protein-1 (Prep1), also suppressed toxicity in the yeast screen. Interestingly, the homeodomain

transcription factor Prep1 can directly regulate apoptotic pathways by controlling the levels of the Bcl-XL protein [367]. Proapoptotic members of the Bcl-2 family are able to increase the permeability of the outer mitochondrial membrane, while antiapoptotic members inhibit their action and maintain mitochondrial homeostasis [493]. Several studies demonstrated that apoptotic cell death may play a critical role in PD [343]. Aggregated alpha-synuclein might sequester Prep1 and thereby decrease the levels of Bcl-XL, leading to induction of apoptosis. Accordingly, overexpression of PKNOX1 could counteract this process. In accordance with this hypothesis, the levels of another nuclear transcription factor, the myocyte enhancer factor 2D (MEF2D), which is known to promote neuronal survival, is downregulated upon accumulation and aggregation of alpha-synuclein [494]. The downregulation was reported both in a cell model and PD patients, and colocalization of MEF2D and alpha-synuclein was demonstrated [494]. A possible beneficial effect of PKNOX1 could be assessed by its overexpression in cell models of PD [109].

6 Outlook

Protein-protein interaction studies can give initial hints to the function of a protein of interest. The main aim of this thesis was the generation of a protein-protein interaction network for alpha-synuclein. Therefore, new methods that allow the identification of protein-protein interactions were devolped. To generate the interaction network, data obtained by these methods was combined with interaction data obtained by already established methods. The work identified numerous proteins interacting with alpha-synuclein that could be potential therapeutic targets for PD. However, additional experiments will have to be performed to prove these hypotheses and investigate the underlying biological mechanisms. Beneficial effects of the interacting proteins could be tested by protein overexpression or knockdown in the cell and animal models of PD. Furthermore, the small molecules targeting interacting proteins identified in this study could be tested for an effect in PD models. Finally, the human proteins that modified alpha-synuclein induced toxicity in yeast could be tested for an effect in cell or animal models of PD.

7 Supplementary Figures and Tables

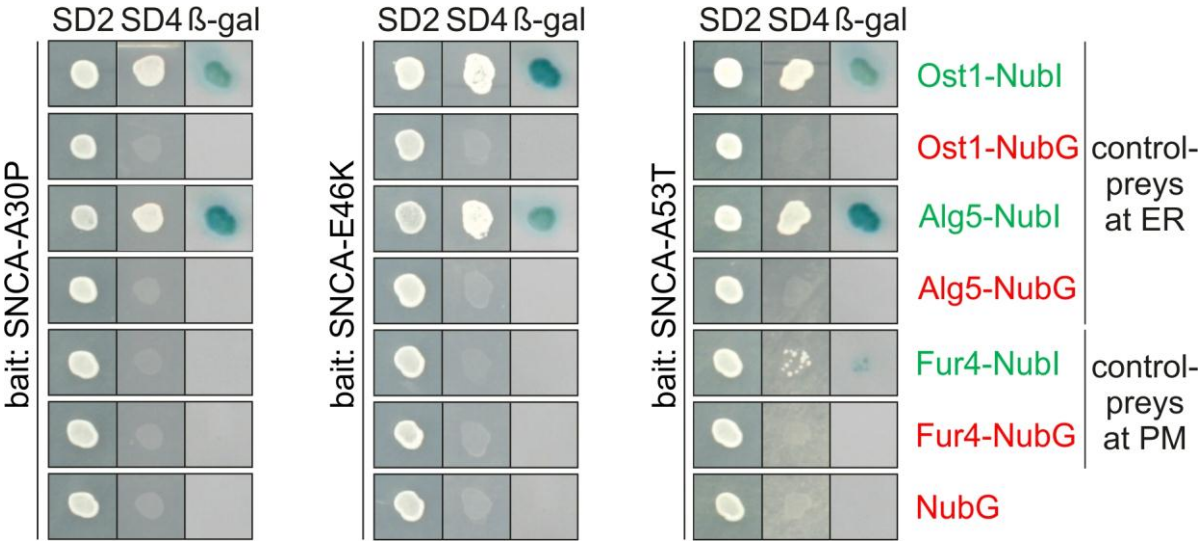

Supplementary Figure 1: Demonstration of cytoY2H bait functionality using the NubG/NubI test. Yeast co-expressing a mutant form of alpha-synuclein (A30P, E46K or A53T) as cytoY2H bait together with positive (green) or negative (red) control preys or NubG alone were plated on SD2 (-Leu-Trp) agar plates selecting for the presence of both bait and prey plasmid. Subsequently, yeast clones were grown on SD4 (-Leu-Trp-Ura-His) agar plates selecting for an interaction of the bait and prey protein. Additionally, yeast cells were spotted onto SD4 plates covered with nylon membranes to detect β-galactosidase (β-gal) activity.

Supplementary Table 1: Published high-confidence alpha-synuclein interactors.

gene symbol	gene name	synonyms	gene ID	HIPPIE score	applied method(s) to detect interaction	Publication
SNCAIP	synuclein, alpha interacting protein	synphilin-1, SYPH1	9627	0.7	Y2H, colocalization (H4 cells, neurons), FRET (H4 cells), AP (COS7 cells)	[116, 495-498]
ASYN	synuclein, alpha	PD1, NACP, PARK1, PARK4	6622	0.69	immuno-FRET (LBs), NMR	[499-502]
BAD	BCL2-associated agonist of cell death	BBC2, BCL2L8	572	0.5	Co-IP (rat brains, HEK and N27 cells)	[176, 177]
MAPT	microtubule-associated protein tau	TAU, MSTD, PPND,DDPAC, MTBT1,MTBT2	4137	0.48	colocalization (rat neurons), AP (human brains), *in vitro* binding	[503]
PLD1	phospholipase D1, phosphatidyl-choline-specific	-	5337	0.48	colocalization (HEK cells, rat brains), Co-IP (HEK cells), binding region determined	[380]
SLC6A3	dopamine transporter	solute carrier family 6 (neurotransmitter transporter) member 3, DAT1	6531	0.48	Y2H, colocalization (Ltk^- cells, HEK cells), Co-IP (Ltk^- cells, rat brains), AP (rat brains)	[327, 377, 378]
MAP1B	microtubule-associated protein 1B	MAP5, FUTSCH	4131	0.45	colocalization (PD brains), *in vitro* binding	[504]
APP	amyloid beta (A4) precursor protein	AAA, AD1, PN2, ABPP, APPI, CVAP	351	0.43	cross-linking (AD brains), cross-linking (*in vitro*, native and recombinant alpha-synuclein), *in situ* staining (AD brains)	[408]
CALM1	calmodulin 1	CAMI, PHKD, DD132, CALML2	801	0.43	AP (rat brains), cross-linking (*in vitro*)	[355]
MT-CO3	cytochrome c oxidase III (mitochondrial encoded)	COIII, MTCO3, COX3	4514	0.36	Y2H, Co-IP (*in vitro*)	[396]
TOR1A	Torsin A	DQ2, DYT1	1861	0.36	immuno-FRET (LBs) with different antibodies	[505]
MAPK1	mitogen-activated protein kinase 1	MAPK, ERK, ERK2, p38, p40, p41, ERT1	5594	0.31	AP (*in vitro*), binding region determined	[465]
PARK2	parkinson protein 2	Parkin, PDJ, PRKN, AR-JP, LPRS2	5071	0.31	colocalization (PD brains), Co-IP (HEK cells, PD brains)	[236, 506, 507]
UBB	ubiquitin B	Ubiquitin	7314	0.31	immuno-FRET (LBs), Co-IP (rat brains)	[499, 508]
YWHAH	14-3-3 eta	YWHA1	7533	0.31	AP (*in vitro*), Co-IP (PD brains)	[390]
SYK	spleen tyrosine kinase	FLJ25043, FLJ37489	6850	0.3	mammalian 2H (neuroblastoma cells), colocalization (mouse brains)	[232, 233, 509]
CYCS	cytochrome c (somatic)	CYC, HCS, THC4	54205	0.28	colocalization (LBs), cross-linking, immuno-FRET (PD brains)	[510-512]
SNCB	synuclein beta	SNCB	6620	0.26	colocalization (HEK cells), Co-IP (mouse brains, HEK cells)	[513]
SEPT4	septin 4	H5, ARTS, MART, CE5B3, PNUTL2, BRADEION, hCDCREL-2	5414	0.21	colocalization (PD and DLB brains), Co-IP (human brain, NIH3T3 cells)	[514]

gene symbol	gene name	also known as	gene ID	HIPPIE score	applied method(s) to detect interaction	PMID(s)
TH	tyrosine hydroxylase	TYH, DYT14, DYT5b	7054	0.21	Co-IP (rat brain, MN9D cells), immunoelectron microscopy	[113]
TPPP	tubulin polymerization promoting protein	p25, TPPP1	11076	0.21	colocalization (LBs, LNs), EM, co-sedimentation	[397, 398]
COL25A1	collagen	CLAC, collagen (type XXV, alpha 1), CLACP	84570	0.18	solid-phase assay	[515]
KLK6	kallikrein-related peptidase 6	Neurosin, Bssp, SP59, PRSS9, PRSS18, KLK6	5653	0.18	colocalization, Co-IP, co-fractionation (all mouse brains)	[516]
TUBA1A	tubulin, alpha 1a	LIS3, TUBA3, B-ALPHA-1	7846	0.18	AP, Co-IP (rat brains), *in vitro binding*	[182, 183]
YWHAB	14-3-3 beta	HS1, GW128, KCIP-1	7529	0.18	Co-IP (rat brains), ASYN was precipitated and co-precipitated	[177]
YWHAE	14-3-3 epsilon	MDCR, KCIP-1, 14-3-3E	7531	0.18	Co-IP (rat brains), ASYN was precipitated and co-precipitated	[177]
AGRN	agrin	FLJ45064	375790	n.a.	colocalization (PD brains), ELISA, *in vitro* binding	[517]
AKT1	v-akt murine thymoma viral oncogene homolog 1	AKT, PKB, RAC; PRKBA, PKB-ALPHA,RAC-ALPHA	207	n.a.	GST-pulldown in HEK-cells, coIP, far western	[518]
CBX4	chromobox homolog 4	hPC2, Human Polycomb protein 2, PC2, NBP16	8535	n.a.	Co-IP (HEK cells), ASYN is sumoylated by CBX4	[519]
CNTFR	ciliary neurotrophic factor receptor	RP11-296L22.1	1271	n.a.	colocalization (MES cells), Co-IP (MES cells)	[520]
CRYAB	crystallin, alpha B	CRYA2, CTPP2, HSPB5	1410	n.a.	NMR, size-exclusion chromatography, AP-MS	[521]
HSPA1A	heat shock 70kDa protein 1A	HSP72, HSPA1, HSP70I, HSP70-1, HSP70-1A	3303	n.a.	addition of binding peptide, Co-IP (MES cells), AP-MS (MES cells), FRET (*in vitro*)	[392]
LAMP2	lysosomal-associated membrane protein 2	LAMPB, CD107b, LGP110	3920	n.a.	Co-IP (isolated lysosomes, PC12 cells)	[79]
LRRK2	leucine-rich repeat kinase 2	PARK8, RIPK7, ROCO2, AURA17, DARDARIN	120892	n.a.	colocalization (LBs, HEK cells), Co-IP (HEK cells)	[490, 491]
PARK7	parkinson protein 7	DJ-1	11315	n.a.	colocalization (LBs), Co-IP (PD brains)	[522]
PLD2	phospholipase D2	-	5538	n.a.	colocalization (HEK cells), Co-IP (HEK cells)	[379-381]
PPP2R4	protein phosphatase 2A activator, regulatory subunit 4	PP2A, PR53, PTPA	5524	n.a.	Co-IP (PC12, rat brains)	[115]
PRKCA	protein kinase C, alpha	AAG6, PKCA, PRKACA	5578	n.a.	Co-IP (HEK cells, rat brains)	[380]
PSMC3	proteasome 26S subunit, ATPase, 3	TBP1	5702	n.a.	Y2H, colocalization (HEK cells), Co-IP (HEK cells)	[235]

gene symbol	gene name	also known as	gene ID	HIPPIE score	applied method(s) to detect interaction	PMID(s)
SIAH1	seven in absentia homolog 1	FLJ08065, SIAH1A	6477	n.a.	colocalization (PC12 cells), Co-IP (HeLa cells, PC12 cells), *in vitro* binding	[118]
TGM2	transglutaminase 2	TG2, TGC, GNAH	7052	n.a.	SPR measurements, Kd determined	[523, 524]
TRAF6	TNF receptor-associated factor 6	RNF85	7189	n.a.	colocalization (LBs in PD brains), Co-IP (HEK cells)	[525]

Abbreviations: n.a.: interaction not annotated in HIPPIE database, AP: affinity purification, AP-MS: affinity-purification mass spectrometry, Co-IP: co-immunoprecipitation, ELISA: enzyme-linked immunosorbent assay, EM: electron microscopy, immuno-FRET: immunofluorescence resonance energy transfer, NMR: nuclear magnetic resonance spectroscopy, SPR: surface plasmon resonance.

Supplementary Table 2: Gene-term enrichment analysis of published high-confidence alpha-synuclein interactors.

Source	Gene Category	associated alpha-synuclein interactors	total annotated alpha-synuclein interactors	associated interactors [%]	associated human genes	total annotated human genes	associated human genes [%]	p-value*
GO Cellular Component	neuron projection	11	38	28.9	342	12782	2.7	5.05E-06
GO Cellular Component	axon	9	38	23.7	159	12782	1.2	2.28E-06
GO Biological Process	regulation of programmed cell death	16	38	42.1	812	13528	6.0	1.19E-06
GO Biological Process	transmission of nerve impulse	10	38	26.3	350	13528	2.6	3.25E-04
GO Biological Process	cell-cell signaling	10	38	26.3	600	13528	4.4	2.66E-02
GO Biological Process	locomotory behavior	10	38	26.3	274	13528	2.0	4.02E-05
GO Biological Process	response to inorganic substance	7	38	18.4	205	13528	1.5	1.85E-02
GO Biological Process	dopamine metabolic process	6	38	15.8	20	13528	0.1	1.84E-06
GO Biological Process	synaptic transmission, dopaminergic	4	38	10.5	9	13528	0.1	1.65E-03
GO Molecular Function	tubulin binding	5	38	13.2	100	12983	0.8	3.19E-02
GO Molecular Function	phosphoprotein binding	4	38	10.5	27	12983	0.2	1.06E-02
KEGG pathway	Parkinson's disease	9	31	29.0	128	5085	2.5	3.52E-05
KEGG pathway	Neurotrophin signaling pathway	8	31	25.8	124	5085	2.4	4.09E-04
KEGG pathway	Alzheimer's disease	7	31	22.6	163	5085	3.2	2.27E-02
KEGG pathway	GnRH signaling pathway	6	31	19.4	98	5085	1.9	1.71E-02
KEGG pathway	Fc gamma R-mediated phagocytosis	6	31	19.4	95	5085	1.9	1.48E-02

* Only statistically significant results (P<0.05, Bonferroni correction) were taken into account.

Supplementary Table 3: Alpha-synuclein interactors detected by automated Y2H screening.

Alpha-synuclein Clone ID	Interactor Clone ID	Interactor Gene ID	Interactor Gene symbol	result SD4*	result LacZ*	svm score	confidence category	interactor used as
CCSB_6120	CCSB_10742	93550	ANUBL1	0	1	0,967838	HC	bait
CCSB_6120	CCSB_4761	163	AP2B1	8	0	-1,002044	LC	bait
CCSB_6120	IOH29583	351	APP	2	1	0,995356	HC	bait
CCSB_6120	CCSB_14684	55738	ARFGAP1	8	2	-0,780188	LC	bait
CCSB_6120	CCSB_4400	26286	ARFGAP3	1	0	-1,143227	LC	bait
CCSB_6120	CCSB_53432	339231	ARL16	4	0	0,465675	HC	bait
CCSB_6120	RZPDo834C1113D	79754	ASB13	1	0	-1,003097	LC	bait
CCSB_6120	CCSB_4958	467	ATF3	7	4	-1,01459	LC	bait
CCSB_6120	RZPDo839C1071	83734	ATG10	1	1	-1,048029	LC	bait
CCSB_6120	IOH13038	581	BAX	2	1	0,934011	HC	bait
CCSB_6120	CCSB_5989	598	BCL2L1	1	0	1,0011	HC	bait
CCSB_6120	CCSB_4441	332	BIRC5	3	1	-1,004315	LC	bait
CCSB_6120	CCSB_52889	338809	C12orf74	1	0	0,967838	HC	bait
CCSB_6120	CCSB_11170	135398	C6orf141	7	1	0,967838	HC	bait
CCSB_6120	CCSB_9298	84254	CAMKK1	3	1	0,991822	HC	bait
CCSB_6120	RZPDo839G05152	823	CAPN1	0	1	0,154554	HC	bait
CCSB_6120	IOH29375	201161	CENPV	7	0	-1,044113	LC	bait
CCSB_6120	CCSB_54986	5119	CHMP1A	2	0	-1,011602	LC	bait
CCSB_6120	RZPDo839F06150	8192	CLPP	1	0	-1,001929	LC	bait
CCSB_6120	CCSB_3700	8533	COPS3	8	8	-1,013145	LC	bait
CCSB_6120	CCSB_14467	51185	CRBN	1	0	-0,996746	LC	bait
CCSB_6120	CCSB_7634	1453	CSNK1D	2	0	-1,013757	LC	bait
CCSB_6120	CCSB_7245	1747	DLX3	6	0	0,183455	HC	bait
CCSB_6120	CCSB_7063	9093	DNAJA3	2	0	-0,991157	LC	bait
CCSB_6120	CCSB_9563	79733	E2F8	1	0	0,629722	HC	bait
CCSB_6120	CCSB_14891	8726	EED	3	0	-1,008022	LC	bait
CCSB_6120	RZPDo839E05126	22936	ELL2	9	5	-1,044928	LC	bait
CCSB_6120	CCSB_1593	219670	ENKUR	8	8	0,433518	HC	bait
CCSB_6120	CCSB_14530	2048	EPHB2	10	4	-	MC	bait
CCSB_6120	CCSB_55650	58489	FAM108C1	5	0	0,967838	HC	bait
CCSB_6120	CCSB_55425	283150	FOXR1	4	1	1,006503	HC	bait
CCSB_6120	CCSB_7125	2783	GNB2	0	1	-1,01035	LC	bait
CCSB_6120	CCSB_56249	23426	GRIP1	12	10	-1,003548	LC	bait
CCSB_6120	CCSB_56643	83933	HDAC10	5	0	-1,004638	LC	bait
CCSB_6120	RZPDo839D04145	57801	HES4	5	1	0,999432	HC	bait
CCSB_6120	CCSB_4764	8357	HIST1H3H	8	1	-1,001088	LC	bait
CCSB_6120	CCSB_8626	126961	HIST2H3C	5	2	-0,999476	LC	bait
CCSB_6120	CCSB_15037	92906	HNRPLL	6	0	-1,036875	LC	bait
CCSB_6120	CCSB_11579	3221	HOXC4	7	0	-1,033558	LC	bait
CCSB_6120	RZPDo839H11146	57549	IGSF9	2	0	-0,323228	LC	bait
CCSB_6120	RZPDo839C0974	9118	INA	2	1	0,317677	HC	bait
CCSB_6120	CCSB_2378	9922	IQSEC1	8	0	0,98417	HC	bait
CCSB_6120	CCSB_14220	22832	KIAA1009	10	6	-1,156796	LC	bait
CCSB_6120	CCSB_9989	28999	KLF15	2	1	0,79042	HC	bait
CCSB_6120	CCSB_9012	27252	KLHL20	1	0	-0,997447	LC	bait
CCSB_6120	CCSB_534	5653	KLK6	1	0	-1,023358	LC	bait
CCSB_6120	CCSB_10868	84456	L3MBTL3	4	1	1,003905	HC	bait
CCSB_6120	CCSB_52874	64211	LHX5	3	0	1,007631	HC	bait
CCSB_6120	CCSB_52814	26468	LHX6	1	0	0,999762	HC	bait
CCSB_6120	CCSB_8141	84708	LNX1	3	0	-1,006202	LC	bait

Alpha-synuclein Clone ID	Interactor Clone ID	Interactor Gene ID	Interactor Gene symbol	result SD4*	result LacZ*	svm score	confidence category	interactor used as
CCSB_6120	CCSB_54982	401296	LOC401296	1	0	0,967838	HC	bait
CCSB_6120	CCSB_52769	139081	MAGEC3	3	0	0,967838	HC	bait
CCSB_6120	RZPDo834G0720	10982	MAPRE2	10	4	-	MC	bait
CCSB_6120	RZPDo839F1288	8932	MBD2	10	4	-	MC	bait
CCSB_6120	CCSB_55542	57591	MKL1	7	4	-1,029336	LC	bait
CCSB_6120	IOH21965	84954	MPND	10	0	0,465675	HC	bait
CCSB_6120	CCSB_6798	22823	MTF2	1	1	-0,876437	LC	bait
CCSB_6120	IOH26774	51691	NAA38	7	3	-0,994965	LC	bait
CCSB_6120	CCSB_4351	4833	NME4	3	1	-0,999622	LC	bait
CCSB_6120	r1d14a12.str.abi_3	27020	NPTN	2	0	-0,865109	LC	bait
CCSB_6120	CCSB_7217	4931	NVL	3	0	-0,974008	LC	bait
CCSB_6120	CCSB_6420	55611	OTUB1	6	1	0,964152	HC	bait
CCSB_6120	IOH12066	56957	OTUD7B	8	0	1,016821	HC	bait
CCSB_6120	CCSB_2185	57097	PARP11	1	0	-0,999569	LC	bait
CCSB_6120	CCSB_9602	10336	PCGF3	2	1	-0,000357	MC	bait
CCSB_6120	CCSB_15059	55251	PCMTD2	5	0	0,969123	HC	bait
CCSB_6120	CCSB_1090	10158	PDZK1IP1	5	1	-0,991235	LC	bait
CCSB_6120	IOH38116	8554	PIAS1	12	8	0,97079	HC	bait
CCSB_6120	CCSB_7513	5700	PSMC1	4	2	-0,999994	LC	bait
CCSB_6120	RZPDo839C0777	5702	PSMC3	4	1	0,98853	HC	bait
CCSB_6120	CCSB_1047	27342	RABGEF1	2	0	-0,521377	LC	bait
CCSB_6120	CCSB_3945	5913	RAPSN	5	0	-1,002258	LC	bait
CCSB_6120	CCSB_8270	54033	RBM11	1	0	-0,834743	LC	bait
CCSB_6120	CCSB_5967	6009	RHEB	0	1	0,214269	HC	bait
CCSB_6120	CCSB_3030	9921	RNF10	1	1	-1,011988	LC	bait
CCSB_6120	CCSB_13709	7732	RNF112	12	0	0,972119	HC	bait
CCSB_6120	CCSB_7469	55658	RNF126	2	0	-1,004559	LC	bait
CCSB_6120	CCSB_797	51444	RNF138	6	0	-1,013562	LC	bait
CCSB_6120	IOH27564	165918	RNF168	3	1	0,390385	HC	bait
CCSB_6120	RZPDo839E0475	8819	SAP30	3	0	-1,013705	LC	bait
CCSB_6120	CCSB_53842	6386	SDCBP	5	3	-1,001879	LC	bait
CCSB_6120	RZPDo839B03148	5414	SEPT4	1	0	1,173365	HC	bait
CCSB_6120	CCSB_53123	129049	SGSM1	5	0	0,24696	HC	bait
CCSB_6120	CCSB_9727	6477	SIAH1	10	4	-0,871076	LC	bait
CCSB_6120	RZPDo839B0677	6620	SNCB	1	0	0,928412	HC	bait
CCSB_6120	CCSB_12140	124460	SNX20	10	4	-	MC	bait
CCSB_6120	CCSB_7188	6672	SP100	1	0	-1,000891	LC	bait
CCSB_6120	CCSB_1414	26206	SPAG8	6	0	-0,984927	LC	bait
CCSB_6120	IOH4396	56928	SPPL2B	3	0	-0,895417	LC	bait
CCSB_6120	RZPDo839B1176	8878	SQSTM1	2	2	0,892675	HC	bait
CCSB_6120	CCSB_1863	10254	STAM2	2	0	0,034432	MC	bait
CCSB_6120	CCSB_9561	25830	SULT4A1	2	0	1,176913	HC	bait
CCSB_6120	CCSB_9643	6996	TDG	3	0	-1,008668	LC	bait
CCSB_6120	CCSB_56266	7003	TEAD1	2	0	-1,00693	LC	bait
CCSB_6120	IOH22127	7014	TERF2	8	6	-1,003149	LC	bait
CCSB_6120	CCSB_3777	7052	TGM2	0	1	1,037277	HC	bait
CCSB_6120	CCSB_381	54472	TOLLIP	1	0	-1,029737	LC	bait
CCSB_6120	RZPDo839F0987	10024	TROAP	10	4	-	MC	bait
CCSB_6120	CCSB_14965	7846	TUBA1A	1	0	0,441444	HC	bait
CCSB_6120	CCSB_12765	117581	TWIST2	7	4	-1,057203	LC	bait
CCSB_6120	r1d10i11,str,abi_1	7311	UBA52	1	0	1,001058	HC	bait

Alpha-synuclein Clone ID	Interactor Clone ID	Interactor Gene ID	Interactor Gene symbol	result SD4*	result LacZ*	svm score	confidence category	interactor used as
CCSB_6120	CCSB_3662	10422	UBAC1	2	0	-1,02168	LC	bait
CCSB_6120	RZPDo839C02123	10537	UBD	2	0	-1,102542	LC	bait
CCSB_6120	CCSB_6778	51035	UBXN1	2	0	-1,006427	LC	bait
CCSB_6120	CCSB_10107	51720	UIMC1	1	0	0,915243	HC	bait
CCSB_6120	CCSB_13320	7428	VHL	3	1	0,974698	HC	bait
CCSB_6120	IOH26580	375260	WASH2P	10	4	-	MC	bait
CCSB_6120	CCSB_6964	80349	WDR61	12	1	-1,009049	LC	bait
CCSB_6120	CCSB_326	11060	WWP2	2	0	-0,045971	MC	bait
CCSB_6120	IOH4929	7533	YWHAH	5	5	1,054502	HC	bait
CCSB_6120	CCSB_10083	9841	ZBTB24	5	1	-0,979967	LC	bait
CCSB_6120	CCSB_13326	153527	ZMAT2	5	0	0,410597	HC	bait
CCSB_6120	CCSB_6279	162979	ZNF296	6	0	-0,698076	LC	bait
CCSB_6120	CCSB_56668	167465	ZNF366	10	6	0,788919	HC	bait
CCSB_6120	CCSB_3850	79230	ZNF557	7	1	-0,041477	MC	bait
CCSB_6120	CCSB_8202	126295	ZNF57	1	0	0,787077	HC	bait
CCSB_6120	CCSB_14172	284312	ZSCAN1	2	0	0,637941	HC	bait
CCSB_6120_A30P	IOH5584	244	ANXA8L2	2	0	0,933819	HC	bait
CCSB_6120_A30P	CCSB_4761	163	AP2B1	7	0	-1,002044	LC	bait
CCSB_6120_A30P	CCSB_9616	8546	AP3B1	1	0	-0,999637	LC	bait
CCSB_6120_A30P	IOH29583	351	APP	4	1	0,995356	HC	bait
CCSB_6120_A30P	CCSB_14684	55738	ARFGAP1	3	0	-0,780188	LC	bait
CCSB_6120_A30P	CCSB_4400	26286	ARFGAP3	5	0	-1,143227	LC	bait
CCSB_6120_A30P	CCSB_14251	10865	ARID5A	3	0	-1,215352	LC	bait
CCSB_6120_A30P	CCSB_53432	339231	ARL16	8	1	0,465675	HC	bait
CCSB_6120_A30P	CCSB_55311	10123	ARL4C	1	0	-0,201723	LC	bait
CCSB_6120_A30P	RZPDo834C1113D	79754	ASB13	1	0	-1,003097	LC	bait
CCSB_6120_A30P	CCSB_56495	121549	ASCL4	4	0	0,679789	HC	bait
CCSB_6120_A30P	CCSB_4958	467	ATF3	8	0	-1,01459	LC	bait
CCSB_6120_A30P	CCSB_3898	7917	BAT3	5	0	-0,972146	LC	bait
CCSB_6120_A30P	CCSB_7342	581	BAX	1	0	0,934011	HC	bait
CCSB_6120_A30P	CCSB_4441	332	BIRC5	3	0	-1,004315	LC	bait
CCSB_6120_A30P	CCSB_55645	90427	BMF	1	1	1,014201	HC	bait
CCSB_6120_A30P	CCSB_52889	338809	C12orf74	3	0	0,967838	HC	bait
CCSB_6120_A30P	CCSB_52979	84709	C4orf49	7	0	-0,759004	LC	bait
CCSB_6120_A30P	CCSB_11170	135398	C6orf141	7	2	0,967838	HC	bait
CCSB_6120_A30P	CCSB_7253	115416	C7orf30	1	0	-0,999807	LC	bait
CCSB_6120_A30P	CCSB_53297	157657	C8orf37	1	1	0,967838	HC	bait
CCSB_6120_A30P	CCSB_3931	79095	C9orf16	3	1	-1,000378	LC	bait
CCSB_6120_A30P	CCSB_395	801	CALM1	1	0	1,017961	HC	bait
CCSB_6120_A30P	CCSB_9298	84254	CAMKK1	10	5	0,991822	HC	bait
CCSB_6120_A30P	CCSB_6129	823	CAPN1	1	0	0,154554	HC	bait
CCSB_6120_A30P	CCSB_53253	445571	CBWD3	1	0	0,465675	HC	bait
CCSB_6120_A30P	IOH22152	317762	CCDC85C	1	0	0,967838	HC	bait
CCSB_6120_A30P	CCSB_55476	440193	CCDC88C	1	1	-1,001221	LC	bait
CCSB_6120_A30P	CCSB_13480	892	CCNC	10	7	-1,025606	LC	bait
CCSB_6120_A30P	CCSB_54986	5119	CHMP1A	1	0	-1,011602	LC	bait
CCSB_6120_A30P	CCSB_14174	1327	COX4I1	2	0	-0,988446	LC	bait
CCSB_6120_A30P	CCSB_14467	51185	CRBN	2	0	-0,996746	LC	bait
CCSB_6120_A30P	CCSB_7634	1453	CSNK1D	1	0	-1,013757	LC	bait
CCSB_6120_A30P	CCSB_6699	1457	CSNK2A1	1	0	1,036604	HC	bait
CCSB_6120_A30P	CCSB_12290	79901	CYBRD1	8	5	-0,367297	LC	bait

Alpha-synuclein Clone ID	Interactor Clone ID	Interactor Gene ID	Interactor Gene symbol	result SD4*	result LacZ*	svm score	confidence category	interactor used as
CCSB_6120_A30P	CCSB_56904	92196	DAPL1	1	0	0,963316	HC	bait
CCSB_6120_A30P	CCSB_52987	1616	DAXX	1	0	0,901766	HC	bait
CCSB_6120_A30P	CCSB_7245	1747	DLX3	1	0	0,183455	HC	bait
CCSB_6120_A30P	CCSB_12820	4733	DRG1	8	1	-1,001981	LC	bait
CCSB_6120_A30P	CCSB_9563	79733	E2F8	5	0	0,629722	HC	bait
CCSB_6120_A30P	CCSB_3183	1937	EEF1G	8	4	-0,604089	LC	bait
CCSB_6120_A30P	CCSB_3148	8665	EIF3F	1	0	0,88199	HC	bait
CCSB_6120_A30P	CCSB_1593	219670	ENKUR	8	7	0,433518	HC	bait
CCSB_6120_A30P	CCSB_11248	10640	EXOC5	4	0	-1,004552	LC	bait
CCSB_6120_A30P	CCSB_55498	2140	EYA3	1	0	-1,266181	LC	bait
CCSB_6120_A30P	CCSB_55650	58489	FAM108C1	8	0	0,967838	HC	bait
CCSB_6120_A30P	CCSB_56659	2280	FKBP1A	1	0	-0,9354	LC	bait
CCSB_6120_A30P	CCSB_55425	283150	FOXR1	4	3	1,006503	HC	bait
CCSB_6120_A30P	IOH21081	2534	FYN	2	1	0,960581	HC	bait
CCSB_6120_A30P	CCSB_2338	8693	GALNT4	2	0	-1,00334	LC	bait
CCSB_6120_A30P	CCSB_4519	29926	GMPPA	8	0	-0,141162	LC	bait
CCSB_6120_A30P	CCSB_56095	55592	GOLGA2B	8	0	0,967838	HC	bait
CCSB_6120_A30P	CCSB_7877	63940	GPSM3	1	0	-1,003645	LC	bait
CCSB_6120_A30P	CCSB_56643	83933	HDAC10	7	0	-1,004638	LC	bait
CCSB_6120_A30P	RZPDo839D04145	57801	HES4	9	0	0,999432	HC	bait
CCSB_6120_A30P	CCSB_8626	126961	HIST2H3C	7	2	-0,999476	LC	bait
CCSB_6120_A30P	CCSB_15037	92906	HNRPLL	10	4	-1,036875	LC	bait
CCSB_6120_A30P	RZPDo839F10150	3430	IFI35	1	0	0,973455	HC	bait
CCSB_6120_A30P	CCSB_2378	9922	IQSEC1	7	0	0,98417	HC	bait
CCSB_6120_A30P	CCSB_9989	28999	KLF15	6	1	0,79042	HC	bait
CCSB_6120_A30P	CCSB_55638	3880	KRT19	1	0	-0,996708	LC	bait
CCSB_6120_A30P	CCSB_54667	337879	KRTAP8-1	1	0	1,056006	HC	bait
CCSB_6120_A30P	CCSB_10868	84456	L3MBTL3	3	1	1,003905	HC	bait
CCSB_6120_A30P	CCSB_1499	92483	LDHAL6B	5	0	-1,09816	LC	bait
CCSB_6120_A30P	CCSB_52874	64211	LHX5	1	1	1,007631	HC	bait
CCSB_6120_A30P	CCSB_52814	26468	LHX6	2	0	0,999762	HC	bait
CCSB_6120_A30P	CCSB_8141	84708	LNX1	3	0	-1,006202	LC	bait
CCSB_6120_A30P	CCSB_54982	401296	LOC401296	1	0	0,967838	HC	bait
CCSB_6120_A30P	CCSB_54938	642947	LOC642947	1	0	0,967838	HC	bait
CCSB_6120_A30P	CCSB_9613	23175	LPIN1	6	0	0,736694	HC	bait
CCSB_6120_A30P	CCSB_54589	4067	LYN	1	0	1,041211	HC	bait
CCSB_6120_A30P	CCSB_52769	139081	MAGEC3	2	0	0,967838	HC	bait
CCSB_6120_A30P	CCSB_53816	7873	MANF	1	1	-1,015417	LC	bait
CCSB_6120_A30P	CCSB_55542	57591	MKL1	8	5	-1,029336	LC	bait
CCSB_6120_A30P	IOH21965	84954	MPND	10	0	0,465675	HC	bait
CCSB_6120_A30P	CCSB_54196	22921	MSRB2	2	0	-0,427748	LC	bait
CCSB_6120_A30P	CCSB_8274	58529	MYOZ1	2	0	-1,00936	LC	bait
CCSB_6120_A30P	CCSB_14229	79612	NAA16	4	1	-1,201046	LC	bait
CCSB_6120_A30P	IOH26774	51691	NAA38	8	6	-0,994965	LC	bait
CCSB_6120_A30P	CCSB_4351	4833	NME4	5	0	-0,999622	LC	bait
CCSB_6120_A30P	CCSB_4747	55611	OTUB1	1	1	0,964152	HC	bait
CCSB_6120_A30P	IOH12066	56957	OTUD7B	2	0	1,016821	HC	bait
CCSB_6120_A30P	IOH29357	55690	PACS1	8	0	-0,893051	LC	bait
CCSB_6120_A30P	CCSB_2185	57097	PARP11	3	0	-0,999569	LC	bait
CCSB_6120_A30P	CCSB_9602	10336	PCGF3	6	0	-0,000357	MC	bait
CCSB_6120_A30P	CCSB_323	84108	PCGF6	0	1	-1,061231	LC	bait

Alpha-synuclein Clone ID	Interactor Clone ID	Interactor Gene ID	Interactor Gene symbol	result SD4*	result LacZ*	svm score	confidence category	interactor used as
CCSB_6120_A30P	CCSB_15059	55251	PCMTD2	1	0	0,969123	HC	bait
CCSB_6120_A30P	CCSB_1090	10158	PDZK1IP1	1	0	-0,991235	LC	bait
CCSB_6120_A30P	IOH38116	8554	PIAS1	12	8	0,97079	HC	bait
CCSB_6120_A30P	CCSB_3826	5434	POLR2E	8	2	-1,009118	LC	bait
CCSB_6120_A30P	CCSB_52968	5578	PRKCA	1	0	1,029495	HC	bait
CCSB_6120_A30P	CCSB_56694	55015	PRPF39	1	0	0,835627	HC	bait
CCSB_6120_A30P	CCSB_7513	5700	PSMC1	4	5	-0,999994	LC	bait
CCSB_6120_A30P	RZPDo839C0777	5702	PSMC3	3	0	0,98853	HC	bait
CCSB_6120_A30P	CCSB_56584	84084	RAB6C	1	1	-0,511619	LC	bait
CCSB_6120_A30P	CCSB_3270	8498	RANBP3	1	0	-1,075297	LC	bait
CCSB_6120_A30P	CCSB_3945	5913	RAPSN	4	3	-1,002258	LC	bait
CCSB_6120_A30P	CCSB_8270	54033	RBM11	1	0	-0,834743	LC	bait
CCSB_6120_A30P	CCSB_5967	6009	RHEB	5	2	0,214269	HC	bait
CCSB_6120_A30P	CCSB_12523	84153	RNASEH2C	2	0	1,027697	HC	bait
CCSB_6120_A30P	CCSB_3030	9921	RNF10	2	0	-1,011988	LC	bait
CCSB_6120_A30P	CCSB_9056	54778	RNF111	4	1	-1,007586	LC	bait
CCSB_6120_A30P	CCSB_13709	7732	RNF112	7	0	0,972119	HC	bait
CCSB_6120_A30P	CCSB_7469	55658	RNF126	1	0	-1,004559	LC	bait
CCSB_6120_A30P	CCSB_6114	138065	RNF183	3	0	-0,991235	LC	bait
CCSB_6120_A30P	CCSB_1644	23429	RYBP	12	0	1,002789	HC	bait
CCSB_6120_A30P	RZPDo839E0475	8819	SAP30	10	0	-1,013705	LC	bait
CCSB_6120_A30P	CCSB_52822	163786	SASS6	1	0	-0,988134	LC	bait
CCSB_6120_A30P	CCSB_53123	129049	SGSM1	6	0	0,24696	HC	bait
CCSB_6120_A30P	CCSB_1414	26206	SPAG8	5	0	-0,984927	LC	bait
CCSB_6120_A30P	CCSB_2101	84690	SPATA22	1	0	0,967838	HC	bait
CCSB_6120_A30P	CCSB_10313	124044	SPATA2L	1	1	-0,999807	LC	bait
CCSB_6120_A30P	IOH4396	56928	SPPL2B	3	0	-0,895417	LC	bait
CCSB_6120_A30P	CCSB_54640	200734	SPRED2	1	0	-1,001489	LC	bait
CCSB_6120_A30P	CCSB_56664	81848	SPRY4	1	0	-0,976083	LC	bait
CCSB_6120_A30P	RZPDo839B1176	8878	SQSTM1	1	1	0,892675	HC	bait
CCSB_6120_A30P	CCSB_4447	246329	STAC3	5	2	-0,999807	LC	bait
CCSB_6120_A30P	CCSB_9561	25830	SULT4A1	5	0	1,176913	HC	bait
CCSB_6120_A30P	IOH22591	8189	SYMPK	1	0	-1,010549	LC	bait
CCSB_6120_A30P	CCSB_53648	10716	TBR1	1	0	-1,068846	LC	bait
CCSB_6120_A30P	CCSB_9643	6996	TDG	7	0	-1,008668	LC	bait
CCSB_6120_A30P	IOH22127	7014	TERF2	8	7	-1,003149	LC	bait
CCSB_6120_A30P	CCSB_3777	7052	TGM2	1	0	1,037277	HC	bait
CCSB_6120_A30P	CCSB_56439	9220	TIAF1	1	1	-0,990868	LC	bait
CCSB_6120_A30P	CCSB_56912	388595	TMEM82	1	1	-0,759004	LC	bait
CCSB_6120_A30P	CCSB_12384	29767	TMOD2	0	1	-0,050922	MC	bait
CCSB_6120_A30P	CCSB_55147	7158	TP53BP1	2	0	-1,001405	LC	bait
CCSB_6120_A30P	CCSB_12402	9537	TP53I11	1	0	0,287357	HC	bait
CCSB_6120_A30P	CCSB_12765	117581	TWIST2	5	0	-1,057203	LC	bait
CCSB_6120_A30P	CCSB_10107	51720	UIMC1	2	0	0,915243	HC	bait
CCSB_6120_A30P	IOH27747	9099	USP2	12	0	0,654428	HC	bait
CCSB_6120_A30P	CCSB_14638	7417	VDAC2	1	0	-0,982452	LC	bait
CCSB_6120_A30P	CCSB_13320	7428	VHL	1	0	0,974698	HC	bait
CCSB_6120_A30P	CCSB_69	7431	VIM	2	0	0,312413	HC	bait
CCSB_6120_A30P	CCSB_56471	338917	VSX2	1	1	0,1562	HC	bait
CCSB_6120_A30P	RZPDo839F04123	155368	WBSCR27	2	0	0,988532	HC	bait
CCSB_6120_A30P	CCSB_6964	80349	WDR61	12	0	-1,009049	LC	bait

Alpha-synuclein Clone ID	Interactor Clone ID	Interactor Gene ID	Interactor Gene symbol	result SD4*	result LacZ*	svm score	confidence category	interactor used as
CCSB_6120_A30P	IOH4929	7533	YWHAH	5	5	1,054502	HC	bait
CCSB_6120_A30P	CCSB_13326	153527	ZMAT2	4	0	0,410597	HC	bait
CCSB_6120_A30P	CCSB_9016	9204	ZMYM6	8	3	-0,093206	MC	bait
CCSB_6120_A30P	CCSB_55412	118738	ZNF488	2	0	-1,196943	LC	bait
CCSB_6120_A30P	CCSB_56039	162968	ZNF497	1	1	0,788919	HC	bait
CCSB_6120_A30P	CCSB_3850	79230	ZNF557	1	0	-0,041477	MC	bait
CCSB_6120_A30P	CCSB_8202	126295	ZNF57	2	0	0,787077	HC	bait
CCSB_6120_A30P	CCSB_14172	284312	ZSCAN1	2	3	0,637941	HC	bait
CCSB_6120_E46K	CCSB_52816	160428	ALDH1L2	1	0	0,30477	HC	bait
CCSB_6120_E46K	CCSB_4761	163	AP2B1	3	0	-1,002044	LC	bait
CCSB_6120_E46K	CCSB_14684	55738	ARFGAP1	2	0	-0,780188	LC	bait
CCSB_6120_E46K	CCSB_53432	339231	ARL16	3	0	0,465675	HC	bait
CCSB_6120_E46K	CCSB_4441	332	BIRC5	3	0	-1,004315	LC	bait
CCSB_6120_E46K	CCSB_7016	79096	C11orf49	1	0	-1,006446	LC	bait
CCSB_6120_E46K	CCSB_4140	28971	C11orf67	1	0	0,967838	HC	bait
CCSB_6120_E46K	CCSB_52889	338809	C12orf74	1	1	0,967838	HC	bait
CCSB_6120_E46K	CCSB_52979	84709	C4orf49	2	0	-0,759004	LC	bait
CCSB_6120_E46K	CCSB_395	801	CALM1	1	0	1,017961	HC	bait
CCSB_6120_E46K	CCSB_7634	1453	CSNK1D	1	0	-1,013757	LC	bait
CCSB_6120_E46K	CCSB_8139	64858	DCLRE1B	1	0	-1,132807	LC	bait
CCSB_6120_E46K	CCSB_12820	4733	DRG1	8	3	-1,001981	LC	bait
CCSB_6120_E46K	CCSB_55498	2140	EYA3	1	0	-1,266181	LC	bait
CCSB_6120_E46K	CCSB_55650	58489	FAM108C1	5	0	0,967838	HC	bait
CCSB_6120_E46K	CCSB_56643	83933	HDAC10	4	0	-1,004638	LC	bait
CCSB_6120_E46K	CCSB_8626	126961	HIST2H3C	4	0	-0,999476	LC	bait
CCSB_6120_E46K	CCSB_15037	92906	HNRPLL	1	0	-1,036875	LC	bait
CCSB_6120_E46K	CCSB_2378	9922	IQSEC1	2	0	0,98417	HC	bait
CCSB_6120_E46K	CCSB_1499	92483	LDHAL6B	6	0	-1,09816	LC	bait
CCSB_6120_E46K	CCSB_54589	4067	LYN	0	1	1,041211	HC	bait
CCSB_6120_E46K	CCSB_6976	80306	MED28	1	0	-0,975844	LC	bait
CCSB_6120_E46K	CCSB_55542	57591	MKL1	4	0	-1,029336	LC	bait
CCSB_6120_E46K	CCSB_5500	4502	MT2A	1	0	-0,991755	LC	bait
CCSB_6120_E46K	CCSB_4351	4833	NME4	1	0	-0,999622	LC	bait
CCSB_6120_E46K	CCSB_4747	55611	OTUB1	0	1	0,964152	HC	bait
CCSB_6120_E46K	IOH29357	55690	PACS1	2	0	-0,893051	LC	bait
CCSB_6120_E46K	CCSB_1090	10158	PDZK1IP1	2	0	-0,991235	LC	bait
CCSB_6120_E46K	IOH38116	8554	PIAS1	3	0	0,97079	HC	bait
CCSB_6120_E46K	CCSB_52968	5578	PRKCA	1	1	1,029495	HC	bait
CCSB_6120_E46K	ORF_SEQ_2C07	5717	PSMD11	1	0	-1,008808	LC	bait
CCSB_6120_E46K	CCSB_3945	5913	RAPSN	5	0	-1,002258	LC	bait
CCSB_6120_E46K	CCSB_9056	54778	RNF111	8	6	-1,007586	LC	bait
CCSB_6120_E46K	CCSB_13709	7732	RNF112	6	0	0,972119	HC	bait
CCSB_6120_E46K	CCSB_1644	23429	RYBP	2	0	1,002789	HC	bait
CCSB_6120_E46K	CCSB_11100	6477	SIAH1	1	0	-0,871076	LC	bait
CCSB_6120_E46K	CCSB_6120	6622	SNCA	1	0	n.a.	n.a.	bait
CCSB_6120_E46K	CCSB_52851	8403	SOX14	1	0	-0,664782	LC	bait
CCSB_6120_E46K	CCSB_1414	26206	SPAG8	6	0	-0,984927	LC	bait
CCSB_6120_E46K	CCSB_10313	124044	SPATA2L	1	0	-0,999807	LC	bait
CCSB_6120_E46K	CCSB_56664	81848	SPRY4	1	0	-0,976083	LC	bait
CCSB_6120_E46K	IOH22127	7014	TERF2	2	0	-1,003149	LC	bait
CCSB_6120_E46K	CCSB_180	23548	TTC33	1	0	0,967838	HC	bait

Alpha-synuclein Clone ID	Interactor Clone ID	Interactor Gene ID	Interactor Gene symbol	result SD4*	result LacZ*	svm score	confidence category	interactor used as
CCSB_6120_E46K	CCSB_6964	80349	WDR61	10	0	-1,009049	LC	bait
CCSB_6120_E46K	IOH4929	7533	YWHAH	5	5	1,054502	HC	bait
CCSB_6120_E46K	CCSB_13326	153527	ZMAT2	5	0	0,410597	HC	bait
RZPDo834A087D	IOH3692	207	AKT1	0	1	0,997669	HC	bait
RZPDo834A087D	RZPDo839D05129	7915	ALDH5A1	2	0	0,194965	HC	prey
RZPDo834A087D	CCSB_11445	338692	ANKRD13D	2	0	0,465675	HC	bait
RZPDo834A087D	CCSB_9616	8546	AP3B1	6	3	-0,999637	LC	bait
RZPDo834A087D	CCSB_13194	525	ATP6V1B1	0	1	-1,007487	LC	bait
RZPDo834A087D	e-ATXN1-Q30_WT	6310	ATXN1	4	0	1,122891	HC	prey
RZPDo834A087D	e-ATXN3-Q71	4287	ATXN3	2	0	0,940724	HC	prey
RZPDo834A087D	CCSB_3898	7917	BAT3	12	2	-0,972146	LC	bait
RZPDo834A087D	CCSB_417	63827	BCAN	2	0	-1,025367	LC	prey
RZPDo834A087D	CCSB_817	590	BCHE	4	0	-0,031829	MC	prey
RZPDo834A087D	CCSB_14984	8553	BHLHE40	2	0	0,093087	MC	prey
RZPDo834A087D	CCSB_52979	84709	C4orf49	6	0	-0,759004	LC	bait
RZPDo834A087D	CCSB_395	801	CALM1	4	1	1,017961	HC	bait
RZPDo834A087D	CCSB_3160	839	CASP6	5	0	1,119784	HC	prey
RZPDo834A087D	CCSB_12521	51379	CRLF3	4	2	0,967838	HC	bait
RZPDo834A087D	CCSB_8833	1488	CTBP2	11	2	-1,003736	LC	prey
RZPDo834A087D	CCSB_7420	54205	CYCS	1	0	0,064622	MC	bait
RZPDo834A087D	CCSB_6848	26999	CYFIP2	2	0	-1,030986	LC	prey
RZPDo834A087D	CCSB_56904	92196	DAPL1	0	1	0,963316	HC	bait
RZPDo834A087D	IOH29409	10522	DEAF1	4	0	-1,091816	LC	bait
RZPDo834A087D	CCSB_12573	1674	DES	12	2	-0,154451	LC	prey
RZPDo834A087D	IOH36584	1742	DLG4	8	5	0,790876	HC	prey
RZPDo834A087D	CCSB_12820	4733	DRG1	4	2	-1,001981	LC	bait
RZPDo834A087D	CCSB_5469	1837	DTNA	6	0	-1,010159	LC	prey
RZPDo834A087D	CCSB_11248	10640	EXOC5	3	1	-1,004552	LC	bait
RZPDo834A087D	CCSB_55446	9637	FEZ2	1	0	-0,983258	LC	bait
RZPDo834A087D	CCSB_56659	2280	FKBP1A	0	1	-0,9354	LC	bait
RZPDo834A087D	CCSB_7395	2512	FTL	1	0	-1,01091	LC	bait
RZPDo834A087D	IOH21081	2534	FYN	2	1	0,960581	HC	bait
RZPDo834A087D	CCSB_5146	2596	GAP43	2	0	0,846302	HC	prey
RZPDo834A087D	CCSB_13820	2668	GDNF	10	1	-1,045688	LC	prey
RZPDo834A087D	CCSB_12739	2773	GNAI3	4	0	-1,002572	LC	prey
RZPDo834A087D	CCSB_5333	9759	HDAC4	2	0	0,735542	HC	prey
RZPDo834A087D	RZPDo839H02145	23394	HOMER2	2	0	-0,64135	LC	prey
RZPDo834A087D	CCSB_7127	9454	HOMER3	12	4	-0,97846	LC	prey
RZPDo834A087D	RZPDo834G0522D	3265	HRAS	2	0	0,591972	HC	prey
RZPDo834A087D	e-HD1223-1941	3064	HTT	2	0	0,95053	HC	prey
RZPDo834A087D	RZPDo839F10150	3430	IFI35	2	0	0,973455	HC	bait
RZPDo834A087D	CCSB_616	9270	ITGB1BP1	10	7	-0,989561	LC	bait
RZPDo834A087D	CCSB_8590	3845	KRAS	2	0	0,117514	HC	prey
RZPDo834A087D	CCSB_53056	83899	KRTAP9-2	2	1	0,43806	HC	bait
RZPDo834A087D	CCSB_3743	3920	LAMP2	1	0	-0,99212	LC	prey
RZPDo834A087D	CCSB_1499	92483	LDHAL6B	7	0	-1,09816	LC	bait
RZPDo834A087D	CCSB_1268	9211	LGI1	2	0	-0,911641	LC	prey
RZPDo834A087D	CCSB_10152	222484	LNX2	1	0	-0,992562	LC	bait
RZPDo834A087D	LRRK2_WD40_G2385A	120892	LRRK2	1	1	-0,241249	LC	prey
RZPDo834A087D	CCSB_54561	4067	LYN	2	1	1,041211	HC	bait
RZPDo834A087D	CCSB_53816	7873	MANF	2	0	-1,015417	LC	bait

Alpha-synuclein Clone ID	Interactor Clone ID	Interactor Gene ID	Interactor Gene symbol	result SD4*	result LacZ*	svm score	confidence category	interactor used as
RZPDo834A087D	CCSB_55860	4137	MAPT	1	0	0,949691	HC	bait
RZPDo834A087D	RZPDo834C0622D	4155	MBP	2	0	0,507632	HC	prey
RZPDo834A087D	CCSB_54196	22921	MSRB2	2	0	-0,427748	LC	bait
RZPDo834A087D	CCSB_5500	4502	MT2A	1	0	-0,991755	LC	bait
RZPDo834A087D	CCSB_389	4504	MT3	10	2	-0,663077	LC	prey
RZPDo834A087D	IOH29357	55690	PACS1	6	0	-0,893051	LC	bait
RZPDo834A087D	CCSB_4845	10298	PAK4	2	0	-1,01207	LC	bait
RZPDo834A087D	CCSB_1392	5071	PARK2	2	1	0,936924	HC	prey
RZPDo834A087D	CCSB_323	84108	PCGF6	0	2	-1,061231	LC	bait
RZPDo834A087D	RZPDo839C08151	5037	PEBP1	2	2	-0,299641	LC	prey
RZPDo834A087D	RZPDo839D09133	10401	PIAS3	2	0	0,767662	HC	prey
RZPDo834A087D	CCSB_1226	9867	PJA2	2	0	-1,006796	LC	prey
RZPDo834A087D	CCSB_10457	219990	PLAC1L	1	0	-0,895417	LC	bait
RZPDo834A087D	CCSB_52968	5578	PRKCA	2	0	1,029495	HC	bait
RZPDo834A087D	CCSB_52967	5581	PRKCE	1	1	1,005953	HC	bait
RZPDo834A087D	CCSB_2589	55660	PRPF40A	3	0	-0,999594	LC	prey
RZPDo834A087D	CCSB_6051	115827	RAB3C	3	0	-1,06559	LC	prey
RZPDo834A087D	CCSB_231	5901	RAN	3	0	-0,998003	LC	prey
RZPDo834A087D	CCSB_9056	54778	RNF111	12	2	-1,007586	LC	bait
RZPDo834A087D	CCSB_6114	138065	RNF183	12	1	-0,991235	LC	bait
RZPDo834A087D	IOH29907	6198	RPS6KB1	2	0	0,953676	HC	prey
RZPDo834A087D	CCSB_1644	23429	RYBP	12	3	1,002789	HC	bait
RZPDo834A087D	CCSB_7641	4735	SEPT2	4	0	-1,004858	LC	prey
RZPDo834A087D	CCSB_12681	5413	SEPT5	12	10	1,009891	HC	prey
RZPDo834A087D	IOH38225	57154	SMURF1	2	0	1,041077	HC	bait
RZPDo834A087D	IOH3724	23557	SNAPIN	6	0	-0,936197	LC	prey
RZPDo834A087D	CCSB_2101	84690	SPATA22	3	0	0,967838	HC	bait
RZPDo834A087D	CCSB_5423	8877	SPHK1	4	0	1,011984	HC	prey
RZPDo834A087D	IOH22591	8189	SYMPK	8	0	-1,010549	LC	bait
RZPDo834A087D	CCSB_53648	10716	TBR1	1	1	-1,068846	LC	bait
RZPDo834A087D	CCSB_56345	11076	TPPP	0	1	-0,730729	LC	bait
RZPDo834A087D	CCSB_130	6737	TRIM21	2	0	-0,141241	LC	bait
RZPDo834A087D	CCSB_3825	203068	TUBB	1	0	1,013654	HC	bait
RZPDo834A087D	IOH27747	9099	USP2	2	1	0,654428	HC	bait
RZPDo834A087D	RZPDo839F04123	155368	WBSCR27	2	1	0,988532	HC	bait

* The sizes of the growing yeast colonies and the size of the blue coloration from the β galactosidase assay were categorized as small, medium or large. 1 point was awarded for a small colony / spot, 2 points for a medium colony / spot and 3 points were awarded for a large colony / spot. For the final “result SD4” or “result lacZ” the points from all four repetitions were added.

Supplementary Table 4: Gene-term enrichment analysis of alpha-synuclein interactors.

Source	Gene category	associated interactors Y2H	total annotated interactors Y2H	associated interactors Y2H [%]	associated genes in Y2H matrix	total annotated genes in Y2H matrix	associated genes in matrix [%]	p-value*
GO Cellular Component	cytoskeletal part	13	49	26.5	621	8504	7.3	2.14E-02
GO Cellular Component	axon	7	49	14.3	110	8504	1.3	5.56E-03
GO Biological Process	regulation of programmed cell death	18	58	31.0	644	9063	7.1	2.95E-04
GO Biological Process	programmed cell death	14	58	24.1	470	9063	5.2	6.36E-03
GO Biological Process	regulation of neuron apoptosis	7	58	12.1	72	9063	0.8	6.83E-03
GO Biological Process	positive regulation of cell proliferation	11	58	19.0	323	9063	3.6	3.51E-02
GO Biological Process	response to radiation	11	58	19.0	146	9063	1.6	2.50E-05
GO Biological Process	response to light stimulus	7	58	12.1	94	9063	1.0	3.16E-02
GO Biological Process	transmission of nerve impulse	10	58	17.2	227	9063	2.5	1.33E-02
GO Biological Process	learning or memory	10	58	17.2	84	9063	0.9	2.61E-06
GO Biological Process	visual behavior	5	58	8.6	24	9063	0.3	1.72E-02
GO Biological Process	visual learning	5	58	8.6	21	9063	0.2	9.88E-03
GO Molecular Function	GTP binding	11	62	17.7	291	8588	3.4	6.38E-03
GO Molecular Function	GTPase activity	9	62	14.5	179	8588	2.1	6.69E-03
KEGG pathway	Fc epsilon RI signaling pathway	7	35	20.0	65	3568	1.8	1.85E-03

* Only statistically significant results (P<0.05, Bonferroni correction) were taken into account.

Supplementary Table 5: Alpha-synuclein interactors detected by automated cytoY2H screening.

Alpha-synuclein Clone ID	Interactor Clone ID	Interactor Gene ID	Interactor Gene symbol	result SD4*	result LacZ*	svm score	confidence category	interactor used as
CCSB_6120	CCSB_2783	18	ABAT	1	0	-0,410704	LC	bait
CCSB_6120	CCSB_53447	340273	ABCB5	8	4	-1,018898	LC	bait
CCSB_6120	CCSB_55490	59272	ACE2	7	2	-0,938171	LC	bait
CCSB_6120	CCSB_54434	102	ADAM10	4	3	-1,014101	LC	bait
CCSB_6120	CCSB_1131	134	ADORA1	3	0	-1,021373	LC	bait
CCSB_6120	CCSB_990	135	ADORA2A	8	5	-1,0046	LC	bait
CCSB_6120	IOH34678	148	ADRA1A	11	10	-1,000619	LC	bait
CCSB_6120	CCSB_2935	183	AGT	1	0	-0,995898	LC	bait
CCSB_6120	CCSB_911	79026	AHNAK	10	8	-1,004345	LC	bait
CCSB_6120	RZPDo839G09133	8165	AKAP1	2	0	-0,250973	LC	bait
CCSB_6120	CCSB_11362	57463	AMIGO1	2	3	-0,758206	LC	bait
CCSB_6120	CCSB_14439	56899	ANKS1B	4	0	-1,003422	LC	bait
CCSB_6120	CCSB_158	322	APBB1	1	1	-0,914535	LC	bait
CCSB_6120	CCSB_8253	323	APBB2	3	1	-0,943147	LC	bait
CCSB_6120	CCSB_5494	325	APCS	1	1	-0,992893	LC	bait
CCSB_6120	RZPDo839G0862	348	APOE	8	5	-0,348046	LC	bait
CCSB_6120	CCSB_8905	351	APP	2	1	0,995356	HC	bait
CCSB_6120	CCSB_7128	23237	ARC	2	1	0,263702	HC	bait
CCSB_6120	CCSB_7252	407	ARR3	5	2	-0,15768	LC	bait
CCSB_6120	CCSB_5430	9114	ATP6V0D1	4	0	-1,020262	LC	bait
CCSB_6120	CCSB_53934	6310	ATXN1	6	1	0,940724	HC	bait
CCSB_6120	CCSB_9771	4287	ATXN3	4	0	1,003328	HC	bait
CCSB_6120	CCSB_12286	10134	BCAP31	10	2	-0,988594	LC	bait
CCSB_6120	CCSB_817	590	BCHE	5	1	-0,031829	MC	bait
CCSB_6120	CCSB_11618	10904	BLCAP	10	6	-0,676302	LC	bait
CCSB_6120	CCSB_2289	144577	C12orf66	5	2	0,27575	HC	bait
CCSB_6120	CCSB_52641	145858	C15orf32	3	2	-0,386366	LC	bait
CCSB_6120	RZPDo839F08145	9478	CABP1	1	0	0,267335	HC	bait
CCSB_6120	CCSB_13920	10369	CACNG2	6	1	-1,005345	LC	bait
CCSB_6120	CCSB_11497	23705	CADM1	4	1	-1,00141	LC	bait
CCSB_6120	CCSB_56868	8618	CADPS	4	0	-1,003472	LC	bait
CCSB_6120	CCSB_8036	800	CALD1	4	0	0,957225	HC	bait
CCSB_6120	CCSB_5208	801	CALM1	10	4	1,017961	HC	bait
CCSB_6120	IOH26807	815	CAMK2A	3	0	0,873351	HC	bait
CCSB_6120	CCSB_55907	84433	CARD11	3	2	-1,010258	LC	bait
CCSB_6120	CCSB_3087	857	CAV1	10	10	0,956533	HC	bait
CCSB_6120	CCSB_5458	858	CAV2	8	6	-0,543296	LC	bait
CCSB_6120	CCSB_13831	859	CAV3	9	9	-0,568914	LC	bait
CCSB_6120	CCSB_13792	140689	CBLN4	8	0	-0,971295	LC	bait
CCSB_6120	CCSB_3454	887	CCKBR	5	1	-0,072835	MC	bait
CCSB_6120	CCSB_134	6347	CCL2	8	10	-0,995069	LC	bait
CCSB_6120	CCSB_53008	908	CCT6A	7	2	-0,686289	LC	bait
CCSB_6120	CCSB_1202	9308	CD83	10	8	0,67	HC	bait
CCSB_6120	IOH46767	999	CDH1	1	0	0,706769	HC	bait
CCSB_6120	CCSB_6327	10668	CGRRF1	10	10	-1,01306	LC	bait
CCSB_6120	CCSB_54886	1103	CHAT	2	0	0,278395	HC	bait
CCSB_6120	CCSB_6592	57132	CHMP1B	3	2	-0,991541	LC	bait
CCSB_6120	CCSB_52695	89832	CHRFAM7A	2	1	-0,850194	LC	bait
CCSB_6120	CCSB_4931	1128	CHRM1	4	2	-1,083496	LC	bait

Alpha-synuclein Clone ID	Interactor Clone ID	Interactor Gene ID	Interactor Gene symbol	result SD4*	result LacZ*	svm score	confidence category	interactor used as
CCSB_6120	CCSB_52939	1129	CHRM2	6	3	-0,985633	LC	bait
CCSB_6120	CCSB_14529	1133	CHRM5	10	9	-0,456391	LC	bait
CCSB_6120	CCSB_4938	1134	CHRNA1	1	0	-1,015747	LC	bait
CCSB_6120	CCSB_5038	1136	CHRNA3	1	0	-0,527701	LC	bait
CCSB_6120	CCSB_9943	1139	CHRNA7	8	4	-0,920086	LC	bait
CCSB_6120	CCSB_53694	55584	CHRNA9	0	2	-0,941979	LC	bait
CCSB_6120	CCSB_2938	23563	CHST5	7	6	0,039365	MC	bait
CCSB_6120	CCSB_3245	1364	CLDN4	10	10	0,493374	HC	bait
CCSB_6120	IOH3475	1201	CLN3	6	4	0,221756	HC	bait
CCSB_6120	CCSB_4981	2055	CLN8	9	10	-0,847748	LC	bait
CCSB_6120	CCSB_9334	9746	CLSTN3	3	0	-0,982704	LC	bait
CCSB_6120	CCSB_12415	1266	CNN3	8	2	-0,601444	LC	bait
CCSB_6120	CCSB_2913	4849	CNOT3	3	2	-1,018566	LC	bait
CCSB_6120	CCSB_6772	1267	CNP	5	0	-0,930971	LC	bait
CCSB_6120	CCSB_14013	1269	CNR2	7	8	-0,642884	LC	bait
CCSB_6120	CCSB_8937	22837	COBLL1	10	8	1,041406	HC	bait
CCSB_6120	CCSB_7000	1312	COMT	4	2	-0,688987	LC	bait
CCSB_6120	CCSB_4196	22818	COPZ1	9	2	-0,999349	LC	bait
CCSB_6120	CCSB_3261	10815	CPLX1	9	8	-1,013188	LC	bait
CCSB_6120	CCSB_52634	339302	CPLX4	6	1	-0,894231	LC	bait
CCSB_6120	CCSB_5546	9419	CRIPT	11	5	-0,958966	LC	bait
CCSB_6120	CCSB_10493	1488	CTBP2	2	1	-1,003736	LC	bait
CCSB_6120	CCSB_8750	9265	CYTH3	10	6	-0,39573	LC	bait
CCSB_6120	CCSB_55164	1612	DAPK1	1	2	-1,048715	LC	bait
CCSB_6120	CCSB_6638	64794	DDX31	2	2	-1,007123	LC	bait
CCSB_6120	CCSB_7241	9093	DNAJA3	6	7	-0,991215	LC	bait
CCSB_6120	CCSB_56401	285489	DOK7	4	0	-1,033003	LC	bait
CCSB_6120	CCSB_12017	1808	DPYSL2	0	1	0,89118	HC	bait
CCSB_6120	IOH29556	1812	DRD1	3	0	-1,000793	LC	bait
CCSB_6120	CCSB_6210	1813	DRD2	11	8	0,235772	HC	bait
CCSB_6120	CCSB_56458	1814	DRD3	6	2	-1,025095	LC	bait
CCSB_6120	CCSB_5469	1837	DTNA	2	0	-1,010159	LC	bait
CCSB_6120	CCSB_131	1906	EDN1	6	1	-1,003289	LC	bait
CCSB_6120	CCSB_5440	1908	EDN3	4	0	-0,986871	LC	bait
CCSB_6120	CCSB_2472	1947	EFNB1	4	3	-1,001776	LC	bait
CCSB_6120	CCSB_4131	2026	ENO2	4	1	0,140901	HC	bait
CCSB_6120	CCSB_8949	23085	ERC1	2	0	-1,008968	LC	bait
CCSB_6120	CCSB_7988	2149	F2R	1	0	-0,726189	LC	bait
CCSB_6120	CCSB_3599	23017	FAIM2	6	2	0,119625	HC	bait
CCSB_6120	CCSB_55296	2339	FNTA	2	0	-0,994419	LC	bait
CCSB_6120	CCSB_52942	11337	GABARAP	12	3	-1,048978	LC	bait
CCSB_6120	RZPDo839G1288	2554	GABRA1	4	2	-0,908146	LC	bait
CCSB_6120	CCSB_1265	2555	GABRA2	2	1	-0,510191	LC	bait
CCSB_6120	CCSB_2189	2565	GABRG1	1	0	-1,002344	LC	bait
CCSB_6120	CCSB_8892	2571	GAD1	2	0	-0,74847	LC	bait
CCSB_6120	CCSB_53270	2572	GAD2	6	4	-0,719511	LC	bait
CCSB_6120	CCSB_5146	2596	GAP43	5	0	0,846302	HC	bait
CCSB_6120	CCSB_53548	2644	GCHFR	4	4	0,31929	HC	bait
CCSB_6120	CCSB_13820	2668	GDNF	6	2	-1,045688	LC	bait
CCSB_6120	CCSB_52569	2691	GHRH	2	0	0,82442	HC	bait
CCSB_6120	CCSB_9462	51738	GHRL	2	0	-0,718237	LC	bait

Alpha-synuclein Clone ID	Interactor Clone ID	Interactor Gene ID	Interactor Gene symbol	result SD4*	result LacZ*	svm score	confidence category	interactor used as
CCSB_6120	CCSB_55761	2695	GIP	9	7	-0,698314	LC	bait
CCSB_6120	CCSB_3443	10755	GIPC1	3	4	-0,57304	LC	bait
CCSB_6120	CCSB_10351	2742	GLRA2	2	1	-0,985048	LC	bait
CCSB_6120	CCSB_2154	8001	GLRA3	1	0	-1,024965	LC	bait
CCSB_6120	RZPDo839A0587	2743	GLRB	2	0	-0,053669	MC	bait
CCSB_6120	RZPDo839F0961	10243	GPHN	1	0	-1,00175	LC	bait
CCSB_6120	CCSB_13725	11245	GPR176	8	2	0,325752	HC	bait
CCSB_6120	IOH43140	2892	GRIA3	0	1	-0,493374	LC	bait
CCSB_6120	CCSB_11433	2894	GRID1	3	1	-1,002693	LC	bait
CCSB_6120	CCSB_10903	2905	GRIN2C	2	0	-1,001833	LC	bait
CCSB_6120	RZPDo839H02145	9455	HOMER2	0	1	-0,995975	LC	bait
CCSB_6120	CCSB_7127	9454	HOMER3	4	3	-0,97846	LC	bait
CCSB_6120	CCSB_55795	3351	HTR1B	8	8	-0,882678	LC	bait
CCSB_6120	CCSB_4968	3352	HTR1D	8	4	-1,098997	LC	bait
CCSB_6120	CCSB_14033	3354	HTR1E	8	5	-0,866066	LC	bait
CCSB_6120	CCSB_13946	3356	HTR2A	7	7	-1,000993	LC	bait
CCSB_6120	CCSB_52795	285242	HTR3E	0	1	-0,734364	LC	bait
CCSB_6120	e-HD513-Q49	3064	HTT	5	0	0,95053	HC	bait
CCSB_6120	CCSB_5776	3382	ICA1	4	0	-1,002994	LC	bait
CCSB_6120	CCSB_2465	30819	KCNIP2	1	0	-0,92099	LC	bait
CCSB_6120	CCSB_14834	3778	KCNMA1	10	10	-1,010644	LC	bait
CCSB_6120	CCSB_8836	3785	KCNQ2	2	0	-0,624273	LC	bait
CCSB_6120	CCSB_9186	23095	KIF1B	2	2	-0,611206	LC	bait
CCSB_6120	CCSB_14124	339451	KLHL17	1	0	-1,011773	LC	bait
CCSB_6120	CCSB_3084	3845	KRAS	8	2	0,117514	HC	bait
CCSB_6120	CCSB_56441	8825	LIN7A	6	1	-1,008234	LC	bait
CCSB_6120	LRRK2_WD40_G2385A	120892	LRRK2	1	0	-0,241249	LC	bait
CCSB_6120	RZPDo834D1012D	57692	MAGEE1	2	2	-0,998812	LC	bait
CCSB_6120	CCSB_4497	4128	MAOA	6	2	-0,179949	LC	bait
CCSB_6120	CCSB_12325	4155	MBP	7	5	0,507632	HC	bait
CCSB_6120	CCSB_4817	4359	MPZ	8	4	-0,930915	LC	bait
CCSB_6120	CCSB_389	4504	MT3	8	8	-0,663077	LC	bait
CCSB_6120	CCSB_53052	4593	MUSK	2	0	-0,254735	LC	bait
CCSB_6120	CCSB_7027	4627	MYH9	3	1	-0,233601	LC	bait
CCSB_6120	CCSB_7027	4627	MYH9	1	1	-0,723041	LC	bait
CCSB_6120	CCSB_13986	85366	MYLK2	4	0	-0,991913	LC	bait
CCSB_6120	CCSB_4378	23413	NCS1	8	8	0,138906	HC	bait
CCSB_6120	CCSB_640	10874	NMU	8	8	0,496239	HC	bait
CCSB_6120	CCSB_55955	2831	NPBWR1	4	3	0,151124	HC	bait
CCSB_6120	CCSB_2181	4852	NPY	2	0	-1,028852	LC	bait
CCSB_6120	RZPDo839D0266	1728	NQO1	8	1	0,560762	HC	bait
CCSB_6120	IOH1768	4893	NRAS	3	5	-1,049054	LC	bait
CCSB_6120	CCSB_14205	9369	NRXN3	4	0	-1,036249	LC	bait
CCSB_6120	CCSB_14027	4908	NTF3	0	1	-1,016242	LC	bait
CCSB_6120	CCSB_1017	26747	NUFIP1	2		-1,00238	LC	bait
CCSB_6120	CCSB_15035	5023	P2RX1	9	7	-0,047681	MC	bait
CCSB_6120	CCSB_2686	11315	PARK7	8	6	-1,050887	LC	bait
CCSB_6120	CCSB_3635	26167	PCDHB5	2	0	0,219576	HC	bait
CCSB_6120	IOH45994	27445	PCLO	6	0	-0,958096	LC	bait
CCSB_6120	CCSB_4549	10611	PDLIM5	1	0	-0,070562	MC	bait
CCSB_6120	CCSB_2192	5037	PEBP1	9	5	-0,299641	LC	bait

Alpha-synuclein Clone ID	Interactor Clone ID	Interactor Gene ID	Interactor Gene symbol	result SD4*	result LacZ*	svm score	confidence category	interactor used as
CCSB_6120	RZPDo839E07161	55361	PI4K2A	8	1	-0,785201	LC	bait
CCSB_6120	CCSB_3625	10401	PIAS3	2	0	0,767662	HC	bait
CCSB_6120	RZPDo839C0769	9463	PICK1	1	0	-0,336597	LC	bait
CCSB_6120	IOH45901	65018	PINK1	2	0	0,527092	HC	bait
CCSB_6120	CCSB_1226	9867	PJA2	1	0	-1,006796	LC	bait
CCSB_6120	CCSB_939	26258	PLDN	8	3	-1,027969	LC	bait
CCSB_6120	CCSB_4062	5354	PLP1	1	1	-0,84505	LC	bait
CCSB_6120	RZPDo839C01131	5573	PRKAR1A	2	0	-1,002821	LC	bait
CCSB_6120	CCSB_53590	5588	PRKCQ	2	1	0,433518	HC	bait
CCSB_6120	CCSB_6988	80758	PRR7	4	3	-0,991235	LC	bait
CCSB_6120	CCSB_12041	5723	PSPH	8	4	-1,003379	LC	bait
CCSB_6120	CCSB_669	5743	PTGS2	8	7	-1,003744	LC	bait
CCSB_6120	RZPDo839C1284	5747	PTK2	4	0	0,920059	HC	bait
CCSB_6120	CCSB_14725	5792	PTPRF	1	0	-0,680115	LC	bait
CCSB_6120	CCSB_7602	54899	PXK	1	0	0,468141	HC	bait
CCSB_6120	CCSB_5952	8766	RAB11A	2	4	-1,006104	LC	bait
CCSB_6120	CCSB_5029	51552	RAB14	0	3	-1,002686	LC	bait
CCSB_6120	CCSB_116	116442	RAB39B	6	4	-0,111676	LC	bait
CCSB_6120	CCSB_6933	5864	RAB3A	7	6	-0,615066	LC	bait
CCSB_6120	CCSB_6051	115827	RAB3C	4	2	-1,06559	LC	bait
CCSB_6120	CCSB_339	5868	RAB5A	3	3	-1,01049	LC	bait
CCSB_6120	CCSB_4757	10567	RABAC1	2	2	-0,985633	LC	bait
CCSB_6120	CCSB_3945	5913	RAPSN	0	2	-1,002258	LC	bait
CCSB_6120	CCSB_1177	79608	RIC3	8	4	-0,305601	LC	bait
CCSB_6120	CCSB_3437	9783	RIMS3	6	2	-1,024299	LC	bait
CCSB_6120	CCSB_1249	6014	RIT2	3	0	0,604519	HC	bait
CCSB_6120	CCSB_1095	390	RND3	10	2	-0,410704	LC	bait
CCSB_6120	CCSB_7765	22895	RPH3A	2	0	-0,426095	LC	bait
CCSB_6120	CCSB_6759	6233	RPS27A	2	0	0,990274	HC	bait
CCSB_6120	IOH29907	6198	RPS6KB1	5	0	0,953676	HC	bait
CCSB_6120	GC-T3314	192683	SCAMP5	9	6	0,414726	HC	bait
CCSB_6120	CCSB_7830	6324	SCN1B	6	5	-0,999878	LC	bait
CCSB_6120	CCSB_10158	6327	SCN2B	4	1	-0,915747	LC	bait
CCSB_6120	CCSB_11456	6383	SDC2	8	10	-1,012478	LC	bait
CCSB_6120	CCSB_6231	9672	SDC3	7	0	-0,022252	MC	bait
CCSB_6120	CCSB_53842	6386	SDCBP	3	0	-1,001879	LC	bait
CCSB_6120	CCSB_56122	55964	SEPT3	7	6	-1,007963	LC	bait
CCSB_6120	CCSB_10416	5270	SERPINE2	2	0	-1,022142	LC	bait
CCSB_6120	RZPDo834B0337D	6456	SH3GL2	2	0	-0,102648	LC	bait
CCSB_6120	CCSB_164	30011	SH3KBP1	2	2	1,077647	HC	bait
CCSB_6120	CCSB_53287	6506	SLC1A2	8	10	-0,767426	LC	bait
CCSB_6120	IOH27697	6507	SLC1A3	8	7	-0,349163	LC	bait
CCSB_6120	RZPDo839D0795	6509	SLC1A4	8	8	0,183495	HC	bait
CCSB_6120	CCSB_2046	6511	SLC1A6	6	4	-1,045951	LC	bait
CCSB_6120	CCSB_2862	291	SLC25A4	3	3	-0,94535	LC	bait
CCSB_6120	CCSB_1592	7781	SLC30A3	8	6	-1,033212	LC	bait
CCSB_6120	CCSB_1298	30061	SLC40A1	9	10	-0,497907	LC	bait
CCSB_6120	CCSB_11159	30061	SLC40A1	8	2	-0,497907	LC	bait
CCSB_6120	CCSB_53032	60482	SLC5A7	2	0	-0,187642	LC	bait
CCSB_6120	CCSB_2003	6529	SLC6A1	2	1	-0,605897	LC	bait
CCSB_6120	CCSB_55877	9152	SLC6A5	6	2	-1,03818	LC	bait

Alpha-synuclein Clone ID	Interactor Clone ID	Interactor Gene ID	Interactor Gene symbol	result SD4*	result LacZ*	svm score	confidence category	interactor used as
CCSB_6120	CCSB_31	8773	SNAP23	2	0	-0,727402	LC	bait
CCSB_6120	CCSB_2998	6616	SNAP25	1	0	0,278535	HC	bait
CCSB_6120	CCSB_137	9342	SNAP29	6	5	-1,041102	LC	bait
CCSB_6120	IOH3724	23557	SNAPIN	4	1	-0,936197	LC	bait
CCSB_6120	CCSB_55457	9627	SNCAIP	4	0	0,89511	HC	bait
CCSB_6120	CCSB_7090	6623	SNCG	6	1	1,040861	HC	bait
CCSB_6120	RZPDo839D0195	6640	SNTA1	1	0	0,418845	HC	bait
CCSB_6120	CCSB_12550	8877	SPHK1	1	0	1,011984	HC	bait
CCSB_6120	IOH23273	80725	SRCIN1	4	0	-1,00048	LC	bait
CCSB_6120	RZPDo834H065D	6804	STX1A	2	0	0,952732	HC	bait
CCSB_6120	CCSB_8013	6810	STX4	9	10	-1,016249	LC	bait
CCSB_6120	CCSB_7652	6812	STXBP1	9	5	0,69001	HC	bait
CCSB_6120	CCSB_9546	55530	SVOP	9	8	-0,844135	LC	bait
CCSB_6120	CCSB_56596	81493	SYNC	6	0	-1,015006	LC	bait
CCSB_6120	CCSB_3594	9145	SYNGR1	5	1	-0,36033	LC	bait
CCSB_6120	CCSB_7106	9143	SYNGR3	10	8	0,744878	HC	bait
CCSB_6120	CCSB_1194	132204	SYNPR	8	6	-0,89142	LC	bait
CCSB_6120	CCSB_12265	6855	SYP	4	0	-0,140467	LC	bait
CCSB_6120	CCSB_12111	6856	SYPL1	6	2	-0,399144	LC	bait
CCSB_6120	CCSB_56313	284612	SYPL2	6	3	-0,979847	LC	bait
CCSB_6120	CCSB_52823	341359	SYT10	6	2	-1,057345	LC	bait
CCSB_6120	CCSB_10205	91683	SYT12	4	1	-0,963121	LC	bait
CCSB_6120	CCSB_4387	51760	SYT17	5	2	-1,032746	LC	bait
CCSB_6120	CCSB_2183	84258	SYT3	1	4	-1,005177	LC	bait
CCSB_6120	CCSB_11334	148281	SYT6	8	2	-1,005466	LC	bait
CCSB_6120	CCSB_56795	9066	SYT7	1	0	-0,780968	LC	bait
CCSB_6120	CCSB_11419	143425	SYT9	6	6	-0,890787	LC	bait
CCSB_6120	CCSB_1164	6863	TAC1	4	3	-1,018716	LC	bait
CCSB_6120	IOH1987	6869	TACR1	4	4	-0,61836	LC	bait
CCSB_6120	CCSB_12384	29767	TMOD2	6	3	-0,050922	MC	bait
CCSB_6120	CCSB_10065	7287	TULP1	1	0	-0,663432	LC	bait
CCSB_6120	CCSB_5572	7336	UBE2V2	10	4	-0,998742	LC	bait
CCSB_6120	CCSB_53026	7349	UCN	11	7	-0,764347	LC	bait
CCSB_6120	CCSB_2588	9094	UNC119	1	0	1,080748	HC	bait
CCSB_6120	CCSB_56075	23326	USP22	2	1	-1,000422	LC	bait
CCSB_6120	CCSB_14197	84669	USP32	5	2	-0,810842	LC	bait
CCSB_6120	CCSB_10047	64854	USP46	3	2	-0,650829	LC	bait
CCSB_6120	CCSB_4137	6844	VAMP2	10	10	-1,000298	LC	bait
CCSB_6120	CCSB_5658	9341	VAMP3	11	9	-1,044739	LC	bait
CCSB_6120	CCSB_3756	9217	VAPB	10	10	-1,035497	LC	bait
CCSB_6120	CCSB_5767	7416	VDAC1	4	0	-0,36847	LC	bait
CCSB_6120	CCSB_12645	65125	WNK1	5	2	-0,581595	LC	bait
CCSB_6120	CCSB_8555	57510	XPO5	1	1	-1,044823	LC	bait
CCSB_6120	CCSB_954	10897	YIF1A	10	10	-0,681216	LC	bait
CCSB_6120	IOH4929	7533	YWHAH	2	0	1,054502	HC	bait
CCSB_6120	RZPDo839D10145	7534	YWHAZ	4	1	0,988134	HC	bait
CCSB_6120	CCSB_56012	353174	ZACN	2	0	-0,288462	LC	bait
CCSB_6120	CCSB_56012	353174	ZACN	4	2	-1,044127	LC	bait
CCSB_6120	CCSB_14719	23503	ZFYVE26	6	2	-1,034981	LC	bait
CCSB_6120	CCSB_2656	116225	ZMYND19	8	8	-1,202834	LC	bait
CCSB_6120	CCSB_56668	167465	ZNF366	2	2	0,788919	HC	bait

Alpha-synuclein Clone ID	Interactor Clone ID	Interactor Gene ID	Interactor Gene symbol	result SD4*	result LacZ*	svm score	confidence category	interactor used as
CCSB_6120	CCSB_5214	84937	ZNRF1	6	1	-1,000965	LC	bait
CCSB_6120_A30P	IOH34678	148	ADRA1A	2	0	-1,000619	LC	bait
CCSB_6120_A30P	CCSB_52942	11337	GABARAP	6	0	-1,048978	LC	bait
CCSB_6120_A30P	CCSB_14834	3778	KCNMA1	2	0	-1,010644	LC	bait
CCSB_6120_A30P	CCSB_53026	7349	UCN	8	2	-0,764347	LC	bait
CCSB_6120_A30P	CCSB_5701	9341	VAMP3	8	2	-1,044739	LC	bait
CCSB_6120_E46K	IOH28586	1132	CHRM4	2	2	-1,136012	LC	bait
CCSB_6120_E46K	CCSB_14834	3778	KCNMA1	2	0	-1,010644	LC	bait
CCSB_6120_E46K	CCSB_53026	7349	UCN	2	0	-0,764347	LC	bait
CCSB_6120_E46K	CCSB_5701	9341	VAMP3	8	2	-1,044739	LC	bait
CCSB_6120_A53T	IOH34678	148	ADRA1A	4	0	-1,000619	LC	bait
CCSB_6120_A53T	CCSB_4981	2055	CLN8	4	0	-0,847748	LC	bait
CCSB_6120_A53T	CCSB_5546	9419	CRIPT	6	0	-0,958966	LC	bait
CCSB_6120_A53T	CCSB_52942	11337	GABARAP	8	2	-1,048978	LC	bait
CCSB_6120_A53T	CCSB_55795	3351	HTR1B	2	0	-0,882678	LC	bait
CCSB_6120_A53T	CCSB_14834	3778	KCNMA1	8	2	-1,010644	LC	bait
CCSB_6120_A53T	CCSB_4497	4128	MAOA	2	0	-0,179949	LC	bait
CCSB_6120_A53T	CCSB_2192	5037	PEBP1	2	0	-0,299641	LC	bait
CCSB_6120_A53T	CCSB_116	116442	RAB39B	2	0	-0,111676	LC	bait
CCSB_6120_A53T	CCSB_7830	6324	SCN1B	2	0	-0,999878	LC	bait
CCSB_6120_A53T	CCSB_8013	6810	STX4	2	0	-1,016249	LC	bait
CCSB_6120_A53T	CCSB_9546	55530	SVOP	2	0	-0,844135	LC	bait
CCSB_6120_A53T	CCSB_53026	7349	UCN	8	4	-0,764347	LC	bait
CCSB_6120_A53T	CCSB_4137	6844	VAMP2	6	4	-1,000298	LC	bait
CCSB_6120_A53T	CCSB_5701	9341	VAMP3	8	8	-1,044739	LC	bait

* The sizes of the growing yeast colonies and the size of the blue coloration from the β galactosidase assay were categorized as small, medium or large. 1 point was awarded for a small colony / spot, 2 points for a medium colony / spot and 3 points were awarded for a large colony / spot. For the final “result SD4” or “result lacZ” the points from all four repetitions were added.

Supplementary Table 6: Published alpha-synuclein interactors detected by subSEQ.

Gene symbol	Gene ID	Unique reads	Multi reads
CALM1	801	553	3308
YWHAE	7531	140	0
APP	351	85	340
HSPA1A	3303	55	0
COL25A1	84570	36	48
CNTFR	1271	34	75
YWHAH	7533	24	73
MAPK1	5594	24	45
SYK	6850	24	41
TOR1A	1861	20	25
SLC6A3	6531	16	0
CBX4	8535	13	161
SEPT4	5414	9	14
ASYN	6622	6	15
AKT1	207	6	0
TRAF6	7189	5	3
PSMC3	5702	0	68
KLK6	5653	0	61
TGM2	7052	0	19
MAPT	4137	0	15
SNCB	6620	0	7
SIAH1	6477	0	3
BAD	572	0	3
TPPP	11076	0	2
CYCS	54205	0	2
PLD2	5538	0	2
LAMP2	3920	0	0
PARK7	11315	0	0
YWHAB	7529	0	0
AGRN	375790	0	0
CRYAB	1410	0	0
LRRK2	120892	0	0
MAP1B	4131	0	0
MT-CO3	4514	0	0
PARK2	5071	0	0
PLD1	5337	0	0
PRKCA	5578	0	0
PRKCD	5580	0	0
SNCAIP	9627	0	0
TH	7054	0	0
TUBA1A	7846	0	0

Supplementary Table 7: Alpha-synuclein interactors detected in subSEQ backmating.

Gene symbol	Gene ID	Clone ID	ORF size	result SD4*	result LacZ*	confidence category	Unique reads	Multi reads
AP1S2	8905	CCSB_6745	474	0	0	LC	16342	14451
BCAP31	10134	CCSB_12286	746	5	1	LC	5115	6006
YIF1A	10897	CCSB_954	882	5	5	LC	2348	3374
VAPB	9217	CCSB_3756	732	5	5	LC	1698	1684
TSPAN7	7102	CCSB_1276	750	0	0	LC	837	640
CALM1	805	CCSB_1	450	5	1	HC	553	3308
CALM1	805	CCSB_55519	342	5	1	HC	553	3308
CALM1	805	CCSB_5697	450	5	3	HC	553	3308
ARV1	64801	CCSB_7486	816	0	0	MC	443	227
CD9	928	CCSB_589	687	0	0	HC	373	159
DISP1	84976	CCSB_2971	2754	0	0	HC	204	101
APCS	325	CCSB_5494	672	1	1	LC	126	47
ABCC6	368	CCSB_56869	4512	0	0	HC	120	62
DDX31	64794	CCSB_6638	2025	1	1	LC	112	0
RTN4R	65078	CCSB_6922	1422	0	0	LC	111	147
CCL2	6347	CCSB_134	300	5	1	LC	107	657
COPZ1	22818	CCSB_4196	534	5	1	LC	99	77
FAM133A	286499	CCSB_53675	747	0	0	MC	98	49
HAGH	3029	CCSB_12139	686	0	0	LC	67	84
PADI4	23569	CCSB_8383	1992	0	0	LC	65	0
CNOT3	4849	CCSB_2913	2262	2	1	LC	61	8
RND3	390	CCSB_1095	735	5	1	LC	61	4
TTC12	54970	CCSB_9723	2199	0	0	HC	56	7
CAV1	857	CCSB_3087	537	5	5	HC	47	0
ARAP3	64411	CCSB_9100	225	0	0	LC	46	119
CARD11	84433	CCSB_55907	3444	2	1	LC	40	146
CCDC37	348807	CCSB_52807	1839	0	0	HC	37	0
SIGLEC12	89858	CCSB_10206	1788	0	0	LC	29	6
DAPK1	1612	CCSB_55164	4293	1	1	LC	21	65
UBE2V2	7336	CCSB_5572	438	5	2	LC	20	42
ZFYVE26	23503	CCSB_14719	989	3	1	LC	18	402
ZNF366	167465	CCSB_56668	2235	1	1	HC	18	21
MATR3	9782	CCSB_282	2544	0	0	LC	16	6
APBB1	322	CCSB_158	2127	1	1	LC	15	67
GUCY1B3	2983	CCSB_10584	1865	0	0	LC	13	47
WDR91	29062	CCSB_7808	2244	0	0	LC	12	22
CNN3	1266	CCSB_12415	995	4	1	LC	12	9
MYH9	4627	CCSB_7027	429	1	1	LC	12	0
SLC14A1	6563	IOH26917	1170	0	0	MC	11	19
XRCC5	7520	CCSB_7362	2204	0	0	LC	10	0
FAM160B1	57700	CCSB_2346	2217	0	0	HC	9	3
USP32	84669	CCSB_14197	1178	3	1	LC	8	74
ABCB5	340273	CCSB_53447	2439	4	2	LC	7	72
PRPS2	5634	CCSB_10375	962	0	0	MC	6	13
PRR3	80742	CCSB_54588	567	0	0	LC	6	13
WASL	8976	CCSB_10576	1523	0	0	LC	5	147
SLC17A5	26503	CCSB_483	1488	0	0	LC	5	10
SLC16A10	117247	CCSB_12896	611	0	0	LC	5	4
VAPA	9218	CCSB_3836	729	0	0	LC	5	0
ZKSCAN2	342357	CCSB_56939	2904	0	0	LC	5	0

Supplementary Table 8: Gene-term enrichment analysis of high-confidence interactors.

Source	Gene Category	associated high-confidence interactors	total annotated high-confidence interactors	percentage associated high-confidence interactors [%]	associated potential alpha-synuclein interactors	total annotated potential alpha-synuclein interactors	percentage potential alpha-synuclein interactors [%]	p-value *	percentage published alpha-synuclein interactors [%]
GO Cellular Component	plasma membrane	59	107	55,1	2253	8504	26,5	1,37E-07	-
GO Cellular Component	cytoskeleton	30	107	28,0	922	8504	10,8	3,96E-04	-
GO Cellular Component	neuron projection	21	107	19,6	239	8504	2,8	2,37E-09	28,9
GO Cellular Component	axon	12	107	11,2	110	8504	1,3	2,49E-05	23,7
GO Cellular Component	synapse	37	107	34,6	245	8504	2,9	2,73E-27	-
GO Cellular Component	dendrite	9	107	8,4	119	8504	1,4	2,69E-02	-
GO Cellular Component	cytoplasmic vesicle	21	107	19,6	480	8504	5,6	3,69E-04	-
GO Cellular Component	membrane-bounded vesicle	17	107	15,9	428	8504	5,0	1,74E-02	-
GO Biological Process	cell-cell signaling	30	115	26,1	412	9063	4,5	2,20E-11	26,3
GO Biological Process	trans-mission of nerve impulse	26	115	22,6	227	9063	2,5	5,44E-14	26,3
GO Biological Process	neuron develop-ment	13	115	11,3	216	9063	2,4	2,69E-02	-
GO Biological Process	regulation of neurotrans mitter levels	7	115	6,1	45	9063	0,5	3,16E-02	-
GO Biological Process	regulation of catechol-amine secretion	5	115	4,3	15	9063	0,2	4,82E-02	-
GO Biological Process	behavior	21	115	18,3	321	9063	3,5	4,24E-06	-
GO Biological Process	learning or memory	12	115	10,4	84	9063	0,9	1,12E-05	-
GO Biological Process	regulation of cellular localization	13	115	11,3	188	9063	2,1	6,58E-03	-
GO Molecular Function	calmodulin binding	8	113	7,1	82	8588	1,0	2,96E-02	-

* Only statistically significant results (P<0.05, Bonferroni correction) were taken into account.

Supplementary Table 9: Proteins screened as alpha-synuclein toxicity modifiers.

Modifier symbol (species)	Publ.	study type	effect in study	Gene symbol human ortholog	Gene ID human ortholog	Clone ID human ortholog	interaction with alpha-synuclein identified by	Modifier effect
glo3 (*S. c.*)	[357]	overex	enh	ARFGAP3	26286	CCSB_4400	subSEQ	enh
sec28 (*S. c.*)	[357]	overex	sup	COPE	11316	CCSB_3874	subSEQ	enh
cax4 (*S. c.*)	[357]	overex	enh	DOLPP1	57171	CCSB_14118	subSEQ	enh
ycr026c (*S. c.*)	[356]	del	sup	ENPP5	59084	CCSB_1625	subSEQ	enh
C35D10.2 (*C. e.*)	[358]	RNAi	sup	GIPC1	10755	CCSB_3443	cytoY2H	enh
glo4 (*S. c.*)	[356]	del	sup	HAGH	3029	CCSB_4075	subSEQ	enh
hbs1 (*S. c.*)	[356]	del	sup	HBS1L	10767	CCSB_7461	subSEQ	enh
ime2 (*S. c.*)	[357]	overex	sup	ICK	22858	CCSB_10179	subSEQ	no effect
fzf1 (*S. c.*)	[357]	overex	sup	KLF15	28999	CCSB_9989	Y2H	enh
lit-1 (*C. e.*)	[359]	RNAi	sup	NLK	51701	CCSB_11819	subSEQ	no effect
nrg1 (*S. c.*)	[100]	overex	enh	NRG1	3084	CCSB_8921	subSEQ	enh
pde2 (*S. c.*)	[357]	overex	sup	PDE1C	5137	RZPDo839F07147	subSEQ	enh
pde2 (*S. c.*)	[357]	overex	sup	PDE4C	5143	CCSB_53018	subSEQ	no effect
pde2 (*S. c.*)	[357]	overex	sup	PDE4D	5144	CCSB_2331	subSEQ	enh
pde2 (*S. c.*)	[357]	overex	sup	PDE6B	5158	CCSB_3372	subSEQ	enh
opi3 (*S. c.*)	[356]	del	sup	PEMT	10400	CCSB_11801	subSEQ	enh
pink-1 (*C. e.*)	[358]	RNAi	sup	PINK1	65018	IOH45901	cytoY2H / subSEQ	enh
cup9 (*S. c.*)	[357]	overex	sup	PKNOX1	5316	CCSB_4897	subSEQ	sup
ppz1 / ppz2 (*S. c.*)	[357]	overex	enh	PPP1CA	5499	CCSB_3788	subSEQ	enh
ptk2 (*S. c.*)	[356]	del	sup	PTK2	5747	RZPDo839C1284	cytoY2H / subSEQ	enh
ptp2 (*S. c.*)	[357]	overex	sup	PTPRE	5791	CCSB_10667	subSEQ	enh
ypt1 (*S. c.*)	[357]	overex	sup	RAB13	5872	CCSB_1781	subSEQ	enh
yip3 (*S. c.*)	[357]	overex	enh	RABAC1	10567	CCSB_4757	cytoY2H	enh
rps31 (*S. c.*)	[100]	overex	sup	RPS27A	6233	CCSB_6759	cytoY2H	enh
sec31 (*S. c.*)	[357]	overex	enh	SEC31A	22872	CCSB_14183	subSEQ	no effect
sec31 (*S. c.*)	[357]	overex	enh	SEC31B	25956	CCSB_14168	subSEQ	sup
smf-1 (*C. e.*)	[358]	RNAi	sup	SLC11A2	4891	RZPDo839F09135	subSEQ	sup
sly41 (*S. c.*)	[100] [357]	overex	enh	SLC35E1	79939	RZPDo834H109D	subSEQ	enh
avt4 (*S. c.*)	[357]	overex	sup	SLC36A2	153201	CCSB_52764	subSEQ	enh
dip5 (*S. c.*)	[357]	overex	sup	SLC7A1	6541	CCSB_10890	subSEQ	enh
dip5 (*S. c.*)	[357]	overex	sup	SLC7A14	57709	CCSB_8179	subSEQ	enh
dip5 (*S. c.*)	[357]	overex	sup	SLC7A3	84889	CCSB_9903	subSEQ	enh
erv29 (*S. c.*) / sft-4 (C. e.)	[100] [357] [358]	overex / RNAi	sup	SURF4	6836	CCSB_12591	subSEQ	enh
cup9 (*S. c.*)	[357]	overex	sup	TGIF1	7050	CCSB_2227	subSEQ	enh
ubc-9 (*C. e.*)	[359]	RNAi	sup	UBE2I	7329	CCSB_3129	subSEQ	enh
vps28 (*S. c.*)	[356]	del	sup	VPS28	51160	CCSB_4587	subSEQ	enh
ydr374c (*S. c.*)	[357]	overex	sup	YTHDF3	253943	CCSB_11612	subSEQ	enh

Abbreviations: *S. c.*: *Saccharomyces cerevisiae*; *C. e.*: *Caenorhabditis elegans*; RNAi: RNAi knockdown study in *C. elegans*; overex: yeast overexpression study; del: yeast deletion strain study; sup: suppressor; enh: enhancer; +: increased growth; 0: no influence on growth; -: slightly reduced growth; --: strong growth reduction; ---: marginal or no growth.

Supplementary Table 10: Gene-term enrichment analysis of alpha-synuclein toxicity.

Source	Gene Category	associated toxcitiy modifiers	total annotated toxcitiy modifiers	percentage associated modifiers [%]	associated human proteins	total annotated human proteins	percentage associated human proteins [%]	p-value*
GO Cellular Component	Golgi apparatus	27	154	17,5	872	12782	6,8	3,19E-03
GO Cellular Component	vesicle coat	6	154	3,9	38	12782	0,3	2,03E-02
GO Biological Process	protein transport	30	183	16,4	762	13528	5,6	4,79E-04
GO Biological Process	vesicle-mediated transport	24	183	13,1	576	13528	4,3	4,02E-03
GO Biological Process	energy reserve metabolic process	8	183	4,4	43	13528	0,3	2,10E-03
GO Molecular Function	amino acid transmembrane transporter activity	8	173	4,6	59	12983	0,5	4,23E-03
GO Molecular Function	protein serine/threonine phosphatase activity	7	173	4,0	45	12983	0,3	9,16E-03
KEGG pathway	Purine metabolism	23	91	25,3	153	5085	3,0	5,16E-13
KEGG pathway	Insulin signaling pathway	11	91	12,1	135	5085	2,7	8,73E-03
SP_PIR_ KEYWORDS	ER-golgi transport	11	203	5,4	83	19235	0,4	4,11E-06
SP_PIR_ KEYWORDS	lipid transport	7	203	3,4	62	19235	0,3	1,18E-02
INTERPRO	3'5'-cyclic nucleotide phosphodiesterase	21	202	10,4	21	16659	0,1	1,16E-35
UP_SEQ_ FEATURE	DNA-binding region:Homeobox; TALE-type	8	203	3,9	19	19113	0,1	3,70E-07

Source	Gene Category	associated interacting modifiers	total annotated interacting modifiers	percentage interacting modifiers [%]	associated human proteins	total annotated human proteins	percentage associated human proteins [%]	p-value *
SP_PIR_ KEYWORDS	ER-golgi transport	5	57	8,8	75	13212	0,6	3,94E-02
INTERPRO	3'5'-cyclic nucleotide phosphodiesterase	6	57	10,5	15	11674	0,1	8,33E-07
KEGG pathway	Purine metabolism	6	23	26,1	117	3763	3,1	1,37E-02
GO Molecular Function	amino acid transmembrane transporter activity	5	47	10,6	50	9076	0,6	2,09E-02

* Only statistically significant results (P<0.05, Bonferroni correction) were taken into account.

8 Bibliography

1. Parkinson, J., *An essay on the shaking palsy. 1817.* J Neuropsychiatry Clin Neurosci, 2002. **14**(2): p. 223-36; discussion 222.
2. Koller, W., et al., *Relationship of aging to Parkinson's disease.* Adv Neurol, 1987. **45**: p. 317-21.
3. Samii, A., J.G. Nutt, and B.R. Ransom, *Parkinson's disease.* Lancet, 2004. **363**(9423): p. 1783-93.
4. Gershanik, O.S. and T.G. Nygaard, *Parkinson's disease beginning before age 40.* Adv Neurol, 1990. **53**: p. 251-8.
5. Chaudhuri, K.R. and A.H. Schapira, *Non-motor symptoms of Parkinson's disease: dopaminergic pathophysiology and treatment.* Lancet Neurol, 2009. **8**(5): p. 464-74.
6. Levy, G., *The relationship of Parkinson disease with aging.* Arch Neurol, 2007. **64**(9): p. 1242-6.
7. Lewy, F.H., ed. *Paralysis agitans*. 2 ed. Handbuch der Neurologie, ed. M. Lewandowsky. Vol. I. Pathologische Anatomie. 1912, Springer-Verlag: Berlin. 920–933.
8. Spillantini, M.G., et al., *Alpha-synuclein in Lewy bodies.* Nature, 1997. **388**(6645): p. 839-40.
9. Tretiakoff, C., *Contribution à l'étude de l'anatomie pathologique du locus niger de Soemmering avec quelques deductions relatives à la pathogénie des troubles du tonus muscolaire et de la maladie de Parkinson.*, in *Univ. Paris*. 1919: Paris.
10. Braak, H. and E. Braak, *Pathoanatomy of Parkinson's disease.* J Neurol, 2000. **247 Suppl 2**: p. II3-10.
11. Dickson, D.W., et al., *Hippocampal degeneration differentiates diffuse Lewy body disease (DLBD) from Alzheimer's disease: light and electron microscopic immunocytochemistry of CA2-3 neurites specific to DLBD.* Neurology, 1991. **41**(9): p. 1402-9.
12. Wenning, G.K., I. Litvan, and E. Tolosa, *Milestones in atypical and secondary Parkinsonisms.* Mov Disord, 2011. **26**(6): p. 1083-95.
13. Chinta, S.J. and J.K. Andersen, *Dopaminergic neurons.* Int J Biochem Cell Biol, 2005. **37**(5): p. 942-6.
14. Forno, L.S. and E.C. Alvord, Jr., *Depigmentation in the nerve cells of the substantia nigra and locus ceruleus in Parkinsonism.* Adv Neurol, 1974. **5**: p. 195-202.
15. Dickson, D.W., et al., *Neuropathology of non-motor features of Parkinson disease.* Parkinsonism Relat Disord, 2009. **15 Suppl 3**: p. S1-5.
16. Wolters, E., *Non-motor extranigral signs and symptoms in Parkinson's disease.* Parkinsonism Relat Disord, 2009. **15 Suppl 3**: p. S6-12.
17. Jellinger, K.A., *Neuropathological spectrum of synucleinopathies.* Mov Disord, 2003. **18 Suppl 6**: p. S2-12.
18. Dick, F.D., et al., *Environmental risk factors for Parkinson's disease and parkinsonism: the Geoparkinson study.* Occup Environ Med, 2007. **64**(10): p. 666-72.
19. Frigerio, R., et al., *Chemical exposures and Parkinson's disease: a population-based case-control study.* Mov Disord, 2006. **21**(10): p. 1688-92.
20. Tanner, C.M., et al., *Occupation and risk of parkinsonism: a multicenter case-control study.* Arch Neurol, 2009. **66**(9): p. 1106-13.
21. Betarbet, R., et al., *Chronic systemic pesticide exposure reproduces features of Parkinson's disease.* Nat Neurosci, 2000. **3**(12): p. 1301-6.

22. Norris, E.H., et al., *Pesticide exposure exacerbates alpha-synucleinopathy in an A53T transgenic mouse model.* Am J Pathol, 2007. **170**(2): p. 658-66.
23. Sherer, T.B., et al., *Subcutaneous rotenone exposure causes highly selective dopaminergic degeneration and alpha-synuclein aggregation.* Exp Neurol, 2003. **179**(1): p. 9-16.
24. Davis, G.C., et al., *Chronic Parkinsonism secondary to intravenous injection of meperidine analogues.* Psychiatry Res, 1979. **1**(3): p. 249-54.
25. Langston, J.W., et al., *Chronic Parkinsonism in humans due to a product of meperidine-analog synthesis.* Science, 1983. **219**(4587): p. 979-80.
26. Ayala, A., et al., *Mitochondrial toxins and neurodegenerative diseases.* Front Biosci, 2007. **12**: p. 986-1007.
27. Olanow, C.W. and W.G. Tatton, *Etiology and pathogenesis of Parkinson's disease.* Annu Rev Neurosci, 1999. **22**: p. 123-44.
28. Wood-Kaczmar, A., S. Gandhi, and N.W. Wood, *Understanding the molecular causes of Parkinson's disease.* Trends Mol Med, 2006. **12**(11): p. 521-8.
29. Zhang, Y., et al., *Parkin functions as an E2-dependent ubiquitin- protein ligase and promotes the degradation of the synaptic vesicle-associated protein, CDCrel-1.* Proc Natl Acad Sci U S A, 2000. **97**(24): p. 13354-9.
30. Kitada, T., et al., *Mutations in the parkin gene cause autosomal recessive juvenile parkinsonism.* Nature, 1998. **392**(6676): p. 605-8.
31. Shimura, H., et al., *Familial Parkinson disease gene product, parkin, is a ubiquitin-protein ligase.* Nat Genet, 2000. **25**(3): p. 302-5.
32. Silvestri, L., et al., *Mitochondrial import and enzymatic activity of PINK1 mutants associated to recessive parkinsonism.* Hum Mol Genet, 2005. **14**(22): p. 3477-92.
33. Petit, A., et al., *Wild-type PINK1 prevents basal and induced neuronal apoptosis, a protective effect abrogated by Parkinson disease-related mutations.* J Biol Chem, 2005. **280**(40): p. 34025-32.
34. Bonifati, V., et al., *DJ-1(PARK7), a novel gene for autosomal recessive, early onset parkinsonism.* Neurol Sci, 2003. **24**(3): p. 159-60.
35. Canet-Aviles, R.M., et al., *The Parkinson's disease protein DJ-1 is neuroprotective due to cysteine-sulfinic acid-driven mitochondrial localization.* Proc Natl Acad Sci U S A, 2004. **101**(24): p. 9103-8.
36. Taira, T., et al., *DJ-1 has a role in antioxidative stress to prevent cell death.* EMBO Rep, 2004. **5**(2): p. 213-8.
37. Shendelman, S., et al., *DJ-1 is a redox-dependent molecular chaperone that inhibits alpha-synuclein aggregate formation.* PLoS Biol, 2004. **2**(11): p. e362.
38. Paisan-Ruiz, C., et al., *Cloning of the gene containing mutations that cause PARK8-linked Parkinson's disease.* Neuron, 2004. **44**(4): p. 595-600.
39. Zimprich, A., et al., *Mutations in LRRK2 cause autosomal-dominant parkinsonism with pleomorphic pathology.* Neuron, 2004. **44**(4): p. 601-7.
40. Di Fonzo, A., et al., *A frequent LRRK2 gene mutation associated with autosomal dominant Parkinson's disease.* Lancet, 2005. **365**(9457): p. 412-5.
41. Gilks, W.P., et al., *A common LRRK2 mutation in idiopathic Parkinson's disease.* Lancet, 2005. **365**(9457): p. 415-6.
42. Polymeropoulos, M.H., et al., *Mutation in the alpha-synuclein gene identified in families with Parkinson's disease.* Science, 1997. **276**(5321): p. 2045-7.
43. Kruger, R., et al., *Ala30Pro mutation in the gene encoding alpha-synuclein in Parkinson's disease.* Nat Genet, 1998. **18**(2): p. 106-8.
44. Zarranz, J.J., et al., *The new mutation, E46K, of alpha-synuclein causes Parkinson and Lewy body dementia.* Ann Neurol, 2004. **55**(2): p. 164-73.

45. Chartier-Harlin, M.C., et al., *Alpha-synuclein locus duplication as a cause of familial Parkinson's disease.* Lancet, 2004. **364**(9440): p. 1167-9.
46. Singleton, A.B., et al., *alpha-Synuclein locus triplication causes Parkinson's disease.* Science, 2003. **302**(5646): p. 841.
47. Fuchs, J., et al., *Phenotypic variation in a large Swedish pedigree due to SNCA duplication and triplication.* Neurology, 2007. **68**(12): p. 916-22.
48. Latourelle, J.C., et al., *Genomewide association study for onset age in Parkinson disease.* BMC Med Genet, 2009. **10**: p. 98.
49. Satake, W., et al., *Genome-wide association study identifies common variants at four loci as genetic risk factors for Parkinson's disease.* Nat Genet, 2009. **41**(12): p. 1303-7.
50. Simon-Sanchez, J., et al., *Genome-wide association study reveals genetic risk underlying Parkinson's disease.* Nat Genet, 2009. **41**(12): p. 1308-12.
51. Chiba-Falek, O., G.J. Lopez, and R.L. Nussbaum, *Levels of alpha-synuclein mRNA in sporadic Parkinson disease patients.* Mov Disord, 2006. **21**(10): p. 1703-8.
52. Baba, M., et al., *Aggregation of alpha-synuclein in Lewy bodies of sporadic Parkinson's disease and dementia with Lewy bodies.* Am J Pathol, 1998. **152**(4): p. 879-84.
53. George, J.M., *The synucleins.* Genome Biol, 2002. **3**(1): p. REVIEWS3002.
54. Goedert, M., *Alpha-synuclein and neurodegenerative diseases.* Nat Rev Neurosci, 2001. **2**(7): p. 492-501.
55. Clayton, D.F. and J.M. George, *The synucleins: a family of proteins involved in synaptic function, plasticity, neurodegeneration and disease.* Trends Neurosci, 1998. **21**(6): p. 249-54.
56. Maroteaux, L., J.T. Campanelli, and R.H. Scheller, *Synuclein: a neuron-specific protein localized to the nucleus and presynaptic nerve terminal.* J Neurosci, 1988. **8**(8): p. 2804-15.
57. Ueda, K., et al., *Molecular cloning of cDNA encoding an unrecognized component of amyloid in Alzheimer disease.* Proc Natl Acad Sci U S A, 1993. **90**(23): p. 11282-6.
58. Weinreb, P.H., et al., *NACP, a protein implicated in Alzheimer's disease and learning, is natively unfolded.* Biochemistry, 1996. **35**(43): p. 13709-15.
59. Davidson, W.S., et al., *Stabilization of alpha-synuclein secondary structure upon binding to synthetic membranes.* J Biol Chem, 1998. **273**(16): p. 9443-9.
60. Bodles, A.M., et al., *Identification of the region of non-Abeta component (NAC) of Alzheimer's disease amyloid responsible for its aggregation and toxicity.* J Neurochem, 2001. **78**(2): p. 384-95.
61. Cookson, M.R., *The biochemistry of Parkinson's disease.* Annu Rev Biochem, 2005. **74**: p. 29-52.
62. Beyer, K., *Alpha-synuclein structure, posttranslational modification and alternative splicing as aggregation enhancers.* Acta Neuropathol, 2006. **112**(3): p. 237-51.
63. Kalivendi, S.V., et al., *Oxidants induce alternative splicing of alpha-synuclein: Implications for Parkinson's disease.* Free Radic Biol Med, 2010. **48**(3): p. 377-83.
64. Gosavi, N., et al., *Golgi fragmentation occurs in the cells with prefibrillar alpha-synuclein aggregates and precedes the formation of fibrillar inclusion.* J Biol Chem, 2002. **277**(50): p. 48984-92.
65. Conway, K.A., et al., *Kinetic stabilization of the alpha-synuclein protofibril by a dopamine-alpha-synuclein adduct.* Science, 2001. **294**(5545): p. 1346-9.

66. Conway, K.A., et al., *Acceleration of oligomerization, not fibrillization, is a shared property of both alpha-synuclein mutations linked to early-onset Parkinson's disease: implications for pathogenesis and therapy.* Proc Natl Acad Sci U S A, 2000. **97**(2): p. 571-6.
67. Dev, K.K., et al., *Part II: alpha-synuclein and its molecular pathophysiological role in neurodegenerative disease.* Neuropharmacology, 2003. **45**(1): p. 14-44.
68. Caughey, B. and P.T. Lansbury, *Protofibrils, pores, fibrils, and neurodegeneration: separating the responsible protein aggregates from the innocent bystanders.* Annu Rev Neurosci, 2003. **26**: p. 267-98.
69. Masliah, E., et al., *Dopaminergic loss and inclusion body formation in alpha-synuclein mice: implications for neurodegenerative disorders.* Science, 2000. **287**(5456): p. 1265-9.
70. Sharon, R., et al., *The formation of highly soluble oligomers of alpha-synuclein is regulated by fatty acids and enhanced in Parkinson's disease.* Neuron, 2003. **37**(4): p. 583-95.
71. Fredenburg, R.A., et al., *The impact of the E46K mutation on the properties of alpha-synuclein in its monomeric and oligomeric states.* Biochemistry, 2007. **46**(24): p. 7107-18.
72. Fujiwara, H., et al., *alpha-Synuclein is phosphorylated in synucleinopathy lesions.* Nat Cell Biol, 2002. **4**(2): p. 160-4.
73. Hashimoto, M., et al., *Oxidative stress induces amyloid-like aggregate formation of NACP/alpha-synuclein in vitro.* Neuroreport, 1999. **10**(4): p. 717-21.
74. Giasson, B.I., et al., *Oxidative damage linked to neurodegeneration by selective alpha-synuclein nitration in synucleinopathy lesions.* Science, 2000. **290**(5493): p. 985-9.
75. Uversky, V.N., *Neuropathology, biochemistry, and biophysics of alpha-synuclein aggregation.* J Neurochem, 2007. **103**(1): p. 17-37.
76. Kim, T.D., S.R. Paik, and C.H. Yang, *Structural and functional implications of C-terminal regions of alpha-synuclein.* Biochemistry, 2002. **41**(46): p. 13782-90.
77. Paxinou, E., et al., *Induction of alpha-synuclein aggregation by intracellular nitrative insult.* J Neurosci, 2001. **21**(20): p. 8053-61.
78. Webb, J.L., et al., *Alpha-Synuclein is degraded by both autophagy and the proteasome.* J Biol Chem, 2003. **278**(27): p. 25009-13.
79. Cuervo, A.M., et al., *Impaired degradation of mutant alpha-synuclein by chaperone-mediated autophagy.* Science, 2004. **305**(5688): p. 1292-5.
80. Lee, H.J., et al., *Clearance of alpha-synuclein oligomeric intermediates via the lysosomal degradation pathway.* J Neurosci, 2004. **24**(8): p. 1888-96.
81. Vogiatzi, T., et al., *Wild type alpha-synuclein is degraded by chaperone-mediated autophagy and macroautophagy in neuronal cells.* J Biol Chem, 2008. **283**(35): p. 23542-56.
82. Mak, S.K., et al., *Lysosomal degradation of alpha-synuclein in vivo.* J Biol Chem, 2010. **285**(18): p. 13621-9.
83. Tofaris, G.K., R. Layfield, and M.G. Spillantini, *alpha-synuclein metabolism and aggregation is linked to ubiquitin-independent degradation by the proteasome.* FEBS Lett, 2001. **509**(1): p. 22-6.
84. Nemani, V.M., et al., *Increased expression of alpha-synuclein reduces neurotransmitter release by inhibiting synaptic vesicle reclustering after endocytosis.* Neuron, 2010. **65**(1): p. 66-79.

85. Garcia-Reitbock, P., et al., *SNARE protein redistribution and synaptic failure in a transgenic mouse model of Parkinson's disease.* Brain, 2010. **133**(Pt 7): p. 2032-44.
86. Scott, D.A., et al., *A pathologic cascade leading to synaptic dysfunction in alpha-synuclein-induced neurodegeneration.* J Neurosci, 2010. **30**(24): p. 8083-95.
87. Alim, M.A., et al., *Demonstration of a role for alpha-synuclein as a functional microtubule-associated protein.* J Alzheimers Dis, 2004. **6**(4): p. 435-42; discussion 443-9.
88. Zhou, R.M., et al., *Molecular interaction of alpha-synuclein with tubulin influences on the polymerization of microtubule in vitro and structure of microtubule in cells.* Mol Biol Rep, 2010. **37**(7): p. 3183-92.
89. Stefanis, L., et al., *Expression of A53T mutant but not wild-type alpha-synuclein in PC12 cells induces alterations of the ubiquitin-dependent degradation system, loss of dopamine release, and autophagic cell death.* J Neurosci, 2001. **21**(24): p. 9549-60.
90. Tanaka, Y., et al., *Inducible expression of mutant alpha-synuclein decreases proteasome activity and increases sensitivity to mitochondria-dependent apoptosis.* Hum Mol Genet, 2001. **10**(9): p. 919-26.
91. Petrucelli, L., et al., *Parkin protects against the toxicity associated with mutant alpha-synuclein: proteasome dysfunction selectively affects catecholaminergic neurons.* Neuron, 2002. **36**(6): p. 1007-19.
92. Snyder, H., et al., *Aggregated and monomeric alpha-synuclein bind to the S6' proteasomal protein and inhibit proteasomal function.* J Biol Chem, 2003. **278**(14): p. 11753-9.
93. Xilouri, M., et al., *Abberant alpha-synuclein confers toxicity to neurons in part through inhibition of chaperone-mediated autophagy.* PLoS One, 2009. **4**(5): p. e5515.
94. Alvarez-Erviti, L., et al., *Chaperone-mediated autophagy markers in Parkinson disease brains.* Arch Neurol, 2010. **67**(12): p. 1464-72.
95. Li, W.W., et al., *Localization of alpha-synuclein to mitochondria within midbrain of mice.* Neuroreport, 2007. **18**(15): p. 1543-6.
96. Devi, L., et al., *Mitochondrial import and accumulation of alpha-synuclein impair complex I in human dopaminergic neuronal cultures and Parkinson disease brain.* J Biol Chem, 2008. **283**(14): p. 9089-100.
97. Loeb, V., et al., *The transgenic overexpression of alpha-synuclein and not its related pathology associates with complex I inhibition.* J Biol Chem, 2010. **285**(10): p. 7334-43.
98. Martin, L.J., et al., *Parkinson's disease alpha-synuclein transgenic mice develop neuronal mitochondrial degeneration and cell death.* J Neurosci, 2006. **26**(1): p. 41-50.
99. Hsu, L.J., et al., *alpha-synuclein promotes mitochondrial deficit and oxidative stress.* Am J Pathol, 2000. **157**(2): p. 401-10.
100. Cooper, A.A., et al., *Alpha-synuclein blocks ER-Golgi traffic and Rab1 rescues neuron loss in Parkinson's models.* Science, 2006. **313**(5785): p. 324-8.
101. Gitler, A.D., et al., *The Parkinson's disease protein alpha-synuclein disrupts cellular Rab homeostasis.* Proc Natl Acad Sci U S A, 2008. **105**(1): p. 145-50.
102. Thayanidhi, N., et al., *Alpha-synuclein delays endoplasmic reticulum (ER)-to-Golgi transport in mammalian cells by antagonizing ER/Golgi SNAREs.* Mol Biol Cell, 2010. **21**(11): p. 1850-63.

103. Kontopoulos, E., J.D. Parvin, and M.B. Feany, *α-synuclein acts in the nucleus to inhibit histone acetylation and promote neurotoxicity.* Human Molecular Genetics, 2006. **15**(20): p. 3012-3023.
104. Bove, J., et al., *Toxin-induced models of Parkinson's disease.* NeuroRx, 2005. **2**(3): p. 484-94.
105. Terzioglu, M. and D. Galter, *Parkinson's disease: genetic versus toxin-induced rodent models.* FEBS J, 2008. **275**(7): p. 1384-91.
106. Falkenburger, B.H. and J.B. Schulz, *Limitations of cellular models in Parkinson's disease research.* J Neural Transm Suppl, 2006(70): p. 261-8.
107. Devine, M.J., et al., *Parkinson's disease induced pluripotent stem cells with triplication of the alpha-synuclein locus.* Nat Commun, 2011. **2**: p. 440.
108. Outeiro, T.F. and S. Lindquist, *Yeast cells provide insight into alpha-synuclein biology and pathobiology.* Science, 2003. **302**(5651): p. 1772-5.
109. Feany, M.B. and W.W. Bender, *A Drosophila model of Parkinson's disease.* Nature, 2000. **404**(6776): p. 394-8.
110. Lakso, M., et al., *Dopaminergic neuronal loss and motor deficits in Caenorhabditis elegans overexpressing human alpha-synuclein.* J Neurochem, 2003. **86**(1): p. 165-72.
111. Matsuoka, Y., et al., *Lack of nigral pathology in transgenic mice expressing human alpha-synuclein driven by the tyrosine hydroxylase promoter.* Neurobiol Dis, 2001. **8**(3): p. 535-9.
112. Kirik, D., et al., *Parkinson-like neurodegeneration induced by targeted overexpression of alpha-synuclein in the nigrostriatal system.* J Neurosci, 2002. **22**(7): p. 2780-91.
113. Perez, R.G., et al., *A role for alpha-synuclein in the regulation of dopamine biosynthesis.* J Neurosci, 2002. **22**(8): p. 3090-9.
114. Liu, D., et al., *Silencing alpha-synuclein gene expression enhances tyrosine hydroxylase activity in MN9D cells.* Neurochem Res, 2008. **33**(7): p. 1401-9.
115. Peng, X., et al., *Alpha-synuclein activation of protein phosphatase 2A reduces tyrosine hydroxylase phosphorylation in dopaminergic cells.* J Cell Sci, 2005. **118**(Pt 15): p. 3523-30.
116. Engelender, S., et al., *Synphilin-1 associates with alpha-synuclein and promotes the formation of cytosolic inclusions.* Nat Genet, 1999. **22**(1): p. 110-4.
117. Smith, W.W., et al., *Synphilin-1 attenuates neuronal degeneration in the A53T alpha-synuclein transgenic mouse model.* Hum Mol Genet, 2010. **19**(11): p. 2087-98.
118. Lee, J.T., et al., *Ubiquitination of alpha-synuclein by Siah-1 promotes alpha-synuclein aggregation and apoptotic cell death.* Hum Mol Genet, 2008. **17**(6): p. 906-17.
119. Fields, S. and O. Song, *A novel genetic system to detect protein-protein interactions.* Nature, 1989. **340**(6230): p. 245-6.
120. Worseck, J.M., et al., *A stringent yeast two-hybrid matrix screening approach for protein-protein interaction discovery.* Methods Mol Biol, 2012. **812**: p. 63-87.
121. Ito, T., et al., *A comprehensive two-hybrid analysis to explore the yeast protein interactome.* Proc Natl Acad Sci U S A, 2001. **98**(8): p. 4569-74.
122. Li, S., et al., *A map of the interactome network of the metazoan C. elegans.* Science, 2004. **303**(5657): p. 540-3.
123. Giot, L., et al., *A protein interaction map of Drosophila melanogaster.* Science, 2003. **302**(5651): p. 1727-36.

124. Goehler, H., et al., *A protein interaction network links GIT1, an enhancer of huntingtin aggregation, to Huntington's disease.* Mol Cell, 2004. **15**(6): p. 853-65.
125. Stelzl, U., et al., *A human protein-protein interaction network: a resource for annotating the proteome.* Cell, 2005. **122**(6): p. 957-68.
126. Rual, J.F., et al., *Towards a proteome-scale map of the human protein-protein interaction network.* Nature, 2005. **437**(7062): p. 1173-8.
127. Vinayagam, A., et al., *A directed protein interaction network for investigating intracellular signal transduction.* Sci Signal, 2011. **4**(189): p. rs8.
128. Mrowka, R., A. Patzak, and H. Herzel, *Is there a bias in proteome research?* Genome Res, 2001. **11**(12): p. 1971-3.
129. von Mering, C., et al., *Comparative assessment of large-scale data sets of protein-protein interactions.* Nature, 2002. **417**(6887): p. 399-403.
130. Stagljar, I. and S. Fields, *Analysis of membrane protein interactions using yeast-based technologies.* Trends Biochem Sci, 2002. **27**(11): p. 559-63.
131. Johnsson, N. and A. Varshavsky, *Split ubiquitin as a sensor of protein interactions in vivo.* Proc Natl Acad Sci U S A, 1994. **91**(22): p. 10340-4.
132. Ozkaynak, E., D. Finley, and A. Varshavsky, *The yeast ubiquitin gene: head-to-tail repeats encoding a polyubiquitin precursor protein.* Nature, 1984. **312**(5995): p. 663-6.
133. Hochstrasser, M., *Ubiquitin-dependent protein degradation.* Annu Rev Genet, 1996. **30**: p. 405-39.
134. Thrower, J.S., et al., *Recognition of the polyubiquitin proteolytic signal.* EMBO J, 2000. **19**(1): p. 94-102.
135. Hershko, A. and A. Ciechanover, *The ubiquitin system for protein degradation.* Annu Rev Biochem, 1992. **61**: p. 761-807.
136. Stagljar, I., et al., *A genetic system based on split-ubiquitin for the analysis of interactions between membrane proteins in vivo.* Proc Natl Acad Sci U S A, 1998. **95**(9): p. 5187-92.
137. Iyer, K., et al., *Utilizing the split-ubiquitin membrane yeast two-hybrid system to identify protein-protein interactions of integral membrane proteins.* Sci STKE, 2005. **2005**(275): p. pl3.
138. Paumi, C.M., et al., *Mapping protein-protein interactions for the yeast ABC transporter Ycf1p by integrated split-ubiquitin membrane yeast two-hybrid analysis.* Mol Cell, 2007. **26**(1): p. 15-25.
139. Schulze, W.X., et al., *Interactions between co-expressed Arabidopsis sucrose transporters in the split-ubiquitin system.* BMC Biochem, 2003. **4**: p. 3.
140. Gisler, S.M., et al., *Monitoring protein-protein interactions between the mammalian integral membrane transporters and PDZ-interacting partners using a modified split-ubiquitin membrane yeast two-hybrid system.* Mol Cell Proteomics, 2008. **7**(7): p. 1362-77.
141. Mockli, N., et al., *Yeast split-ubiquitin-based cytosolic screening system to detect interactions between transcriptionally active proteins.* Biotechniques, 2007. **42**(6): p. 725-30.
142. Rigaut, G., et al., *A generic protein purification method for protein complex characterization and proteome exploration.* Nat Biotechnol, 1999. **17**(10): p. 1030-2.
143. Gavin, A.C., et al., *Functional organization of the yeast proteome by systematic analysis of protein complexes.* Nature, 2002. **415**(6868): p. 141-7.
144. Gregan, J., et al., *Tandem affinity purification of functional TAP-tagged proteins from human cells.* Nat Protoc, 2007. **2**(5): p. 1145-51.

145. Forler, D., et al., *An efficient protein complex purification method for functional proteomics in higher eukaryotes.* Nat Biotechnol, 2003. **21**(1): p. 89-92.
146. Rohila, J.S., et al., *Improved tandem affinity purification tag and methods for isolation of protein heterocomplexes from plants.* Plant J, 2004. **38**(1): p. 172-81.
147. Gully, D., et al., *New partners of acyl carrier protein detected in Escherichia coli by tandem affinity purification.* FEBS Lett, 2003. **548**(1-3): p. 90-6.
148. Piehler, J., *New methodologies for measuring protein interactions in vivo and in vitro.* Curr Opin Struct Biol, 2005. **15**(1): p. 4-14.
149. Barrios-Rodiles, M., et al., *High-throughput mapping of a dynamic signaling network in mammalian cells.* Science, 2005. **307**(5715): p. 1621-5.
150. Miller, B.W., et al., *Application of an integrated physical and functional screening approach to identify inhibitors of the Wnt pathway.* Mol Syst Biol, 2009. **5**: p. 315.
151. Pfefferle, S., et al., *The SARS-coronavirus-host interactome: identification of cyclophilins as target for pan-coronavirus inhibitors.* PLoS Pathog, 2011. **7**(10): p. e1002331.
152. Vizoso Pinto, M.G., et al., *LuMPIS--a modified luminescence-based mammalian interactome mapping pull-down assay for the investigation of protein-protein interactions encoded by GC-low ORFs.* Proteomics, 2009. **9**(23): p. 5303-8.
153. Palidwor, G.A., et al., *Detection of alpha-rod protein repeats using a neural network and application to huntingtin.* PLoS Comput Biol, 2009. **5**(3): p. e1000304.
154. Gietz, R.D. and R.A. Woods, *Transformation of yeast by lithium acetate/single-stranded carrier DNA/polyethylene glycol method.* Methods Enzymol, 2002. **350**: p. 87-96.
155. Kiernan, J.A., *Indigogenic substrates for detection and localization of enzymes.* Biotech Histochem, 2007. **82**(2): p. 73-103.
156. Ma, H., et al., *Plasmid construction by homologous recombination in yeast.* Gene, 1987. **58**(2-3): p. 201-16.
157. Boussif, O., et al., *A versatile vector for gene and oligonucleotide transfer into cells in culture and in vivo: polyethylenimine.* Proc Natl Acad Sci U S A, 1995. **92**(16): p. 7297-301.
158. Keshava Prasad, T.S., et al., *Human Protein Reference Database--2009 update.* Nucleic Acids Res, 2009. **37**(Database issue): p. D767-72.
159. Chaurasia, G., et al., *UniHI: an entry gate to the human protein interactome.* Nucleic Acids Res, 2007. **35**(Database issue): p. D590-4.
160. Ceol, A., et al., *MINT, the molecular interaction database: 2009 update.* Nucleic Acids Res, 2010. **38**(Database issue): p. D532-9.
161. Salwinski, L., et al., *The Database of Interacting Proteins: 2004 update.* Nucleic Acids Res, 2004. **32**(Database issue): p. D449-51.
162. Huang da, W., B.T. Sherman, and R.A. Lempicki, *Systematic and integrative analysis of large gene lists using DAVID bioinformatics resources.* Nat Protoc, 2009. **4**(1): p. 44-57.
163. Huang da, W., B.T. Sherman, and R.A. Lempicki, *Bioinformatics enrichment tools: paths toward the comprehensive functional analysis of large gene lists.* Nucleic Acids Res, 2009. **37**(1): p. 1-13.
164. Schlicker, A., T. Lengauer, and M. Albrecht, *Improving disease gene prioritization using the semantic similarity of Gene Ontology terms.* Bioinformatics, 2010. **26**(18): p. i561-7.

165. Yellaboina, S., et al., *DOMINE: a comprehensive collection of known and predicted domain-domain interactions.* Nucleic Acids Res, 2011. **39**(Database issue): p. D730-5.
166. Su, A.I., et al., *A gene atlas of the mouse and human protein-encoding transcriptomes.* Proc Natl Acad Sci U S A, 2004. **101**(16): p. 6062-7.
167. Langfelder, P. and S. Horvath, *WGCNA: an R package for weighted correlation network analysis.* BMC Bioinformatics, 2008. **9**: p. 559.
168. Zhang, B. and S. Horvath, *A general framework for weighted gene co-expression network analysis.* Stat Appl Genet Mol Biol, 2005. **4**: p. Article17.
169. Brown, K.R. and I. Jurisica, *Online predicted human interaction database.* Bioinformatics, 2005. **21**(9): p. 2076-82.
170. Lehner, B. and A.G. Fraser, *A first-draft human protein-interaction map.* Genome Biol, 2004. **5**(9): p. R63.
171. Schaefer, M.H., et al., *HIPPIE: Integrating Protein Interaction Networks with Experiment Based Quality Scores.* PLoS One, 2012. **7**(2): p. e31826.
172. Chang, C. and C. Lin, *LIBSVM: A library for support vector machines.* ACM Trans. Intell. Syst. Technol., 2011. **2**(3).
173. Pruitt, K.D., et al., *NCBI Reference Sequences: current status, policy and new initiatives.* Nucleic Acids Res, 2009. **37**(Database issue): p. D32-6.
174. Alibes, A., et al., *IDconverter and IDClight: conversion and annotation of gene and protein IDs.* BMC Bioinformatics, 2007. **8**: p. 9.
175. Hashimoto, M., et al., *alpha-Synuclein protects against oxidative stress via inactivation of the c-Jun N-terminal kinase stress-signaling pathway in neuronal cells.* J Biol Chem, 2002. **277**(13): p. 11465-72.
176. Nagano, Y., et al., *Lack of binding observed between human alpha-synuclein and Bcl-2 protein family.* Neurosci Lett, 2001. **316**(2): p. 103-7.
177. Ostrerova, N., et al., *alpha-Synuclein shares physical and functional homology with 14-3-3 proteins.* J Neurosci, 1999. **19**(14): p. 5782-91.
178. Kaul, S., et al., *Wild-type alpha-synuclein interacts with pro-apoptotic proteins PKCdelta and BAD to protect dopaminergic neuronal cells against MPP+-induced apoptotic cell death.* Brain Res Mol Brain Res, 2005. **139**(1): p. 137-52.
179. Curtin, F. and P. Schulz, *Multiple correlations and Bonferroni's correction.* Biol Psychiatry, 1998. **44**(8): p. 775-7.
180. Vila, M. and S. Przedborski, *Targeting programmed cell death in neurodegenerative diseases.* Nat Rev Neurosci, 2003. **4**(5): p. 365-75.
181. Hornykiewicz, O. and S.J. Kish, *Biochemical pathophysiology of Parkinson's disease.* Adv Neurol, 1987. **45**: p. 19-34.
182. Payton, J.E., et al., *Protein-protein interactions of alpha-synuclein in brain homogenates and transfected cells.* Brain Res Mol Brain Res, 2001. **95**(1-2): p. 138-45.
183. Alim, M.A., et al., *Tubulin seeds alpha-synuclein fibril formation.* J Biol Chem, 2002. **277**(3): p. 2112-7.
184. Trojanowski, J.Q., et al., *Fatal attractions: abnormal protein aggregation and neuron death in Parkinson's disease and Lewy body dementia.* Cell Death Differ, 1998. **5**(10): p. 832-7.
185. Zweifel, L.S., R. Kuruvilla, and D.D. Ginty, *Functions and mechanisms of retrograde neurotrophin signalling.* Nat Rev Neurosci, 2005. **6**(8): p. 615-25.
186. Dawbarn, D. and S.J. Allen, *Neurotrophins and neurodegeneration.* Neuropathol Appl Neurobiol, 2003. **29**(3): p. 211-30.

187. Groves, E., et al., *Molecular mechanisms of phagocytic uptake in mammalian cells.* Cell Mol Life Sci, 2008. **65**(13): p. 1957-76.
188. McGeer, P.L., et al., *Reactive microglia are positive for HLA-DR in the substantia nigra of Parkinson's and Alzheimer's disease brains.* Neurology, 1988. **38**(8): p. 1285-91.
189. Sauer, H. and W.H. Oertel, *Progressive degeneration of nigrostriatal dopamine neurons following intrastriatal terminal lesions with 6-hydroxydopamine: a combined retrograde tracing and immunocytochemical study in the rat.* Neuroscience, 1994. **59**(2): p. 401-15.
190. Lee, C.S., H. Sauer, and A. Bjorklund, *Dopaminergic neuronal degeneration and motor impairments following axon terminal lesion by instrastriatal 6-hydroxydopamine in the rat.* Neuroscience, 1996. **72**(3): p. 641-53.
191. Carbon, S., et al., *AmiGO: online access to ontology and annotation data.* Bioinformatics, 2009. **25**(2): p. 288-9.
192. Lotharius, J. and P. Brundin, *Pathogenesis of Parkinson's disease: dopamine, vesicles and alpha-synuclein.* Nat Rev Neurosci, 2002. **3**(12): p. 932-42.
193. Bruckner, A., et al., *Yeast two-hybrid, a powerful tool for systems biology.* Int J Mol Sci, 2009. **10**(6): p. 2763-88.
194. Estojak, J., R. Brent, and E.A. Golemis, *Correlation of two-hybrid affinity data with in vitro measurements.* Mol Cell Biol, 1995. **15**(10): p. 5820-9.
195. Vinayagam, A., U. Stelzl, and E. Wanker, *Repeated two-hybrid screening detects transient protein–protein interactions.* Theoretical Chemistry Accounts: Theory, Computation, and Modeling (Theoretica Chimica Acta), 2010. **125**(3): p. 613-619.
196. Miller, D.W., et al., *Alpha-synuclein in blood and brain from familial Parkinson disease with SNCA locus triplication.* Neurology, 2004. **62**(10): p. 1835-8.
197. Fletcher, D.A. and R.D. Mullins, *Cell mechanics and the cytoskeleton.* Nature, 2010. **463**(7280): p. 485-92.
198. McMurray, C.T., *Neurodegeneration: diseases of the cytoskeleton?* Cell Death Differ, 2000. **7**(10): p. 861-5.
199. Perier, C., J. Bove, and M. Vila, *Mitochondria and Programmed Cell Death in Parkinson's Disease: Apoptosis and Beyond.* Antioxid Redox Signal, 2011.
200. Hoglinger, G.U., et al., *Dopamine depletion impairs precursor cell proliferation in Parkinson disease.* Nat Neurosci, 2004. **7**(7): p. 726-35.
201. Halliwell, B., *Reactive Oxygen Species and the Central Nervous System.* Journal of Neurochemistry, 1992. **59**(5): p. 1609-1623.
202. Bonini, N.M. and B.I. Giasson, *Snaring the function of alpha-synuclein.* Cell, 2005. **123**(3): p. 359-61.
203. Cabin, D.E., et al., *Synaptic vesicle depletion correlates with attenuated synaptic responses to prolonged repetitive stimulation in mice lacking alpha-synuclein.* J Neurosci, 2002. **22**(20): p. 8797-807.
204. Bienenstock, J., et al., *Mast cell involvement in various inflammatory processes.* Am Rev Respir Dis, 1987. **135**(6 Pt 2): p. S5-8.
205. Tuncel, N., et al., *Brain mast cells and therapeutic potential of vasoactive intestinal peptide in a Parkinson's disease model in rats: brain microdialysis, behavior, and microscopy.* Peptides, 2005. **26**(5): p. 827-36.
206. Vukosavic, S., et al., *Bax and Bcl-2 interaction in a transgenic mouse model of familial amyotrophic lateral sclerosis.* J Neurochem, 1999. **73**(6): p. 2460-8.
207. Gonzalez de Aguilar, J.L., et al., *Alteration of the Bcl-x/Bax ratio in a transgenic mouse model of amyotrophic lateral sclerosis: evidence for the implication of the p53 signaling pathway.* Neurobiol Dis, 2000. **7**(4): p. 406-15.

208. Zhu, S., et al., *Minocycline inhibits cytochrome c release and delays progression of amyotrophic lateral sclerosis in mice.* Nature, 2002. **417**(6884): p. 74-8.
209. *A novel gene containing a trinucleotide repeat that is expanded and unstable on Huntington's disease chromosomes. The Huntington's Disease Collaborative Research Group.* Cell, 1993. **72**(6): p. 971-83.
210. Teles, A.V., et al., *Increase in bax expression and apoptosis are associated in Huntington's disease progression.* Neurosci Lett, 2008. **438**(1): p. 59-63.
211. Wang, X., et al., *Inhibitors of cytochrome c release with therapeutic potential for Huntington's disease.* J Neurosci, 2008. **28**(38): p. 9473-85.
212. Lesort, M., et al., *Tissue transglutaminase is increased in Huntington's disease brain.* J Neurochem, 1999. **73**(5): p. 2018-27.
213. Orr, H.T., et al., *Expansion of an unstable trinucleotide CAG repeat in spinocerebellar ataxia type 1.* Nat Genet, 1993. **4**(3): p. 221-6.
214. Takiyama, Y., et al., *The gene for Machado-Joseph disease maps to human chromosome 14q.* Nat Genet, 1993. **4**(3): p. 300-4.
215. Mouillet-Richard, S., et al., *Signal transduction through prion protein.* Science, 2000. **289**(5486): p. 1925-8.
216. Kang, J., et al., *The precursor of Alzheimer's disease amyloid A4 protein resembles a cell-surface receptor.* Nature, 1987. **325**(6106): p. 733-6.
217. O'Day, D.H. and M.A. Myre, *Calmodulin-binding domains in Alzheimer's disease proteins: extending the calcium hypothesis.* Biochem Biophys Res Commun, 2004. **320**(4): p. 1051-4.
218. Nixon, R.A., *The calpains in aging and aging-related diseases.* Ageing Res Rev, 2003. **2**(4): p. 407-18.
219. Ballatore, C., V.M. Lee, and J.Q. Trojanowski, *Tau-mediated neurodegeneration in Alzheimer's disease and related disorders.* Nat Rev Neurosci, 2007. **8**(9): p. 663-72.
220. Ross, C.A. and M.A. Poirier, *Protein aggregation and neurodegenerative disease.* Nat Med, 2004. **10 Suppl**: p. S10-7.
221. McGrath, J.P., et al., *Structure and organization of the human Ki-ras proto-oncogene and a related processed pseudogene.* Nature, 1983. **304**(5926): p. 501-6.
222. Carpten, J.D., et al., *A transforming mutation in the pleckstrin homology domain of AKT1 in cancer.* Nature, 2007. **448**(7152): p. 439-44.
223. Degenhardt, K., et al., *BAX and BAK mediate p53-independent suppression of tumorigenesis.* Cancer Cell, 2002. **2**(3): p. 193-203.
224. Boise, L.H., et al., *bcl-x, a bcl-2-related gene that functions as a dominant regulator of apoptotic cell death.* Cell, 1993. **74**(4): p. 597-608.
225. Vaughn, A.E. and M. Deshmukh, *Glucose metabolism inhibits apoptosis in neurons and cancer cells by redox inactivation of cytochrome c.* Nat Cell Biol, 2008. **10**(12): p. 1477-83.
226. Lacal, J.C., P.S. Anderson, and S.A. Aaronson, *Deletion mutants of Harvey ras p21 protein reveal the absolute requirement of at least two distant regions for GTP-binding and transforming activities.* EMBO J, 1986. **5**(4): p. 679-87.
227. Li, H., et al., *Telomerase is controlled by protein kinase Calpha in human breast cancer cells.* J Biol Chem, 1998. **273**(50): p. 33436-42.
228. Latif, F., et al., *Identification of the von Hippel-Lindau disease tumor suppressor gene.* Science, 1993. **260**(5112): p. 1317-20.

229. Morris, L.G., S. Veeriah, and T.A. Chan, *Genetic determinants at the interface of cancer and neurodegenerative disease.* Oncogene, 2010. **29**(24): p. 3453-64.
230. Herrup, K. and J.C. Busser, *The induction of multiple cell cycle events precedes target-related neuronal death.* Development, 1995. **121**(8): p. 2385-95.
231. Chen, L. and M.B. Feany, *Alpha-synuclein phosphorylation controls neurotoxicity and inclusion formation in a Drosophila model of Parkinson disease.* Nat Neurosci, 2005. **8**(5): p. 657-63.
232. Nakamura, T., et al., *Activated Fyn phosphorylates alpha-synuclein at tyrosine residue 125.* Biochem Biophys Res Commun, 2001. **280**(4): p. 1085-92.
233. Negro, A., et al., *Multiple phosphorylation of alpha-synuclein by protein tyrosine kinase Syk prevents eosin-induced aggregation.* FASEB J, 2002. **16**(2): p. 210-2.
234. Qing, H., et al., *Lrrk2 phosphorylates alpha synuclein at serine 129: Parkinson disease implications.* Biochem Biophys Res Commun, 2009. **387**(1): p. 149-52.
235. Ghee, M., A. Fournier, and J. Mallet, *Rat alpha-synuclein interacts with Tat binding protein 1, a component of the 26S proteasomal complex.* J Neurochem, 2000. **75**(5): p. 2221-4.
236. Choi, P., et al., *Co-association of parkin and alpha-synuclein.* Neuroreport, 2001. **12**(13): p. 2839-43.
237. Tyers, M. and R. Rottapel, *VHL: a very hip ligase.* Proc Natl Acad Sci U S A, 1999. **96**(22): p. 12230-2.
238. Walter, J., et al., *Phosphorylation of presenilin-2 regulates its cleavage by caspases and retards progression of apoptosis.* Proc Natl Acad Sci U S A, 1999. **96**(4): p. 1391-6.
239. Puthalakath, H., et al., *Bmf: a proapoptotic BH3-only protein regulated by interaction with the myosin V actin motor complex, activated by anoikis.* Science, 2001. **293**(5536): p. 1829-32.
240. Sousa, V.L., et al., *{alpha}-synuclein and its A30P mutant affect actin cytoskeletal structure and dynamics.* Mol Biol Cell, 2009. **20**(16): p. 3725-39.
241. Hamosh, A., et al., *Online Mendelian Inheritance in Man (OMIM), a knowledgebase of human genes and genetic disorders.* Nucleic Acids Res, 2005. **33**(Database issue): p. D514-7.
242. Knox, C., et al., *DrugBank 3.0: a comprehensive resource for 'omics' research on drugs.* Nucleic Acids Res, 2011. **39**(Database issue): p. D1035-41.
243. Safran, M., et al., *GeneCards Version 3: the human gene integrator.* Database (Oxford), 2010. **2010**: p. baq020.
244. Williams, S.R., et al., *Haploinsufficiency of HDAC4 causes brachydactyly mental retardation syndrome, with brachydactyly type E, developmental delays, and behavioral problems.* Am J Hum Genet, 2010. **87**(2): p. 219-28.
245. Majdzadeh, N., et al., *HDAC4 inhibits cell-cycle progression and protects neurons from cell death.* Dev Neurobiol, 2008. **68**(8): p. 1076-92.
246. Zhou, W., et al., *Phenylbutyrate up-regulates the DJ-1 protein and protects neurons in cell culture and in animal models of Parkinson disease.* J Biol Chem, 2011. **286**(17): p. 14941-51.
247. Outeiro, T.F., et al., *Sirtuin 2 inhibitors rescue alpha-synuclein-mediated toxicity in models of Parkinson's disease.* Science, 2007. **317**(5837): p. 516-9.

248. Kazantsev, A.G. and L.M. Thompson, *Therapeutic application of histone deacetylase inhibitors for central nervous system disorders.* Nat Rev Drug Discov, 2008. **7**(10): p. 854-68.
249. Johnston, J.A., C.L. Ward, and R.R. Kopito, *Aggresomes: a cellular response to misfolded proteins.* J Cell Biol, 1998. **143**(7): p. 1883-98.
250. Tanaka, M., et al., *Aggresomes formed by alpha-synuclein and synphilin-1 are cytoprotective.* J Biol Chem, 2004. **279**(6): p. 4625-31.
251. Ikeda, D., et al., *Carnosine stimulates vimentin expression in cultured rat fibroblasts.* Cell Struct Funct, 1999. **24**(2): p. 79-87.
252. Hipkiss, A.R., *Could carnosine or related structures suppress Alzheimer's disease?* J Alzheimers Dis, 2007. **11**(2): p. 229-40.
253. Boldyrev, A., et al., *Chemical intervention in senescence-accelerated mice metabolism for modeling neurodegenerative diseases: an overview.* International Congress Series, 2004. **1260**(0): p. 109-115.
254. Boldyrev, A., et al., *Carnosine [corrected] increases efficiency of DOPA therapy of Parkinson's disease: a pilot study.* Rejuvenation Res, 2008. **11**(4): p. 821-7.
255. Li, F., et al., *Control of apoptosis and mitotic spindle checkpoint by survivin.* Nature, 1998. **396**(6711): p. 580-4.
256. Altieri, D.C., *Validating survivin as a cancer therapeutic target.* Nat Rev Cancer, 2003. **3**(1): p. 46-54.
257. Hoglinger, G.U., et al., *The pRb/E2F cell-cycle pathway mediates cell death in Parkinson's disease.* Proc Natl Acad Sci U S A, 2007. **104**(9): p. 3585-90.
258. Betarbet, R., T.B. Sherer, and J.T. Greenamyre, *Animal models of Parkinson's disease.* Bioessays, 2002. **24**(4): p. 308-18.
259. Yang, K., et al., *Fyn, a potential target for Alzheimer's disease.* J Alzheimers Dis, 2011. **27**(2): p. 243-52.
260. Ho, G.J., et al., *Altered p59Fyn kinase expression accompanies disease progression in Alzheimer's disease: implications for its functional role.* Neurobiol Aging, 2005. **26**(5): p. 625-35.
261. McLean, P.J., et al., *Membrane association and protein conformation of alpha-synuclein in intact neurons. Effect of Parkinson's disease-linked mutations.* J Biol Chem, 2000. **275**(12): p. 8812-6.
262. Breeden, L. and K. Nasmyth, *Regulation of the yeast HO gene.* Cold Spring Harb Symp Quant Biol, 1985. **50**: p. 643-50.
263. Chang, C.N., et al., *Saccharomyces cerevisiae secretes and correctly processes human interferon hybrid proteins containing yeast invertase signal peptides.* Mol Cell Biol, 1986. **6**(5): p. 1812-9.
264. Jacobs, M.D. and S.C. Harrison, *Structure of an IkappaBalpha/NF-kappaB complex.* Cell, 1998. **95**(6): p. 749-58.
265. Deloulme, J.C., et al., *S100A6 and S100A11 are specific targets of the calcium- and zinc-binding S100B protein in vivo.* J Biol Chem, 2000. **275**(45): p. 35302-10.
266. Yang, Q., et al., *Demonstration of heterodimer formation between S100B and S100A6 in the yeast two-hybrid system and human melanoma.* Exp Cell Res, 1999. **246**(2): p. 501-9.
267. Matlashewski, G., et al., *Isolation and characterization of a human p53 cDNA clone: expression of the human p53 gene.* EMBO J, 1984. **3**(13): p. 3257-62.
268. Wang, B., et al., *The yeast split-ubiquitin membrane protein two-hybrid screen identifies BAP31 as a regulator of the turnover of endoplasmic reticulum-*

associated protein tyrosine phosphatase-like B. Mol Cell Biol, 2004. **24**(7): p. 2767-78.
269. Dixon, C., et al., *Alpha-synuclein targets the plasma membrane via the secretory pathway and induces toxicity in yeast.* Genetics, 2005. **170**(1): p. 47-59.
270. Kornfeld, R. and S. Kornfeld, *Assembly of asparagine-linked oligosaccharides.* Annu Rev Biochem, 1985. **54**: p. 631-64.
271. Heesen, S., et al., *Isolation of the ALG5 locus encoding the UDP-glucose:dolichyl-phosphate glucosyltransferase from Saccharomyces cerevisiae.* Eur J Biochem, 1994. **224**(1): p. 71-9.
272. Chevallier, M.R. and F. Lacroute, *Expression of the cloned uracil permease gene of Saccharomyces cerevisiae in a heterologous membrane.* EMBO J, 1982. **1**(3): p. 375-7.
273. Orlean, P., C. Albright, and P.W. Robbins, *Cloning and sequencing of the yeast gene for dolichol phosphate mannose synthase, an essential protein.* J Biol Chem, 1988. **263**(33): p. 17499-507.
274. Hitzeman, R.A., L. Clarke, and J. Carbon, *Isolation and characterization of the yeast 3-phosphoglycerokinase gene (PGK) by an immunological screening technique.* J Biol Chem, 1980. **255**(24): p. 12073-80.
275. Nevalainen, L.T., J. Louhelainen, and M. Makarow, *Post-translational modifications in mitotic yeast cells.* European Journal of Biochemistry, 1989. **184**(1): p. 165-172.
276. Clayton, D.F. and J.M. George, *Synucleins in synaptic plasticity and neurodegenerative disorders.* J Neurosci Res, 1999. **58**(1): p. 120-9.
277. Zhang, W., et al., *SynDB: a Synapse protein DataBase based on synapse ontology.* Nucleic Acids Res, 2007. **35**(Database issue): p. D737-41.
278. Uetz, P., et al., *Herpesviral protein networks and their interaction with the human proteome.* Science, 2006. **311**(5758): p. 239-42.
279. Rozen, R., et al., *Virion-wide protein interactions of Kaposi's sarcoma-associated herpesvirus.* J Virol, 2008. **82**(10): p. 4742-50.
280. Kirschner, L.S. and C.A. Stratakis, *Structure of the human ubiquitin fusion gene Uba80 (RPS27a) and one of its pseudogenes.* Biochem Biophys Res Commun, 2000. **270**(3): p. 1106-10.
281. Huang, L., Y.M. Kuo, and J. Gitschier, *The pallid gene encodes a novel, syntaxin 13-interacting protein involved in platelet storage pool deficiency.* Nat Genet, 1999. **23**(3): p. 329-32.
282. Kohn, W.D., C.T. Mant, and R.S. Hodges, *Alpha-helical protein assembly motifs.* J Biol Chem, 1997. **272**(5): p. 2583-6.
283. Yakovleva, T., et al., *Prodynorphin storage and processing in axon terminals and dendrites.* FASEB J, 2006. **20**(12): p. 2124-6.
284. *Isolation of a novel gene underlying Batten disease, CLN3. The International Batten Disease Consortium.* Cell, 1995. **82**(6): p. 949-57.
285. Guilford, P., et al., *E-cadherin germline mutations in familial gastric cancer.* Nature, 1998. **392**(6674): p. 402-5.
286. Smith, M.T., *Benzene, NQO1, and genetic susceptibility to cancer.* Proc Natl Acad Sci U S A, 1999. **96**(14): p. 7624-6.
287. Wible, B.A., et al., *Increased K+ efflux and apoptosis induced by the potassium channel modulatory protein KChAP/PIAS3beta in prostate cancer cells.* J Biol Chem, 2002. **277**(20): p. 17852-62.

288. Guan, J.L. and D. Shalloway, *Regulation of focal adhesion-associated protein tyrosine kinase by both cellular adhesion and oncogenic transformation.* Nature, 1992. **358**(6388): p. 690-2.
289. Ji, H., et al., *Identification of a breast cancer-specific gene, BCSG1, by direct differential cDNA sequencing.* Cancer Res, 1997. **57**(4): p. 759-64.
290. Edmondson, D.E., et al., *Structure and mechanism of monoamine oxidase.* Curr Med Chem, 2004. **11**(15): p. 1983-93.
291. Naoi, M. and W. Maruyama, *Monoamine oxidase inhibitors as neuroprotective agents in age-dependent neurodegenerative disorders.* Curr Pharm Des, 2010. **16**(25): p. 2799-817.
292. Lin, R.C. and R.H. Scheller, *Structural organization of the synaptic exocytosis core complex.* Neuron, 1997. **19**(5): p. 1087-94.
293. Burre, J., et al., *Alpha-synuclein promotes SNARE-complex assembly in vivo and in vitro.* Science, 2010. **329**(5999): p. 1663-7.
294. Lovejoy, D.A. and R.J. Balment, *Evolution and physiology of the corticotropin-releasing factor (CRF) family of neuropeptides in vertebrates.* Gen Comp Endocrinol, 1999. **115**(1): p. 1-22.
295. Pedersen, W.A., et al., *Urocortin, but not urocortin II, protects cultured hippocampal neurons from oxidative and excitotoxic cell death via corticotropin-releasing hormone receptor type I.* J Neurosci, 2002. **22**(2): p. 404-12.
296. Abuirmeileh, A., et al., *The corticotrophin-releasing factor-like peptide urocortin reverses key deficits in two rodent models of Parkinson's disease.* Eur J Neurosci, 2007. **26**(2): p. 417-23.
297. Salkoff, L., et al., *High-conductance potassium channels of the SLO family.* Nat Rev Neurosci, 2006. **7**(12): p. 921-31.
298. Sausbier, M., et al., *Cerebellar ataxia and Purkinje cell dysfunction caused by Ca2+-activated K+ channel deficiency.* Proc Natl Acad Sci U S A, 2004. **101**(25): p. 9474-8.
299. Fader, C.M., et al., *TI-VAMP/VAMP7 and VAMP3/cellubrevin: two v-SNARE proteins involved in specific steps of the autophagy/multivesicular body pathways.* Biochim Biophys Acta, 2009. **1793**(12): p. 1901-16.
300. Irrcher, I. and D.S. Park, *Parkinson's disease: to live or die by autophagy.* Sci Signal, 2009. **2**(65): p. pe21.
301. Jin, J., et al., *Identification of novel proteins affected by rotenone in mitochondria of dopaminergic cells.* BMC Neurosci, 2007. **8**: p. 67.
302. Kabeya, Y., et al., *LC3, GABARAP and GATE16 localize to autophagosomal membrane depending on form-II formation.* J Cell Sci, 2004. **117**(Pt 13): p. 2805-12.
303. O'Sullivan, G.A., et al., *GABARAP is not essential for GABA receptor targeting to the synapse.* Eur J Neurosci, 2005. **22**(10): p. 2644-8.
304. Przedborski, S. and M. Vila, *The 1-Methyl-4-Phenyl-1,2,3,6-Tetrahydropyridine Mouse Model.* Annals of the New York Academy of Sciences, 2003. **991**(1): p. 189-198.
305. Okubo, Y., et al., *Decreased prefrontal dopamine D1 receptors in schizophrenia revealed by PET.* Nature, 1997. **385**(6617): p. 634-6.
306. Zhang, Y., et al., *Polymorphisms in human dopamine D2 receptor gene affect gene expression, splicing, and neuronal activity during working memory.* Proc Natl Acad Sci U S A, 2007. **104**(51): p. 20552-7.

307. Schmauss, C., et al., *Selective loss of dopamine D3-type receptor mRNA expression in parietal and motor cortices of patients with chronic schizophrenia.* Proc Natl Acad Sci U S A, 1993. **90**(19): p. 8942-6.
308. Seeman, P. and H.B. Niznik, *Dopamine receptors and transporters in Parkinson's disease and schizophrenia.* FASEB J, 1990. **4**(10): p. 2737-44.
309. Kurz, A., et al., *A53T-alpha-synuclein overexpression impairs dopamine signaling and striatal synaptic plasticity in old mice.* PLoS One, 2010. **5**(7): p. e11464.
310. Kim, S.J., et al., *Alpha-synuclein enhances dopamine D2 receptor signaling.* Brain Res, 2006. **1124**(1): p. 5-9.
311. Diaz, J., et al., *Selective expression of dopamine D3 receptor mRNA in proliferative zones during embryonic development of the rat brain.* J Neurosci, 1997. **17**(11): p. 4282-92.
312. Van Kampen, J.M. and C.B. Eckman, *Dopamine D3 receptor agonist delivery to a model of Parkinson's disease restores the nigrostriatal pathway and improves locomotor behavior.* J Neurosci, 2006. **26**(27): p. 7272-80.
313. Cash, R., et al., *Adrenergic receptors in Parkinson's disease.* Brain Res, 1984. **322**(2): p. 269-75.
314. Henry, B., et al., *The alpha2-adrenergic receptor antagonist idazoxan reduces dyskinesia and enhances anti-parkinsonian actions of L-dopa in the MPTP-lesioned primate model of Parkinson's disease.* Mov Disord, 1999. **14**(5): p. 744-53.
315. Axelrod, J. and R. Tomchick, *Enzymatic O-methylation of epinephrine and other catechols.* J Biol Chem, 1958. **233**(3): p. 702-5.
316. Williams, H.J., M.J. Owen, and M.C. O'Donovan, *Is COMT a susceptibility gene for schizophrenia?* Schizophr Bull, 2007. **33**(3): p. 635-41.
317. Mannisto, P.T. and S. Kaakkola, *Rationale for selective COMT inhibitors as adjuncts in the drug treatment of Parkinson's disease.* Pharmacol Toxicol, 1990. **66**(5): p. 317-23.
318. Lin, L., et al., *GDNF: a glial cell line-derived neurotrophic factor for midbrain dopaminergic neurons.* Science, 1993. **260**(5111): p. 1130-1132.
319. Gill, S.S., et al., *Direct brain infusion of glial cell line-derived neurotrophic factor in Parkinson disease.* Nat Med, 2003. **9**(5): p. 589-95.
320. Slevin, J.T., et al., *Improvement of bilateral motor functions in patients with Parkinson disease through the unilateral intraputaminal infusion of glial cell line-derived neurotrophic factor.* J Neurosurg, 2005. **102**(2): p. 216-22.
321. Quartara, L. and C.A. Maggi, *The tachykinin NK1 receptor. Part II: Distribution and pathophysiological roles.* Neuropeptides, 1998. **32**(1): p. 1-49.
322. Barker, R., *Substance P and neurodegenerative disorders. A speculative review.* Neuropeptides, 1991. **20**(2): p. 73-8.
323. Yu, J., J.L. Cadet, and J.A. Angulo, *Neurokinin-1 (NK-1) receptor antagonists abrogate methamphetamine-induced striatal dopaminergic neurotoxicity in the murine brain.* J Neurochem, 2002. **83**(3): p. 613-22.
324. Hong, C.J., et al., *Association study of PICK1 rs3952 polymorphism and schizophrenia.* Neuroreport, 2004. **15**(12): p. 1965-7.
325. Zhang, B., et al., *Protein interacting with C alpha kinase 1 (PICK1) is involved in promoting tumor growth and correlates with poor prognosis of human breast cancer.* Cancer Sci, 2010. **101**(6): p. 1536-42.
326. Torres, G.E., et al., *Functional interaction between monoamine plasma membrane transporters and the synaptic PDZ domain-containing protein PICK1.* Neuron, 2001. **30**(1): p. 121-34.

327. Lee, F.J., et al., *Direct binding and functional coupling of alpha-synuclein to the dopamine transporters accelerate dopamine-induced apoptosis.* FASEB J, 2001. **15**(6): p. 916-26.
328. Mander, A., C.P. Hodgkinson, and G.J. Sale, *Knock-down of LAR protein tyrosine phosphatase induces insulin resistance.* FEBS Lett, 2005. **579**(14): p. 3024-8.
329. Morris, J.K., et al., *Measures of striatal insulin resistance in a 6-hydroxydopamine model of Parkinson's disease.* Brain Res, 2008. **1240**: p. 185-95.
330. Xie, Y., et al., *Protein-tyrosine phosphatase (PTP) wedge domain peptides: a novel approach for inhibition of PTP function and augmentation of protein-tyrosine kinase function.* J Biol Chem, 2006. **281**(24): p. 16482-92.
331. Bentley, D.R., et al., *Accurate whole human genome sequencing using reversible terminator chemistry.* Nature, 2008. **456**(7218): p. 53-9.
332. Mardis, E.R., *Next-generation DNA sequencing methods.* Annu Rev Genomics Hum Genet, 2008. **9**: p. 387-402.
333. Craig, D.W., et al., *Identification of genetic variants using bar-coded multiplexed sequencing.* Nat Methods, 2008. **5**(10): p. 887-93.
334. Quail, M.A., et al., *A large genome center's improvements to the Illumina sequencing system.* Nat Methods, 2008. **5**(12): p. 1005-10.
335. DeAngelis, M.M., D.G. Wang, and T.L. Hawkins, *Solid-phase reversible immobilization for the isolation of PCR products.* Nucleic Acids Res, 1995. **23**(22): p. 4742-3.
336. Vrouwe, E.X., et al., *Chip-based capillary electrophoresis with an electrodeless nanospray interface.* Rapid Commun Mass Spectrom, 2000. **14**(18): p. 1682-8.
337. Benson, D.A., et al., *GenBank.* Nucleic Acids Res, 2011. **39**(Database issue): p. D32-7.
338. Cohen, A.W., et al., *Role of caveolae and caveolins in health and disease.* Physiol Rev, 2004. **84**(4): p. 1341-79.
339. Madeira, A., et al., *Caveolin-1 interacts with alpha-synuclein and mediates toxic actions of cellular alpha-synuclein overexpression.* Neurochem Int, 2011. **59**(2): p. 280-9.
340. Cousin, E., et al., *A risk for early-onset Alzheimer's disease associated with the APBB1 gene (FE65) intron 13 polymorphism.* Neurosci Lett, 2003. **342**(1-2): p. 5-8.
341. Nishimura, A.L., et al., *A mutation in the vesicle-trafficking protein VAPB causes late-onset spinal muscular atrophy and amyotrophic lateral sclerosis.* Am J Hum Genet, 2004. **75**(5): p. 822-31.
342. Inbal, B., et al., *Death-associated protein kinase-related protein 1, a novel serine/threonine kinase involved in apoptosis.* Mol Cell Biol, 2000. **20**(3): p. 1044-54.
343. Tatton, W.G., et al., *Apoptosis in Parkinson's disease: signals for neuronal degradation.* Ann Neurol, 2003. **53 Suppl 3**: p. S61-70; discussion S70-2.
344. Zhang, Y., et al., *SAP30, a novel protein conserved between human and yeast, is a component of a histone deacetylase complex.* Mol Cell, 1998. **1**(7): p. 1021-31.
345. Mahul-Mellier, A.L., et al., *De-ubiquitinating protease USP2a targets RIP1 and TRAF2 to mediate cell death by TNF.* Cell Death Differ, 2011.
346. Stevenson, L.F., et al., *The deubiquitinating enzyme USP2a regulates the p53 pathway by targeting Mdm2.* EMBO J, 2007. **26**(4): p. 976-86.

347. Hellman, M., et al., *Mesencephalic astrocyte-derived neurotrophic factor (MANF) has a unique mechanism to rescue apoptotic neurons.* J Biol Chem, 2011. **286**(4): p. 2675-80.
348. Garami, A., et al., *Insulin activation of Rheb, a mediator of mTOR/S6K/4E-BP signaling, is inhibited by TSC1 and 2.* Mol Cell, 2003. **11**(6): p. 1457-66.
349. Kim, S.R., et al., *AAV Transduction of Dopamine Neurons With Constitutively Active Rheb Protects From Neurodegeneration and Mediates Axon Regrowth.* Mol Ther, 2012. **20**(2): p. 275-86.
350. Somia, N.V., et al., *LFG: an anti-apoptotic gene that provides protection from Fas-mediated cell death.* Proc Natl Acad Sci U S A, 1999. **96**(22): p. 12667-72.
351. Fernandez, M., et al., *Lifeguard/neuronal membrane protein 35 regulates Fas ligand-mediated apoptosis in neurons via microdomain recruitment.* J Neurochem, 2007. **103**(1): p. 190-203.
352. Yeung, K.C., et al., *Raf kinase inhibitor protein interacts with NF-kappaB-inducing kinase and TAK1 and inhibits NF-kappaB activation.* Mol Cell Biol, 2001. **21**(21): p. 7207-17.
353. Ghosh, A., et al., *Selective inhibition of NF-kappaB activation prevents dopaminergic neuronal loss in a mouse model of Parkinson's disease.* Proc Natl Acad Sci U S A, 2007. **104**(47): p. 18754-9.
354. Larsen, K.E., et al., *Alpha-synuclein overexpression in PC12 and chromaffin cells impairs catecholamine release by interfering with a late step in exocytosis.* J Neurosci, 2006. **26**(46): p. 11915-22.
355. Lee, D., et al., *alpha-Synuclein exhibits competitive interaction between calmodulin and synthetic membranes.* J Neurochem, 2002. **82**(5): p. 1007-17.
356. Willingham, S., et al., *Yeast genes that enhance the toxicity of a mutant huntingtin fragment or alpha-synuclein.* Science, 2003. **302**(5651): p. 1769-72.
357. Yeger-Lotem, E., et al., *Bridging high-throughput genetic and transcriptional data reveals cellular responses to alpha-synuclein toxicity.* Nat Genet, 2009. **41**(3): p. 316-23.
358. Hamamichi, S., et al., *Hypothesis-based RNAi screening identifies neuroprotective genes in a Parkinson's disease model.* Proc Natl Acad Sci U S A, 2008. **105**(2): p. 728-33.
359. Kuwahara, T., et al., *A systematic RNAi screen reveals involvement of endocytic pathway in neuronal dysfunction in alpha-synuclein transgenic C. elegans.* Hum Mol Genet, 2008. **17**(19): p. 2997-3009.
360. Sayers, E.W., et al., *Database resources of the National Center for Biotechnology Information.* Nucleic Acids Res, 2011. **39**(Database issue): p. D38-51.
361. Carlsson, T., et al., *Systemic administration of neuregulin-1beta1 protects dopaminergic neurons in a mouse model of Parkinson's disease.* J Neurochem, 2011. **117**(6): p. 1066-74.
362. Todd, A.M. and B.E. Staveley, *Pink1 suppresses alpha-synuclein-induced phenotypes in a Drosophila model of Parkinson's disease.* Genome, 2008. **51**(12): p. 1040-6.
363. Salazar, J., et al., *Divalent metal transporter 1 (DMT1) contributes to neurodegeneration in animal models of Parkinson's disease.* Proc Natl Acad Sci U S A, 2008. **105**(47): p. 18578-83.
364. Liu, X., et al., *Functional characterization of novel human ARFGAP3.* FEBS Lett, 2001. **490**(1-2): p. 79-83.

365. Stafa, K., et al., *GTPase Activity and Neuronal Toxicity of Parkinson's Disease–Associated LRRK2 Is Regulated by ArfGAP1.* PLoS Genet, 2012. **8**(2): p. e1002526.
366. Mata, I.F., et al., *LRRK2 in Parkinson's disease: protein domains and functional insights.* Trends Neurosci, 2006. **29**(5): p. 286-93.
367. Micali, N., et al., *Prep1 directly regulates the intrinsic apoptotic pathway by controlling Bcl-XL levels.* Mol Cell Biol, 2009. **29**(5): p. 1143-51.
368. Soper, J.H., et al., *Alpha-synuclein-induced aggregation of cytoplasmic vesicles in Saccharomyces cerevisiae.* Mol Biol Cell, 2008. **19**(3): p. 1093-103.
369. Braak, H., et al., *Staging of brain pathology related to sporadic Parkinson's disease.* Neurobiol Aging, 2003. **24**(2): p. 197-211.
370. Edwards, T.L., et al., *Genome-wide association study confirms SNPs in SNCA and the MAPT region as common risk factors for Parkinson disease.* Ann Hum Genet, 2010. **74**(2): p. 97-109.
371. Clayton, D.F. and J.M. George, *Synucleins in synaptic plasticity and neurodegenerative disorders.* Journal of Neuroscience Research, 1999. **58**(1): p. 120-129.
372. Armstrong, R.A., P.L. Lantos, and N.J. Cairns, *Overlap between neurodegenerative disorders.* Neuropathology, 2005. **25**(2): p. 111-124.
373. Abeliovich, A., et al., *Mice lacking alpha-synuclein display functional deficits in the nigrostriatal dopamine system.* Neuron, 2000. **25**(1): p. 239-52.
374. Giros, B., et al., *Hyperlocomotion and indifference to cocaine and amphetamine in mice lacking the dopamine transporter.* Nature, 1996. **379**(6566): p. 606-12.
375. Reith, M.E., C. Xu, and N.H. Chen, *Pharmacology and regulation of the neuronal dopamine transporter.* Eur J Pharmacol, 1997. **324**(1): p. 1-10.
376. Jones, S.R., et al., *Profound neuronal plasticity in response to inactivation of the dopamine transporter.* Proc Natl Acad Sci U S A, 1998. **95**(7): p. 4029-34.
377. Wersinger, C. and A. Sidhu, *Attenuation of dopamine transporter activity by alpha-synuclein.* Neurosci Lett, 2003. **340**(3): p. 189-92.
378. Wersinger, C., et al., *Mutations in the lipid-binding domain of alpha-synuclein confer overlapping, yet distinct, functional properties in the regulation of dopamine transporter activity.* Mol Cell Neurosci, 2003. **24**(1): p. 91-105.
379. Jenco, J.M., et al., *Regulation of phospholipase D2: selective inhibition of mammalian phospholipase D isoenzymes by alpha- and beta-synucleins.* Biochemistry, 1998. **37**(14): p. 4901-9.
380. Ahn, B.H., et al., *alpha-Synuclein interacts with phospholipase D isozymes and inhibits pervanadate-induced phospholipase D activation in human embryonic kidney-293 cells.* J Biol Chem, 2002. **277**(14): p. 12334-42.
381. Payton, J.E., et al., *Structural determinants of PLD2 inhibition by alpha-synuclein.* J Mol Biol, 2004. **337**(4): p. 1001-9.
382. Olanow, C.W. and G.W. Arendash, *Metals and free radicals in neurodegeneration.* Curr Opin Neurol, 1994. **7**(6): p. 548-58.
383. Offen, D., et al., *Oxidative stress and neuroprotection in Parkinson's disease: implications from studies on dopamine-induced apoptosis.* Adv Neurol, 1999. **80**: p. 265-9.
384. Venda, L.L., et al., *alpha-Synuclein and dopamine at the crossroads of Parkinson's disease.* Trends Neurosci, 2010. **33**(12): p. 559-68.
385. Jao, C.C., et al., *Structure of membrane-bound alpha-synuclein from site-directed spin labeling and computational refinement.* Proc Natl Acad Sci U S A, 2008. **105**(50): p. 19666-71.

386. Madine, J., A.J. Doig, and D.A. Middleton, *A study of the regional effects of alpha-synuclein on the organization and stability of phospholipid bilayers.* Biochemistry, 2006. **45**(18): p. 5783-92.
387. Varkey, J., et al., *Membrane curvature induction and tubulation are common features of synucleins and apolipoproteins.* J Biol Chem, 2010. **285**(42): p. 32486-93.
388. Auluck, P.K., G. Caraveo, and S. Lindquist, *alpha-Synuclein: membrane interactions and toxicity in Parkinson's disease.* Annu Rev Cell Dev Biol, 2010. **26**: p. 211-33.
389. Zhu, M., et al., *Alpha-synuclein can function as an antioxidant preventing oxidation of unsaturated lipid in vesicles.* Biochemistry, 2006. **45**(26): p. 8135-42.
390. Sato, S., et al., *14-3-3eta is a novel regulator of parkin ubiquitin ligase.* EMBO J, 2006. **25**(1): p. 211-21.
391. Bridges, D. and G.B. Moorhead, *14-3-3 proteins: a number of functions for a numbered protein.* Sci STKE, 2005. **2005**(296): p. re10.
392. Roodveldt, C., et al., *Chaperone proteostasis in Parkinson's disease: stabilization of the Hsp70/alpha-synuclein complex by Hip.* EMBO J, 2009. **28**(23): p. 3758-70.
393. Chandra, S., et al., *Alpha-synuclein cooperates with CSPalpha in preventing neurodegeneration.* Cell, 2005. **123**(3): p. 383-96.
394. Rizo, J. and C. Rosenmund, *Synaptic vesicle fusion.* Nat Struct Mol Biol, 2008. **15**(7): p. 665-74.
395. Zhang, N.Y., Z. Tang, and C.W. Liu, *alpha-Synuclein protofibrils inhibit 26 S proteasome-mediated protein degradation: understanding the cytotoxicity of protein protofibrils in neurodegenerative disease pathogenesis.* J Biol Chem, 2008. **283**(29): p. 20288-98.
396. Elkon, H., et al., *Mutant and wild-type alpha-synuclein interact with mitochondrial cytochrome C oxidase.* J Mol Neurosci, 2002. **18**(3): p. 229-38.
397. Lindersson, E., et al., *p25alpha Stimulates alpha-synuclein aggregation and is co-localized with aggregated alpha-synuclein in alpha-synucleinopathies.* J Biol Chem, 2005. **280**(7): p. 5703-15.
398. Olah, J., et al., *Interaction of TPPP/p25 protein with glyceraldehyde-3-phosphate dehydrogenase and their co-localization in Lewy bodies.* FEBS Lett, 2006. **580**(25): p. 5807-14.
399. Qureshi, H.Y. and H.K. Paudel, *Parkinsonian neurotoxin 1-methyl-4-phenyl-1,2,3,6-tetrahydropyridine (MPTP) and alpha-synuclein mutations promote Tau protein phosphorylation at Ser262 and destabilize microtubule cytoskeleton in vitro.* J Biol Chem, 2011. **286**(7): p. 5055-68.
400. Kontopoulos, E., J.D. Parvin, and M.B. Feany, *Alpha-synuclein acts in the nucleus to inhibit histone acetylation and promote neurotoxicity.* Hum Mol Genet, 2006. **15**(20): p. 3012-23.
401. Austin, S.A., et al., *Alpha-synuclein expression modulates microglial activation phenotype.* J Neurosci, 2006. **26**(41): p. 10558-63.
402. Uetz, P., et al., *A comprehensive analysis of protein-protein interactions in Saccharomyces cerevisiae.* Nature, 2000. **403**(6770): p. 623-7.
403. Braun, P., et al., *An experimentally derived confidence score for binary protein-protein interactions.* Nat Methods, 2009. **6**(1): p. 91-7.
404. Dunker, A.K., et al., *Intrinsically disordered protein.* J Mol Graph Model, 2001. **19**(1): p. 26-59.

405. Wright, P.E. and H.J. Dyson, *Intrinsically unstructured proteins: re-assessing the protein structure-function paradigm.* J Mol Biol, 1999. **293**(2): p. 321-31.
406. Bonar, L., A.S. Cohen, and M.M. Skinner, *Characterization of the amyloid fibril as a cross-beta protein.* Proc Soc Exp Biol Med, 1969. **131**(4): p. 1373-5.
407. Glenner, G.G. and C.W. Wong, *Alzheimer's disease: initial report of the purification and characterization of a novel cerebrovascular amyloid protein.* Biochem Biophys Res Commun, 1984. **120**(3): p. 885-90.
408. Jensen, P.H., et al., *Binding of Abeta to alpha- and beta-synucleins: identification of segments in alpha-synuclein/NAC precursor that bind Abeta and NAC.* Biochem J, 1997. **323 (Pt 2)**: p. 539-46.
409. Komano, H., et al., *Involvement of cell surface glycosyl-phosphatidylinositol-linked aspartyl proteases in alpha-secretase-type cleavage and ectodomain solubilization of human Alzheimer beta-amyloid precursor protein in yeast.* J Biol Chem, 1998. **273**(48): p. 31648-51.
410. Luthi, U., et al., *Human beta-secretase activity in yeast detected by a novel cellular growth selection system.* Biochim Biophys Acta, 2003. **1620**(1-3): p. 167-78.
411. Hogl, S., et al., *Determination of the proteolytic cleavage sites of the amyloid precursor-like protein 2 by the proteases ADAM10, BACE1 and gamma-secretase.* PLoS One, 2011. **6**(6): p. e21337.
412. Kawashima, M., et al., *alpha-Synuclein is expressed in a variety of brain tumors showing neuronal differentiation.* Acta Neuropathol, 2000. **99**(2): p. 154-60.
413. Fung, K.M., et al., *Expression of alpha-, beta-, and gamma-synuclein in glial tumors and medulloblastomas.* Acta Neuropathol, 2003. **106**(2): p. 167-75.
414. Bruening, W., et al., *Synucleins are expressed in the majority of breast and ovarian carcinomas and in preneoplastic lesions of the ovary.* Cancer, 2000. **88**(9): p. 2154-63.
415. Ye, Q., et al., *Expression of alpha-, beta- and gamma-synuclein in colorectal cancer, and potential clinical significance in progression of the disease.* Oncol Rep, 2010. **23**(2): p. 429-36.
416. Matsuo, Y. and T. Kamitani, *Parkinson's disease-related protein, alpha-synuclein, in malignant melanoma.* PLoS One, 2010. **5**(5): p. e10481.
417. Feddersen, R.M., et al., *Disrupted cerebellar cortical development and progressive degeneration of Purkinje cells in SV40 T antigen transgenic mice.* Neuron, 1992. **9**(5): p. 955-66.
418. Anderson, J.P., et al., *Phosphorylation of Ser-129 is the dominant pathological modification of alpha-synuclein in familial and sporadic Lewy body disease.* J Biol Chem, 2006. **281**(40): p. 29739-52.
419. Billich, A., et al., *Basal and induced sphingosine kinase 1 activity in A549 carcinoma cells: function in cell survival and IL-1beta and TNF-alpha induced production of inflammatory mediators.* Cell Signal, 2005. **17**(10): p. 1203-17.
420. Ishikawa, Y., et al., *Identification and characterization of novel components of a Ca2+/calmodulin-dependent protein kinase cascade in HeLa cells.* FEBS Lett, 2003. **550**(1-3): p. 57-63.
421. Alvarez-Castelao, B. and J.G. Castano, *Synphilin-1 inhibits alpha-synuclein degradation by the proteasome.* Cell Mol Life Sci, 2011. **68**(15): p. 2643-54.
422. Bussell, R., Jr. and D. Eliezer, *Residual structure and dynamics in Parkinson's disease-associated mutants of alpha-synuclein.* J Biol Chem, 2001. **276**(49): p. 45996-6003.

423. Perrin, R.J., et al., *Interaction of human alpha-Synuclein and Parkinson's disease variants with phospholipids. Structural analysis using site-directed mutagenesis.* J Biol Chem, 2000. **275**(44): p. 34393-8.
424. Jo, E., et al., *Defective membrane interactions of familial Parkinson's disease mutant A30P alpha-synuclein.* J Mol Biol, 2002. **315**(4): p. 799-807.
425. Jensen, P.H., et al., *Binding of alpha-synuclein to brain vesicles is abolished by familial Parkinson's disease mutation.* J Biol Chem, 1998. **273**(41): p. 26292-4.
426. Stockl, M., et al., *Alpha-synuclein selectively binds to anionic phospholipids embedded in liquid-disordered domains.* J Mol Biol, 2008. **375**(5): p. 1394-404.
427. Yonetani, M., et al., *Conversion of wild-type alpha-synuclein into mutant-type fibrils and its propagation in the presence of A30P mutant.* J Biol Chem, 2009. **284**(12): p. 7940-50.
428. Rospigliosi, C.C., et al., *E46K Parkinson's-linked mutation enhances C-terminal-to-N-terminal contacts in alpha-synuclein.* J Mol Biol, 2009. **388**(5): p. 1022-32.
429. Biere, A.L., et al., *Parkinson's disease-associated alpha-synuclein is more fibrillogenic than beta- and gamma-synuclein and cannot cross-seed its homologs.* J Biol Chem, 2000. **275**(44): p. 34574-9.
430. Conway, K.A., J.D. Harper, and P.T. Lansbury, *Accelerated in vitro fibril formation by a mutant alpha-synuclein linked to early-onset Parkinson disease.* Nat Med, 1998. **4**(11): p. 1318-20.
431. Giasson, B.I., et al., *Mutant and wild type human alpha-synucleins assemble into elongated filaments with distinct morphologies in vitro.* J Biol Chem, 1999. **274**(12): p. 7619-22.
432. Hashimoto, M., et al., *Human recombinant NACP/alpha-synuclein is aggregated and fibrillated in vitro: relevance for Lewy body disease.* Brain Res, 1998. **799**(2): p. 301-6.
433. Sayed, M., et al., *Protein kinase CK2 is involved in G2 arrest and apoptosis following spindle damage in epithelial cells.* Oncogene, 2001. **20**(48): p. 6994-7005.
434. Ishii, A., et al., *Casein kinase 2 is the major enzyme in brain that phosphorylates Ser129 of human alpha-synuclein: Implication for alpha-synucleinopathies.* FEBS Lett, 2007. **581**(24): p. 4711-7.
435. Rochet, J.C., et al., *Interactions among alpha-synuclein, dopamine, and biomembranes: some clues for understanding neurodegeneration in Parkinson's disease.* J Mol Neurosci, 2004. **23**(1-2): p. 23-34.
436. Savitt, J.M., V.L. Dawson, and T.M. Dawson, *Diagnosis and treatment of Parkinson disease: molecules to medicine.* J Clin Invest, 2006. **116**(7): p. 1744-54.
437. Skovronsky, D.M., V.M. Lee, and J.Q. Trojanowski, *Neurodegenerative diseases: new concepts of pathogenesis and their therapeutic implications.* Annu Rev Pathol, 2006. **1**: p. 151-70.
438. Bilen, J. and N.M. Bonini, *Drosophila as a model for human neurodegenerative disease.* Annu Rev Genet, 2005. **39**: p. 153-71.
439. Israeli, E., et al., *alpha-Synuclein expression selectively affects tumorigenesis in mice modeling Parkinson's disease.* PLoS One, 2011. **6**(5): p. e19622.
440. Ling, X., et al., *Induction of survivin expression by taxol (paclitaxel) is an early event, which is independent of taxol-mediated G2/M arrest.* J Biol Chem, 2004. **279**(15): p. 15196-203.

441. Zhang, B., et al., *Microtubule-binding drugs offset tau sequestration by stabilizing microtubules and reversing fast axonal transport deficits in a tauopathy model.* Proc Natl Acad Sci U S A, 2005. **102**(1): p. 227-31.
442. Talpaz, M., et al., *Dasatinib in imatinib-resistant Philadelphia chromosome-positive leukemias.* N Engl J Med, 2006. **354**(24): p. 2531-41.
443. Chen, L., et al., *Tyrosine and serine phosphorylation of α-synuclein have opposing effects on neurotoxicity and soluble oligomer formation.* The Journal of Clinical Investigation, 2009. **119**(11): p. 3257-3265.
444. Spiro, R.G., *Protein glycosylation: nature, distribution, enzymatic formation, and disease implications of glycopeptide bonds.* Glycobiology, 2002. **12**(4): p. 43R-56R.
445. Shimura, H., et al., *Ubiquitination of a new form of alpha-synuclein by parkin from human brain: implications for Parkinson's disease.* Science, 2001. **293**(5528): p. 263-9.
446. Jung, T., N. Bader, and T. Grune, *Lipofuscin: formation, distribution, and metabolic consequences.* Ann N Y Acad Sci, 2007. **1119**: p. 97-111.
447. Ulfig, N., *Altered lipofuscin pigmentation in the basal nucleus (Meynert) in Parkinson's disease.* Neurosci Res, 1989. **6**(5): p. 456-62.
448. Jarvela, I., et al., *Defective intracellular transport of CLN3 is the molecular basis of Batten disease (JNCL).* Hum Mol Genet, 1999. **8**(6): p. 1091-8.
449. Tuxworth, R.I., et al., *The Batten disease gene CLN3 is required for the response to oxidative stress.* Hum Mol Genet, 2011. **20**(10): p. 2037-47.
450. Jenner, P., *Oxidative stress in Parkinson's disease.* Ann Neurol, 2003. **53 Suppl 3**: p. S26-36; discussion S36-8.
451. Valente, E.M., et al., *PARK6 is a common cause of familial parkinsonism.* Neurol Sci, 2002. **23 Suppl 2**: p. S117-8.
452. Liu, W., et al., *PINK1 defect causes mitochondrial dysfunction, proteasomal deficit and alpha-synuclein aggregation in cell culture models of Parkinson's disease.* PLoS One, 2009. **4**(2): p. e4597.
453. Kamp, F., et al., *Inhibition of mitochondrial fusion by alpha-synuclein is rescued by PINK1, Parkin and DJ-1.* EMBO J, 2010. **29**(20): p. 3571-89.
454. Takeuchi, H., et al., *Characterization of PXK as a protein involved in epidermal growth factor receptor trafficking.* Mol Cell Biol, 2010. **30**(7): p. 1689-702.
455. Iwakura, Y., et al., *Influences of dopaminergic lesion on epidermal growth factor-ErbB signals in Parkinson's disease and its model: neurotrophic implication in nigrostriatal neurons.* J Neurochem, 2005. **93**(4): p. 974-83.
456. Henchcliffe, C. and M.F. Beal, *Mitochondrial biology and oxidative stress in Parkinson disease pathogenesis.* Nat Clin Pract Neurol, 2008. **4**(11): p. 600-9.
457. Kean, M.J., et al., *VAMP3, syntaxin-13 and SNAP23 are involved in secretion of matrix metalloproteinases, degradation of the extracellular matrix and cell invasion.* J Cell Sci, 2009. **122**(Pt 22): p. 4089-98.
458. Klebig, C., et al., *Characterization of {gamma}-aminobutyric acid type A receptor-associated protein, a novel tumor suppressor, showing reduced expression in breast cancer.* Cancer Res, 2005. **65**(2): p. 394-400.
459. Schwarten, M., et al., *Nix directly binds to GABARAP: a possible crosstalk between apoptosis and autophagy.* Autophagy, 2009. **5**(5): p. 690-8.
460. Dreifuss, J.J. and M. Raggenbass, *Tachykinins and bombesin excite non-pyramidal neurones in rat hippocampus.* J Physiol, 1986. **379**: p. 417-28.
461. Rioux, L. and J.N. Joyce, *Substance P receptors are differentially affected in Parkinson's and Alzheimer's disease.* J Neural Transm Park Dis Dement Sect, 1993. **6**(3): p. 199-210.

462. Munoz, M., M. Rosso, and R. Covenas, *The NK-1 receptor: a new target in cancer therapy.* Curr Drug Targets, 2011. **12**(6): p. 909-21.
463. Staudinger, J., J. Lu, and E.N. Olson, *Specific interaction of the PDZ domain protein PICK1 with the COOH terminus of protein kinase C-alpha.* J Biol Chem, 1997. **272**(51): p. 32019-24.
464. Joch, M., et al., *Parkin-mediated monoubiquitination of the PDZ protein PICK1 regulates the activity of acid-sensing ion channels.* Mol Biol Cell, 2007. **18**(8): p. 3105-18.
465. Iwata, A., et al., *alpha-Synuclein forms a complex with transcription factor Elk-1.* J Neurochem, 2001. **77**(1): p. 239-52.
466. Pan, Z.Z., et al., *Gamma-synuclein promotes cancer cell survival and inhibits stress- and chemotherapy drug-induced apoptosis by modulating MAPK pathways.* J Biol Chem, 2002. **277**(38): p. 35050-60.
467. Dunah, A.W., et al., *LAR receptor protein tyrosine phosphatases in the development and maintenance of excitatory synapses.* Nat Neurosci, 2005. **8**(4): p. 458-67.
468. Fisher, D., et al., *Leukocyte common antigen-related phosphatase is a functional receptor for chondroitin sulfate proteoglycan axon growth inhibitors.* J Neurosci, 2011. **31**(40): p. 14051-66.
469. Yu, H., et al., *Next-generation sequencing to generate interactome datasets.* Nat Methods, 2011. **8**(6): p. 478-80.
470. Bader, J.S., *Grand network convergence.* Genome Biol, 2011. **12**(6): p. 306.
471. Ward, M.W., et al., *The amyloid precursor protein intracellular domain(AICD) disrupts actin dynamics and mitochondrial bioenergetics.* J Neurochem, 2010. **113**(1): p. 275-84.
472. Lin, M.T. and M.F. Beal, *Mitochondrial dysfunction and oxidative stress in neurodegenerative diseases.* Nature, 2006. **443**(7113): p. 787-795.
473. Kanekura, K., et al., *ER stress and unfolded protein response in amyotrophic lateral sclerosis.* Mol Neurobiol, 2009. **39**(2): p. 81-9.
474. Bialik, S. and A. Kimchi, *The death-associated protein kinases: structure, function, and beyond.* Annu Rev Biochem, 2006. **75**: p. 189-210.
475. Schumacher, A.M., et al., *DAPK catalytic activity in the hippocampus increases during the recovery phase in an animal model of brain hypoxic-ischemic injury.* Biochim Biophys Acta, 2002. **1600**(1-2): p. 128-37.
476. Djaldetti, R., N. Lev, and E. Melamed, *Lesions outside the CNS in Parkinson's disease.* Mov Disord, 2009. **24**(6): p. 793-800.
477. Pan-Montojo, F., et al., *Progression of Parkinson's disease pathology is reproduced by intragastric administration of rotenone in mice.* PLoS One, 2010. **5**(1): p. e8762.
478. Kuo, Y.M., et al., *Extensive enteric nervous system abnormalities in mice transgenic for artificial chromosomes containing Parkinson disease-associated alpha-synuclein gene mutations precede central nervous system changes.* Hum Mol Genet, 2010. **19**(9): p. 1633-50.
479. Mavrakis, K.J. and H.G. Wendel, *Translational control and cancer therapy.* Cell Cycle, 2008. **7**(18): p. 2791-4.
480. Zhou, X., et al., *Rheb controls misfolded protein metabolism by inhibiting aggresome formation and autophagy.* Proc Natl Acad Sci U S A, 2009. **106**(22): p. 8923-8.
481. Tatton, W.G., et al., *Apoptosis in Parkinson's disease: Signals for neuronal degradation.* Annals of Neurology, 2003. **53**(S3): p. S61-S72.

482. Mattson, M.P. and M.K. Meffert, *Roles for NF-kappaB in nerve cell survival, plasticity, and disease.* Cell Death Differ, 2006. **13**(5): p. 852-60.
483. Chua, C.E. and B.L. Tang, *alpha-synuclein and Parkinson's disease: the first roadblock.* J Cell Mol Med, 2006. **10**(4): p. 837-46.
484. Stenmark, H., *Rab GTPases as coordinators of vesicle traffic.* Nat Rev Mol Cell Biol, 2009. **10**(8): p. 513-25.
485. Jahn, R. and R.H. Scheller, *SNAREs--engines for membrane fusion.* Nat Rev Mol Cell Biol, 2006. **7**(9): p. 631-43.
486. Sharma, M., J. Burre, and T.C. Sudhof, *CSPalpha promotes SNARE-complex assembly by chaperoning SNAP-25 during synaptic activity.* Nat Cell Biol, 2011. **13**(1): p. 30-9.
487. Darios, F., et al., *Alpha-synuclein sequesters arachidonic acid to modulate SNARE-mediated exocytosis.* EMBO Rep, 2010. **11**(7): p. 528-33.
488. Dogic, D., et al., *The ADP-ribosylation factor GTPase-activating protein Glo3p is involved in ER retrieval.* Eur J Cell Biol, 1999. **78**(5): p. 305-10.
489. Saitoh, A., et al., *Three homologous ArfGAPs participate in coat protein I-mediated transport.* J Biol Chem, 2009. **284**(20): p. 13948-57.
490. Qing, H., et al., *Lrrk2 interaction with alpha-synuclein in diffuse Lewy body disease.* Biochem Biophys Res Commun, 2009. **390**(4): p. 1229-34.
491. Perry, G., et al., *Leucine-rich repeat kinase 2 colocalizes with alpha-synuclein in Parkinson's disease, but not tau-containing deposits in tauopathies.* Neurodegener Dis, 2008. **5**(3-4): p. 222-4.
492. Smith, W.W., et al., *Leucine-rich repeat kinase 2 (LRRK2) interacts with parkin, and mutant LRRK2 induces neuronal degeneration.* Proc Natl Acad Sci U S A, 2005. **102**(51): p. 18676-81.
493. Desagher, S. and J.C. Martinou, *Mitochondria as the central control point of apoptosis.* Trends Cell Biol, 2000. **10**(9): p. 369-77.
494. Chu, Y., A.L. Mickiewicz, and J.H. Kordower, *alpha-synuclein aggregation reduces nigral myocyte enhancer factor-2D in idiopathic and experimental Parkinson's disease.* Neurobiol Dis, 2011. **41**(1): p. 71-82.
495. Kawamata, H., et al., *Interaction of alpha-synuclein and synphilin-1: effect of Parkinson's disease-associated mutations.* J Neurochem, 2001. **77**(3): p. 929-34.
496. Nagano, Y., et al., *Lack of binding observed between human α-synuclein and Bcl-2 protein family.* Neuroscience Letters, 2001. **316**(2): p. 103-107.
497. Neystat, M., et al., *Analysis of synphilin-1 and synuclein interactions by yeast two-hybrid beta-galactosidase liquid assay.* Neurosci Lett, 2002. **325**(2): p. 119-23.
498. Xie, Y.Y., et al., *Interaction with synphilin-1 promotes inclusion formation of alpha-synuclein: mechanistic insights and pathological implication.* FASEB J, 2010. **24**(1): p. 196-205.
499. Sharma, N., et al., *Alpha-synuclein has an altered conformation and shows a tight intermolecular interaction with ubiquitin in Lewy bodies.* Acta Neuropathol, 2001. **102**(4): p. 329-34.
500. Du, H.N., et al., *Acceleration of alpha-synuclein aggregation by homologous peptides.* FEBS Lett, 2006. **580**(15): p. 3657-64.
501. Vilar, M., et al., *The fold of alpha-synuclein fibrils.* Proc Natl Acad Sci U S A, 2008. **105**(25): p. 8637-42.
502. McFarland, M.A., et al., *Proteomics analysis identifies phosphorylation-dependent alpha-synuclein protein interactions.* Mol Cell Proteomics, 2008. **7**(11): p. 2123-37.

503. Jensen, P.H., et al., *alpha-synuclein binds to Tau and stimulates the protein kinase A-catalyzed tau phosphorylation of serine residues 262 and 356.* J Biol Chem, 1999. **274**(36): p. 25481-9.
504. Jensen, P.H., et al., *Microtubule-associated protein 1B is a component of cortical Lewy bodies and binds alpha-synuclein filaments.* J Biol Chem, 2000. **275**(28): p. 21500-7.
505. Sharma, N., et al., *A close association of torsinA and alpha-synuclein in Lewy bodies: a fluorescence resonance energy transfer study.* Am J Pathol, 2001. **159**(1): p. 339-44.
506. Kawahara, K., et al., *alpha-Synuclein aggregates interfere with Parkin solubility and distribution: role in the pathogenesis of Parkinson disease.* J Biol Chem, 2008. **283**(11): p. 6979-87.
507. Hampe, C., et al., *Biochemical analysis of Parkinson's disease-causing variants of Parkin, an E3 ubiquitin-protein ligase with monoubiquitylation capacity.* Hum Mol Genet, 2006. **15**(13): p. 2059-75.
508. Monti, B., et al., *Alpha-synuclein protects cerebellar granule neurons against 6-hydroxydopamine-induced death.* J Neurochem, 2007. **103**(2): p. 518-30.
509. Nakamura, T., et al., *Activation of Pyk2/RAFTK induces tyrosine phosphorylation of alpha-synuclein via Src-family kinases.* FEBS Lett, 2002. **521**(1-3): p. 190-4.
510. Hashimoto, M., et al., *Role of cytochrome c as a stimulator of alpha-synuclein aggregation in Lewy body disease.* J Biol Chem, 1999. **274**(41): p. 28849-52.
511. Lim, J., et al., *A protein-protein interaction network for human inherited ataxias and disorders of Purkinje cell degeneration.* Cell, 2006. **125**(4): p. 801-14.
512. Bayir, H., et al., *Peroxidase mechanism of lipid-dependent cross-linking of synuclein with cytochrome C: protection against apoptosis versus delayed oxidative stress in Parkinson disease.* J Biol Chem, 2009. **284**(23): p. 15951-69.
513. Hashimoto, M., et al., *beta-Synuclein inhibits alpha-synuclein aggregation: a possible role as an anti-parkinsonian factor.* Neuron, 2001. **32**(2): p. 213-23.
514. Ihara, M., et al., *Association of the cytoskeletal GTP-binding protein Sept4/H5 with cytoplasmic inclusions found in Parkinson's disease and other synucleinopathies.* J Biol Chem, 2003. **278**(26): p. 24095-102.
515. Soderberg, L., et al., *Characterization of the Alzheimer's disease-associated CLAC protein and identification of an amyloid beta-peptide-binding site.* J Biol Chem, 2005. **280**(2): p. 1007-15.
516. Iwata, A., et al., *Alpha-synuclein degradation by serine protease neurosin: implication for pathogenesis of synucleinopathies.* Hum Mol Genet, 2003. **12**(20): p. 2625-35.
517. Liu, I.H., et al., *Agrin binds alpha-synuclein and modulates alpha-synuclein fibrillation.* Glycobiology, 2005. **15**(12): p. 1320-31.
518. Chung, J.Y., et al., *Direct interaction of alpha-synuclein and AKT regulates IGF-1 signaling: implication of Parkinson disease.* Neurosignals, 2011. **19**(2): p. 86-96.
519. Oh, Y., et al., *Human Polycomb protein 2 promotes alpha-synuclein aggregate formation through covalent SUMOylation.* Brain Res, 2011. **1381**: p. 78-89.
520. Liu, J., et al., *Identification of ciliary neurotrophic factor receptor alpha as a mediator of neurotoxicity induced by alpha-synuclein.* Proteomics, 2010. **10**(11): p. 2138-50.

521. Rekas, A., et al., *Interaction of the molecular chaperone alphaB-crystallin with alpha-synuclein: effects on amyloid fibril formation and chaperone activity.* J Mol Biol, 2004. **340**(5): p. 1167-83.
522. Meulener, M.C., et al., *DJ-1 is present in a large molecular complex in human brain tissue and interacts with alpha-synuclein.* J Neurochem, 2005. **93**(6): p. 1524-32.
523. Andringa, G., et al., *Tissue transglutaminase catalyzes the formation of alpha-synuclein crosslinks in Parkinson's disease.* FASEB J, 2004. **18**(7): p. 932-4.
524. Segers-Nolten, I.M., et al., *Tissue transglutaminase modulates alpha-synuclein oligomerization.* Protein Sci, 2008. **17**(8): p. 1395-402.
525. Zucchelli, S., et al., *TRAF6 promotes atypical ubiquitination of mutant DJ-1 and alpha-synuclein and is localized to Lewy bodies in sporadic Parkinson's disease brains.* Hum Mol Genet, 2010. **19**(19): p. 3759-70.